Effects of *Vigna mungo* (cv.T9) Seed Proteinase Inhibitor on Larval Growth and Expression of Midgut Proteins in Noctuid Lepidopteran Pests – A Comparative Study

A thesis submitted to the University of Hyderabad for the award of

DOCTOR OF PHILOSOPHY

By

V. SWAROOP KUMAR

(Enrolment No: 11LTPH16)

Supervisor: Prof. K.P.M.S.V. Padmasree



(A Central University established in 1974 by an Act of Parliament)

Department of Biotechnology & Bioinformatics, School of Life Sciences University of Hyderabad Hyderabad-500 046, INDIA

October 2019



(A Central University established in 1974 by an Act of Parliament)

Department of Biotechnology & Bioinformatics School of Life Sciences University of Hyderabad-500046 India

DECLARATION

I hereby declare that the work presented in this thesis entitled "Effects of Vigna mungo (cv.T9) Seed Proteinase Inhibitor on Larval Growth and Expression of Midgut Proteins in Noctuid Lepidopteran Pests – A Comparative Study" has been carried out by me under the supervision of Prof. K.P.M.S.V. Padmasree in the Department of Biotechnology & Bioinformatics, School of Life Sciences, University of Hyderabad. This work has not been submitted for any degree or diploma of any other University or Institute.

V. Swaroop kumar

V. Swaroop Omar

(Candidate)

Enrol. No. 11LTPH16

Dr. K.P.M.S.V. Padmasree

(Supervisor)

Dr. K.P.M.S.V. Padmasree, Ph.D.,
Professor & AvH Research Fellow
Dept. of Biotechnology & Bioinformatics
School of Life Sciences
University of Hyderabad
Hyderabad-500 046
Telangana, INDIA



(A Central University established in 1974 by an Act of Parliament)

CERTIFICATE

This is to certify that the thesis entitled "Effects of Vigna mungo (cv.T9) Seed Proteinase Inhibitor on Larval Growth and Expression of Midgut Proteins in Noctuid Lepidopteran Pests - A Comparative Study " submitted by V. Swaroop Kumar, bearing registration number 11LTPH16 in partial fulfilment of the requirements for award of Doctor of Philosophy in the Department of Biotechnology & Bioinformatics, School of Life Sciences is a bonafide work carried out by him under my supervision and guidance.

This thesis is free from plagiarism and has not been submitted previously in part or in full to this or any other University or Institution for the award of any degree or diploma.

Parts of the work performed in close relation to this thesis have been:

A. Published in the following peer-reviewed journals.

- 1. Plant Physiology and Biochemistry, DOI: 10.1016/j.plaphy.2014.07.009
- 2. Acta Physiologiae Plantarum, DOI: 10.1007/s11738-015-1991-8
- 3. Frontiers in Physiology (Invertebrate Physiology), DOI: 10.3389/fphys.2016.00388

B. Presented in the following conferences.

- 1. "ISPP South Zonal Seminar on Crop Physiology-Emerging Challenges and Opportunities for Sustainable Agriculture" held at S.V. University, Tirupathi on 3rd March 2015.
- 2. "International Conference on Innovations in Pharma and Biopharma Industry", held at the University of Hyderabad, Hyderabad, on 20-22nd December 2017.
- 3. "Eighth International Symposium on Molecular Insect Science", held at Melia Sitges. Sitges, Spain on 7-10th July 2019.

Further, the student has passed the following courses towards the fulfilment of the coursework requirement for PhD.

S. No.	Course Code	Name	Credits	Pass/Fail
1	BT 801	Seminar	1	Pass
2	BT 802	Research Ethics & Management	2	Pass
3	BT 803	Biostatistics	2	Pass
4	BT 804	Analytical Techniques	3	Pass
5	BT 805	Lab Work	4	Pass

Supervisor Dr. K.P.M.S.V. Padmasree, Ph.D., Professor & AvH Research Fellow Dept. of Biotechnology & Bioinformatics School of Life Sciences University of Hyderabad Hyderabad-500 046 Telangana, INDIA

Head of the Department

HEAD

Dept. of Biotechnology & Bioinformatics University of hyderabad Hyderabad.

DEAN School of Life Sciences University of Hyderabad Hyderabad - 500 046.

Acknowledgements

The process of earning a Ph.D. is a long and arduous endeavour that is certainly not an individual experience; rather it takes place in a collective context and includes many people, whom I would like to thank sincerely. Gratitude is an emotion least expressible in words. However, this limitation, I would like the reader to know that the following words are sincere feelings which I shall cherish for a lifetime.

First and foremost I would like to express my profound gratitude to my supervisor **Prof. K.P.M.S.V. Padmasree** for her guidance, constant encouragement and precious suggestions throughout my Ph.D.

I thank my doctoral committee members **Prof. Sarada Devi Tetali** and **Prof. P. Prakash Babu**, for their critical comments and valuable suggestions.

I would like to extend my sincere thanks to **Prof. Sarada Devi Tetali** for her critical suggestions while implementing molecular biology experiments and extending their lab facilities.

I am grateful to **Prof. Aparna Dutta Gupta** for her critical inputs, support and allowing me to use their lab facilities.

I thank, **Prof. K.P.M.S.V. Padmasree**, Head, Dept. of Biotechnology & Bioinformatics, and former Heads **Prof. J.S.S. Prakash**, **Prof. Anand K. Kondapi**, **Prof. Niyaz Ahmad** and **Prof. P. Prakash Babu** for providing the necessary facilities in the department to carry out my research work.

I thank Prof. S. Dayananda Dean, School of Life Sciences and former Deans Prof. K.V. Ramaiah, Prof. P. Reddanna, Prof. A.S. Raghavendra, Prof. R.P. Sharma, Prof. Aparna Dutta Gupta and Prof. M. Ramanadham for providing all the facilities in the school.

I am thankful to my senior labmates **Dr. Mohanraj** S.S, **Dr. Srinivasa Rao Yearla**, **Dr. Swathi Marri** and **Dr. Abhay Pratap Vishwakarma** for their encouragement and support during my entire Ph.D. duration. I also thank **Dr. Prasad** and **Dr. Dinakar** for their contribution to this laboratory.

I thank Dr. Vinod Kumar, Mr. Naren Dania, Dr. R. Kiran Kumar, Mr. Vamshi, Ms. Lalitha Niharika, Nanak Ram and Satya for their help and support.

I am grateful to my lab mates Mr. Lokya, Mr. Sankar, Ms. Mariyamma, Ms. Mahati and Ms. Fouzia for being kind and creating friendly environment to work in. Special thanks to my batch mates Dr. Lokya, Mr. Durgeshwar, Mr. Sireesh, Mr. Suresh, Mr. Lingaswamy Bantu, Dr. Ashwini, Dr. Prasanna, Mr. Chaitanya, Dr. Santosh, and Dr. Naresh.

I am always be grateful to have friends Mr. Pandu, Dr. Vikranth, Dr. Chandra, Dr. Kiran, Dr. Sateesh, Dr. Vamsi, Mr. Prakash, Mr. Shyam, Mr. Uma

maheshwar, Dr. Hari, Dr. Satish suthari, Dr. Ravi for making happy and wonderful days during this time.

My special thanks to my friend **Durgeshwar** and **his family members**, **Prakash** and **Suresh** for providing accommodation with tasty food, during Corona pandemic time.

My special thanks to Sirish, Ashwini, Lokya, Sankar, Suresh, Varaprasad anna for their moral support.

I would like to thank Divya, Sai, Deviram anna, Preetham, Sravan, Madhu, Ramana master, Praneeth, Nagaraju, Goutham, Ramji, Naresh, Abhilash, sekhar, Dr. Ramjee, Mr. Sattiraju for their chill time.

I am thankful to Mrs. Monika kannan and Mrs. Kalpana for all this support whenever I needed in Proteomics Facility.

I would also like to thank all the **Faculty** and **Research scholars** of the School of Life Sciences.

I am grateful to all my teachers, who taught me and are instrumental in shaping up my life.

I thank Mr. Arun, Mr. Prashanth Kumar and Mr. Mallesh for their assistance in the lab. I also extend my thanks to dept. technical staff members for their assistance.

I'm very thankful to the sources that have supported me financially! Funding from the **UPE**, **DBT-CREBB**, and **DST-FIST** to School and Department, CSIR, **UGC**, **DBT**, **DST** and **UPE** II for lab and fellowship by **DBT** is greatly acknowledged.

I am thankful to University of Hyderabad and Dept. of Biotechnology and Bioinformatics for giving this opportunity to pursue my Ph.D. degree.

I am always grateful to my family members Sukumar, Vadhina, Dhatri papa, Suji, Suneel baava, Varshu papa and Sobharaj.

I am always grateful to my brother **Sukumar**, because of his encouragement and support I have finished my PhD.

Special thanks to my brother **Sobharaj** for his support.

I wish to express my deepest gratitude and reverence to my parents for their epitome of patience in allowing me to choose the career of my interest.

Above all, I owe my thanks to *Almighty*, for giving me the patience to wade through the ebbs and tides of my research.

Vanka Swaroop Kumar

Abbreviations

A. janata	Achaea janata
AGPIs	A. janata trypsin-like midgut protease inhibitors
AGPs	A. janata midgut proteases
AK	Arginine kinase
BAPNA	N - α -benzoyl-DL-arginine- p -nitroanilide hydrochloride
BBI	Bowman-Birk inhibitor
CI	Chymotrypsin inhibitor
CSN	COP-9 signalosome
Cyc-C	Cyclin-C
Cyt-P450	Cytochrome-P450
GLUPHEPA	<i>N</i> -glutaryl-L-phenylalanine- <i>p</i> -nitroanilide
GST	Glutathione S-transferase
H. armigera	Helicoverpa armigera
HGPIs	H. armigera trypsin-like midgut protease inhibitors
HGPs	H. armigera midgut proteases
HSPs	Heat shock proteins
IDA	Iodoacetamide
IEF	Isoelectric focusing
IPG	Immobiline pH gradient
IPTG	Isopropyl-β-D-1-thiogalactopyranoside
MALDI-TOF/TOF MS	Matrix assisted laser desorption ionization time of flight mass spectroscopy
PDH	Pigment dispersing hormone
PIs	Protease inhibitors
PMF	Peptide mass fingerprinting
PVP	Poly vinyl pyrrolidone
rT9BBI	Recombinant Bowman-Birk inhibitor
S. litura	Spodoptera litura
SGPs	S. litura midgut proteases
SGPIs	S. litura trypsin-like midgut protease inhibitors

SBBI	Soybean Bowman-Birk inhibitor
T9BBI	Bowman-Birk inhibitor (cv.T9)
TI	Trypsin inhibitor
Трх	Thioredoxin peroxidase
V. mungo	Vigna mungo
2-DE	Two-dimensional gel electrophoresis

Contents

Chapter 1: General Introduction

Chapter 2: Rationale of the Study, Objectives and Approach

Chapter 3: Materials and Methods

Chapter 4: Purification and Partial Characterization of Proteinase

Inhibitor from the Seeds of *Vigna mungo* (cv.T9)

Chapter 5: Insecticidal Potential of T9BBI on larval growth and

development of a non-host insect pest *Achaea janata*: Modulation in expression of midgut tissue proteins

Chapter 6: Insecticidal Potential of T9BBI on Larval Growth and

Development of a Host Insect Pest *Spodoptera litura*: Modulation in the Expression of Midgut Tissue Proteins

Chapter 7: Insecticidal Potential of T9BBI on Larval Growth and

Development of a Host Insect Pest *Helicoverpa armigera*: Modulation in the Expression of Midgut Tissue Proteins

Chapter 8: Cloning of *T9BBI1* from the seeds of *V. mungo* (*cv*.T9) and

its expression in *E.coli* shuffle cells using pET-32a vector.

Chapter 9: Summary and Conclusions

Chapter 10: Literature Cited

Publications & Conference Attended

Plagiarism Report

This Thesis Dedicated to My Parents & My brother Sukumar

Chapter 1 General introduction

Chapter 1

General Introduction

The enormous increase in population worldwide alarms requirement of appropriate food security for which beneficial crop cultivation practices and crop protection strategies play an essential role. The overall loss in crop yield generated by insect pests during the pre-harvest and post-harvest period of cultivation is very high. Approximately, more than 10,000 species of insects are known to cause severe damage to several economically important food crops (Kalavagunta et al., 2014).

Use of chemical or synthetic pesticides is an instant approach to control insect pests on various crops throughout the world. However, excessive and improper usage of agrochemicals causes adverse effects on the environment and human health (Briones, 2005). Moreover, the usage of traditional pesticides like organochlorides or organophosphates (DDT, Endosulfan, Malathion, Monocrotophos and Chlorpyrophis) are found to be lethal to birds as well as wildlife creatures (Clothianidin, 2014 and Extoxnet, 2014) and caused many diseases to humanity (Bouchard et al., 2010; Kashyap et al., 2010). Also, the usage of pesticides raised concern on several issues related to food safety among domestic consumers and impeded trade in agricultural commodities for export (Gupta and Dikxit. 2010). Thus, the deleterious consequences of synthetic pesticides have driven scientific community to search for alternative eco-friendly approaches such as "Biopesticides".

The usage of biopesticides along with bio-fertilizers (also known as Bio-agents) has gained significant attention in agricultural research due to their sustainability in nature. Biological pesticides are categorized into biochemical, microbial and natural type (animal and plant origin) pesticides (Kumar singh, 2014). Biological pesticides are much safer and not hazardous to mankind and animals as much as compared to synthetic pesticides. These biological pesticides are host specific with minimal or no risk to the non-target organisms

(such as parasitoids, predators and many vertebrates). They are also safe to habitat and environment. The biopesticides are known to affect the metabolism of pests and delay the life cycle of target pests but do not eradicate the pests.

Thus, there is a need to develop new biopesticides which can effectively control the pests in the field while allowing the significant species remain unaffected. These goals can be achieved by developing transgenic plants expressing various defensive traits such as protease inhibitors (PIs), lectins or amylase inhibitors from selected plants to combat insect pests (Foissac et al., 2000). However, screening of several wild species, host and non-host plants for these defensive traits would be a foremost step towards the development of transgenic crops/plants resistant to their respective pest species. Several transgenic crop plants resistant to various insect pests are developed by incorporating several PI genes belonging to different families.

Transgenic tomato (*Lycopersicum esculentum*) with two barley PIs showed defence response and enhanced resistance against *Tuta absoluta* (Hamza *et al.*, 2018). Also, transgenic tomato with Oryzacystatin PIs (OCI & OCII) showed resistance against Colorado potato beetle. Similarly, potato (*Solanum tuberosum*) transformed with OCI and OCII showed resistance against potato beetle (Cingel *et al.*, 2014). Further, transgenic tomato with *Capsicum annum* protease inhibitor (Can PI7) showed tolerance against *Helicoverpa armigera* (Tanpure *et al.*, 2017). Transgenic rice with maize protease inhibitor (MPI) and potato carboxypeptidase inhibitor (PCI) showed resistance against *Chilo suppressalis* (Quilis *et al.*, 2014). Furthermore, feeding of *Nicotiana benthamiana* transformed with serine PI gene from *Beta vulgaris* (BvSTI) considerably reduced the weight of the following larvae: *Agrotis ipsilon, Heliothis virescens, Manduca sexta, Spodoptera exigua and S. frugiperda* (Smigocki et al., 2013). Similarly, Chinese cabbage (*Brassica campestris sp. Chinensis var. parachinensis*) transformed with sporamin from sweet potato showed insect resistance against

Plutella xylostella (Qiu et al., 2013). Transgenic sugarcane (Saccharum officinarum) with soybean (Glycine max) Kunitz inhibitor (SKI) and Bowman-Birk inhibitor (SBBI) showed resistance against Diatraea sacccharalis (Falco et al., 2003). Transgenic Nicotiana tabacum with tomato showed resistance against Manduca sexta larvae. Trypsin inhibitor gene NtPI from N. tabaccum showed resistance against insect pests S. litura and H. armigera (Srinivasan et al., 2009). However, in some cases, the transgenic plants failed to protect themselves from the invading pests, possibly due to the development of resistance in the pest species to the PI and/or development of specialized adaptive strategies in the pest themselves when exposed to the PI(s). It is well known that few lepidopteran and coleopteran pests have evolved such adaptive strategies.

Adaptation of insect pests towards plant toxins, allelochemicals or insecticidal compounds depends on the presence of a variety of midgut detoxifying enzymes such as cytochrome P-450, esterase (EST), glutathione S-transferase (GST) and monooxygenase (P450) (Franscis et al., 2005). They are expressed in the midgut, either constitutively or induced on exposure to a secondary metabolite (War et al., 2013). Contrarily, adaptation in insect pests towards phenols is due to the lower oxygen levels and higher gut pH, which prevent the auto-oxidation of tannins to toxic compounds. Nevertheless, some insects are not only adapted to the tannins but also utilized them for their growth and development (War & Sharma 2014). Adaptation of insect pests against protease inhibitors (PIs) could be due to the overproduction of proteases which are insensitive to PIs (Zhu-salzman and Zeng, 2015). The following are few examples of insects which showed adaptation against PIs by overproducing proteases in their midguts: *A. ipsilon, C. maculatus H. zea* and *L. decemlineata* and *Anagasta kuehniella* (Oliveira et al., 2013). Thus, considering the various adaptive mechanisms exhibited by the insect pests, the identification of novel defensive traits in the host plants or wild species and developing pest-resistant crops is a continuous thirst of agricultural research.

Helicoverpa armigera, Spodoptera litura and Achaea janata are the three major cropdamaging pests among the lepidopteran insects.

Helicoverpa armigera:

The cotton bollworm, *Helicoverpa armigera* is economically a critical polyphagous pest in the world (Tay et al., 2017). It is the most global widespread species due to its ability to spread via long-range migration (Goergen et al., 2016). The estimated loss of annual production cost due to *H. armigera* alone in the world is ~5 billion US dollars (Sharma et al., 2005). Many approaches, including generation of *Bt* crops, were used to overcome the infestation by *H. armigera*. *Bt* crops are harmful to some devastating pests, including *H. armigera* abut are non-toxic to other organisms (Swiatkiewicz et al., 2014). But, the development of resistance in *H. armigera* threatens the massive environmental and economic benefits to *Bt*-resistant crops (Tabashnik et al., 2013). However, the introduction of multiple *Bt* genes prolonged the efficacy of various crop species. A synergistic effect of *Cry2Ab* and *Cry1AC* delayed the development of resistance in Cotton bollworm (Wei et al., 2015). Other approaches used to manage the *H. armigera* are RNAi technology (Zhang et al., 2017) and CRISPR (clustered regularly interspaced short palindromic repeats)/Cas9 (CRISPR associated proteins) technology (Wang et al., 2017).

Several other measures also established to control the *H. armigera* by using plant growth regulators such as abscisic, gibberellic-(GA₃) and indole-3-acetic- acid (Kaur and Rup 2002; Er and Keskin 2016). GA₃ treatment is not only active on plant growth but it also negatively affected the survival of insects (Altuntas et al., 2012). The studies of Shayegan et al. (2019) have shown the impact of different concentrations of GA₃ on larval development, pupal duration, adult longevity, growth, reproductive parameters and survival rates in

H. armigera. Similarly, several studies used secondary metabolites such as Caffeic acid and PIs, to control *H. armigera* (Joshi et al., 2014).

Further, the purified Bowman-Birk and Kunitz inhibitors from pigeon pea seeds showed inhibitory activity against trypsin-like gut enzymes of *H. armigera* (Mohan raj et al., 2018, 2019). The purified PIs or trypsin inhibitors from *Cajanus platycarpus* (Swathi et al., 2015, 2016), soapnut seeds (Gandreddi et al., 2015) and transgenic tomato with *Capsicum annuum* PI genes (Tanpure et al., 2017) declined the growth of *H. armigera*.

Spodoptera litura:

Spodoptera litura, a tobacco caterpillar, is a polyphagous pest feeding on ~87 plant species spanning 40 families related to fruits, pulses and vegetables including castor, cauliflower, cotton, groundnut, ladyfinger and tobacco in many Asian countries (Datta et al., 2019). The use of synthetic organic insecticides to control this pest lead to increase in resistance against different groups of insecticidal compounds. Therefore, alternative control measures used to manage this pest (Srivastava et al., 2015).

Insect resistant plants are developed by expressing defence traits against insects using genetic engineering technology (Tabashnik et al., 2014). Recent reports showed that overexpression of *Cry1Aa* gene in sweet potato reduced the pest damage significantly by disrupting the midgut membrane of *S. litura* larvae (Zhong et al., 2019). Insect bioassay with *S. litura* showed up to 93% mortality with dual gene transgenic crops (Siddiqui et al., 2019). Gene pyramiding is another approach to control lepidopteran and hemipteran insect pests. The synergistic effect of expressed toxins combined with plant lectin showed 100% mortality against *S. litura* (Rauf et al., 2019). Also, herbicides and plant growth regulators (PGRs) are useful to control the growth and development of *S. litura* (Sing et al., 2002).

Achaea janata:

The castor semi looper, *A. janata* is an important pest on crops such as castor, rose and pomegranate. Several studies showed the usage of *Bt* based biopesticides to control *A. janata* (Dhania et al., 2019 and Muddanuru et al., 2019). However, the unlimited use of *Bt*-biopesticides may develop resistance in the larvae (Dhania et al., 2019). Alternatively synthetic and purified naphthol derivatives (Kalvagunta et al., 2014), limonoids from the leaves of *Soymida febrifuga* (Yadav et al., 2014) and terpene compounds (alpha-pinene and linalool) formulated with silica nanoparticles (Rani et al., 2014) are found to be useful to control *A. janata*.

Further, the crude leaf extracts from Argemone mexicana, C. annuum, C. multiflorum, Clerodendrum splendens, L. esculentum, S. melongena and Vitex negundo (Devanand and Rani 2011; Devarshi et al., 2017). Also, benzyl derivatives from the root extract of Derris scandens, synthesized Plumbagin derivative, Triterpenes from the leaves of Walsura trifoliata (Rao et al., 2015) and kairomonal attractants (Duraimurugan et al., 2017) were useful to control this voracious feeder. Further feeding with PVP coated silver nanoparticles (Yasur et al., 2015) and intercropping cultural practices helped to control the A. janata (Srinivasa et al., 2012).

In the present study, efforts are made to examine the proteinase inhibitor (PI) based pest management strategy to control all the lepidopteran pests described above.

Protease inhibitors (PIs):

PIs are proteins which are ubiquitously expressed in plants as a part of defensive mechanism against insect pests (Foissac *et al.*, 2000; Shamsi *et al.*, 2016 and Clemente *et al.*,

2019). In the plant kingdom, they are mainly present in three families such as Gramineae, Leguminosae and Solanaceae (Katoch *et al.*, 2014), and concentrated in stems, leaves, flowers, seeds and tubers (Browse and Howe 2008). As PIs show specificity for Aspartic, Cysteine, Serine and Metallo-proteases, they are classified as Aspartic PIs, cysteine PIs, respectively. Serine PIs and Metallo PIs, respectively. Among Serine PI family includes Kunitz, Cereal, Squash, Potato type I & II, Mustard and Bowman-Birk type inhibitors. However, Kunitz and BBI are found to be most prominent inhibitors (Prasad et al., 2011; **Table. 1.1**).

In the last decade, studies have been focused on commonly occurring SPIs due to two main reasons: Firstly, it controls the functions of fundamental mechanisms in insects such as digestive and immune system and provides protection against predators. Secondly, due to its low molecular weight, they became interesting tools to investigate the common aspects of protein conformation as well as protein-protein interactions (Kellenberger et al., 2005).

Mechanism of Inhibition:

The mechanism of molecular interaction of protease and PIs are mainly of three types such as canonical, non-canonical and serpins (Otlewski et al., 1998). PIs bind to the active site of protease with a complementary reactive loop similar to the enzyme-substrate interaction in the canonical model (Silverman. 2001). SPIs, metalloprotease inhibitors and cysteine protease inhibitors adopted this standard mechanism for efficient inhibition (Seeram et al., 1997). In the case of the non-canonical model, inhibitor slowly binds to the secondary binding site, which is followed by binding of the N-terminus to the active site of protease (Fig.1.1). Cystatins undergo this type of inhibitory mechanism (Page and Dicera et al., 2008). In contrary, serpins bind to the proteases in a substrate-like manner while structural modifications cleave the peptide bond in the binding loop (Krowarsch et al., 2003).

Table.1.1. Classification, distribution, and target proteases of plant protease inhibitors (PPIs): Adapted (Rai et al., 2017) and modified

Sl. No	Families and	Progenitors	Type of Inhibitors	Protein restrained	References
	Subfamilies				
1	Serine PIs				
1.1	Kunitz	G. max, Hordeum vulgare, Psophocarpus Tetragonolobus, Cajanus platycarpus and Rhynchosia sublobata	Soybean, barley subtilisin, winged bean inhibitors, <i>R. sublobata</i> Kunitz inhibitor, <i>C. platycarpus</i> Kunitz inhibitor	Trypsin, Chymotrypsin, Subtilisin and α-trypsin	Vallee et al. (1998) Oliva et al. (2010) Swathi et al. (2016) Mohanraj et al. (2019)
1.2	Potato type I and II	Hordeum vulgare, Triticum estivum and Momordica charantia	Wheat chymotrypsin inhibitor, mustard and rape trypsin inhibitor	Trypsin, Chymotrypsin and Subtilisin	Greagg et al. (1994); Dunse et al. (2010)
1.3	Squash	Momordica acharantia; Momordica Cochinchinensis	Trypsin inhibitor MCTI-I and II Macrocyclic squash inhibitor	Pancreatic elastase and trypsin	Huang et al. (1992); Daly and Craik (2011),
1.4	Cereal	Hordeum vulgare, Triticum aestivum, Zea mays	Wheat, maize, and barley alpha- amylase inhibitor	Alpha-amylase and trypsin	Akande et al. (2010)
1.5	Bowman-Birk	Glycine max, Arachis hypogaea, Helianthus annuus, V. mungo (TAU-1), C. cajan (ICP-7118)	Bowman-Birk trypsin/chymotrypsin Inhibitor and sunflower cyclic trypsin inhibitor	Trypsin and Chymotrypsin	Mulvenna et al. (2005) Prasad et al. (2010 a,b) Swathi et al. (2014)

1.6	Mustard	Sinapis alba and Brassica napus	Mustard and rapeseed inhibitor	Trypsin and Chymotrypsin	Menengatti et al. (1992), Jongsma and Beekwilder (2011)
2	Cysteine PIs				
2.1	Cystatin	Onchocerca volvulus and Oryza Sativa	Onchocystain and ovocystain	Cysteine and thiol protease	Lustigman et al. (1992), Benchabane et al. (2010)
2.2	Cystatins	Chlorella, pearl millet	Celostatin and sarcocystatin	Cysteine and thiol protease	Ryan and Pearce (1998)
3	Aspartic PIs				
3.1	Aspartyl protease inhibitors	Cynara cardunculus flowers and in potato tubers	Aspartyl protease inhibitor	Aspartyl protease	Park et al. (2000)
3.2	Cathepsin D inhibitor	potato tubers	Soybean type inhibitor	Trypsin and Chymotrypsin	Lawrence and Koundal (2002)
3.3	Pepstatin	Colorado potato Beetle	Aspartyl protease inhibitor	Aspartyl proteases	Wolfson and Murdock (1987)

4	Metallocarboxy	Solanaceous plants,	Carboxypeptidase A	Carboxypeptidase	Liu et al.
	peptidase	Hirudomedicinalis		inhibitor	(2000)

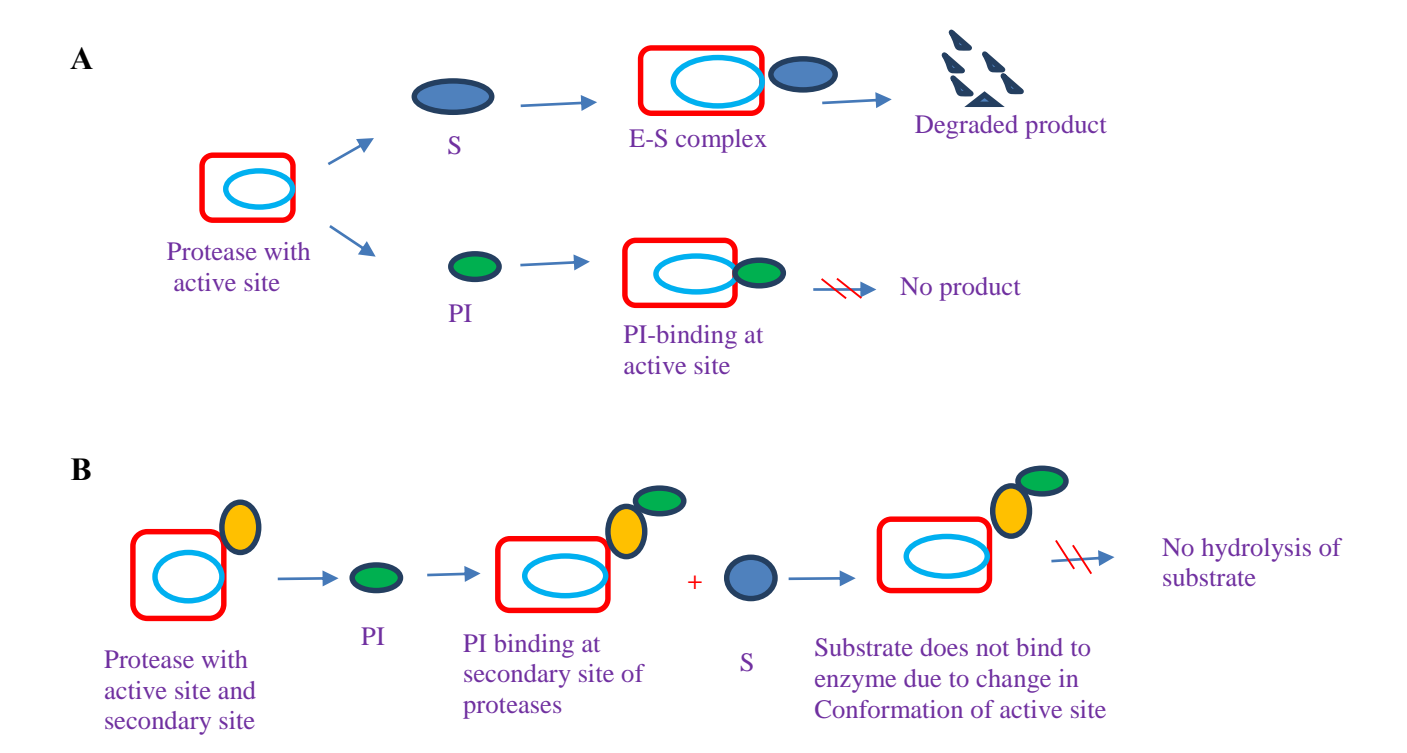


Fig. 1.1. Diagrammatic representation of the mode of inhibition of PIs: (A) Canonical and (B) Non-canonical type.

Different Families of PIs:

Serine PIs (SPIs):

The serine PIs specifically bind to elastase, trypsin and chymotrypsin proteases of the serine family. The BBI(s) and KI(s) from SPI(s) are well characterized. In addition to the crop protection, they possessed pharmacological properties as evident by their inhibitory action against serine proteases implied in several diseases (Clemente et al., 2019; Shamsi et al., 2016).

Bowman-Birk inhibitors (BBIs):

BBIs belongs to serine-type of PIs named after D.E. Bowman and Y. Birk (Habib and Fazil. 2007) and are present in both dicots and monocots (Law et al., 2006).

Dicot BBIs are very strongly conserved, showing negligible discrepancy at the moment of their evolution, whereas monocot BBIs are highly flexible, showing a convincing evolutionary mechanism based on gene duplication and mutation incidence (Rai et al., 2017). Dicotyledonous BBIs contains a single polypeptide chain (8-10 kDa) with two reactive sites (double-headed) rich in cysteine amino acids which are bridged by seven conserved disulphide bonds (Richardson.1991, Rai et al., 2017). Monocotyledonous plant BBIs are grouped into two types. One group with a single polypeptide chain with a single reactive site having mass of ~8 kDa and other group having two polypeptide chains with two reactive sites having the mass of 16kDa (Habib and Fazil, 2007). Dicotyledonous BBIs consist of a cysteine-rich polypeptide chain (8-10 kDa) which is bridged by seven conserved disulfide bonds with two reactive sites (Richardson.1991, Rai et al., 2017). The disulphide bonds provide stability to the structure and function of BBIs when heated or treated with denaturing agents (Kumar et al., 2013). BBIs consists of several iso-inhibitors due to variations in genetic polymorphism or post-translational protein modifications (Quillien et al., 1997; Mello et al., 2003). Due to its two functional reactive sites, BBIs can inhibit two diverse proteases concurrently by forming a ternary complex. The reactive sites are exposed peripherally on the surface of a stringent disulphide-linked β-sheet loop (Fig. 1.2) which is extremely conserved and generally contain nine residues (Rai et al., 2017).

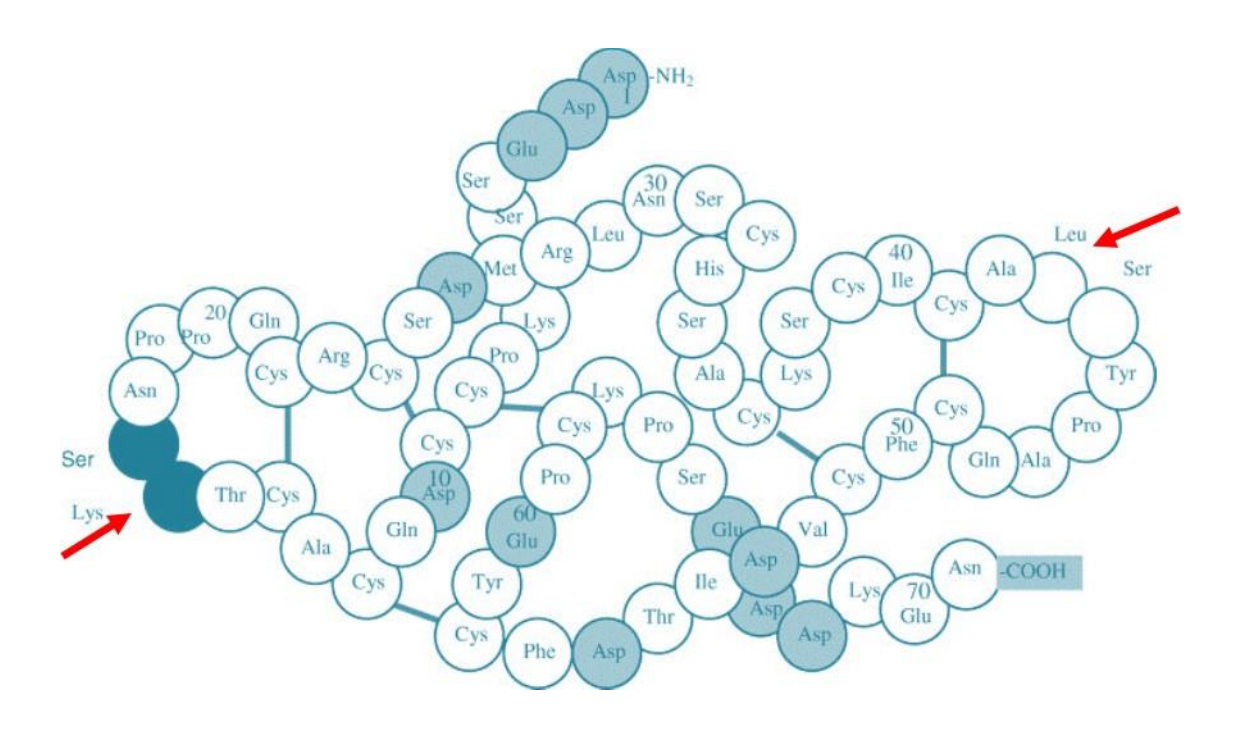


Fig. 1. 2. Primary structure of soybean Bowman-Birk inhibitor showing an arrangement of disulfide bonds. Lys and Leu are the P1 residues indicated in red colour arrow at tryspin inhibitory (Left-side) and chymotrypsin inhibitory (Right-side) domains (Adapted from Odani and Ikenaka)

Kunitz inhibitors (KIs):

The KI family is also well characterized among all the plant PIs. These are extensively studied in different families such as Solanaceae, Fabaceae and Poaceae (Habib and Fazil, 2007). They are 18-22 kDa proteins containing two di-sulphide bonds with a single reactive site. They are very effective against serine proteases and exhibit moderate inhibition towards aspartic, cysteine proteases like cathepsin D and papain (Rai et al., 2017). However, KIs, which are devoid of disulphide bonds, are also reported in *Archidendron ellipticum* (Bhattacharya et al., 2006), *Cassia grandis* and *Leucaena leucocephala* (Oliva et al., 2000).

The reactive site of these PI's range from 50-60 amino acids length. Due to their distinct sequence homology, they are placed into the separate family of inhibitors which are

active against serine proteases along with other class of proteases (Laing and McManus 2002). The reversible interaction exhibited by KIs towards the target proteases leads to the formation of stable complexes, inhibiting their active catalytic sites through a competitive or non-competitive manner. These structural characteristics helped in understanding the mechanism and biological activities with which they bring about specificity in their binding to various kinds of coagulation factors and tumour cells (Oliva et al., 2008; 2010). KIs have potential inhibitory activity against many insect pests (Jamal and Pandey, 2014). The antifungal activity of KIs was described in potato tubers (Wang and Ng 2006) and root extracts of ginseng under stress conditions (Ledoigt et al., 2006). Besides, KIs also showed antimicrobial (Macedo et al., 2016), anti-coagulant (Nakahata et al., 2006) and anti-tumour properties (Oliva and Sampaio 2008; Bortolozzo et al., 2018).

Cystatin family:

Cystatin family includes the group of cysteine protease inhibitors isolated from the seeds and leaves of various crop species like corn, soybean, rice, Chinese cabbage and cowpea (Jacinto et al., 1998). The cystatin superfamily is characterized by a group of endogenous cysteine PIs containing multiple cystatin-like protein motifs. Majority of cystatin inhibitors span about 11-16kDa (Barnet et al., 1987) and this superfamily includes 1) Stefin, 2) Cystatin, 3) Kininogen and 4) Phytocystatin families (Barnet et al., 1987). Stefin family comprise of 11kDa proteins and cystatins range about 13.4-14.4 kDa (Gatehouse. 2002). This superfamily inhibits the activity of thiol and cysteine proteinases. Cystatins forms tight complex and inhibits the action of proteases such as papain and cathepsin B, H and L (Kennedy et al., 2012). The proteins from kininogen family are glycosylated and grouped under three major classes. They are with high molecular weight kininogens with 120 kDa molecular weight, low molecular weight kininogens with 60–80 kDa MW and type T-kininogens having 68 kDa. These are considered as markers for kidney dysfunction and they

have anti-bacterial, anti-viral properties along with antifungal activities. They play a main function in different cellular systems, mainly in tumour metastasis, inflammatory response, growth and cell proliferation (McPhalen et al., 1985).

Phytocystatins are 17-19 kDa proteins mainly reported from different plant species of alfalfa, rice (Wang et al., 2015) and potato (Bouchard et al., 2003). Phytocystatins are ubiquitously expressed in different parts of the plant, control the cysteine protease activity during seed germination and development as well as programmed cell death (Solomon et al., 1999). These are known to accumulate in response to many abiotic stress conditions such as alkali (Sun *et al.*, 2014), drought (Tan et al., 2015), heat (Je *et al.*, 2014) and salinity (Li et al., 2015). So far, the defensive role of Phytocystatins towards coleopteran insects was well documented (Martinez et al., 2016).

Aspartyl PI family (APIs):

APIs inhibits the catalytic activity of an aspartyl protease such as pepsin and retro pepsin which contains an aspartate residue (Asp) in the active site. These family members are found in barley, cardoon flowers and potato tubers (Cater *et al.*, 2002). These inhibitors are 27 kDa proteins and inhibit aspartyl protease cathepsin D besides serine proteases. Pepstatin inhibits the aspartyl proteases and in nature it occurs as a hexapeptide containing the unusual amino acid statin, which inhibits the midgut proteases of Colorado potato beetle (Wolfson and Murdock, 1987). They are also isolated from the various species of actinomyces cultures. The aspartic proteases are associated with nitrogen recycling in crops deprived of nutrients as the second-biggest family of plant proteases (Rustgi et al., 2018).

Metalloprotease Inhibitors (MPIs):

MPIs are the main cellular inhibitors of the matrix metalloproteinases (MMPs) which exhibit a variable degree of activity in various tissues. These are small peptides having

molecular mass of ~4.2 kDa (Hass et al., 1975). MMPs degrade the extracellular matrix during tissue differentiation, morphogenesis and wound healing which might be a suitable target during the treatment of diseases such as cancer and arthritis (Browner et al., 1995). They strongly inhibit a wide range of carboxypeptidases of both plant and animal origin, but not from the yeast (Havkioja and Neuvonen 1985). Carboxypeptidase inhibitor (PCI) contains 39 amino acids with a molecular weight of 4,295 Da, forms a globular core with 27 residues which are stabilized by three disulfide bridges and a C-terminal tail from 35-39 residues (Winer et al., 2018).

The various PI structures from different families are shown in Fig. 1.3.

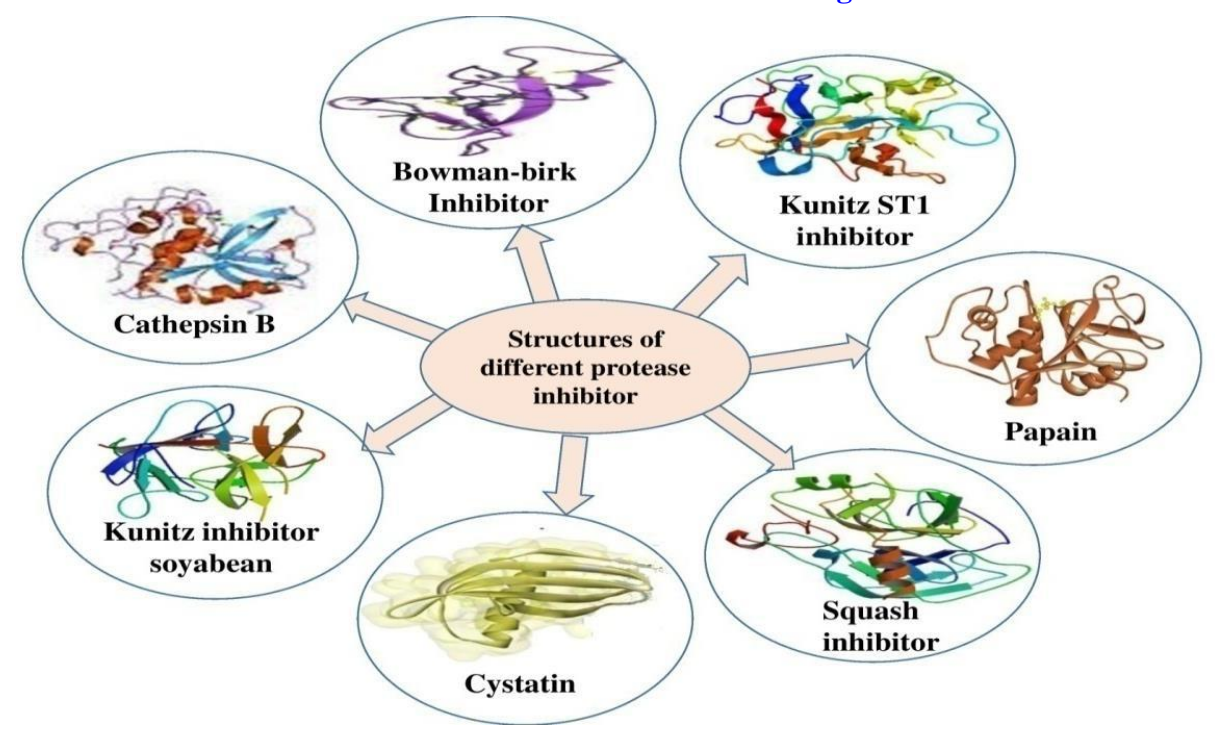


Fig. 1.3. The structures of different protease inhibitors (adapted from Rai et al., 2017).

Applications of PIs:

Plant organs such as seed, fruit and tubers usually contain a relatively large quantity of PIs and they have been well exploited in the agricultural and medicinal fields as antagonists of digestive proteases of economically important insect pests as well as proteases associated with the pathophysiological state in several human diseases. In general, lepidopteran and dipteran order of insects predominantly uses serine proteases for their

digestion. Contrarily, Homoptera and Coleoptera insect's midguts are dominated with cysteine proteases (Srinivasan et al. 2006).

PIs and their role in agriculture:

The initial studies demonstrated the failure of certain insect larvae to grow on soybean products. The cause for such failure was later discovered to the presence of trypsin inhibitors in soybean, which are toxic to insect larvae (Lawrence and Koundal, 2002; Clemente et al., 2019). In recent years, the use of PIs in insect pest management has gained more attention due to the hazardous nature of synthetic pesticides on human and environment. Among PIs, both KIs and BBIs impaired the larval growth of Tribolium confusum, H. virescens and T. castaneum (Ryan, 1990, Gatehouse et al., 1993), and Cysteine PIs and oryzacystatin showed inhibitory activity against Diabrotica undecium punctata larvae (Edmonds et al., 1996). Further, it has been demonstrated that the heterologous expression of inhibitors in transgenic plants reduces the growth rates of several insect larvae (Gatehouse et al., 1997; Jouanin et al., 1998). KIs isolated from Arabidopsis thaliana showed inhibitory activity against serine and cysteine proteases of spider mite and caused a negative effect on their fecundity and mortality (Arnaiz et al., 2018). The chymotrypsin/subtilisin inhibitor 2, amylase/ subtilisin inhibitor, Kazal-type inhibitors from A. thaliana, BBIs isolated from Hordeum vulgare (Periani et al., 2016) and Vicia faba (Pekkarinen et al., 2007) showed protection against fungal diseases. The PIs isolated from microorganisms such as aminopeptidase inhibitors, Pepstatin A and leupeptin from actinomycetes were also used as insecticidal agents against T. castaneum, Callosobruchus maculatus and D. virgifera (Kim and Mullin, 2003; Amirhusin et al., 2007). Cysteine PI E-64 isolated from A. japonicas was used against Colorado potato beetle (Bolter and green., 1997).

Transgenic Plants:

The genes of Plant PIs (PPIs) against common proteases found in larval gut have been transferred to plants through genetic engineering to enhance the level of pest resistance in plants (Fig. 1.4). The over-expression of many PPI genes in transgenic plants were shown to have an antagonistic effect on insect feeding and impaired larval growth and development (Clemente et al., 2019). For instance, enhanced resistance to Heliothis obsolete and Liriomyza trifolii larvae was observed by the leaf-specific overexpression of the potato PI-II and PCI genes in homozygous tomato lines (Abdeen et al., 2005). Similarly, when transgenic apple leaves expressing N. alata protease inhibitor (Na-PI) was fed to light-brown apple moth, it showed reduced larval and pupal body weight after several days of feeding (Maheswaran et al., 2007)., In contrary, when the transgenic tobacco expressing Na-PI gene and barley gene for β -hordothionin (β -HTH) was ingested by *H. armigera* larvae, a higher mortality rate and slower development was observed when compared with larvae fed on non-transgenic tobacco (Charity et al., 2005). The studies conducted on transgenic Medicago sativa expressing wound-inducible Oryza cystatin II (OCII) gene (a cysteine PI) revealed that about 80% of the second and third instar larvae were found to be mortal after two days of feeding (Ninkovic et al. 2007). Besides, there are many more promising candidates for improving plant defences such as ApTI (Adenanthera pavonina trypsin inhibitor, Richardson et al., 1986) and chymotrypsin inhibitors WCI2 and WCI5 from winged bean (Psophocarpus tetragonolobus, Telang et al. 2009). Some plant PIs with potential application in agriculture and molecular farming are summarised in Table 1.2. In Molecular farming, the crops are genetically modified to produce the proteins and chemicals for medicinal and commercial purposes (Ahmed, 2014).

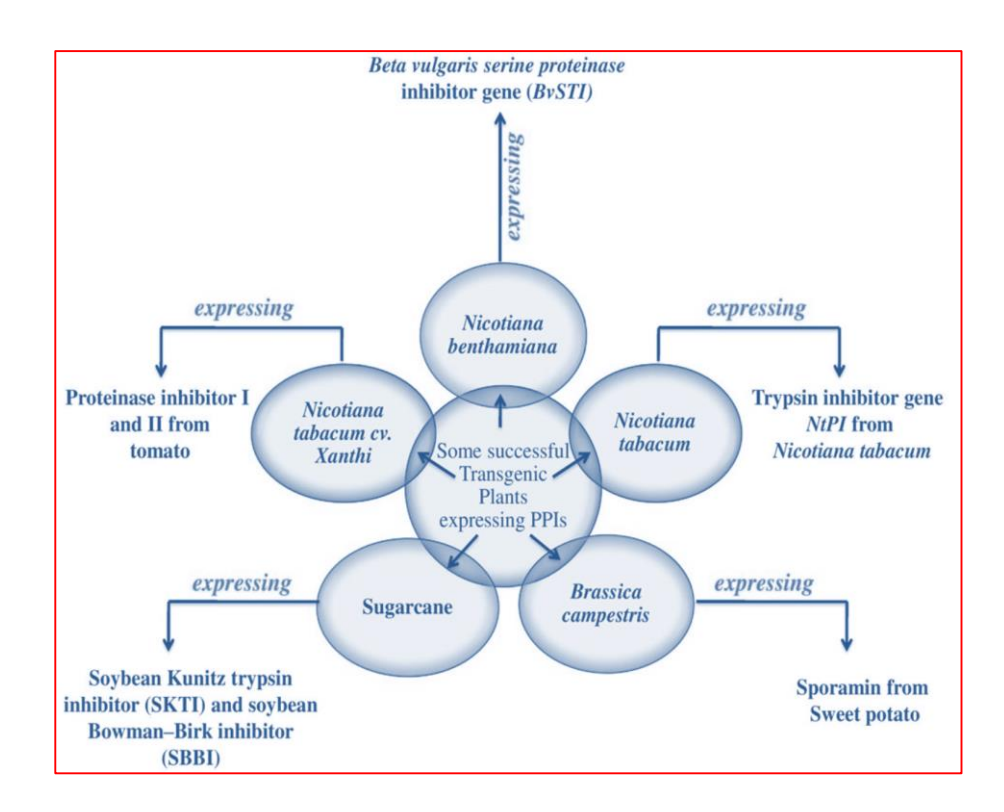


Fig.1.4. Some successful examples of transgenic plants expressing plant protease inhibitors (PPIs) (Adapted from Rai et al., 2017).

Therapeutic applications of PIs:

PIs also have many therapeutic applications which include anti-tumour (Kennedy et al., 1998; Laparra et al., 2019), anti-coagulant (Salu et al., 2019) and anti-inflammatory (Losso et al., 2008) activities.

PIs and cancer:

MMPs degrade the inflammatory tissues which cause severe inflammatory diseases and it destroys the collagen basement membrane, which leads to cancer cell metastasis (Dufour, 2013; Srikanth and Chen, 2016). Generally, extracellular metal-dependent proteases reconstitute the cell surface proteins and thereby controls the cell behaviour, its shape, activity and differentiation, and causes abnormal growth.

Table	Table.1.2. Plant PIs application in agriculture and molecular farming: (Table adapted from Clemente et al., 2019)						
S. No	SPI name	Origen	Role and Function	Biotechnology application	Ref		
1	A. thaliana Kunitz trypsin inhibitors (AtKTI4, AtKTI5)	A. thaliana	Inhibitory activity against serine and cysteine protease; effect on mite performance (fecundity and mortality)	Protection against spider mite	Arnaiz et al., 2018		
2	AtSerpin1	A. thaliana	Inhibition of digestive protease activity; inhibition of larval growth	inhibition of RD21 activity Protection against insect disease	Rustgi et al., 2017		
3	Kunitz type protease inhibitor (AtWSCP)	A. thaliana	Arabidopsis thaliana Inhibition of cysteine RD21 activity; controlling cell death	Protection against herbivore attack	Roberts at al., 2011		
4	Potato type 1 inhibitors	Solanum tuberosum	Differential expression pattern after wounding and nematode infection	Protection against nematodes	Turra et al., 2009		
5	Bowman-Birk-type inhibitor	Oryza sativa	Arrest fungal invasion, inhibition of fungal growth	Protection against fungal disease	Qu et al., 2003		
6	Phloem serpin-1(CmPS-1)	Cucurbita maxima	Inhibition of elastase activity; the increase of the aphid mortality	Protection against insect disease	Yoo et al., 2000		

7	Cowpea trypsin inhibitor gene (CPTI)	Vigna unguiculata	Inhibition of larval growth	Protection against insect disease	Ling et al., 2005
8	Potato carboxypeptidase inhibitor (PCI)	Solanum tuberosum	Antifungal activity; inhibition of larval growth	Protection against fungal and insect disease	Quilis et al., 2007
9	Maize proteinase inhibitor (MPI)	Zea mays	Inhibition of digestive Serine proteinases; inhibition of larval and fungal growth	Protection against fungal and insect disease	Azzouz et al., 2005
10	Soybean Kunitz inhibitor (SKTI)	Glycine max	Inhibition of digestive proteases present in insects and parasites	Protection against parasitic and insect disease	Azzouz et al., 2005
11	Soybean Bowman-Birk inhibitor (SbBBI)	Glycine max	Inhibition of digestive protease activity; inhibition of aphid growth	Protection against aphid parasitoids	Major et al., 2008
12	Poplar Kunitz trypsin inhibitor	Populus trichocarpa x Populus	Inhibition of midgut protease present in lepidopteran pests	Protection against insect disease	Botelho et al., 2014
13	Passion fruit Kunitz type inhibitors	Passiflora edulis	Inhibition of midgut proteases present in lepidopteran and coleopteran pests and <i>Aedes aegypti</i>	Protection against insect disease and control of vectors of neglected tropical diseases	Migliolo et al., 2010
14	Kunitz trypsin inhibitor (ApKTI)	Adenanthara pavonia	Inhibitory activity against trypsin and papain proteases; inhibition of midgut	Protection against insect disease	Laluk et al., 2011

			proteases and larval growth		
15	Unusual serine protease inhibitor (UPI)	Arabidopsis thaliana	Chymotrypsin inhibitory activity; effect on the fungal larval growth	Protection against fungal and insect disease	Smigocki et al., 2013
16	Serine proteinase inhibitor (BvSTI)	Beta vulgaris	Trypsin inhibitor activity; effect on larval weights	Protection against lepidopteran insect disease	Altpeter et al., 1999
17	Serine protease inhibitor	Barley (Hordeum vulgare)	growth and inhibition of midgut protease activity; effect on larval survival of insects	Protection against insect disease	Dunse et al., 2010
18	Potato type-I and type-II inhibitor	Nicotiana alata	Protease inhibitory activity; effect on larval growth	Protection against Helicoverpa spp.	Altpeter et al., 1999
19	PI-I and PI-II-class inhibitors	Solanum nigrum	Serine protease inhibitory activity	Protection against insect disease	Dunse et al., 2010
20	Potato Type II Proteinase Inhibitors (SaPIN2b)	Solanum americanum	Inhibition of midgut protease activity	Protection against insect disease	Cheng et al., 2015
21	Serine protease inhibitor (BWI-1a)	Fagopyrum sculentum	Inhibition of spore germination, mycelial growth, bacterial growth and survival of insects	Protection against insect, fungal and bacterial disease	Valueva et al., 1998
22	Serine protease inhibitors (PSPI-21, PSPI-22)	Solanum tuberosum	Trypsin and chymotrypsin inhibitory activity; inhibition of mycelial growth	Protection against fungal disease	Ye et al., 2001
23	Bowman-Birk-type inhibitor	Vicia faba	Trypsin and chymotrypsin inhibitory activity; inhibition of mycelial growth	Protection against fungal disease	Pekkarinen et al., 2007

24	Chymotrypsin inhibitor amylase/subtilisin	Hordeum Vulgare	Inhibition of subtilisin and trypsin proteases of <i>Fusarium culmorum</i>	Protection against fungal disease	Periani et al., 2016
25	inhibitor, BBI Kazal type inhibitor (AtKPI-1)	Arabidopsis thaliana	Inhibition of conidial germination	Protection against fungal disease	Pariani et al., 2016

However, inhibition of these proteases by the action of PIs could hamper the abnormal growth of the tumour (Rudek et al., 2002). PIs can prevent tumour invasion through the formation of complexes with plasma Kallikreins and trypsin (Goetting et al., 2010; Nobar et al., 2004). Several studies reported that the consumption of seeds which contain higher PIs reduced the incidence of the different cancers such as breast, colon and pharyngeal (Jedinak and Maliar; 2005; Aoki et al., 1995; Meyskens and Szabo, 2005; Shamsi et al., 2016). For example, BBIs from soybean prevent *in-vivo* carcinogenesis and *in-vitro* malignant transformation (Kennedy et al., 1993). Similarly, several *in-vitro* studies revealed that PIs have promoted cell growth and are involved in tissue repair. Failure in the expression of serine PIs are associated with tumour growth in ductal carcinoma of the breast, which supports the potential of PIs in cancer therapy (Maass et al., 2001).

PIs in AIDS:

The combination of PIs with anti-HIV therapy has shown to be a promising approach for treating AIDS. These PIs are targeted towards the mature proteases and arrest the processing of Gag and Gag-pol as a consequence, and it prevents the viral particle maturation (Davis et al., 2012). Therefore, numerous effective PIs are implicated in treating HIV/AIDS patients as a combination therapy with drugs (Llibre, 2009; Naggie and Hicks et al., 2010; Shamsi et al., 2016). So far, there are nine-PIs identified in clinical use. All PIs are acting as peptidomimetic agents except tipranavir which mimics like a substrate for viral protease receptor (Ridky and Leis, 1995; Schon et al., 2003; Pettit et al., 2004). Darunavir and saquinavir arrest the initial autocatalytic step, which inhibits the Gag-pol processing in HIV infected patients that leads to incomplete viral maturation at the early stages (La porte. 2009). The PIs from *Glycine max* and *Phaseolus lunatus* inhibited the HIV-1 reverse transcriptase (Wang & Ng., 2001).

Chapter 2

Rationale of the Study, Objectives and Approach

Chapter 2

Rationale of the Study, Objectives and Approach

Rationale of the study:

Destabilization of crop productivity by insect pests is a major threat to agricultural ecosystems. The yield losses due to pest damage is severely impacting the economy of agricultural farmers. There are 10,000 species of insect pests which cause economic loss to food crops (Kalavagunta et al., 2014). Among them, *H. armigera*, *S. litura*, and *A. janata* belonging to Noctuidae family and Lepidopteran order are considered as most devastating as they cause significant yield losses to their host plants. The development of efficient, cost-effective and eco-friendly approaches are necessary to improve pest resistance in host plants. Biochemical molecules such as PIs, α -amylase inhibitors, lectins, ribosome-inactivating proteins, defensins and chitinases which act an integral components of plant defence system are being exploited as insecticidal agents.

The cotton bollworm *H. armigera* and armyworm *S. litura* are cosmopolitan polyphagous pests which attack above 100 plant species, in addition to economically important crops like tomato, cotton, corn, tobacco, groundnut, chilli, bhendi, pigeon pea and chickpea (Talekar et al., 2006; Elumalai et al., 2010; Rauf et al., 2019). The annual loss caused by *H. armigera* is estimated at ~2 billion dollars (Smith-pardo, 2014). Apart, *S. litura* and *A. janata* (castor semi looper) are defoliators of castor, which is extensively grown as an industrial crop in India (Narayana and Raoof, 2005; Sujatha et al., 2011). In fact, *A. janata* alone is known to cause 30-50% yield loss in castor crop (Dunse et al., 2010).

Black gram (*Vigna mungo*) is a globally grown essential pulse crop consumed regularly in the diet. It is widely cultivated in India which contributes to one-fifth global production (~8.5 million tonnes) annually. However, the insect pests cause ~2.4 million tonnes loss in annual yield accounting for ~798 million USD globally. *H. armigera*, being a

pod borer, is an important economic pest of black gram, majorly limiting the yield and productivity (Kumar et al., 2017). The usage of synthetic pesticides as instant or eventive strategy creates not only environmental hazards but also raises health concerns among farmers and other domestic consumers (Briones 2005; Gupta and Dikxit 2010). Therefore, several integrated pest management techniques are adopted to manage various devastating insect pests (Meiners and Elden, 1978). The usage of plant-derived protease inhibitors (PIs) are accepted as a part of Integrated Pest Management (IPM). They are extensively studied by various biochemical and molecular approaches and exploited by conventional breeding and transgenic approaches to develop resistance in both host and non-host plants (Foissac et al., 2000; Shamsi et al., 2016). Hierarchical classification of *A. janata*, *S. litura*, *H. armigera* and *V. mungo* were shown in Figure 2.1.

Plant PIs, which are proteinaceous in nature act as natural agonists of digestive proteases that play a pivotal role in hydrolyzing peptides and nutrients absorption in insect pests. PIs are constitutively expressed as part of the plant defence mechanisms during development and also induced during biotic stress of herbivory or pathogen attack (Oliveira et al., 2007; Furstenberg-Hagg et al., 2013). They are usually identified in the storage organs like seeds and tubers at ~1-10% as soluble proteins (Jamal et al., 2013). PIs are more prominent in leguminous plants and are known to accumulate gradually accumulate during seed maturation as part of plant defence (Zhu et al., 2015). So far, various studies reported that PIs are particularly present in three families: Leguminosae, Solanaceae and Gramineae (Richardson, 1991). PIs are broadly classified based on the specificity of amino acids in the active site of their cognate proteases such as aspartic, cysteine, serine, and metalloproteases. Among these, serine PIs are the most prominent and well-studied family of PIs and they include majorly Bowman-Birk (BBIs) and Kunitz inhibitors (KIs). Soybean BBIs are the most extensively studied and well-characterized among all Bowman-Birk family proteins

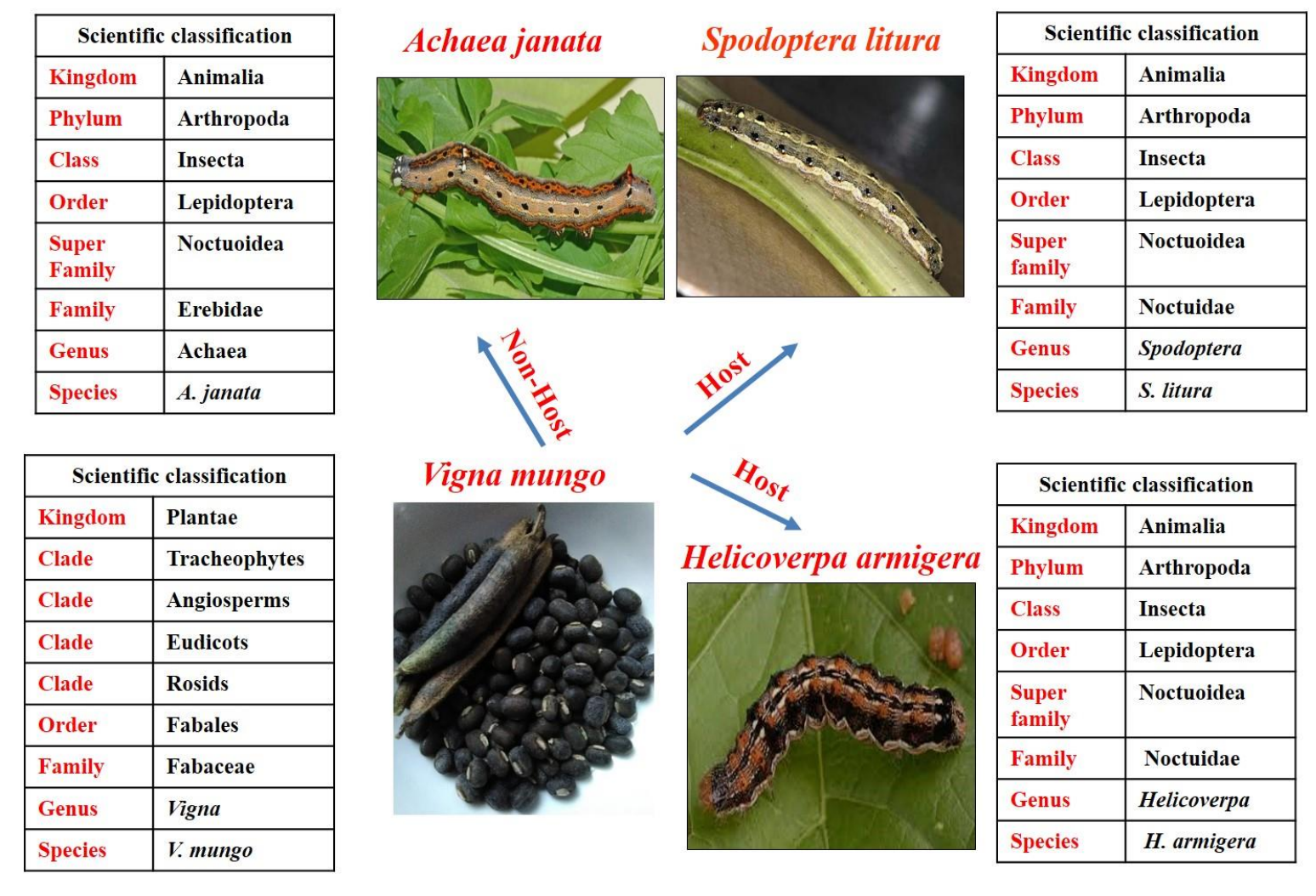


Fig. 2.1. Taxonomic classification of *A. janata*, *S. litura*, *H. armigera* and *V.mungo*. *H. armigera and S. litura* are the host pests and *A. janata* is the non-host pest for *V. mungo*. Seeds of *V. mungo* (cv. T9) are used in this study.

and several of them were cloned and sequenced (Clemente et al., 2019). The major digestive serine proteases present in the midgut of the lepidopteran larvae are the trypsin and chymotrypsin, which are responsible for insect's proteolytic activity, growth and survival (Srinivasan et al., 2006)

Several research groups widely studied the effect of PIs purified from various host, non-host, wild relatives and cultivars on activity and modulation in larval digestive enzymes, and eventually the growth as well as the survival of the pest (Chougule et al., 2003; Telang et al., 2003; Prasad et al., 2009; 2010b; Parde et al., 2010; Swathi et al., 2014, 2016; Mohanraj et al., 2018). Several studies (*in vitro* and *in vivo*) has demonstrated the efficacy of PIs in hampering the breakdown and absorption of dietary amino acids which eventually lead to retarded growth and development of larvae along with impaired fertility and fecundity of the adult moths (Babu et al., 2012). Due to their promising results as insecticidal agents, several attempts were made to develop insect-resistant plants and thereby increase crop productivity for human welfare. However, as host-pest co-evolution is a continuous process, it is essential to continue the screening, identification and test the efficacy of new PIs against insect pests. Also, exploration of new PIs from the host and non-host plants as pest-resistant traits and their incorporation into susceptible lines remained as a continuous thrust of IPM strategy (Ghodke et al., 2013).

A previous report on purified BBIs from *V. mungo* cultivar TAU-1 showed significant insecticidal potential against host pest *Spodoptera litura* and non-host pest *Achaea janata* by feeding assays until 3rd instar stage (Prasad et al., 2010b). However, the changes in the growth and development of larvae upon feeding with BBI until last instar stage is not known. If the larvae survive even upon feeding, it would be interesting to understand the molecular basis behind its survival. Further, to develop transgenics in this direction it would be appropriate to examine in detail other available domestic varieties of a black gram to

understand the redundancy in inhibitory activities of BBI and its efficacy to combat with a broad range of insect pests. In the present study, we chose a T9 variety of black gram for our studies. The insecticidal potential of BBI purified from this seed variety was tested against larvae of two host insect pests *H. armigera* and *S. litura*. We also tested the efficacy of T9BBI on *A. janata* larvae to explore its use as a biopesticide against a non-host insect pest.

Considering the importance of black gram as staple food and lacunae identified in the existing literature, the following objectives were framed in the present study:

Objectives of the thesis:

- 1) Isolation of serine PI (T9BBI) from the seeds of *V. mungo* (*cv*.T9) and its partial characterization.
- 2) A comparative study on the insecticidal potential of purified T9BBI on larval growth and development of two host insect pests *S. litura* and *H. armigera*, and a non-host insect pest *A. janata*.
- 3) Identification of protein spots which showed significant differential expression pattern in midgut tissues of larvae fed upon T9BBI.
- 4) Cloning of *T9BB11* from the seeds of *V. mungo* (*cv*.T9) and its expression in *E.coli* shuffle cells using pET-32a vector.

Approach of the study undertaken:

In the present study, BBI was purified from *V. mungo* (T9 variety) seeds and evaluated its insecticidal potential against gut proteases of *S. litura*, *H. armigera* and *A. janata*. BBI is easily quantified by using two synthetic chromogenic substrates that are found to be specific for trypsin and chymotrypsin proteases. The substrate specificity of trypsin cleaves C-terminal of arginine residues of benzoyl-DL-arginine-*p*-nitroanilide (BAPNA), while chymotrypsin cleaves C-terminal of phenylalanine of 3-Glutaryl-L-phenylalanine-4-nitroanilide (GLUPHEPA). The released *p*-nitro anilide product can be monitored spectrophotometrically at 410 nm (Erlanger et al., 1961; Mueller and Weder,

1989). The formation of colour intensity is negatively correlated with the level of trypsin inhibitory (TI) and chymotrypsin-inhibitory (CI) activities respectively.

The insecticidal properties of purified PIs from *V. mungo* seeds was assessed using both *in vitro* assays and *in vivo* feeding assays. The impact of T9BBI on growth and development of insect larvae was monitored by a comparative examination of the larval weight, retarded growth including the formation of larval-pupal as well as pupal-adult intermediates and finally determined the mortality/survival rates of the pest. Further, the differentially expressed proteins in insect midgut tissues upon feeding with T9BBI are identified by the comparative proteomic approach of two-dimensional gel electrophoresis (2-DE) followed by MALDI-TOF-TOF analysis. The functions of the selected proteins with significant change was further elucidated by matching with the similar peptides in the NCBI database.

Chapter 3 Materials and Methods

Materials and Methods

3.1. Seed material and Insects

Black gram (*Vigna mungo, cv*.T9) seeds were obtained from a local market in Hyderabad, Telangana, India. The egg mass of *S. litura* and *H. armigera* egg were obtained from NBAIR, Bangalore, India while the egg mass/larvae of *A. janata* was obtained from the castor plants grown on the landscape of the University of Hyderabad.

Chemicals

BSA (Bovine serum albumin), N-α-benzoyl-DL-arginine-*p*-nitroanilide (BAPNA), Bicinchoninic acid protein estimation kit, Bovine trypsin and Bovine chymotrypsin were procured from Thermo scientific (USA). DEAE-cellulose, Coomassie brilliant blue (R and G-250), Sephadex G-50, Cyanogen bromide activated Sepharose 4B, Soybean trypsin-chymotrypsin inhibitor (SBBI), Tricine and Gelatin were obtained from Sigma (USA). Restriction enzymes BamH1 HF and Sac1 HF are procured from New England Biolabs, cDNA synthesis kit from Thermo scientific, plasmid isolation and gel extraction kits are procured from Qiagen. Other reagents and chemicals used in this study are of analytical grade. Urea and Iodoacetamide are procured from GE Healthcare.

3. 2. Purification of PIs from V. mungo cv. T9 (Black gram)

Crude protein extraction from *V. mungo* seeds and ammonium sulfate fractionation of seed proteins was performed according to Prasad et al. (2010a). The precipitated fraction with high trypsin inhibitor (TI) activity was further purified using Ion exchange chromatography by DEAE-cellulose column, affinity chromatography by trypsin-CNBr activated Sepharose 4B column and Gel filtration chromatography by Sephadex G-50 column with the help of FPLC (Fast Protein Liquid Chromatography) Acta prime plus, GE Healthcare) as described

in Mohanraj et al. (2019). The eluted fractions from each column chromatography were assessed for TI activity and total protein content (A_{280}). The fractions with prominent TI activity after gel filtration are pooled and dialysed using dialysis bags with 3 kDa pore size. Further, amicon filters with 3 kDa cut off are used to concentrate the dialyzed protein.

3.3. Protein estimation

The protein content was estimated by the Bicinchoninic acid assay method (Kit method) using bovine serum albumin as a standard. The protein content in the crude seed extracts, eluted fractions from the different chromatography columns and larval midgut tissue extracts was estimated by UV absorbance at 280 nm.

3.4. Proteinase inhibitor (PI) activity assay

Trypsin, chymotrypsin and larval gut (*S. litura, H. armigera* and *A. janata*) trypsin-like protease inhibitory activities were estimated by addition of a required volume of crude or purified PIs, which decrease 40-60% of respective enzyme activity. Tris- HCl containing (0.05M) 0.02 M CaCl₂ was used as assay buffer for trypsin (pH 8.2) and chymotrypsin (pH 7.2) inhibitory assays while BAPNA (Erlanger et al., 1961) and GLUPHEPA (Mueller and Weder, 1989) were used as substrates in the corresponding assay mixture. Further, 0.05 M glycine-NaOH (pH 10.0) was used for the analysis of trypsin-like enzymes from larval guts of *S. litura* (SGPs) and *H. armigera* (HGPs) while 0.05M Tris-HCl containing 0.02 M CaCl₂ (pH 8.2) was used for the analysis of trypsin-like enzymes from larval guts of *A. janata* (AGPs).

The assay was initiated by addition of an appropriate amount of crude PI or Purified PI into respective assay buffer in the presence of trypsin (10 µg) or chymotrypsin (80µg) or suitable volume of gut enzymes of *S. litura / H. armigera / A. janata* and incubated for 15 min at 37°C. This is followed by the addition of respective substrates (BAPNA/GLUPHEPA)

and incubated for 45 min at 37° C. The reaction was stopped by addition of 30% acetic acid (v/v). In the absence of PI, the proteases act on substrates BAPNA (1.0 mM) and GLUPHEPA (1.0 mM) and convert them into *p*-nitroanilides (control sample). In the presence of crude or purified PI, the protease activity is blocked and the conversion of the substrates to their corresponding *p*-nitroanilides is decreased. Thus, the inhibitory activity of protease inhibitors was determined by monitoring the decrease in OD of the assay mixture at A₄₁₀. One inhibitory unit (TI/CI/SGPI/AGPI/HGPI) is defined as the minimum quantity of PI utilized to reduce the initial OD of the assay mixture by 50% under optimal conditions (Swathi et al., 2014, Mohanraj et al., 2019).

3.5. Rearing of insects and extraction of midgut proteases

The egg masses of *S. litura / H. armigera / A. janata* were incubated in insect culture room at 25±1°C temperature and 60±5% relative humidity for 14:10 hr light-dark photoperiod. The hatched larvae of *H. armigera* and *S. litura* were reared on the artificial diet supplemented with or without T9BBI while the larvae of *A. janata* are reared on fresh castor leaves coated with or without T9BBI. In the control diet, an equal aliquot of buffer was used in place of the T9BBI.

The midguts were isolated from the larvae which are in last but one late-instar stage by narcotizing on ice (20-25 min) followed by dissecting them in the presence of Ringer solution (0.13 M NaCl, 1mM PMSF, 0.1 mM CaCl₂ and 0.5M KCl (Girard et al., 1998). The dissected midguts were homogenised in presence of respective pH buffers and centrifuged at 12,000 rpm for 10 min at 4°C to remove the debris. The clear supernatants obtained from midgut tissues of larvae fed upon T9BBI diet and control diet were collected and stored at -20°C for further use to analyze the trypsin-like digestive proteases and for 2-D gel electrophoresis (Arunprasanna et al., 2017, Yang et al., 2017).

3.6. Efficacy of T9BBI on growth and development of insects

Feeding experiments were performed using newly hatched larvae reared on an artificial diet containing different concentrations of T9BBI (0.01%, 0.025%, 0.05%, and 0.1%) for *S. litura / H. armigera* and fresh castor leaf coated with various concentrations (0.5, 1, 2, 4 and 8 μg/ cm² leaf area) of T9BBI was used for *A. janata*. Control insects were reared on same diet/castor leaves incorporated with 50 mM Tris-HCl, pH 8.0, which was devoid of PIs.

The artificial diet was prepared by addition of nutrient agar (6.5g) to ddw (260 ml). The mixture was boiled and cooled down to 40°C temperature. This was followed by the addition of yeast extract (10g), Bengal gram powder (55gms), Vitamin E (400mg) and Multivitamin (400mg), Ascorbic acid (1.3g), Methyl parahydroxybenzoate (1g), Casein (5g), Cholesterol (55mg), Streptomycin sulphate (100mg) and Sorbic acid (250 mg) to 100 ml of water and mixed with molten agar using the blender. The prepared diet was poured into sterile glass plates and mixed with specific concentrations of T9BBI and allowed to solidify.

The antifeedant effect of T9BBI on growth and development of different larvae was monitored periodically by recording larval weights, capturing photographs and observing morphological changes such as intermediates formation (larval- pupal and pupal-adult) between control and treated larvae.

3.7. SDS-PAGE profiling of T9BBI

The molecular weight of T9BBI was monitored electrophoretically by Tricine SDS-PAGE (4% stacking and 15% separating gel at 100 V) according to the method of Schagger and von Jagow (1987) under non-reducing conditions. The molecular weight standard (PMWL, Puregene, Genetix) ranging from 4.6-180 kDa was used to compare the molecular weight of the purified protein. The commercial soybean trypsin chymotrypsin inhibitor (8.0 kDa) was

used as a reference standard to analyse the Electrophoretic pattern of BBI. Gels were stained with silver nitrate or Coomassie brilliant blue (CBB) G-250.

3.8. Activity staining of T9BBI

Gelatin–polyacrylamide gel electrophoresis (PAGE) activity staining method was used to visualize the trypsin inhibitory (TI) or chymotrypsin inhibitory bands under both reducing and non-reducing conditions (Felicioli et al., 1997). This was performed by adding 0.1% (w/v) gelatin to the final concentration of resolving gel during the time of casting. After the completion of electrophoresis, the gels were incubated at 4°C for 5 min in either 0.1M Tris-HCl (pH 8.2) containing trypsin (0.1 mg/ml) or chymotrypsin (0.2 mg/ml) followed by incubation at 37°C for 5 min. After the incubation period, these gels were rinsed with double distilled water and stained with Coomassie brilliant blue (CBB R-250, 0.1%) followed by destaining with the MilliQ. The inhibitory bands are appeared in dark blue colour in a clear background. This is due to the formation of the undigested gelatin with the stain. Soybean BBI (SBBI, Commercially available) is used as a marker in gelatin-PAGE.

3.9. Two-dimensional gel electrophoresis (2-DE) of Midgut tissue protein

The supernatant obtained from midgut tissues (please refer to section 3.5) was subjected to 10% TCA precipitation. The pellet was washed twice with chilled acetone, air dried and resuspended in 100µl rehydration buffer [7M Urea, 2M Thiourea, 4% CHAPS (w/v), pH 4-7 IPG buffer (0.2% v/v), 30 mM DTT, 0.002% bromophenol blue]. The isoelectric focusing (IEF) of protein extract prepared from midgut tissues of larvae (*A. janata, S. litura and H. armigera*) fed on the control diet and T9BBI supplemented diet was performed using 11 cm, non-linear (pH 4-7) IPG strips (GE Healthcare). Protein from each sample (400 µg) was mixed with 100 µl of rehydration buffer and subjected to passive rehydration for 12 h at 20°C. This is followed by isoelectric focusing (Ettan IPG phor 3 isoelectric focusing system,

GE Healthcare) for segregation of proteins according to their isoelectric points. Following the first dimension, the strips were sequentially equilibrated using 75mM Tris-HCl (pH 8.5) containing 2% SDS (w/v), 6M Urea, 30% glycerol (v/v). In the initial steps (15 min), the strips were equilibrated with the above buffer containing DTT (2%, w/v). Later, the strips were equilibrated (15 min) with buffer containing iodoacetamide (2.5% w/v). The equilibrated strips are positioned horizontally and second dimension electrophoresis was performed using 15% Tricine SDS-PAGE under non-reducing conditions at 20°C and 100V using EttanDalt6 vertical electrophoresis system. This is followed by incubation of gels in fixative reagent (Water, Methanol and acetic acid in 5:4:1 ratio) for one hour, staining in 0.1% Coomassie Brilliant Blue G-250 for 3 hours and destaining with Milli-Q water.

3.10. Image and data analysis

Magic image scanner was used to scan the 2-DE gel spots after staining the gels with the CBB-G250. These scanned gels were analyzed by using the 2-D image master platinum software (version 7.0) to identify the differences in protein spots between the two gels of comparison. Spots were discerned automatically after aligning the control and treated gel images. The differential comparison was performed by cropping each spot according to match set classes and further arranged by giving the spot numbers. Protein normalization was considered by taking into account the following parameters: For example, for any given spot, the percent size is determined by taking into account the average size of all spots on the gel. The differential abundance with respect to relative spot volume between control and treated were determined by comparing the gels of control to that of treated. If the change in expression levels of protein spots between controls versus treated is ≥ 1.5 fold it is considered as "up-regulation". In contrast, if the change in expression levels is ≤ 0.6 , it is considered as "down-regulation". However, we considered to choose spots with expression levels of \geq or \leq 1.5 in our studies.

3.11. Protein identification

Protein identification was done by using the protocol of Rani and Podile (2014). The differentially expressed spots were selected and excised manually and destained with 0.05 M NH₄HCO₃ in 50% acetonitrile and subjected to trypsin digestion. MALDI-TOF-TOF analysis was done for these digested peptides by using the instrument Bruker Auto flex III smart beam (Germany) which will generate the ions for the query peptide. The peptides contaminated with keratin and trypsin were omitted by using the mass tolerance of \pm 0.5 Dalton (Da).

The ions generated were identified by using the mascot search engine and Biotools 3.1 software. The different parameters used for identification of proteins are (1) Taxonomic is set to lepidopteran insects; 2) Identification of protein, is set to NCBI and swissprot; (3) Modifications are set to Carbamidomethyl, (4) Enzymes used is set to trypsin and MS/MS tolerance is set to 100 ppm and 0.4 Da. After setting all these parameters, the protein was confirmed only after the threshold values are significant ($P \le 0.05$) and that peptides have matches greater than two.

3.12. Arginine kinase (AK) assay

The assay of AK is performed spectrophotometrically by coupled enzymatic assasy (Blethen, 1970) as shown below:

Pyruvate +
$$\beta$$
-NADH \longrightarrow Lactate + β -NAD

ADP + PEP — Pyruvate + ATP

The activity of AK is determined by monitoring the rate of oxidation of NADH at 340 nm as shown above at 30°C for 5 min. The reaction mixture contained: glycine (178 mM), 2-mercaptoethanol (0.33 mM), potassium chloride (133 mM), magnesium sulphate (13 mM), PEP (20 mM), ATP (6.7 mM), NADH (0.13 mM), 2 U of Pyruvate kinase (PK), 3U Lactate

dehydrogenase (LDH), L-arginine (17 mM) at pH 8.6. The reaction was initiated by the addition of 100 μg of midgut tissue protein extract (as described in section 3.8) which possessed arginine kinase. The reference cuvette contained all components of the assay medium except AK enzyme, i.e., midgut tissue protein extract. One unit of AK is referred to as "The minimum concentration of enzyme that produces 1.0 μmol of N-phospho-L-arginine min⁻¹ by using substrates ATP and L-arginine at pH 8.6 and 30°C".

3.13. Cloning of T9BBI gene

RNA was isolated from dry, mature seeds (200 mg) of *V. mungo* by Lithium chloride (Li-Cl) method (Matilla et al., 1980) and quantified using Nanodrop. This was reverse transcribed to cDNA at 42°C for 30 min and 94°C for 2 min using dNTPs, RT (reverse transcriptase) enzyme, RT buffer and oligo dT primers as per manufacturer's instructions (verso cDNA synthesis kit). The synthesized cDNA was amplified for T9BBI gene using forward 5'ATG ATG GTG CTA AAG GTG TGT G 3' and reverse 5' CCA ACT TTT ATT CTG TCT TCC C 3' primers designed from complete CDS of *V. radiata* proteinase inhibitor gene (NCBI Acc. No. AY713305.2). A gradient from 48°C to 62°C was used to optimize the annealing temperature. The best annealing temperature for amplification of T9BBI gene was obtained at 54°C. Thus, the amplification conditions were maintained as 30 sec at 94°C for denaturation, 15 sec at 54°C for annealing and 72°C for 15 sec for extension with a final hold for an extra 10 min at 72°C. A 1% agarose gel was used for analysis of the amplified product. The amplified product was sliced and DNA was eluted using Gel elution kit (Qiagen gel extraction kit).

The gel elution product was further cloned into a TA cloning vector, pTZ57R/T (Fermentas). The differences in nucleotide and amino acid sequences of the commercially sequenced clones with that of the non-redundant sequences available in the NCBI (National Centre for Biotechnology) data base was made with the help of BLAST (Basic Local

Alignment Search Tool) search. The amino acid sequence of the recombinant T9BBI was analysed using Expasy translation software.

3.14. Expression and purification of T9BBI

Primers were designed for the cloned sequence with the incorporation of restriction sites of BamH1 HF and Sac1 HF (Forward primer sequence: 5' TCG GAT CCG ATG ATG GTG CTA AAG GTG 3' and Reverse primer sequence 5'CCT GAG CTC TTA GAC ATC ATC TTC ATC CAT3'). Red colour indicates the restriction enzyme sites. The sequence was amplified and ligated into the pET32a expression vector. PET32a-T9BBI plasmid construct was further transformed into E.coli shuffle competent cells on an ampicillin agar plate. To confirm the presence of insert in the expression vector, BamH1 HF and Sac1 HF are subjected to restriction digestion. An overnight primary culture (Luria broth and 0.01% Ampicillin) of E. coli shuffle cells containing the recombinant gene was used for a secondary culture in presence of 0.1mg/ml ampicillin. The protein induction was done by using 0.4 mM Isopropyl β-D-1-thiogalactopyranoside (IPTG) which was visualized on 12.5% SDS-PAGE. The protein was purified by passing the supernatant collected from lysed cells on Ni-NTA agarose column equilibrated with 10 ml of equilibration buffer [50mM Tris-HCl containing 300 mM NaCl and 10 mM imidazole at pH 8.0]. The column was washed with wash buffer (50 mM Tris-HCl containing 30 mM NaCl and 20 mM imidazole at pH 8.0) and protein elution was performed with 5 ml of elution buffer (50mM Tris-HCl containing 300 mM NaCl and 250 mM imidazole at pH 8.0). The purified protein was confirmed by western blot analysis.

3.15. Statistical analysis

Statistical analysis was done by using the Sigma plot version 12.0, Systat software. The data shown was mean \pm SE of three biological replicates.

Purification and Partial Characterization of Proteinase Inhibitor from the Seeds of *Vigna mungo* (*cv*.T9)

Purification and Partial Characterization of Proteinase Inhibitors from the Seeds of *Vigna mungo*

In general, proteolysis is an important functional process in the living organisms such as animals, microorganisms and plants (Lopez-Otin and Bond, 2009). The proteolytic activity of different proteases such as Aspartate, Cysteine, Metallo and Serine type was regulated by their respective PIs. In plants, PIs are expressed constitutively in the storage organs and induced in response to insect pest invasion or microbial pathogen attack and wounding (Ryan, 1990). In the agricultural field, many researchers used the PIs to manage the commercially significant insect pests (Shamsi et al., 2016). However, serine PIs (BBIs and KIs) are known to play a key role in integrated pest management (IPM) (Srinivasan et al., 2006).

In the present study, a PI is purified from the black gram (*Vigna mungo*), an important pulse crop and partially characterized for its purity, mass, presence of isoforms, self-association pattern and inhibitory activity against proteases such as bovine trypsin and chymotrypsin.

Results and Discussion:

4.1. Purification of PI:

The protein level in crude extract of *V. mungo* was found to be 3.56g per 50 g seed and specific activity was found to be 8.5 TIU/mg protein. This crude protein extract was further subjected to ammonium sulphate precipitation. The 20-80% fraction showed a specific activity of 22 TIU/mg protein. A total protein of 1222 mg was recovered with 2.56 fold purity. Salting-out with 70% ammonium sulphate has increased the specific activity and purity of TPBI in tepary bean seeds (Al-Maiman et al., 2019). Corroborating with these studies, specific activity of the PI was increased by more than 2-fold. This salting out

procedure not only remove the coloured materials but also concentrate the protein to a workable volume (Ahmed et al., 2009). The precipitated protein was dissolved in 50mM Tris-HCl (pH 8.0) and dialysed against 2M Tris-HCl (pH 8.0) using 3.0 kDa cut off membrane. The sample was subjected to further purification process by using ion-exchange chromatography on a DEAE-cellulose matrix and the bound proteins were eluted with a linear gradient of 0.1 to 1.0 M NaCl in 50 mM Tris-HCl, pH 8.0 (Fig.4.1A). The total protein was eluted into two major peaks and the TI active fractions were recovered in the peak II with a specific activity of 30.5 TIU/mg protein and yield recovery of 696 mg protein with 3.59 fold purity. The active fractions from peak II were further passed through affinity chromatography column using Trypsin-Sepharose-4B matrix and the bound proteins were eluted with 0.01 N HCl at a flow rate of 60ml/hr (Fig.4.1B). After affinity chromatography, the yield of the total protein was reduced to 35 mg, however, with a specific activity of 314 TIU/mg protein and 36.94 fold purity. To remove minor contaminants, TI active fractions from affinity column were pooled and dialyzed, and further purified by passing through a gelfiltration chromatography column using Sephadex G-50 matrix and eluted with 50 mM Tris-HCl, pH 8.0 at 60ml/hr flow rate (Fig.4. 1C). A total protein of 10.2 mg was recovered from the gel filtration column with a specific activity of 980TIU/mg protein and 115.29-fold purity (Table.4.1). Our results correlated with the studies of mung bean seeds which showed an increase in the inhibitory activity when Sephadex G-50 was used as the matrix in the gel filtration column during final purification step (Klomklao et al., 2011).

4.2. Electrophoresis and matrix-assisted laser desorption ionization time-of-flight (MALDI-TOF) analysis of Purified PI:

The purified PI showed four bands with an approximate molecular mass of 8kDa (monomer), 16kDa (dimer), 24 kDa (trimer) and 32 kDa (tetramer) on Tricine-SDS-PAGE under non-

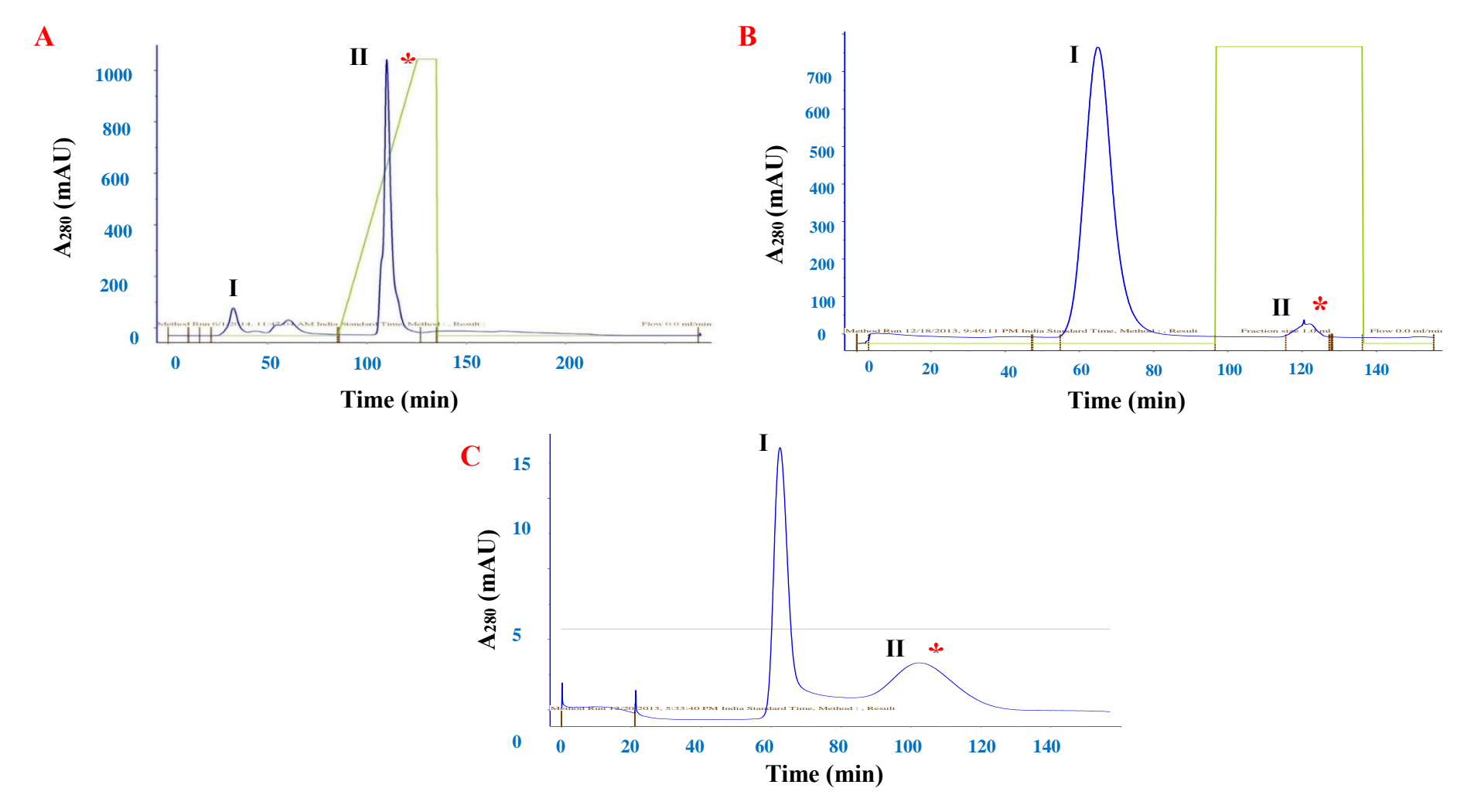


Figure. 4.1. FPLC purification of PIs from *V. mungo* seeds: Elution profiles of (A) Ion-exchange column loaded with 20-80% (NH₄)₂SO₄ fraction (B) trypsin affinity column loaded with active fraction pool from the ion-exchange column and (C) gel filtration column loaded with active fraction pool from affinity column. The protein peaks active against trypsin were marked with an asterisk (*).

Table 4.1: Purification of PIs from V. mungo (cv. T9) seeds (50 g)

Purification step	Total protein (mg)	Total activity (TI units) ^a	Yield recovery (%)	Specific activity ^b (TI units/mg protein)	Purification (fold)
Crude extract	3556	30,400	100	8.5	1
(NH ₄) ₂ S0 ₄ fraction (20-80%)	1222	26,666	88	22	2.56
DEAE-Cellulose column	696	21,246	70	30.5	3.59
Trypsin- Sepharose-4B column	35	11,000	36	314	36.94
Sephadex-G-50 column	10.2	10,000	33	980	115.29

^a One TI unit is defined as the amount of T9BBI required to inhibit 50% of BAPNA hydrolysis by trypsin.

^b Specific activity is defined as the number of TI units/mg protein.

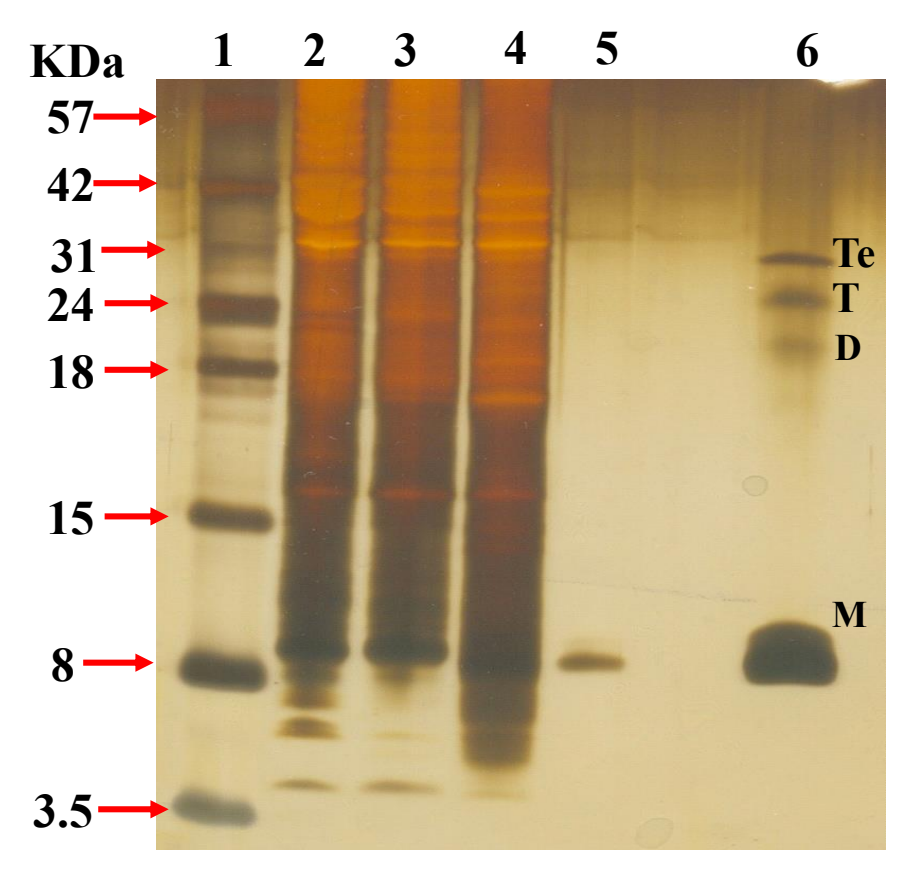


Fig.4.2. Purification profile of T9BBI on Tricine-SDS-PAGE (15%). Lane 1: Protein molecular weight (PMW) marker from Bangalore genei, Lane 2: Crude protein (25 μ g), Lane 3: Ammonium sulphate fractionation (25 μ g), Lane 4: Ion exchange column (25 μ g), Lane 5: Affinity column (10 μ g) and Lane 6: gel-filtration column (25 μ g). M- monomer, D-Dimer, T- trimer, Te-Tetramer.

reducing condition (**Fig. 4.2**). A molecular weight range of 0.8-13 kDa, reported for various Bowman-birk inhibitors (BBIs) isolated from different plants such as *Phaseolus* species (Campos et al., 2004; Pereira et al., 2007), *V. mungo*-TAU1 variety (Prasad et al., 2010), Glycine *soja* (Deshimaru et al., 2002), *Dolichos biflorus* (Kuhar et al., 2013), and *Clitoria fairchildiana* (Dantzer et al., 2015) supported that the PI purified in the present study might belong to BBI.

Further, MALDI-TOF was used to determine both accurate molecular weight and purity of PIs. Intact mass analysis of the purified PI showed the presence of a high-intensity peak at 8209.0 Da and a less intensified peak at 16574.6 Da which represent the monomeric and dimeric forms of PI (Fig. 4.3A). The PIs isolated from kidney bean (Kumar et al., 2004), *Camaratus* bean (Paiva et al., 2006), *V. mungo-TAU1* (Prasad et al., 2010), *Dolichos biflorus* (Kuhar et al., 2013) and *Clitoria fairchildiana* (Dantzer et al., 2015) showed a self-association tendency in the solution and this could be the possible reason for the observed multimers of 8-kDa protein such as dimer, trimer or tetramer in SDS-PAGE and/or MALDI-TOF mass spectrum (Figs. 4.2 and 4.3A). Also, the PI existed as several isoinhibitors (Fig. 4.3B). Taken together, these results suggest that the purified protein existed as an oligomer of different isoinhibitors under native conditions which is essential for its molecular packing as a seed storage protein (Barbosa et al., 2007; Prasad et al., 2010b; Swathi et al., 2014).

4.3. Activity staining:

Gelatin activity staining of purified PI showed inhibitory bands against both trypsin and chymotrypsin on Native and SDS-PAGE, a common feature of BBI. It has shown 8 isoinhibitory bands in native-PAGE against trypsin and chymotrypsin and 2 bands in SDS-PAGE against trypsin (Figs. 4.4A-C). BBIs are products of multigene families that justify the existence of multiple isoforms (Domoney et al., 1995). During the period of plant-insect evolution, the isoinhibitors were produced in the plants to overcome the new proteases

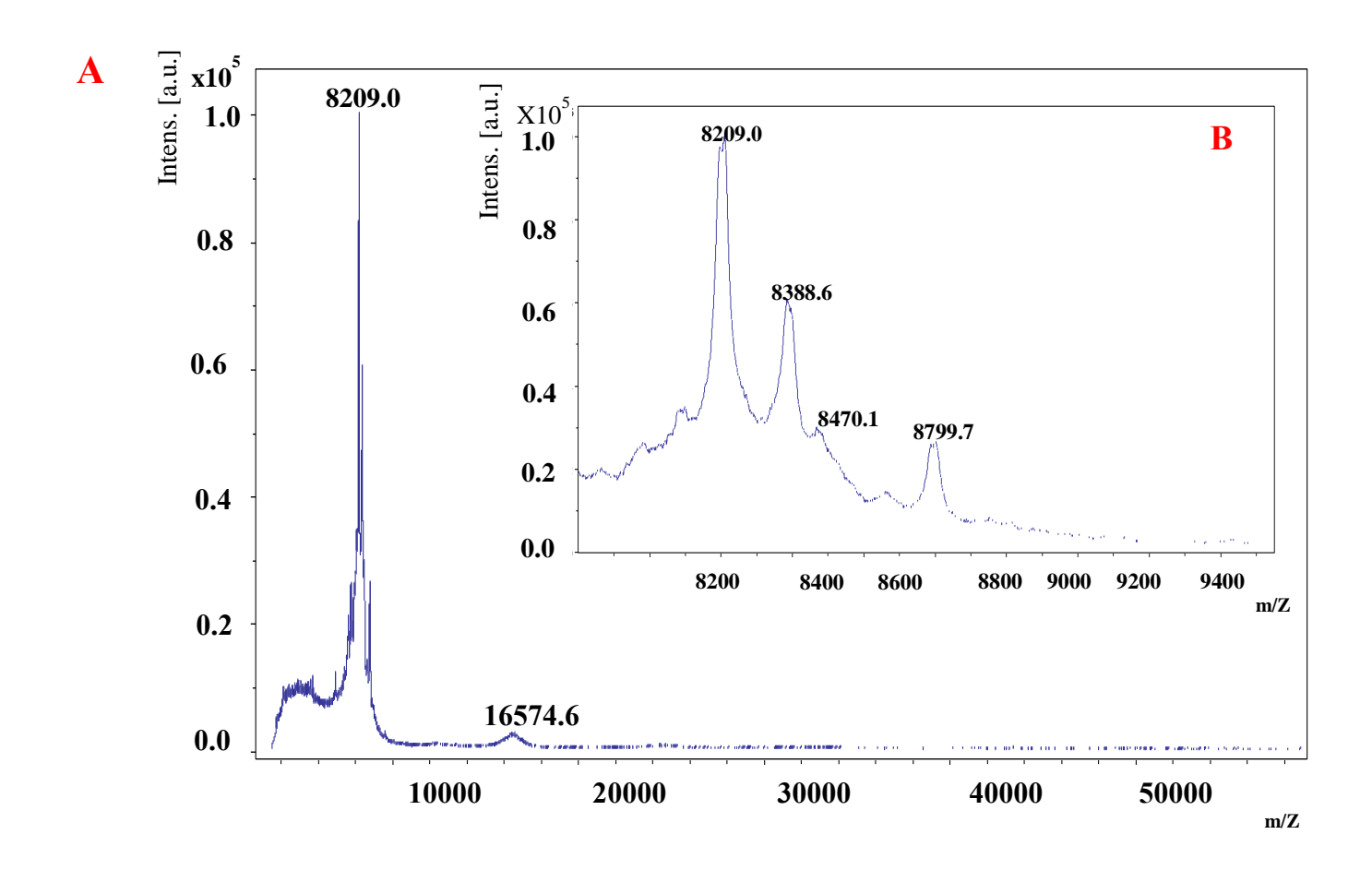


Fig.4.3. **MALDI-TOF mass spectrum of T9BBI**. **(A)** Between m/z 2,000-50,000 under non-reducing conditions, representing monomer (m/z 8209.0) and dimer (m/z 16,574.6). **(B)** The monomer was zoomed between m/z 8000-9500 for representing the isoforms.

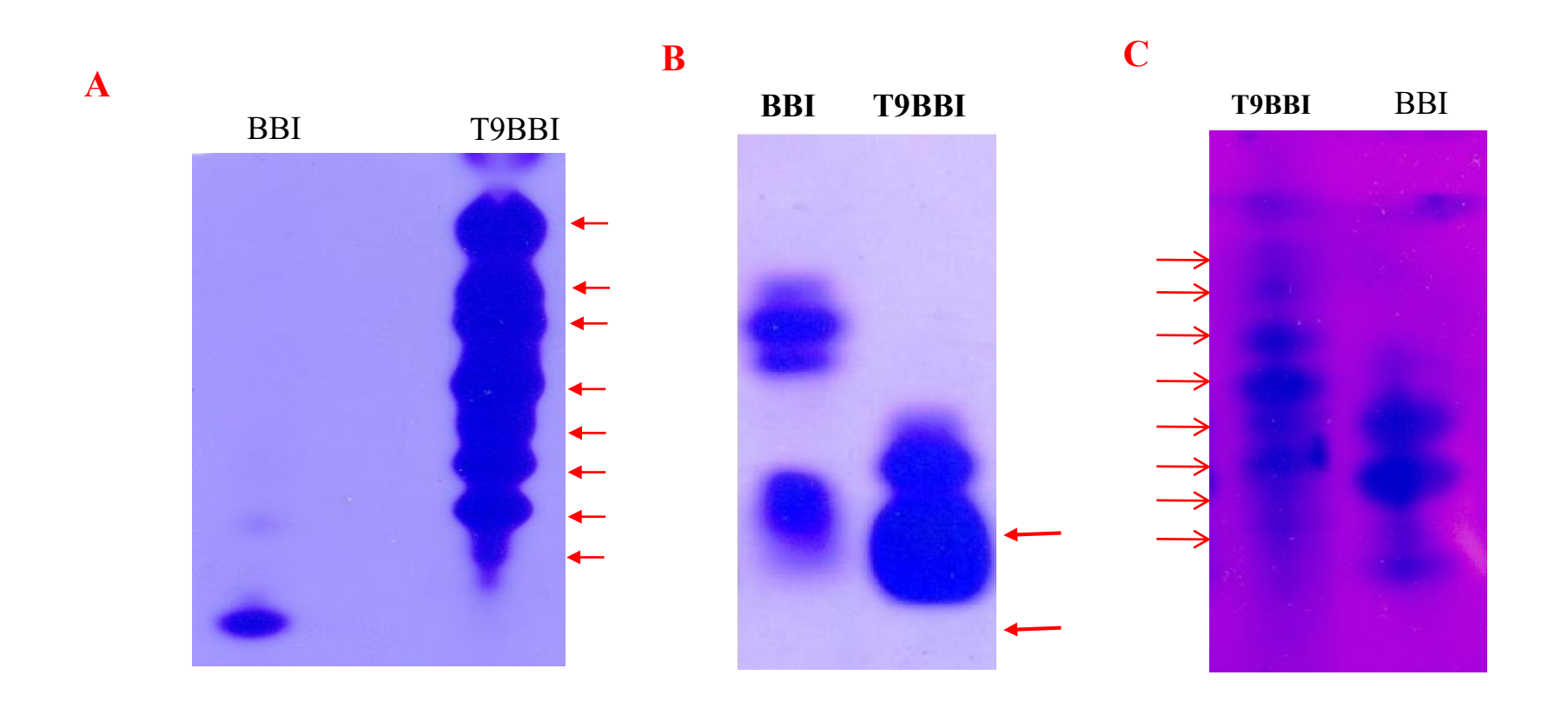


Fig.4.4. Gelatin activity staining (12.5%) of T9BBI. **(A)** Trypsin inhibitory bands on native-PAGE; **(B)** Trypsin inhibitory bands on SDS-PAGE and **(C)** Chymotrypsin (0.1 mg/ml) inhibitory bands on native PAGE

synthesized in the midguts of insects on exposure to PI (Lopes et al., 2004). Legume BBIs contain two individual binding loops which forms the inhibitory domains. Due to the presence of these two binding loops it looks like a double-headed structure. Specificity of the inhibitory domains was determined by the amino acids which are present in the P1 posotion (De Paola et al., 2012; Laskoswski and Kato, 1980). The amino acid of P1 position (Lys/Arg) in the first inhibitory domain has specificity towards trypsin. The presence of amino acids Arg, Lys or Ser in the P1 position of the second inhibitory domain shows the specificity towards chymotrypsin. Similarly, the presence of Ala at P1 position shows the specificity for elastage (Laskowski and Kato, 1980. Prakash et al., 1996).

The mode of action of PI is similar to that of enzyme-substrate interaction and the specificity is determined by whether the P1 position amino acid can fit into the S1 pocket of proteases. Mechanism of interaction not only depend on the amino acid effect alone, but also is associated with their steric conformation. This gives the explanation for "why not all the Arg and Lys residue-containing sequences have the ability to inhibit trypsin and Phe containing peptides to inhibit chymotrypsin" (Wu et al., 2017). Also, the secondary structure and the conserved disulfide-bridges are crucial for their bioactivity.

Previous reports indicated that BBI family of PIs present in the seeds of *Cajanus cajan* (Prasad et al., 2009), *C. fairchildiana* (Dantzger et al., 2015), *V. radiata* (Wilson and Chen, 1983) have shown inhibitory activities against both trypsin and chymotrypsin. Thus based on the inhibitory activity against both trypsin and chymotrypsin, and molecular weight, the PI purified in this study is suggested to the BBI family (**Figs. 4.2, 4.3 and 4.4**; Kuhar et al., 2013).

Thus, the PI isolated from the *V. mungo* T9 variety is named as 'T9BBI' and used in further studies.

High Lights of the Study:

- ➤ PI from seeds of *V. mungo* (*cv.* T9) was purified by using Akta prime plus FPLC purification system and it showed the molecular mass of 8.2 kDa in Mass spectrometry (MALDI-TOF) studies.
- ➤ Yield recovery of PI was 33% and purification fold was 115%.
- ➤ Purified protein showed both Trypsin inhibitory bands and Chymotrypsin inhibitory bands on Gelatin PAGE in activity staining studies.
- The low molecular mass, existence of self-association pattern, presence of several isoforms and presence of activity against trypsin and chymotrypsin is a characteristic feature of Bowman-Birk Inhibitor (BBI). Hence it is named as "T9BBI".

Insecticidal Potential of T9BBI on larval growth and development of a non-host insect pest *Achaea janata*: Modulation in expression of midgut tissue proteins

Insecticidal Potential of T9BBI on larval growth and development of a non-host insect pest *Achaea janata*: Modulation in expression of midgut tissue proteins

A. janata (Lepidoptera, Noctuidae), the castor semi looper is the main defoliator of castor crop (Sujatha et al., 2011). Severe loss in castor crop occurs during July-October in the Indian subcontinent during which A. janata larvae completely defoliates its plantation. It is estimated that A. janata alone reduces the castor yields around 30-50% (Dunse et al., 2010). Farmers use a broad range of chemical pesticides like quinalphos, endosulfan, chlorpyrophis and monocrotophos to manage A. janata, in spite of their harmful nature to both environment and human health (Gahukar, 2015). To overcome the harmful effects of regularly used chemical pesticides, agricultural scientists focused their research on making use of proteinase inhibitors (PIs), the defensive proteins of a plant system in the management of A. janata.

The serine PIs from several cultivars and wild relatives of pigeon pea (Prasad et al., 2009, Swathi et al., 2014, Mohanraj et al., 2018 and 2019) and *Solanum melanogena* (Devanand and Rani, 2011) showed significant inhibitory activity against AGPs. The studies of Prasad et al. (2010a, b) from our laboratory identified that PIs from *V. mungo* (TAU1 variety) were very effective in inhibiting the activity of *A. janata* trypsin-like midgut proteases (AGPs) and retarding the growth of larvae. However, these studies were limited by feeding the larvae with PI during the early instars, i.e., up to third instar stage. These preliminary studies raised the following key questions such as: 1) Does all the domestic varieties of *V. mungo* possesses PIs which are active against AGPs; 2) If yes, what is their effect on larval and pupal growth when fed throughout their larval stage. Also, in general, the larvae are very well known for their dynamism to adapt to any new feeding habits. In this context, it would be interesting to monitor the changes that occur in the midgut tissue proteome of *A. janata* larvae upon feeding with T9BBI. This study also would pave the path to understand the biochemical/molecular strategies adapted by *A. janata* larvae to compensate for the loss in function of trypsin-like proteases in its midgut tissue.

Results and Discussion:

5.1. *In-vitro* inhibitory effect of T9BBI on *A. janata* trypsin-like midgut proteases (AGPs):

In the present study, our results revealed that the purified T9BBI showed significant inhibitory potential against *A. janata* gut proteases with 6250±25 AGPI units/mg protein when compared with its crude protein extract which showed 400±25 AGPI units/mg protein (**Fig. 5.1**). Further inhibitory potential of T9BBI was also assessed against commercially available bovine trypsin as a positive control. The T9BBI showed 6.35 fold higher inhibitory potential towards AGPs as compared to bovine trypsin (983±25 TI units/ mg protein) which indicate that it is a potential inhibitor of AGPs.

5.2. Effect of *in-vivo* feeding of T9BBI on *A. janata* larval growth and development:

A. janata were allowed to feed on castor leaves coated with buffer (50mM Tris-HCl, pH 8.0) alone (controls) or buffer with T9BBI at different concentrations (0.5, 1, 2, 4 and 8 μg/cm² leaf area). Though, the feeding of the larvae with T9BBI was started at the 1st instar stage, major changes in growth and development was observed only at the 3rd instar stage. Hence, the changes in larval weights were monitored from 3rd instar stage. The average weight of the 3rd instar larvae fed on control diet was 352±49 mg. In contrast, the larvae fed on T9BBI coated castor leaves showed significant retardation in their larval growth by 12.5±0.6% (0.5 μg/cm²), 37±2.29% (1 μg/cm²), 50±3.9% (2 μg/cm²), 65±5.9% (4 μg/cm²) and 72±4.11% (8 μg/cm²), respectively, as compared to control diet-fed larvae (Fig. 5.2A and B). The average weight of the 4th instar stage control larvae was 619±78 mg. After feeding with T9BBI, the larval weight was found to be retarded by 31±3.8%, 42±2.9%, 52±4.4%, 70±6.7% and 77±8.7% (Fig.5.3A and B), respectively, as compared to control diet-fed larvae.

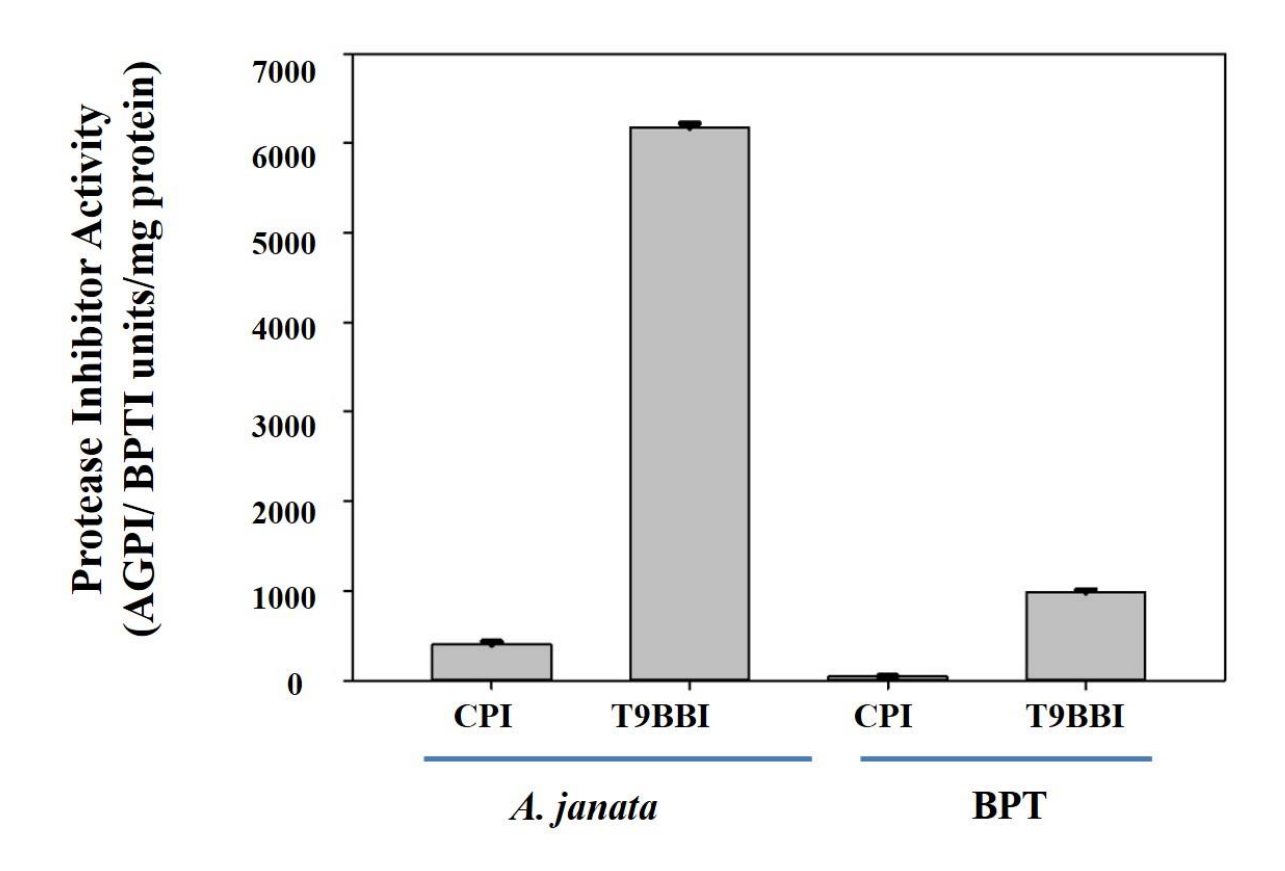


Fig. 5.1. A comparative inhibitory potential of crude proteinase inhibitor (CPI) extract and purified T9BBI from seeds of *V. mungo* (T9 variety) towards *A. janata* midgut trypsin-like proteases (AGPs) collected from 5th instar larvae and bovine pancreatic trypsin (BPT), which is used as a control. The specific activity of CPI and T9BBI was determined as the number of *A. janata* midgut trypsin-like proteinase inhibitor (AGPI) units mg⁻¹ protein and Bovine pancreatic trypsin inhibitor (BPTI) units mg⁻¹ protein, respectively. Further details were described in materials and methods.

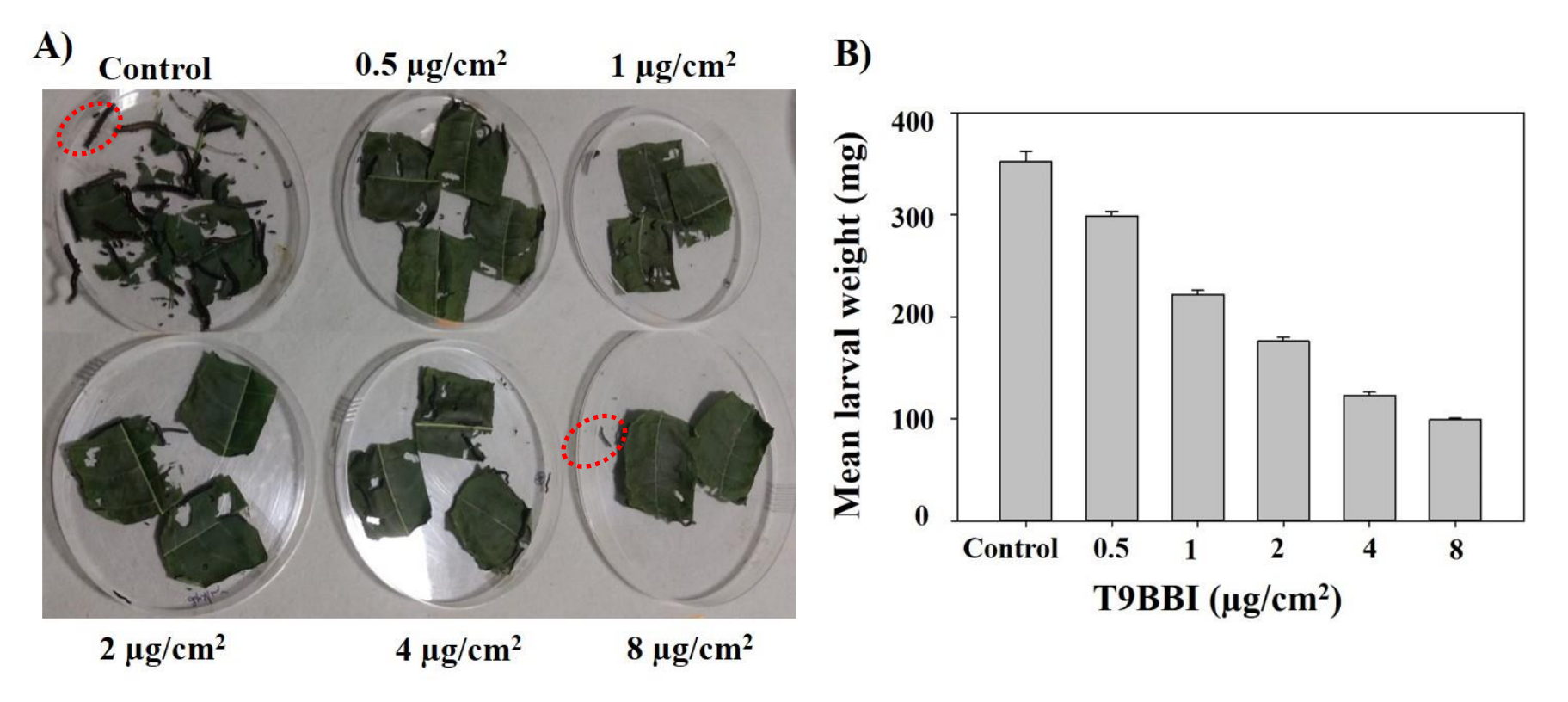


Fig. 5.2. Effect of T9BBI on the growth of 3rd instar larvae of *A. janata*. (A) Pictorial depiction of larvae reared on castor leaf coated with buffer alone (control) and different concentrations of T9BBI (treated), and (B) Mean body weight of the corresponding larvae. A single larva from control and T9BBI treated (8μg/cm²) groups are encircled with dashed line (red) to depict the differences in the growth. Further details were described in materials and methods.

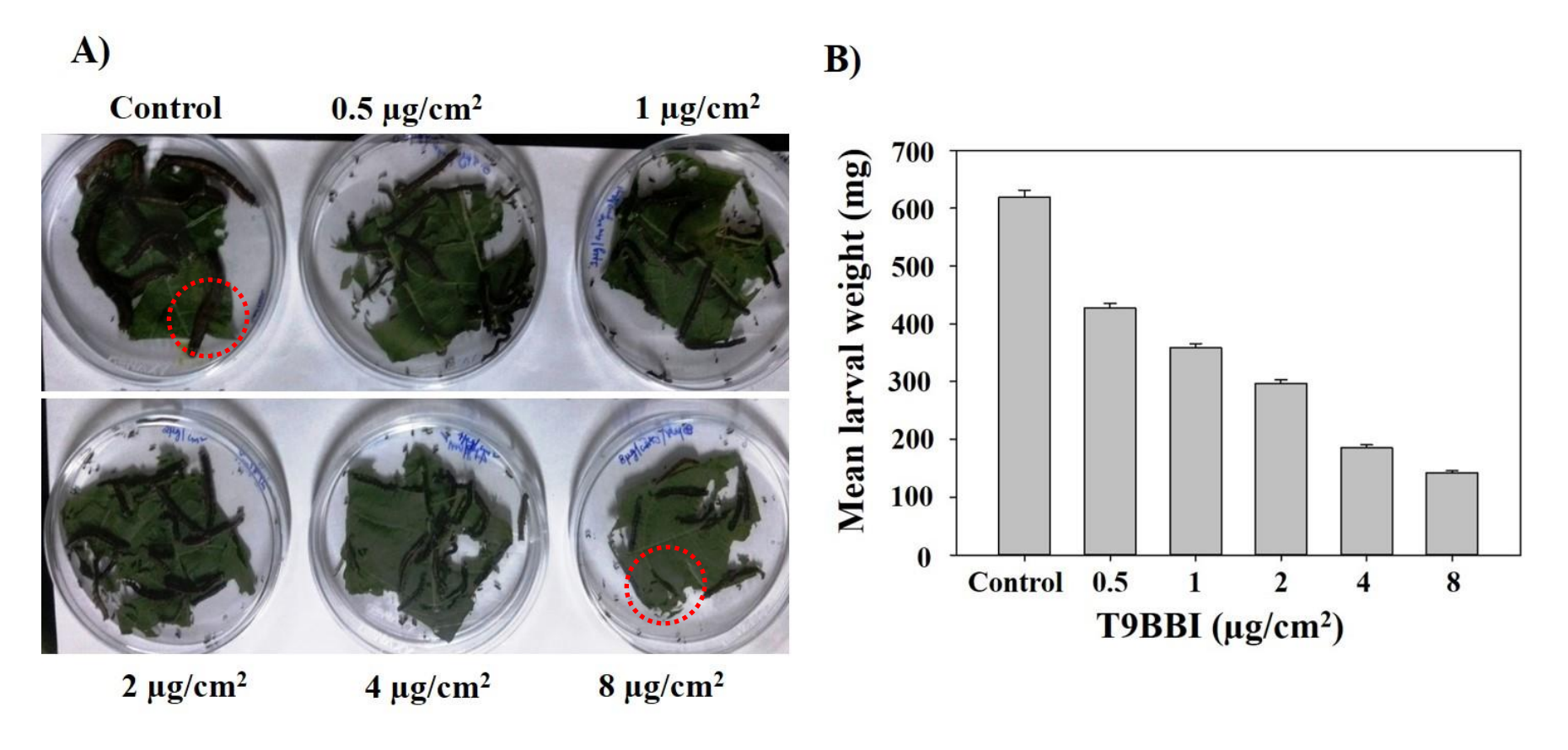


Fig. 5.3. Effect of T9BBI on the growth of 4th instar larvae of *A. janata*. (A) Pictorial depiction of larvae reared on castor leaf coated with buffer alone (control) and different concentrations of T9BBI (treated), and (B) Mean body weight of the corresponding larvae. A single larva from control and T9BBI treated (8μg/cm²) groups are encircled with dashed line (red) to depict the differences in the growth. Further details were described in materials and methods.

In the final instar (5th) stage, the average weight of the larvae fed upon the control diet was 916±116 mg. After feeding with T9BBI, the larval weight was found to be retarded by $47\pm4.0\%$ (0.5 µg/cm²), $56\pm5.9\%$ (1 µg/cm²), $61\pm5.0\%$ (2 µg/cm²), $72\pm6.9\%$ (4 µg/cm²) and $80\pm7.7\%$ (8 µg/cm²), respectively as compared to their corresponding control larvae (Fig. 5.4A and B; Table 5.1).

After completion of 5th instar stage, the mortality rate of larvae fed upon T9BBI was found to be $25\pm2.9\%$ (0.5 µg/cm²), $38\pm4.4\%$ (1 µg/cm²), $42\pm3.3\%$ (2 µg/cm²) $58\pm1.7\%$ (4 µg/cm²) and $80\pm2.9\%$ (8 µg/cm²) of their respective control larvae. The larvae which survived were further converted into pupae, but a delay in pupal formation was observed from 2-7 days in T9BBI fed larvae when compared with their respective control larvae (Table.5. 1).

Further, a weight reduction in the pupae emerged from T9BBI fed larvae was observed. With an increase in the concentration of T9BBI in the diet, there was a gradual reduction in the weight of the pupae by 46 to 85% when compared to the pupae emerged from larvae fed on control diet. Furthermore, the emergence of abnormal larval-pupal intermediates was observed from larvae fed upon leaves coated with high concentration (8 μ g/cm²) of T9BBI (Fig 5.5A and B). In addition, these abnormal larval-pupal intermediates did not turn into adult moth during the process of metamorphosis. In contrast, the pupae that emerged from larvae fed upon T9BBI from 0.5 μ g/cm² to 4 μ g/cm² are metamorphosized into physiologically active moths (Fig. 5.5C).

The results obtained in the present study correlated well with previous studies performed with PIs from *C. cajan* wild relatives and cultivars. (Prasad et al., 2010b; Swathi et al., 2014 and Mohanraj et al., 2018). The studies of Mohanraj et al. (2018) demonstrated that when *A. janata* larvae were fed with bacterially expressed recombinant BBI from *R. sublobata* (rRsBBI from 2 to 8 μ g/cm² on castor leaf) up to 5th instar stage, the larvae

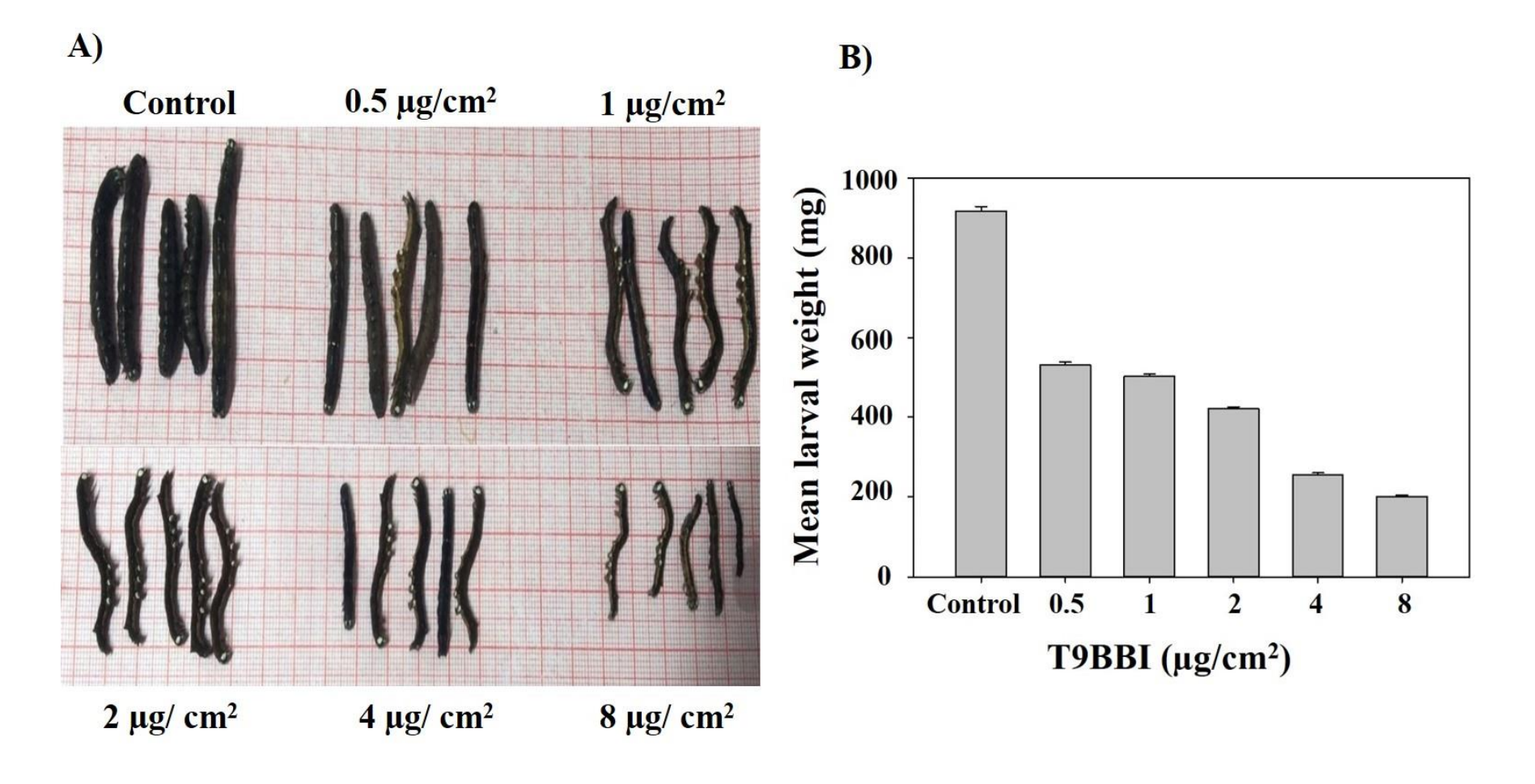


Fig. 5.4. Effect of T9BBI on the growth of 5th instar larvae of A. janata. (A) Pictorial depiction of larvae reared on castor leaf coated with buffer alone (control) and different concentrations of T9BBI (treated), and (B) Mean body weight of the corresponding larvae. Further details were described in materials and methods.

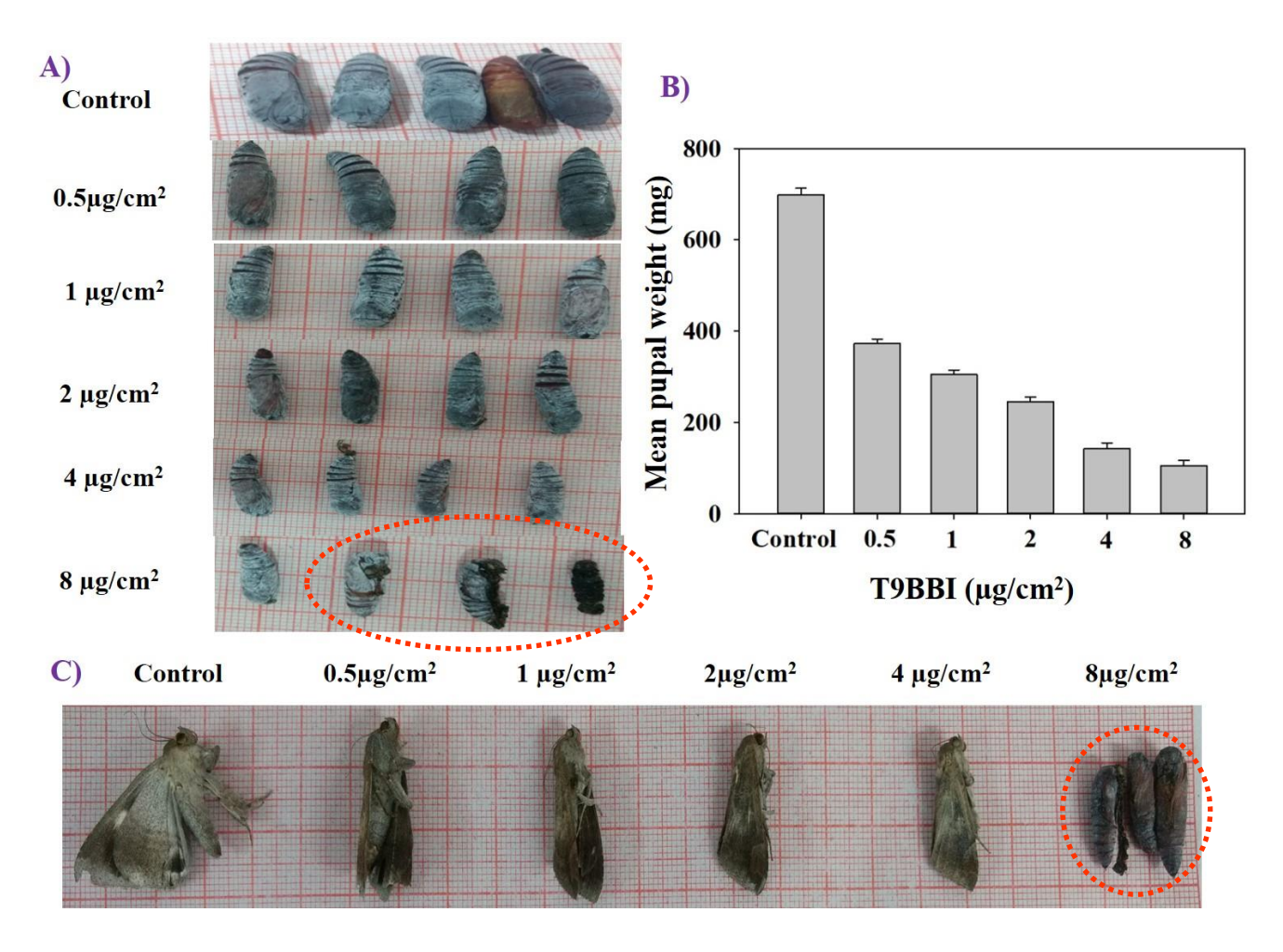


Fig. 5.5. Effect of T9BBI on development of *A. janata*. (A) Pictorial depiction of pupae formed from larvae fed up on castor leaf coated with buffer (control) and T9BBI (treated), respectively; (B) Mean pupal weight and (C) Pictorial depiction of adults emerged from corresponding pupae. The larval-pupal intermediates emerged from larval upon feeding on T9BBI at 8μg/cm² did not transform into adults (shown in dotted red line). Further details were described in materials and methods.

Table. 5.1: Anti metabolic effect of T9BBI on larval growth and development of *A. janata*: Reduction in larval growth was represented after 4^{th} instar stage (8 days of feeding), while survival and mortality rate of larvae was represented after 5^{th} instar stage (10 days of feeding), respectively. Data shown here is the mean \pm SE values of three independent experiments (n=20). Further details were described in materials and methods.

Concentration of T9BBI on	Reduction in larval growth (% control)	Survival rate (% control)	Mortality rate (% control)	Pupal formation time (days)	Intermediate formation		Adult emergence
artificial diet (μg/ Cm ⁻²)					Larval-pupal	Pupal-adult	
0 (Control)	100	100	0	10-16	No	No	Yes
0.5	47±4.0	75±2.9	25±2.8	14-18	No	No	Yes
1	56±5.9	61±4.5	38±4.4	16-22	No	No	Yes
2	61±5.0	58±3.3	42±3.3	16-22	No	No	Yes
4	72±6.9	42±1.4	58±1.7	17-22	No	No	Yes
8	80±7.7	20±2.9	80±2.9	18-23	Yes	NA	No

showed significant growth retardation up to 84% and mortality rate up to 60%, respectively when compared with control larvae. Similarly, the PIs purified from *C. cajan* (*cv.* ICP 7118) when fed to second instar larvae throughout their growth at different concentrations on castor leaf, it resulted in growth retardation of larvae from 45 to 70% of control and mortality rate from 13 to 88% of control, respectively. In addition, abnormalities also observed and delay in the transformation of larvae to pupae (6 days) was also observed when larvae were fed with *C. cajan* PIs (Swathi et al., 2014).

The studies of Prasad et al. (2010b) demonstrated that A. janata larvae when continuously fed with PIs from redgram (RgPI) and black gram (BgPI) for 6 days, maximum retardation in growth was observed up to 92%. Further, when the A. janata larvae were allowed to grow for twenty days on the castor leaf without any inhibitor, 100% mortality rate was observed with both RgPI and BgPI at concentrations used in the present study. Furthermore, defective larval-pupal development was also observed in their study. A similar type of study was performed on A. janata using caffeic acid methyl ester purified from Solanum melongena fruit extract. After 7 days of feeding with different concentrations (30 & 40 μg/cm² leaf area), larval growth retardation and pupal weight reduction was observed up to 93% and 48%, respectively (Rani et al., 2013). Anagasta kuehniella is a polyphagous pest and when the larvae of this pest were fed with trypsin inhibitors purified from Adenanthara pavonia seeds, they showed growth retardation up to 79% of control and mortality rate up to 50% of control while the delay in pupal development was observed up to 10 days (Macedo et al., 2010). Further, the Kunitz inhibitors purified from Acacia polyphylla seeds also showed retardation in growth of Anagasta kuehniella. The growth of 5th instar larvae was retarded up to 57% of control when fed with different concentrations (0.5, 1 and 2%) of Kunitz inhibitors (Machado et al., 2013). The PIs isolated from Adenanthara pavonia seeds showed an inhibitory effect on Aedes aegypti with different concentrations (from 0.12 to 1 mg/ml) at different time periods (24, 48, 72 and 96 hrs). Its growth was retarded up to 69% of control, while 100% mortality was observed at 1mg/ml concentration (Sasaki et al., 2013).

5.3. Differential expression of proteins in midgut tissue of *A. janata* larvae fed with T9BBI:

The protein extract prepared from midgut tissue of late 4th instar larvae feeding on a diet containing T9BBI (8 µg/cm²) and control diet were separated on IPG strips in the pH range from 4-7 followed by SDS-PAGE in the second dimension. The proteome profile from these tissues were Compared for differentially expressed proteins by using image master platinum 7.0 software. A total of 256 protein spots were observed in 5 to 100 kDa range when separated in second dimension using SDS-PAGE (**Fig. 5.6**). Eight protein spots which showed significant differences in their expression (>2-fold), separated conspicuously and placed far off from other protein spots were considered for identification. The partial maps and 3-D views of the corresponding spots were represented in **Figure 5.7**.

All the protein spots (Spot 1 to 8) were subjected to tryptic digestion followed by MALDI-TOF-TOF analysis to identify the molecular mechanisms by which *A. janata* larvae become susceptible to T9BBI and attain mortality.

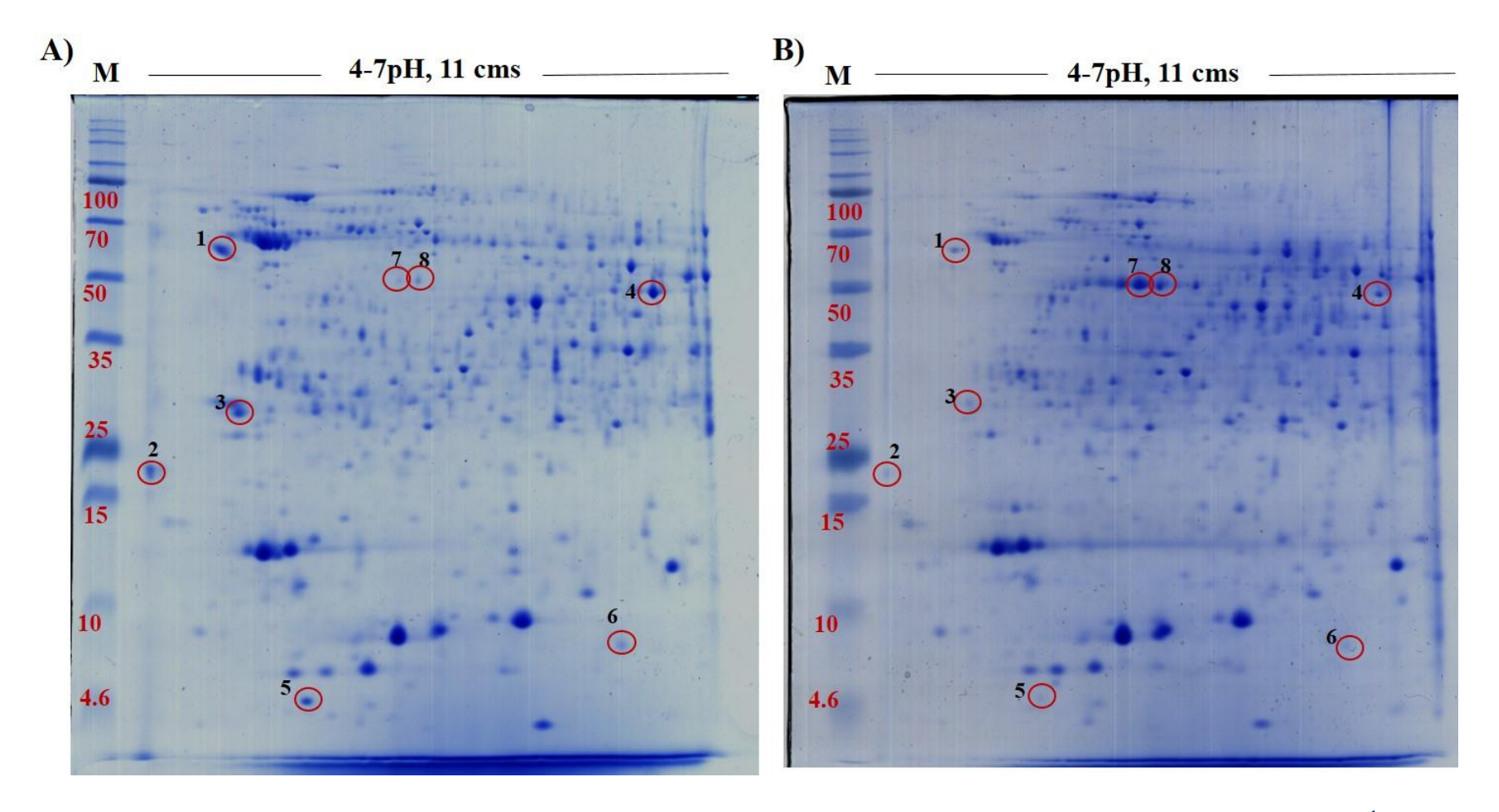


Fig. 5.6. Two dimensional gel electrophoresis of midgut tissue proteome from *A. janata* larvae (early 5th instar stage) fed up on (**A**) control leaf coated with buffer and (**B**) leaf coated with T9BBI (8 μg/cm²), respectively. Among several spots which showed significant differences (> 2-fold), spots labelled as 1 to 8 (indicated with red circles) which are clearly separated from other spots are chosen for further studies, i.e., MALDI-TOF-TOF analysis. Further details were described in materials and methods.

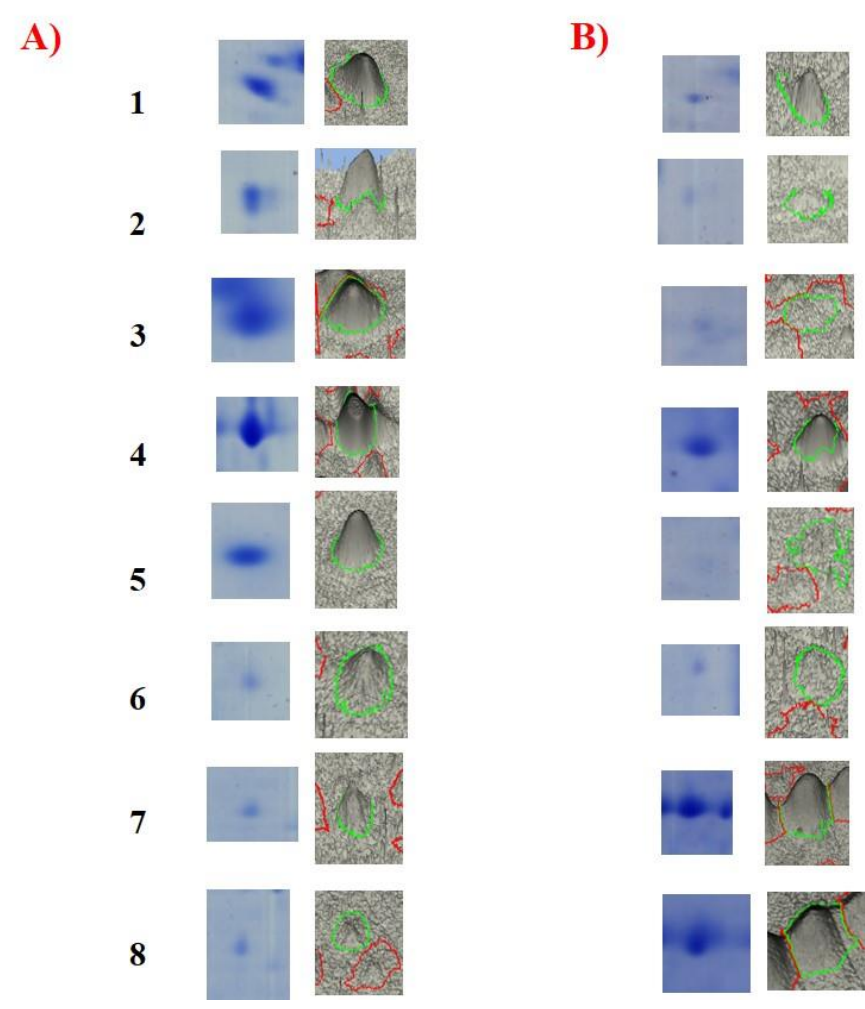
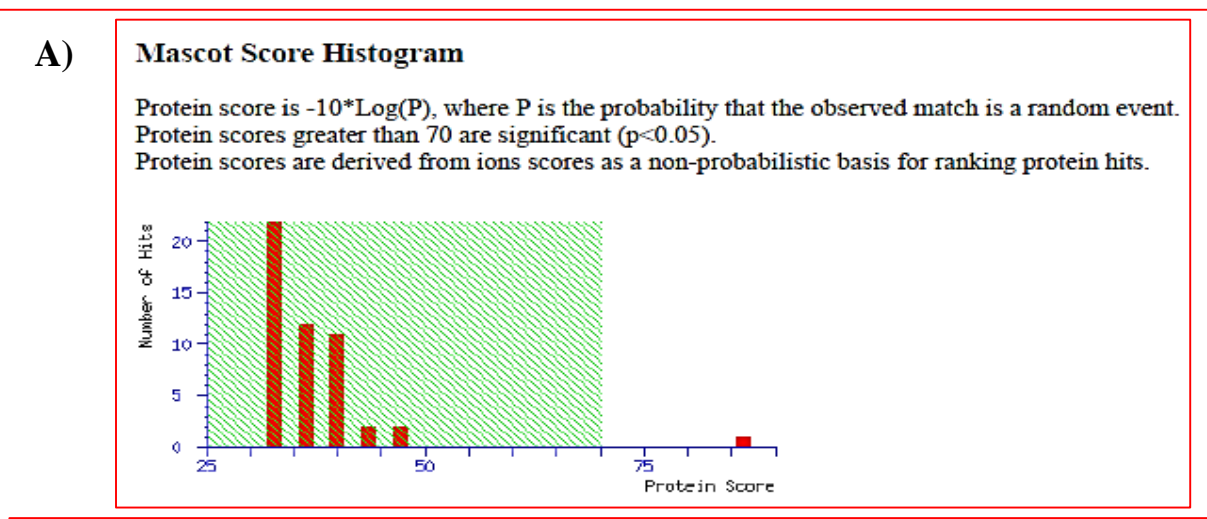


Fig. 5.7. Three-dimensional view of differentially expressed protein spots (1-8) labelled in 2-DE of fig 5.6 using Image Master Platinum software. Panels (A) and (B) represent protein spots from midgut proteome of *A. janata* larvae (early 5th instar stage) fed up on (A) control leaf coated with buffer and (B) leaf coated with T9BBI (8 μg/cm²), respectively.

5.4. Mass spectrometric analysis of differentially expressed proteins:

5.4.1. Identification of Spot 1 as COP-9 Signalosome (CSN) complex-3 subunit:

Mascot search results for various ions generated from spot 1 on subjecting to tryptic digestion followed by MALDI-TOF-TOF analysis showed a significant score of 86 with CSN complex-3 subunit of *Drosophila melanogaster* (Fig. **5.8A**). The spectrum corresponding to peptide mass fingerprint (PMF) data was represented in Figure 5.8B. When the peak with m/z 1173 from PMF spectrum was ionized further in MALDI-TOF-TOF, the resulting lift spectrum showed the following de novo sequence 'VQLASAVEAER' when analyzed using Biotools software (Figs. **5.8C** and **D**). Further, the various ions generated during MALDI-TOF-TOF studies showed 44% identity with the amino acid sequence of CSN complex-3 subunit (Uniprot Acc No. Q8SYG2). Also, the de novo sequence obtained from PMF peak with m/z 1173 showed over-lapping with one of the internal amino acid sequence recognised for CSN complex-3 subunit during MS/MS ion search (Fig. 5.8E). Furthermore, clustal alignment of this de novo sequence showed significant (82-100%) matching with the CSN complex-3 subunits from different *Drosophila* species available in NCBI database (Fig. 5.8F). These results confirm that CSN complex-3 subunit is down-regulated by 5.2-fold in A. janata larvae upon feeding on a diet supplemented with T9BBI. CSN is a nuclear enriched multiprotein complex found mainly in plants, mammals, insects and yeast (Wei et al., 1994; Deng et al., 2000). It plays a pivotal role in the growth and development as well as to acquire stress tolerance in plants (Zhou et al., 2019). It shares homology with the 26S proteasome complex, which is involved in the degradation of proteins (Wei et al., 1999; Schwechheimer et al., 2000). CSN is also known to



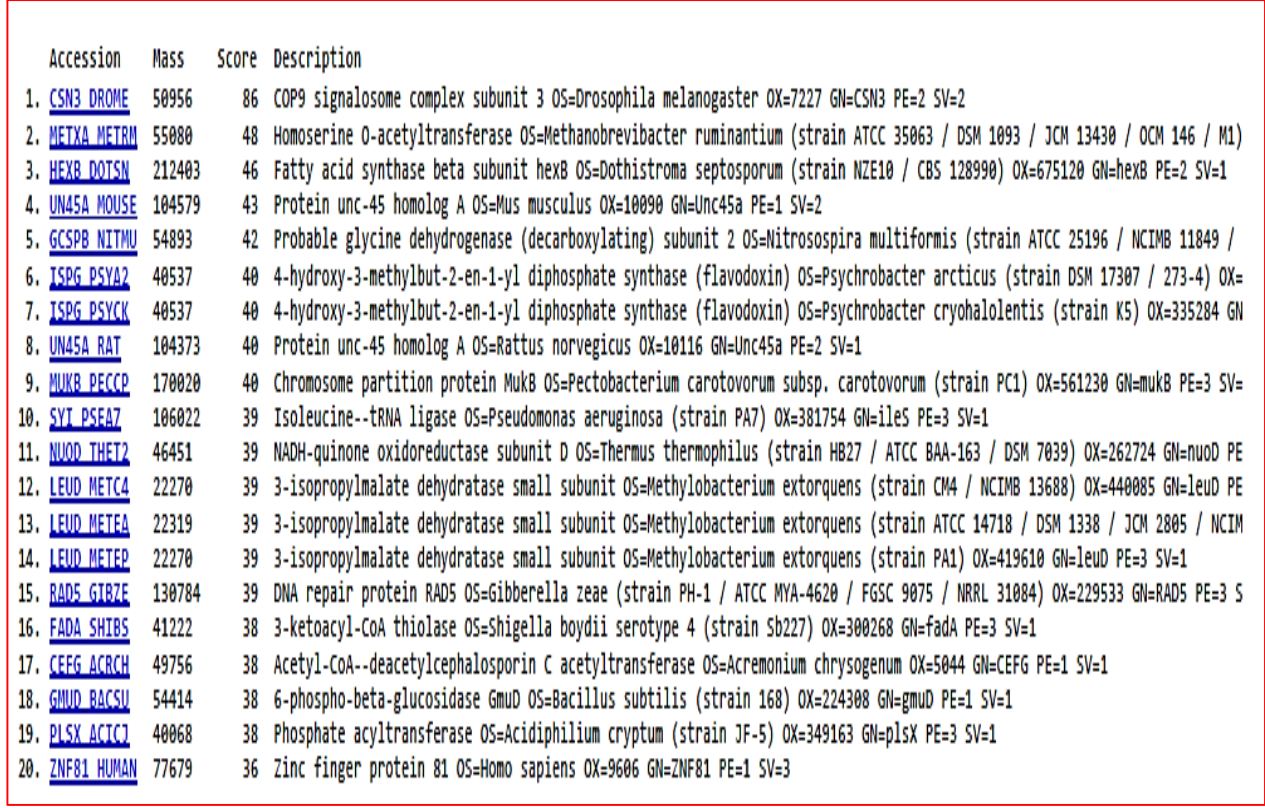
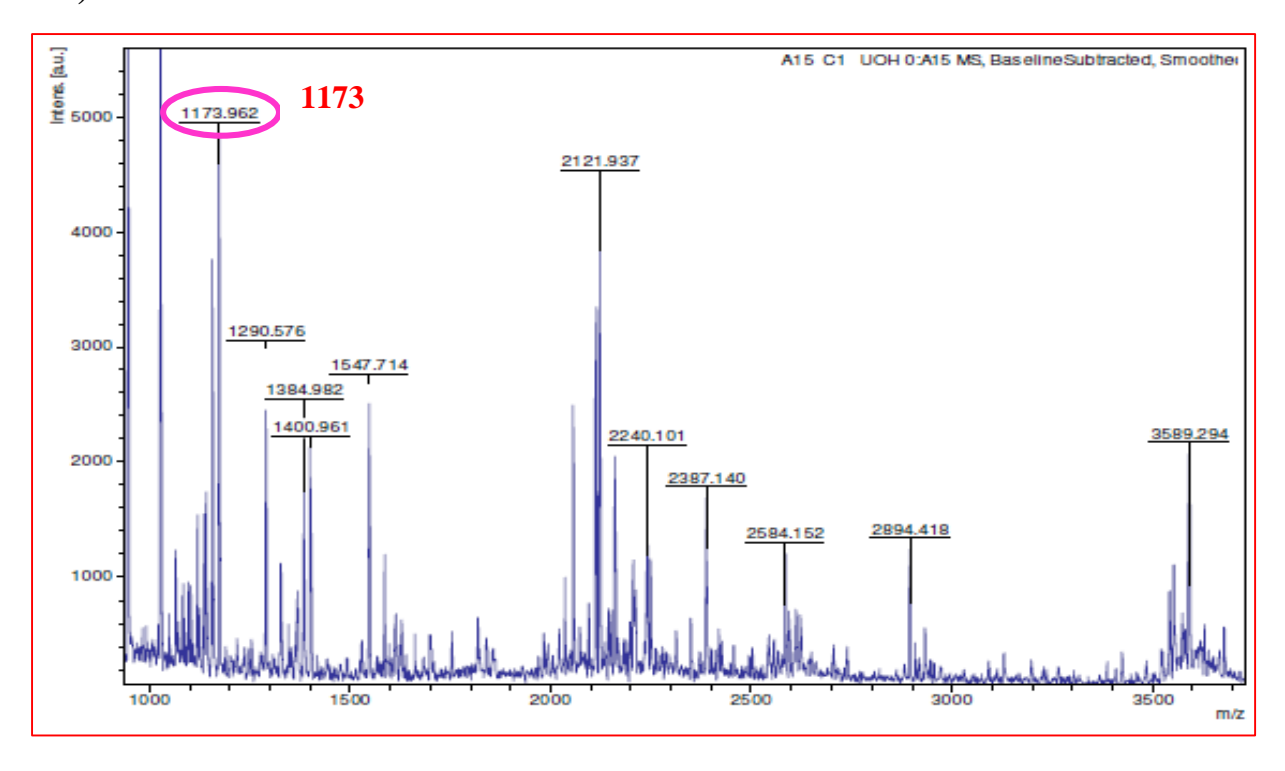


Fig. 5.8. Identification of spot 1 as COP-9 signalosome after tryptic digestion and MALDI-TOF-TOF analysis. (A) Histogram of MASCOT search results and corresponding protein hits.

B)



C)

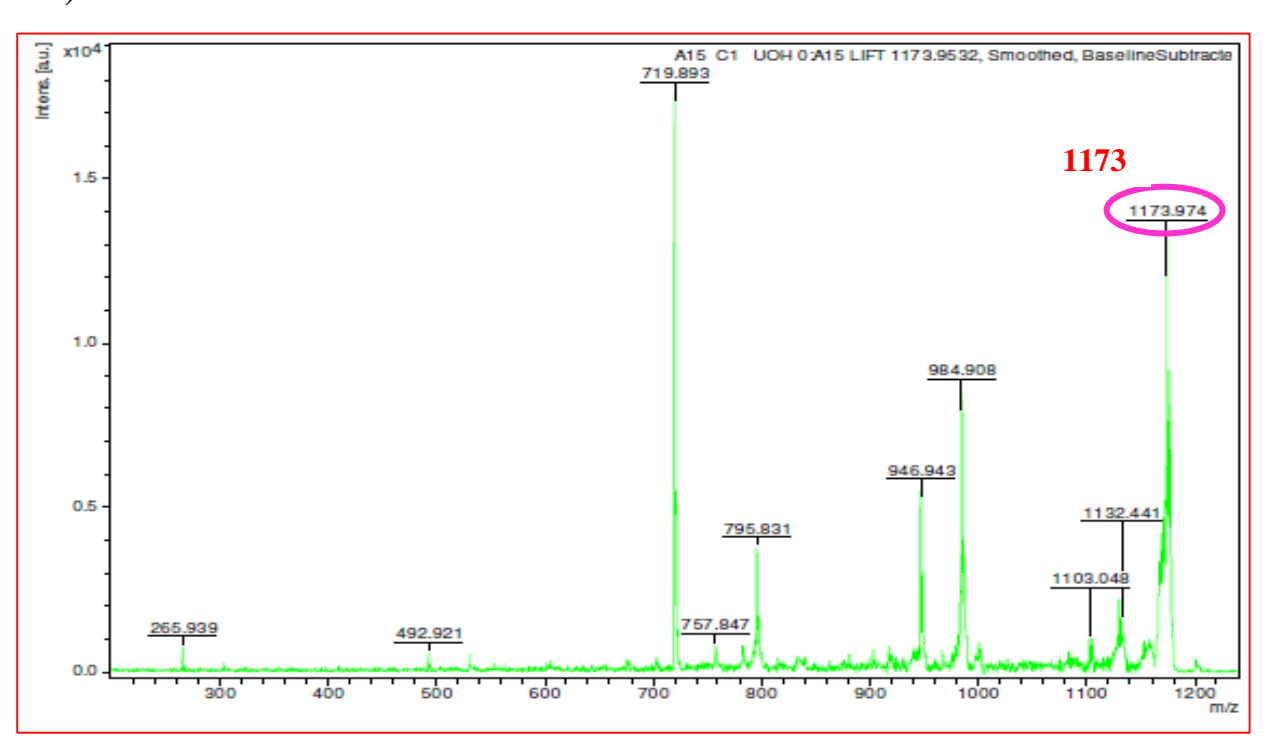


Fig. 5.8. (B): PMF spectrum of spot 1 highlighting peak 1173 (m/z); **(C)** Lift spectrum of PMF peak with m/z 1173

D)

	Alculated Masses: VQLASAVEAER OLASAVEAER							Peak: 1173		
N-Term.	Ion	8	b	1	a-17	b-17	V	C-Term.	lor	
1	٧	72.081	100.076	72.081	55.054	83.049	175.119	11	R	
2	Q	200.139	228.134	101.071	183.113	211.108	304.162	10	E	
3	L	313.223	341.218	86.096	296.197	324.192	375,199	9	Α	
4	A	384.261	412.255	44.049	367.234	395.229	504.241	8	E	
5	S	471.293	499.287	60.044	454.266	482,261	603.310	7	V	
6	A	542,330	570.325	44.049	525.303	553,298	674.347	6	A	
7	V	641.398	669.393	72.081	624.372	652.366	761.379	5	S	
8	E	770.441	798.436	102.055	753.414	781.409	832,416	4	A	
9	A	841.478	869.473	44.049	824,451	852.446	945.500	3	L	
10	E	970.520	998.515	102.055	953,494	981.489	1073,559	2	(
11	R	1126.621	1154,616	129.113	1109,595	1137,590	1172.627	1	١	

E)

Sequence coverage: 44%

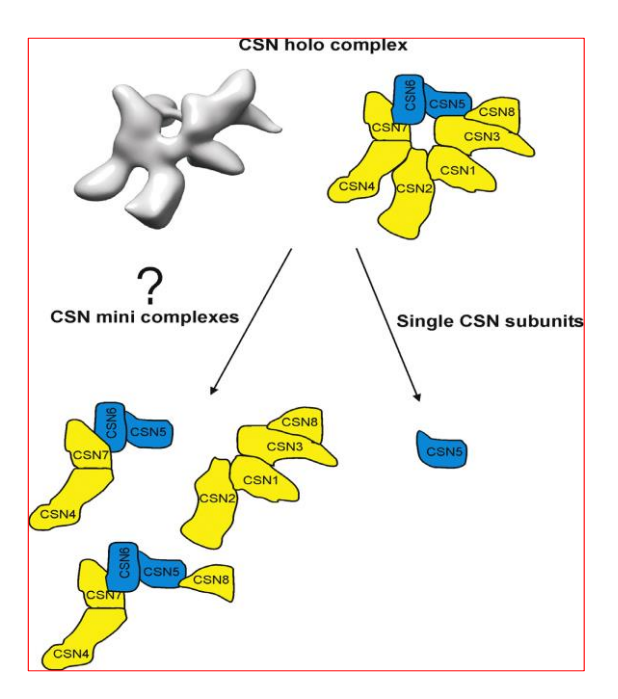
MGSALENYVNQVRTLSASGSYRELAEELPESLSLLARNWSILDNVLETLDM QQHSLGVLYVLLAKLHSASTANPEPVQLIQLMRDFVQRNNNEQLRYAVCAFY ETCHLFTEFVVQKNLSILGIRIISRAIDQIRQLETQLTPIHADLCLLSLKAKNFS VVLPYLDADITDISTVAAECKTQQQQQSQHADANNDAKYFLLYFYYGGMIYT AVKNYERALYFFEVCITTPAMAMSHIMLEAYKKFLMVSLIVEGKIAYIPKNTQ VIGRFMKPMANHYHDLVNVYANSSSEELRIIILKYSEAFTRDNNMGLAKQVAT SLYKRNIQRLTKTFLTLSLSDVASFVQLASAVEAERYILNMIKSGEIYASINQK DGMVLFKDDPEKYNSPEMFLNVQNNITHVLDQVRQINKMEEEIILNPMYVK KALGSQDDDLTSQHPKTFSGDPTD

Fig. 5.8. (D): Analysis of Lift spectrum from peak m/z 1173 using Biotools; **(E)** COP-9 signalosome (CSN3 DROME / Uniprot Acc. No. Q8SYG2) sequence. Red colour indicates the partial sequence coverage by various ions generated from spot1 while blue box indicate the matching of de novo (m/z 1173) sequence obtained from Biotools with one of the peptides identified by Mascot search engine.

F)

Accession number	Protein name/Source	Sequence	Similarity (%)
Spot number 1, (de	e novo sequence from PMF peak with m/z 1173)	VQLSSAAEAER	100
XP_001956992.1	COP9-signalosome-complex-subunit-3/Drosophila-ananassae	VQLSSAAEAER	100
XP_020816114.1	COP9-signalosome-complex-subunit-3/Drosophila-serrata	VQLSSAAEAER	100
XP_016984327.1	COP9-signalosome-complex-subunit-3/Drosophila-rhopaloa	VQLSSAVEAER	91
XP_001973550.1	COP9-signalosome-complex-subunit-3/Drosophila-erecta	VQLSSAVEAER	91
XP_017041430.1	COP9-signalosome-complex-subunit-3/Drosophila-ficusphila	VQLSSAVEAER	91
XP_017005528.1	COP9-signalosome-complex-subunit-3/Drosophila-takahashii	VQLSSAVEAER	91
XP_002046288.1	COP9-signalosome-complex-subunit-3/Drosophila-virilis	VQLSSAVEAER	91
NP_524190.2	COP9-signalosome-subunit-3/Drosophila-melanogaster	VQLPSAVEAER	82
XP_002040729.1	COP9-signalosome-complex-subunit-3/Drosophila-sechellia	VQLASAVEAER *** ** ****	82

Fig. 5.8 F): Clustal alignment of *de novo* sequence from PMF peak (m/z 1173) with signalosome complexes identified in NCBI database.



Supplementary Figure 5.1. CSN holo and mini complexes, the release of CSN 5 subunit from CSN holo complex (Adapted from Dubiel et al., 2015)

be involved in (i) interaction of integrins, (ii) stabilization of Jun transcription factors (Doronkin et al., 2003). Thus, the functional diversity and flexibility in CSN is brought about mainly by its holo complex, which helps in the formation of many smaller complexes and free subunits (Dubiel et al., 2015).

In addition to the above, it was also found to be essential for proper development in *Drosophila* and cell-cycle control in fission yeast (Freilich et al., 1999; Mundt et al., 1999). The studies of Moon et al. (2004) reported that the feeding of cowpea bruchid with a diet containing soybean cysteine protease inhibitor 'soyacystatin N (scN)' downregulated the expression of CSN complex subunit1 gene. Thus, taken together the results from the present study and literature cited above suggest that the 'CSN complex-3 subunit' possibly play a significant role in the sustenance of growth and development of *A. janata* larvae and the

larvae might have lost their ability to adapt to T9BBI challenge due to down regulation of CSN complex-3 subunit (Figs. 5.2-5.8 and Table 5.1).

5.4.2. Identification of Spot 2 as protein SOEM-1 (Suppressor of ectopic mig-13):

The various ions generated from spot 2 when subjected to tryptic digestion and MALDI-TOF-TOF analysis showed matching to a protein 'SOEM-1' of *Caenorhabditis elegans* with a significant score of 92 during Mascot MS/MS ion search (Fig. 5.9A). The PMF spectrum corresponding to spot 2 was represented in Figure 5.9B. When the PMF peaks with m/z 1173 (lift spectrum shown) and m/z 1545 (lift spectrum not shown) were further ionized in MALDI-TOF-TOF, the following *de novo* sequences 'WVIGEGPLFR' and 'RRPSDSEIYMEQNMNR', were resulted through Biotools software (Figs. 5.9C and D). Also, the various ions generated during MALDI-TOF-TOF studies showed partial sequence coverage of up to 77% with protein SOEM-1 (Uniprot Acc No. Q7YWN4). Further, the two *de novo* sequences obtained through Biotools showed overlapping with the partial amino acid sequences recognised for protein SOEM-1 during MS-MS ion search (Fig. 5.9E). Furthermore, the *de novo* sequence 'RRPSDSEIYMEQNMNR' showed 100% matching with the SOEM-1 protein of *C. elegans* from the data available in the NCBI database (Fig.

5.9F).



Supplementary Fig. 5.2. SOEM downstream signalling (Adapted from Zhu et al., 2016)

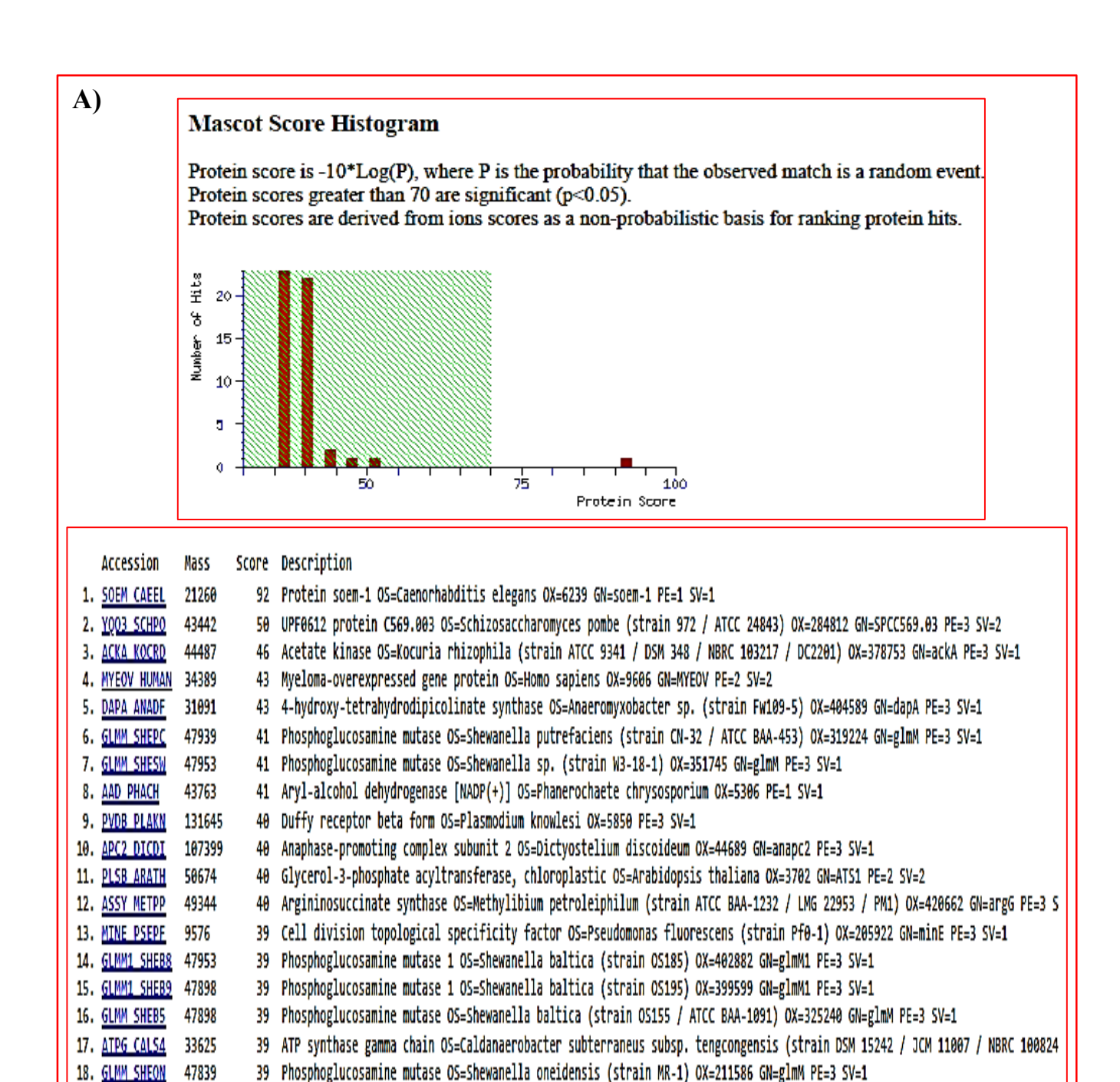


Fig. 5.9. Identification of spot 2 as SOEM-1 after tryptic digestion and MALDI-TOF-TOF analysis. (A) Histogram of MASCOT search results and corresponding protein hits.

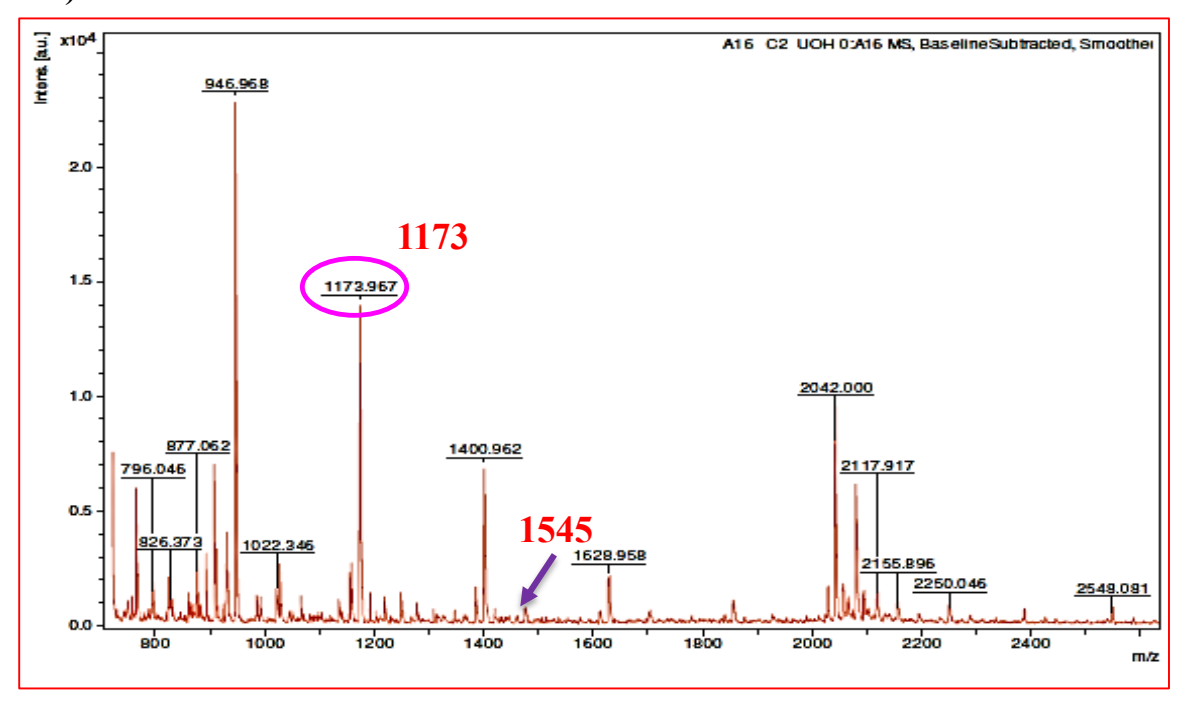
39 Phosphoglucosamine mutase OS=Shewanella sp. (strain ANA-3) OX=94122 GN=glmM PE=3 SV=1

39 Interferon alpha/beta receptor 2 OS=Ovis aries OX=9940 GN=IFNAR2 PE=2 SV=2

19. GLMM SHESA 47855

20. INAR2 SHEEP 61021







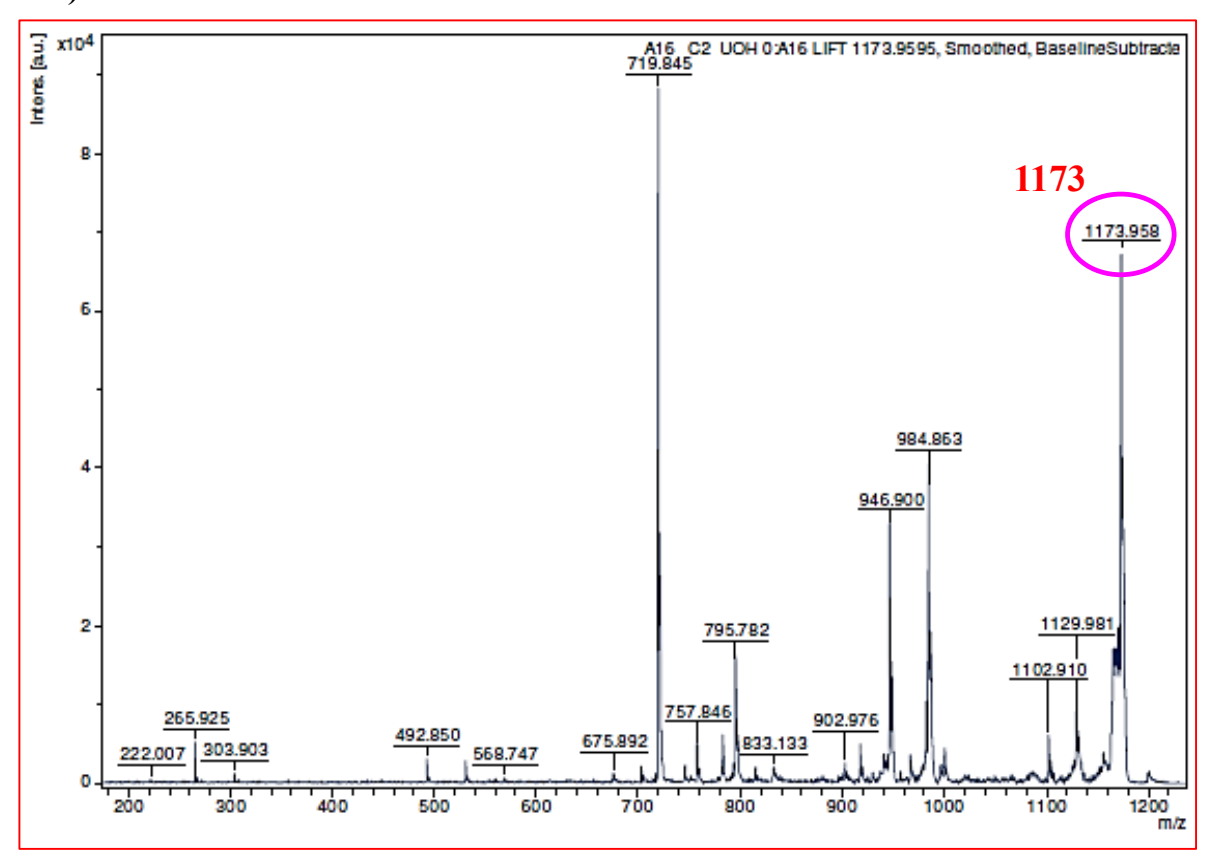


Fig. 5.9. (B): PMF spectrum of spot 2 highlighting peaks 1173 and (m/z) and 1545 (m/z); **(C)** Lift spectrum of PMF peak with m/z 1173

D)

/VIGEGF	LFR		WVIGEGI	PLFR			Peak	: 1173	
N-Term.	Ion	a	b	I	a-17	b-17	Y	C-Term.	ю
1	W	159.092	187.087	159.092	142.065	170.060	175.119	10	F
2	٧	258.160	296.155	72.081	241.134	269.128	322.187	9	I
3		371.244	399.239	86.096	354.218	382.213	435.271	8	П
4	G	428.266	456.261	30.034	411.239	439.234	532.324	7	I
5	Ε	557.308	585.303	102.055	540.282	568.277	589.346	6	(
6	G	614.330	642.325	30.034	597.303	625.298	718.388	5	
7	Р	711.382	739.377	70.065	694.356	722.351	775.410	4	(
8	L	824.466	852.461	86.096	807.440	835.435	888.494	3	
9	F	971.535	999.530	120.081	954.508	982.503	987.562	2	١
10	R	1127.636	1155.631	129,113	1110.609	1138.604	1173,642	1	N

alculated Masses: IRPSDSEIYMEQNMNR 10: Oxidation (M) RRPSDSEIYMEQNMNR							Peak: 1545		
N-Term.	lon	8	b	I	a-17	b-17	у	C-Term.	lon
1	R	129.113	157.108	129.113	112.087	140.082	175.119	16	B
2	R	285.215	313.209	129.113	268.188	296.183	289.162	15	N
3	Р	382.267	410.262	70.065	365.241	393.236	420.202	14	M
4	S	469.299	497.294	60.044	452.273	480.268	534.245	13	N
5	D	584.326	612.321	88.039	567.300	595.295	662.304	12	0
6	S	671.358	699.353	60.044	654.332	682.327	791.346	11	Е
7	E	800.401	828.396	102.055	783.374	811.369	938.382	10	M.
8		913.485	941.480	86.096	896.458	924.453	1101.445	9	Y
9	Υ	1076.548	1104.543	136.076	1059.522	1087.517	1214.529	8	
10	M*	1223.584	1251.579	120.048	1206.557	1234.552	1343,572	7	E
11	Ε	1352.626	1380.621	102.055	1335,600	1363.595	1430.604	6	(A)
12	Q	1490.685	1508.680	101.071	1463.658	1491.653	1545,631	5	

E)

Protein sequence coverage: 77%

MMMTMAADYGSSEGHYDTPWEFLARPNSVRFSTADVRLSTSAAGDAKVSPHGSP
SLCSSSSFVNQLVQIGNSAVDARRKVPRDESKRRRPSDSEIYMEONMNRVEAEKRL
ENRNLGDYLLRSRGEGSAALSLRATKGVVHIKIEWNGEKWVIGEGPLFRSISSAISF
YRRHPLPIRGADHLVLKNQLKPV

Fig. 5.9. (D): Analysis of Lift spectrum from peaks m/z 1173 & 1545 using Biotools; **(E)** SOEM-1 (SOME CAEEL /Uniprot Acc. Q7YWN4) sequence. Red colour indicates the partial sequence coverage by various ions generated from spot 2 while blue box indicate the matching of *denovo* (m/z 1173 & 1545) sequences obtained from Biotools with the peptides identified by Mascot search engine.

F)

Accession number	Protein name/ Source	Sequence	Similarity (%)
Spot number xx (a	de novo sequence from PMF peak with m/z 1545)	RRPSDSEIYMEQNMNR	100
NP_001021833.1	Protein SOEM-1/ Caenorhabditis elegans	RRPSDSEIYMEQNMNR ********	100

Fig. 5.9. F): Clustal alignment of *de novo* sequence from PMF peak (m/z 1545) with SOEM-1, identified in NCBI database.

These results confirm that SOEM-1protein is down-regulated by 3.4-fold when the *A. janata* larvae were fed upon a diet supplemented with T9BBI. Suppressor of ectopic mig-13 shortly called as 'SOEM-1' protein acts as a downstream regulator of migratory protein mig-13 and is known to play a role in the regulation of Q neuroblast migration during larval growth (Zhu et al., 2016). Also, actin mediated cytoskeleton rearrangements are necessary for a migratory cell to respond to extracellular signals. During this process, Arp 2/3 acts as an upstream regulator of actin and is involved in the nucleation of actin, an essential step required for the migration of the cell (Swaney and Li, 2016). Further, WASP (Wiskott–Aldrich syndrome protein) and WAVE (WASP family verprolin-homologous protein) together act as the nucleation promoting factors of the Arp 2/3 while the transmembrane proteins Mig-13/Lrp 12 are involved in Arp 2/3 complex formation. Loss in any of these proteins prevent cell migration and known to cause cell lethality (Pollard and cooper, 2009; Swaney and Li, 2016).

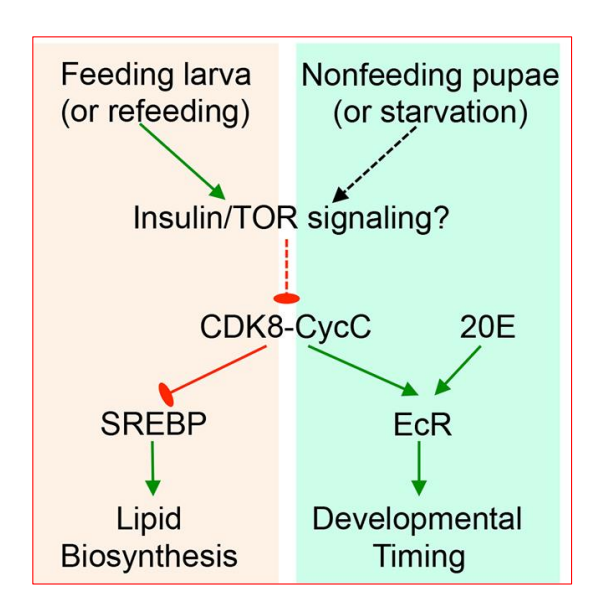
Considering the role of SOEM-1, its down-regulation in the *A. janata* larvae fed on a diet containing T9BBI might have lead to loss of regulatory control on cell migration which in turn affected the growth and development of *A. janata* larvae (**Figs. 5.2-5.7 and 5.9**; **Table 5.1**).

5.4.3. Identification of Spot 3 as Cyclin-C:

Tryptic digestion of spot 3 followed by MALDI-TOF-TOF analysis resulted in the generation of various ions which showed matching to Cyc-C of *D. pseudoobscura* with a significant score of 66 using a Mascot search engine (**Fig. 5.10A**). The spectrum corresponding to PMF data was represented in **Figure 5.10B**. When the peak with m/z 1154 from PMF spectrum was ionized in MALDI-TOF-TOF, the resulting lift spectrum showed the following *de novo* sequence '**RFYARNSLK**' when analyzed using Biotools software (**Figs. 5.10C and D**).

The various ions generated during MALDI-TOF-TOF studies showed partial sequence coverage up to 46% with Cyc-C (Acc. No. CCNC DROPS). Further, the *de novo* sequence obtained from PMF peak with m/z 1154 showed overlapping with one of the partial amino acid sequence recognised for Cyc-C (Uniprot Acc No. Q29AII) during MS-MS ion search (Fig. 5.10E). Furthermore, Clustal alignment of this *de novo* sequence with various sequences available in NCBI database showed 100% matching with the Cyc-C sequences from different insects such as *Bicyclusanyana*, *Halyomorphahalys*, *Drosophila busckii*, *D. willistoni*, *Manduca sexta*, *Pieris-rapae*, *S. litura*, *Bombyx mori* and *Aedes aegypti* (Fig. 5. 10F). These results confirm that Cyc-C is down-regulated by 5.2-fold when the *A. janata* larvae were exposed to a diet containing T9BBI.

In *Drosophila*, nutritional control of developmental transition, completed by the ecdysone receptor is known to be mediated by CDK8-Cyc-C. Further, the CDK8-Cyc-C complex is also known to bind to SREBPs (Sterol regulatory element-binding protein) to inhibit its transcriptional activity and thereby regulate the lipid synthesis in both mammals and *Drosophila*. Thus, the control of both EcR (positively) and SREBP (negatively) with the help of CDK8-Cyc-C suggests that it can assimilate feeding-stimulated lipid synthesis and ecdysone-controlled metamorphosis during the larval-pupal alteration (Xie et al., 2015). In corroboration with these studies, the down regulation of Cyc-C in the midgut tissues of T9BBI fed larvae indicates its potential role in growth retardation by inhibiting Cyc-C (Figs. 5.2-5.7 and 5.10; Table 5.1). Further, the inhibition of Cyc-C might have lead to the disruption of metamorphosis, resulting in the emergence of abnormal larval-pupal intermediates in T9BBI fed larvae.



Supplementary Fig. 5.3. Model for the CDK8-SREBP/EcR regulatory network (Adapted from Xie et al., 2015)

A)

31664 114792

235067

16463

23123

23135

75318

74517

34203

77158

58562

11. RTEL1 AEDAE
12. PLXB DROME

13. CPLX DROME

18. PA1 POLAN

19. NONA DROME

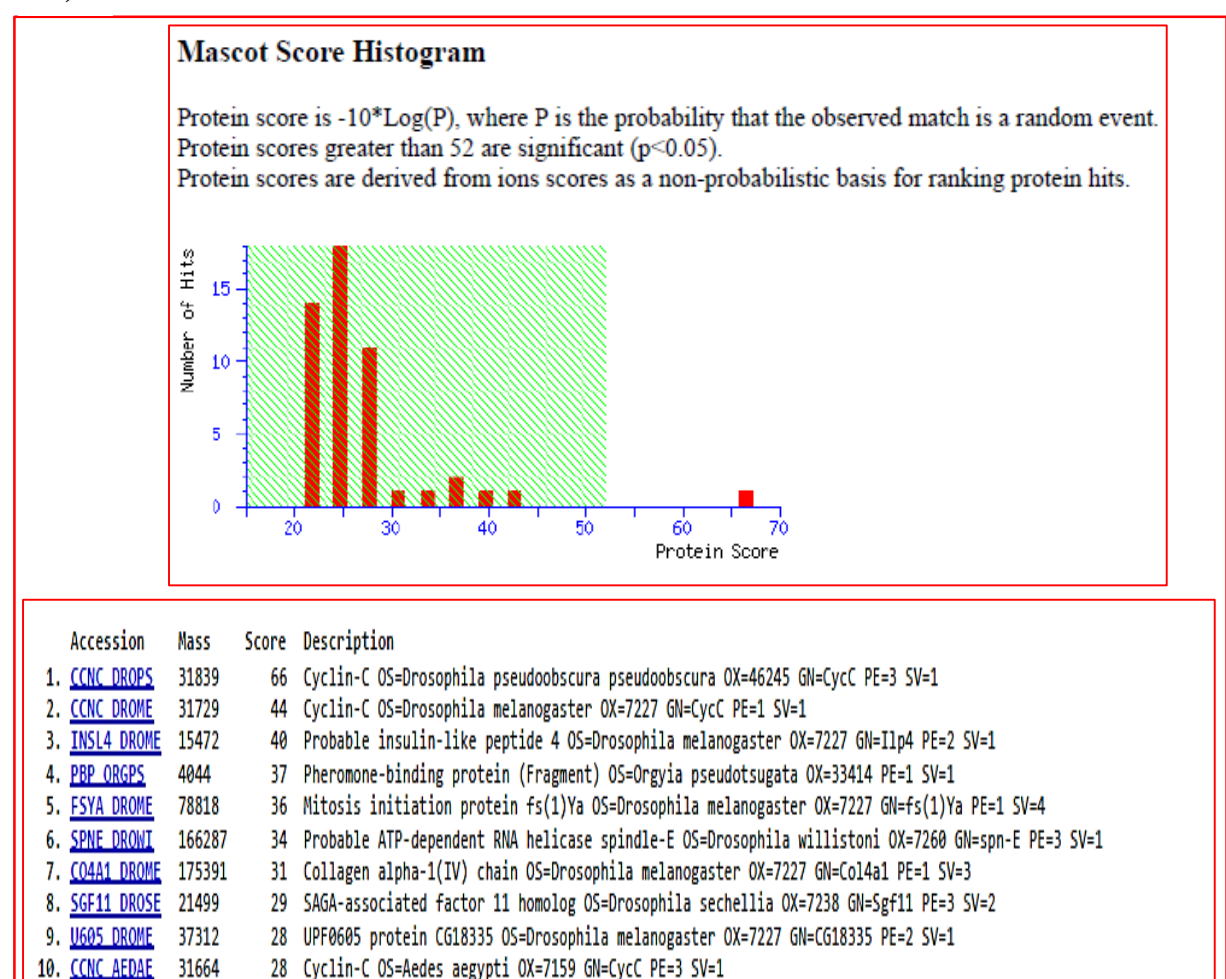


Fig. 5.10. Identification of spot 3 as Cyclin-C after tryptic digestion and MALDI-TOF-TOF analysis. (A) Histogram of MASCOT search results and corresponding protein hits.

26 Protein no-on-transient A OS=Drosophila melanogaster OX=7227 GN=nonA PE=1 SV=2

26 Cyclin-dependent kinase 8 OS=Aedes aegypti OX=7159 GN=Cdk8 PE=3 SV=2

27 Plexin-B OS=Drosophila melanogaster OX=7227 GN=PlexB PE=1 SV=2

27 Complexin OS=Drosophila melanogaster OX=7227 GN=cpx PE=2 SV=1

26 Phospholipase A1 OS=Polistes annularis OX=27505 PE=2 SV=1

28 Regulator of telomere elongation helicase 1 homolog OS=Aedes aegypti OX=7159 GN=AAEL008960 PE=3 SV=1

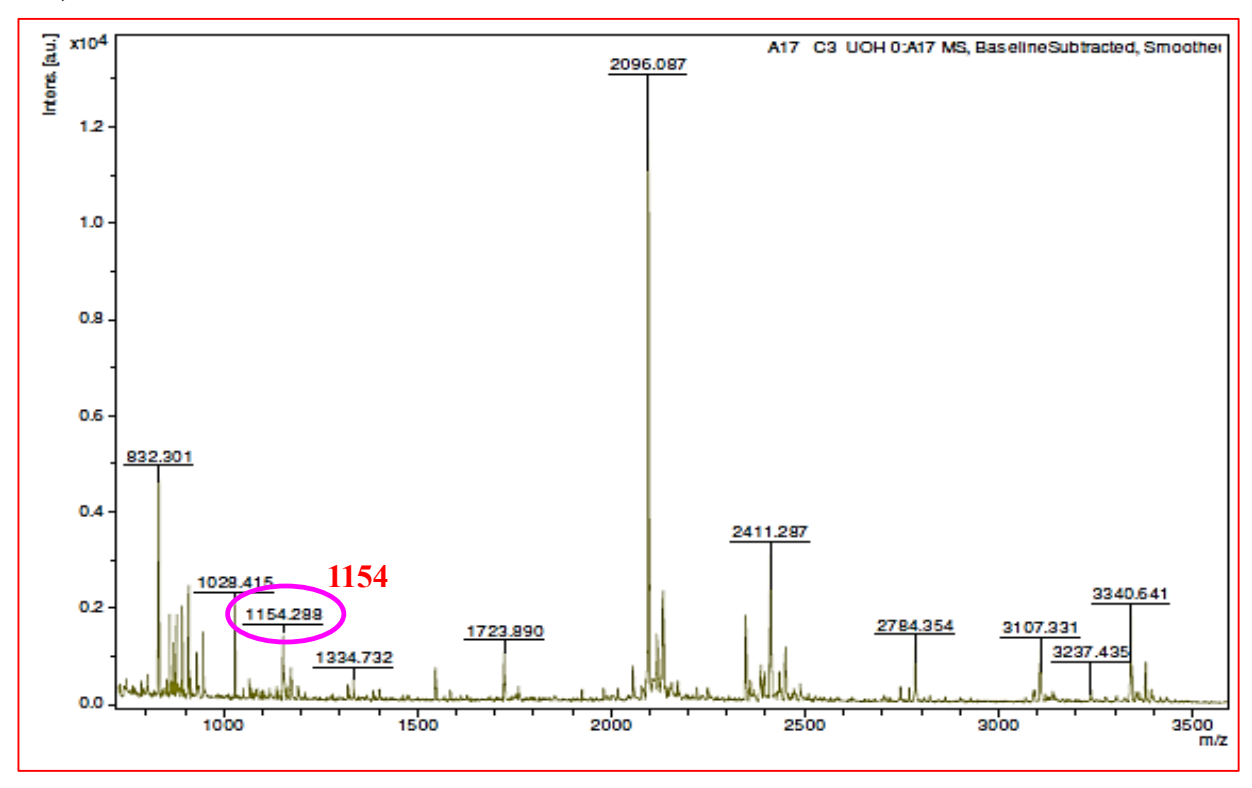
27 Mannosyl-oligosaccharide alpha-1,2-mannosidase IA OS-Drosophila melanogaster OX-7227 GN-alpha-Man-Ia PE-2 SV-2

27 SAGA-associated factor 11 homolog 1 OS=Drosophila grimshawi OX=7222 GN=Sgf11-1 PE=3 SV=1

27 SAGA-associated factor 11 homolog 2 OS=Drosophila grimshawi OX=7222 GN=Sgf11-2 PE=3 SV=1

26 Inner nuclear membrane protein Man1 OS=Drosophila melanogaster OX=7227 GN=MAN1 PE=1 SV=1

B)





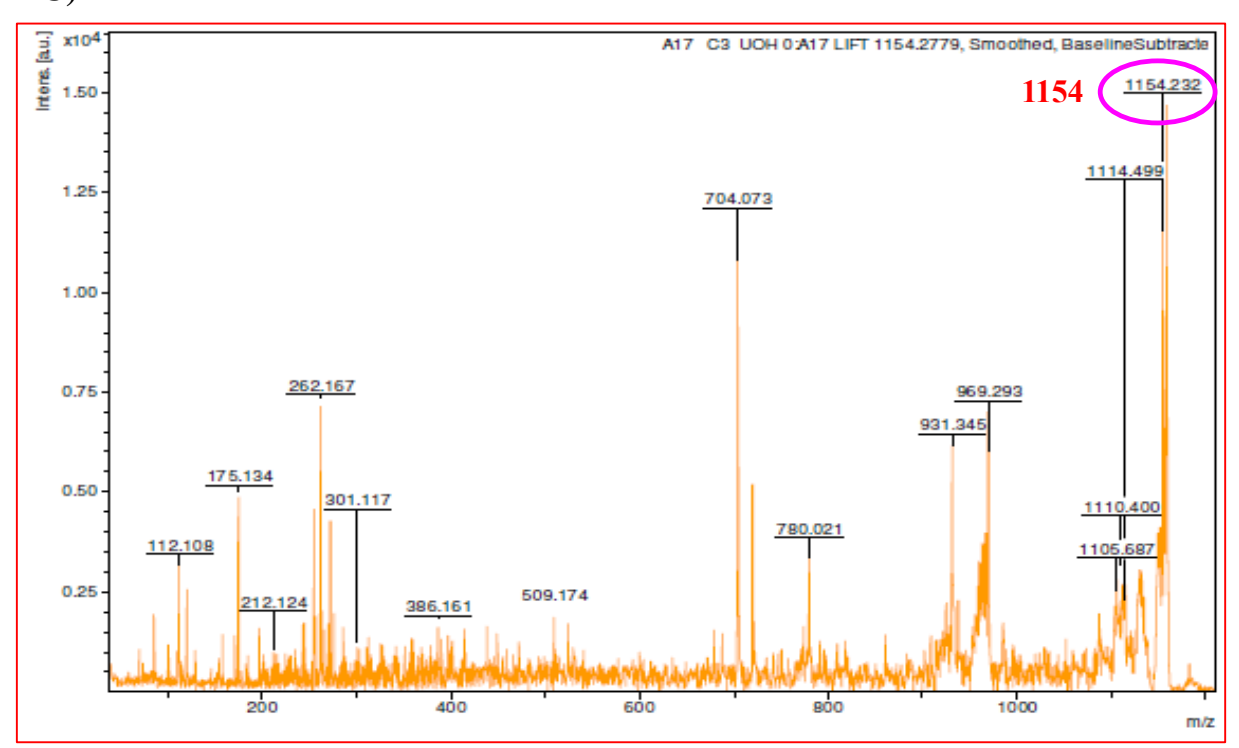


Fig. 5.10. (B): PMF spectrum of spot 3 highlighting peak 1154 (m/z); **(C)** Lift spectrum of PMF peak with m/z 1154

D)

Calculațe (RFYARNS		Peak: 1154							
N-Term.	Ion	8	b		a-17	b-17	y	C-Term.	lon
1	R	129,113	157.108	129.113	112.087	140.082	147.113	9	K
2	F	276.182	304.177	120.081	259.155	287.150	260.197	8	L
3	Υ	439.245	467.240	136.076	422.219	450.214	347.229	- 7	- 8
4	Α	510.282	538.277	44.049	493,256	521.251	461.272	6	N
5	R	666.383	694.378	129,113	649.357	677.352	617.373	5	R
6	N	780.426	808.421	87.055	763.400	791.395	688.410	4	Α
7	S	867.458	895.453	60.044	850.432	878.427	851.473	3	Υ
8	L	980.542	1008.537	86.096	963.516	991.511	998.542	2	F
9	K	1108.637	1136.632	101.107	1091.611	1119,606	1154.643	1	R

E)

Sequence coverage: 46%

MAGNFWQSSHSQQWILDKQDLLRERQHDLLSLNEDEYQKVFIFFANVIQ VLGEQLKLRQQVIATATVYFKRFYARNSLKNIDPLLLAPTCILLASKVEEFGV ISNSRLISICQSAIKTKFSYAYTQEFPYRTNHILECEFYLLENLDCCLIVYQPYR PLLQLVQDMGQEDQLLTLSWRIVNDSLRTDVCLLYPPYQIAIACLQIACVILQ KDSTKQWFAELNVDLDKVQEIVRAIVNLYEMWKDWKEKDEIQMLLS KIPKPKPPPQR

Fig. 5.10. (D): Analysis of Lift spectrum from peak m/z 1154 using Biotools; **(E)** Cyclin-C (CCNC DROPS/ Uniprot Acc. Q29AI1) sequence. Red colour indicates the partial sequence coverage by various ions generated from spot 3 while blue box indicate the matching of *denovo* (m/z 1154) sequence obtained from Biotools with one of the peptides identified by Mascot search engine.

Accession number	Protein name/Source	sequence	Similarity
			(%)
Spot number 3, (de no	vo sequence from PMF peak with m/z 1154)	RFYARNSLK	100
XP_023940149.1	Cyclin-C/ Bicyclusanyana	RFYARNSLK	100
XP_014284839.1	Cyclin-C/Halyomorphahalys	RFYARNSLK	100
XP_017847104.1	Cyclin-C/Drosophila busckii	RFYARNSLK	100
XP_030027080.1	Cyclin-C/ Manduca sexta	RFYARNSLK	100
XP_022122868.1	Cyclin-C/ Pieris-rapae	RFYARNSLK	100
XP_022826111.1	Cyclin-C/ Spodoptera litura	RFYARNSLK	100
XP_012544554.1	Cyclin-C/ Drosphila willistoni	RFYARNSLK	100
XP_002072863.1	Cyclin-C/Bombyx mori	RFYARNSLK	100
XP_0016635484.2	Cyclin-C/Aedes aegypti	RFYARNSLK *******	100

Fig. 5.10. F): Clustal alignment of *de novo* sequence from PMF peak (m/z 1154) with Cyclin-C complex, identified in NCBI database.

5.4.4. Identification of Spot 4 as Heat shock 70 kDa protein cognate 4:

Tryptic digestion of spot 4 followed by MALDI-TOF-TOF analysis showed matching to a Heat shock 70 kDa protein cognate 4 from Manduca sexta with a significant score of 354 in the Mascot search engine (Fig. 5.11A). The mass spectrum corresponding to the PMF data was represented in Figure 5.11B. When the PMF peaks with m/z 2022 (lift spectrum shown), 1691 (lift spectrum not shown) and 1215 (Lift spectrum not shown) were further ionized MALDI-TOF-TOF, the following denovo sequences 'TVQNAVITVPAYFNDSQR', 'STAGDTHLGGEDFDNR' and 'DAGTISGLNYLR' were resulted when the corresponding lift spectra are analyzed using Biotools software (Figs. **5.11C** and **D**). The various ions generated during MALDI-TOF-TOF studies showed partial sequence coverage up to 21% with Heat shock 70 kDa protein cognate 4 (Uniprot Acc No. Q9U639). Further, the de novo sequences obtained from all the above PMF peaks showed overlapping with the partial amino acid sequences recognised for Heat shock 70 kDa protein cognate 4 during MALDI-TOF-TOF analysis (Fig. 5.11E). Furthermore, Clustal alignment of the de novo sequence 'TVQNAVITVPAYFNDSQR' with available sequences in the NCBI database showed 100% matching to a Heat shock 70 kDa protein cognate from different insects such as Danaus plexippus, Papilio machaon, P. xuthus, Sesamia inferens, Leguminivora glycinivorella, Agrotis ipsilon, Helicoverpa, Trichoplusia ni and Xestia cnigrum, respectively (Fig. 5.11F). The remaining two de novo sequences also showed 100% similarity with the Heat shock 70 kDa protein cognate 4 (Clustal alignment data not shown). These results confirm that Heat shock 70 kDa protein cognate is down-regulated by 5.5-fold in the midgut tissues of the A. janata larvae when fed upon a diet containing T9BBI.

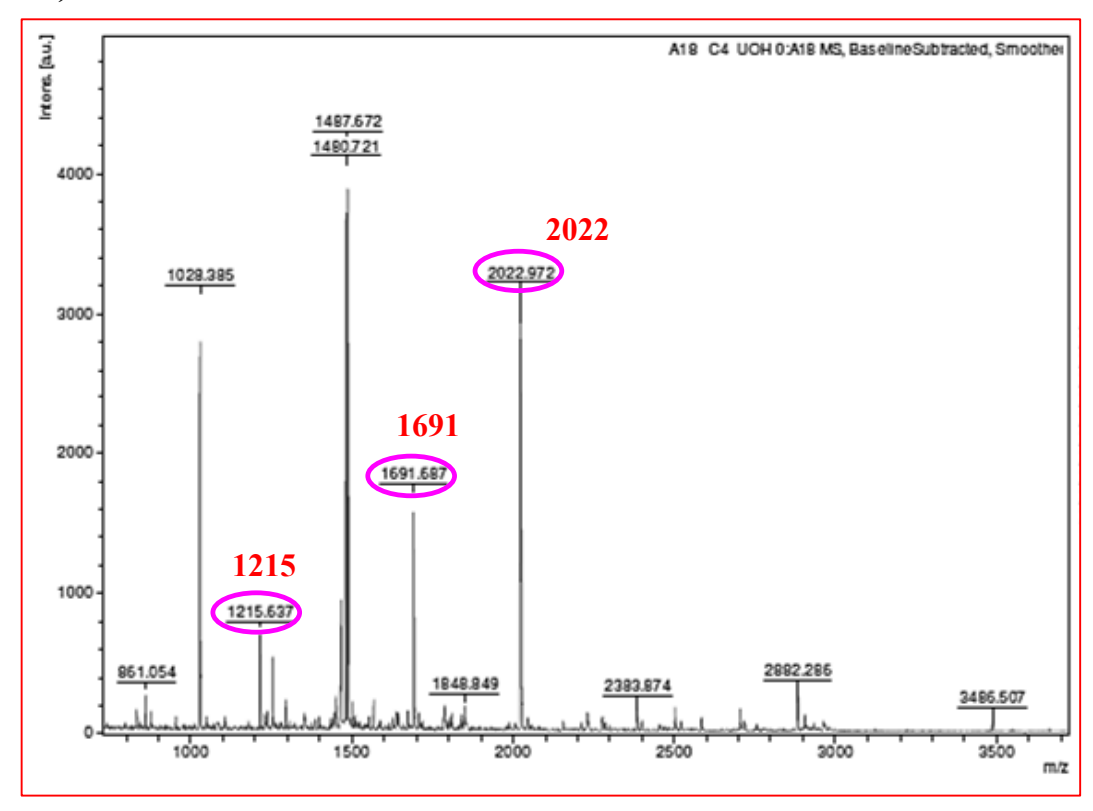
A)

Protein score is -10*Log(P), where P is the probability that the observed match is a random event. Protein scores greater than 52 are significant (p<0.05). Protein scores are derived from ions scores as a non-probabilistic basis for ranking protein hits.

ı					
		Accession	Mass	Score	Description
	1.	HSP7D_MANSE	71672	354	Heat shock 70 kDa protein cognate 4 OS=Manduca sexta OX=7130 PE=2 SV=1
	2.	HSP7D DROME	71372	159	Heat shock 70 kDa protein cognate 4 OS=Drosophila melanogaster OX=7227 GN=Hsc70-4 PE=1 SV=3
	3.	HSP68_DROME	70043	103	Heat shock protein 68 OS=Drosophila melanogaster OX=7227 GN=Hsp68 PE=1 SV=1
	4.	HSP71 DROSI	70660	101	Major heat shock 70 kDa protein Ab OS=Drosophila simulans OX=7240 GN=Hsp70Ab PE=3 SV=2
	5.	HSP70 DROME	70516	101	Major heat shock 70 kDa protein Aa OS=Drosophila melanogaster OX=7227 GN=Hsp70Aa PE=2 SV=2
	6.	HSP71 DROME	70516	101	Major heat shock 70 kDa protein Ab OS=Drosophila melanogaster OX=7227 GN=Hsp70Ab PE=2 SV=3
	7.	HSP72_DROSI	70716	101	Major heat shock 70 kDa protein Ba OS=Drosophila simulans OX=7240 GN=Hsp70Ba PE=3 SV=2
	8.	HSP72 DROME	70551	99	Major heat shock 70 kDa protein Ba OS=Drosophila melanogaster OX=7227 GN=Hsp70Ba PE=2 SV=2
	9.	HSP73 DROME	70551	99	Major heat shock 70 kDa protein Bb OS=Drosophila melanogaster OX=7227 GN=Hsp70Bb PE=2 SV=2
	10.	HSP74_DROME	70609	99	Major heat shock 70 kDa protein Bbb OS=Drosophila melanogaster OX=7227 GN=Hsp70Bbb PE=3 SV=2
	11.	HSP75 DROME	70551	99	Major heat shock 70 kDa protein Bc OS=Drosophila melanogaster OX=7227 GN=Hsp70Bc PE=2 SV=2
	12.	HSP74_ANOAL	70566	97	Heat shock protein 70 B2 OS=Anopheles albimanus OX=7167 GN=HSP70B2 PE=3 SV=1
	13.	DUOX DROME	179058	49	Dual oxidase OS=Drosophila melanogaster OX=7227 GN=Duox PE=1 SV=2
	14.	HSP7A DROSI	24100	48	Heat shock 70 kDa protein cognate 1 (Fragments) OS=Drosophila simulans OX=7240 GN=Hsc70-1 PE=2 SV=1
	15.	ACES CULPI	78758	46	Acetylcholinesterase OS=Culex pipiens OX=7175 GN=ACHE1 PE=2 SV=2
	16.	HSP7A_DROME	70871	45	Heat shock 70 kDa protein cognate 1 OS=Drosophila melanogaster OX=7227 GN=Hsc70-1 PE=1 SV=1
	17.	ACTN DROME	107636	38	Alpha-actinin, sarcomeric OS=Drosophila melanogaster OX=7227 GN=Actn PE=1 SV=2
	18.	ACTN_ANOGA	107087	35	Alpha-actinin, sarcomeric OS=Anopheles gambiae OX=7165 GN=Actn PE=3 SV=2
	19.	BRA2 CHITH	28670	34	Balbiani ring A 28 kDa protein OS=Chironomus thummi thummi OX=7155 PE=2 SV=1
	20.	RPA1 DROME	186718	34	DNA-directed RNA polymerase I subunit RPA1 OS=Drosophila melanogaster OX=7227 GN=RpI1 PE=1 SV=2

Fig. 5.11. Identification of spot 4 as Heat shock 70 kDa protein cognate 4 after tryptic digestion and MALDI-TOF-TOF analysis. (A) Histogram of MASCOT search results and corresponding protein hits.





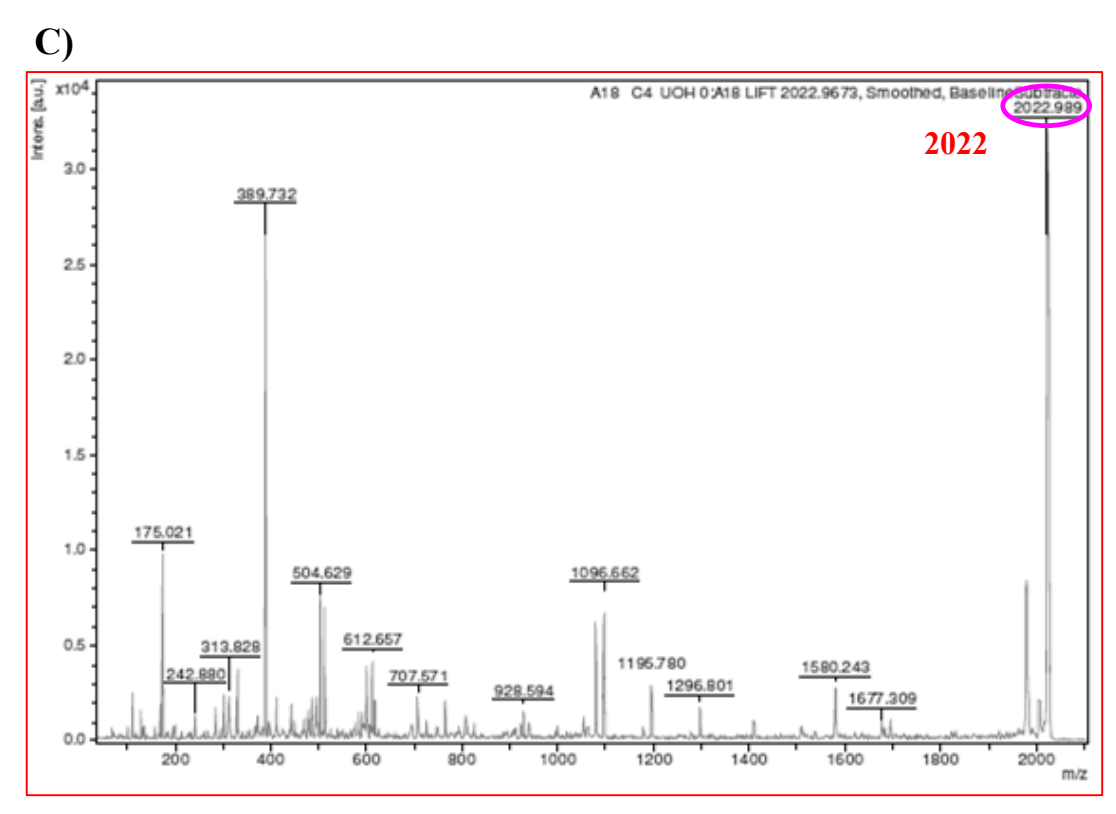


Fig. 5.11. (B): PMF spectrum of spot 4 highlighting peaks (m/z): 1215, 1691 and 2022; **(C)** Lift spectrum of PMF peak with m/z 2022.

		NDSQR	QNAVITVP					
N-Term.	Ion	а	b	I	a-17	b-17	V	C-Term.
1	T	74.060	102.055	74.060	57.033	85.028	175.119	18
2	V	173.128	201.123	72.081	156.102	184.097	303.178	17
3	Q	301.187	329.182	101.071	284.160	312.155	390.210	16
4	N	415.230	443.225	87.055	398.203	426.198	505.236	15
- 5	Α	486,267	514.262	44.049	469.241	497.235	619.279	14
6	V	585.335	613.330	72.081	568.309	596.304	766.348	13
7		698.420	726,414	86.096	681.393	709.388	929,411	12
8	Т	799,467	827,462	74.060	782,441	810,436	1000.448	- 11
9	V	898.536	926.531	72.081	881.509	909.504	1097.501	10
10	Р	995.588	1023.583	70.065	978.562	1006.557	1196,569	9
11	Α	1066,626	1094.620	44.049	1049.599	1077.594	1297.617	8
12	Y	1229,689	1257.684	136.076	1212.662	1240.657	1410.701	7
13	Ė	1376,757	1404.752	120.081	1359.731	1387.726	1509.770	6
14	N	1490.800	1518.795	87.055	1473.774	1501.769	1580.807	5
15	Ď	1605.827	1633.822	88.039	1588,801	1616.795	1694,850	4
16	S	1692.859	1720.854	60.044	1675.833	1703.828	1822,908	3
17	Q	1820.918	1848.913	101.071	1803.891	1831.886	1921.977	2
18	R	1977.019	2005.014	129,113	1959.992	1987.987	2023.024	
10	-11	1977.019	2000.014	128.118	1000.00E	1007.501	2023.024	
Calculated Masses: DAGTISGLNVLR Peak: 1215								
N-Term.	Ion	a	b	1	a-17	b-17	V.	C-Term.
1	D	88.039	116.034	88.039	71.013	99.008	175.119	12
2	A	159.076	187.071	44.049	142.050	170.045	288.203	11
3	G	216.098	244.093	30.034	199.071	227.066	387.271	10
4		317.146	345.140	74.060	300.119	328.114	501.314	9
6	S	430.230 517.262	458.225 545.257	86.096 60.044	413.203 500.235	441.198 528.230	614.398 671.420	8 7
7	G	574.283	602.278	30.034	557.257	585.251	758.452	6
8	L	687.367	715.362	86.096	670.341	698.336	871.536	5
9	Ň	901.410	829.405	87.055	784.384	812.378	972.584	4
			025.400	0,,000				
4.0	V	900.479	928.473	72.081	883,452	911.447	1029.605	3
10								
10	L	1013.563	1041.557	86.096	996.536	1024.531	1100.642	
$\overline{}$	L R	1013.563 1169.664	1041.557 1197.659	86.096 129.113	996.536 1152.637		1100.642 1215.669	
11 12 Calculated STAGDTH	d Mass	es: STA	GDTHLGG	129.113	1152.837	1024.531 1180.632	1215.869 Pea	2 1 ak: 169
11 12 Calculated STAGDTH N-Term.	d Mass LGGED	es: STA	d GDTHLGG	129.113 SEDFDNR	1152.637 a-17	1024.531 1180.632 b-17	1215.869 Pea	2 1 ak: 169
11 12 Calculated STAGDTH	d Mass	es: STA	GDTHLGG	129.113	1152.837	1024.531 1180.632	1215.869 Pea	2 1 ak: 169
11 12 Calculated STAGDTH N-Term. 1	d Mass ILGGED Ion	1169.664 es: STA DFDNR a 60.044	1197.659 GDTHLGG b 88.039	129.113 GEDFDNR I 60.044	a-17 43.018	b-17 71.013	1215.869 Pea y 175.119	2 1 ak: 169 C-Term
11 12 Calculated STAGDTH N-Term. 1	d Mass	1169.664 es: STA DFDNR a 60.044 161.092	b 88.039	129.113 EEDFDNR I 60.044	a-17 43.018	b-17 71.013	Pea y 175.119 289.162	2 1 ak: 169 C-Term 16
11 12 Calculated STAGDTH N-Term. 1	d Mass	1169.664 es: STA DFDNR a 60.044 161.092 232.129	1197.659 GDTHLGG b 88.039 189.087 260.124	129.113 EEDFDNR I 60.044 74.060 44.049	a-17 43.018 144.066 215.103	b-17 71.013 172.060 243.098	Pea y 175.119 289.162 404.189	2 1 ak: 169 C-Term 16
11 12 Calculated STAGDTH N-Term. 1	ION S	1169.664 es: STA DFDNR a 60.044 161.092 232.129 289.151	1197.659 CGDTHLGG b 88.039 189.087 260.124 317.146	129.113 EEDFDNR 1 60.044 74.060 44.049 30.034	a-17 43.018 144.066 215.103 272.124	b-17 71.013 172.060 243.098 300.119	Pea y 175.119 289.162 404.189 551.257	2 1 1 1 1 1 1 1 1 1 1 1 1 1 1 1 1 1 1 1
Calculated STAGDTH N-Term. 1 2 3 4 5	ILGGED	1169.664 es: STA DFDNR a 60.044 161.092 232.129 289.151 404.178	1197.659 D 88.039 189.087 260.124 317.146 432.173	129.113 EEDFDNR 60.044 74.060 44.049 30.034 88.039	a-17 43.018 144.066 215.103 272.124 387.151	b-17 71.013 172.060 243.098 300.119 415.146	Pea y 175.119 289.162 404.189 551.257 666.284	2 1 1 ak: 169 C-Term 16 15 14 13 12
Calculated STAGDTH N-Term. 1 2 3 4 5 6	ILGGED ION S T A G	1169.664 es: STA DFDNR 8 60.044 161.092 232.129 289.151 404.178 505.225	1197.659 D 88.039 189.087 260.124 317.146 432.173 533.220	129.113 EDFDNR 60.044 74.060 44.049 30.034 88.039 74.060	a-17 43.018 144.066 215.103 272.124 387.151 488.199	b-17 71.013 172.060 243.098 300.119 415.146 516.194	Pea y 175.119 289.162 404.189 551.257 666.284 795.327	2 1 1 ak: 169 C-Term 16 15 14 13 12 11
11 12 Calculated STAGDTH N-Term. 1 2 3 4 5 6 7	ILGGED	1169.664 es: STA DFDNR 8 60.044 161.092 232.129 289.151 404.178 505.225 642.284	1197.659 b 88.039 189.087 260.124 317.146 432.173 533.220 670.279	129.113 EDFDNR 60.044 74.060 44.049 30.034 88.039 74.060 110.071	a-17 43.018 144.066 215.103 272.124 387.151 488.199 625.258	b-17 71.013 172.060 243.098 300.119 415.146 516.194 653.253	Pea y 175.119 289.162 404.189 551.257 668.284 795.327 852.348	2 1 1 ak: 169 C-Term 16 15 14 13 12 11 10
Calculated STAGDTH N-Term. 1 2 3 4 5 6	ILGGED ION S T A G	1169.664 es: STA DFDNR 8 60.044 161.092 232.129 289.151 404.178 505.225	1197.659 D 88.039 189.087 260.124 317.146 432.173 533.220	129.113 EDFDNR 60.044 74.060 44.049 30.034 88.039 74.060	a-17 43.018 144.066 215.103 272.124 387.151 488.199	b-17 71.013 172.060 243.098 300.119 415.146 516.194	Pea y 175.119 289.162 404.189 551.257 666.284 795.327	2 1 1 ak: 169 C-Term 16 15 14 13 12 11 10
11 12 Calculated STAGDTH N-Term. 1 2 3 4 5 6 7	ILGGED S ILGGED S I T A G D	1169.664 es: STA DFDNR 8 60.044 161.092 232.129 289.151 404.178 505.225 642.284	1197.659 b 88.039 189.087 260.124 317.146 432.173 533.220 670.279 783.363	129.113 EDFDNR 60.044 74.060 44.049 30.034 88.039 74.060 110.071	a-17 43.018 144.066 215.103 272.124 387.151 488.199 625.258	b-17 71.013 172.060 243.098 300.119 415.146 516.194 653.253	Pea y 175.119 289.162 404.189 551.257 668.284 795.327 852.348	2 1 1 ak: 169 C-Term 16 15 14 13 12 11 10 9
11 12 Calculated STAGDTH N-Term. 1 2 3 4 5 6 7 8	Ion S G D T H L G	1169.664 es: STA DFDNR 8 60.044 161.092 232.129 289.151 404.178 505.225 642.284 755.368 812.390	1197.659 D 88.039 189.087 260.124 317.146 432.173 533.220 670.279 783.363 840.385	74.060 44.049 30.034 88.039 74.060 110.071 86.096 30.034	a-17 43.018 144.066 215.103 272.124 387.151 488.199 625.258 738.342 795.363	b-17 71.013 172.060 243.098 300.119 415.146 516.194 653.253 766.337 823.358	y 175.119 289.162 404.189 551.257 668.284 795.327 852.348 909.370 1022.454	2 1 1 ak: 169 C-Term 16 15 14 13 12 11 10 9
11 12 Calculated STAGDTH N-Term. 1 2 3 4 5 6 7 8 9	ILGGED ION S IT A G D T H L G G G	1169.664 es: STA DFDNR a 60.044 161.092 232.129 289.151 404.178 505.225 642.284 755.368 812.390 869.411	1197.659 D 88.039 189.087 260.124 317.146 432.173 533.220 670.279 783.363 840.385 897.406	74.060 44.049 30.034 88.039 74.060 110.071 88.096 30.034 30.034	a-17 43.018 144.066 215.103 272.124 387.151 488.199 625.258 738.342 795.363 852.385	b-17 71.013 172.060 243.098 300.119 415.146 516.194 653.253 766.337 823.358 890.380	Y 175.119 289.162 404.189 551.257 668.284 795.327 852.348 909.370 1022.454 1159.513	2 1 1 ak: 169 C-Term 16 15 14 13 12 11 10 9 8 7
11 12 Calculated STAGDTH N-Term. 1 2 3 4 5 6 7 8 9 10	I Mass	1169.664 es: STA DEDNR 8 60.044 161.092 232.129 289.151 404.178 505.225 642.284 755.368 812.390 869.411 996.454	1197.659 D 88.039 189.087 260.124 317.146 432.173 533.220 670.279 783.363 840.385 897.406 1026.449	74.060 44.049 30.034 88.039 74.060 110.071 88.096 30.034 30.034 102.055	a-17 43.018 144.066 215.103 272.124 387.151 488.199 625.258 738.342 795.363 852.385 981.427	b-17 71.013 172.060 243.098 300.119 415.146 516.194 653.253 766.337 823.358 880.380 1009.422	Y 175.119 289.162 404.189 551.257 668.284 795.327 852.348 909.370 1022.454 1159.513 1260.560	2 1 1 ak: 169 C-Term 16 15 14 13 12 11 10 9 8 7
11 12 Calculated STAGDTH N-Term. 1 2 3 4 5 6 7 8 9 10 11	I Mass	1169.664 es: STA DEDNR 8 60.044 161.092 232.129 289.151 404.178 505.225 642.284 755.368 812.390 869.411 996.454 1113.481	1197.659 b 88.039 189.087 260.124 317.146 432.173 533.220 670.279 783.363 840.385 897.406 1026.449 1141.476	74.060 44.049 30.034 88.039 74.060 110.071 86.096 30.034 30.034 102.055 88.039	a-17 43.018 144.066 215.103 272.124 387.151 488.199 625.258 738.342 795.363 852.385 981.427 1096.454	b-17 71.013 172.060 243.098 300.119 415.146 516.194 653.253 766.337 823.358 890.390 1009.422 1124.449	y 175.119 289.162 404.189 551.257 666.284 795.327 852.348 909.370 1022.454 1159.513 1260.560	2 1 1 ak: 169 C-Term 16 15 14 13 12 11 10 9 8 7 6
11 12 Calculated STAGDTH N-Term. 1 2 3 4 5 6 7 8 9 10 11 12 13	ILGGED ION S IT A G D T H L G G E D F	1169.664 es: STA DEDNR 8 60.044 161.092 232.129 289.151 404.178 505.225 642.284 755.368 812.390 889.411 998.454 1113.481 1260.549	1197.659 b 88.039 189.087 260.124 317.146 432.173 533.220 670.279 783.363 840.385 897.406 1026.449 1141.476 1289.544	74.060 44.049 30.034 88.039 74.060 110.071 86.096 30.034 30.034 102.055 88.039 120.081	a-17 43.018 144.066 215.103 272.124 387.151 488.199 625.258 738.342 795.363 852.385 981.427 1096.454 1243.523	b-17 71.013 172.060 243.098 300.119 415.146 516.194 653.253 766.337 823.358 880.380 1009.422 1124.449 1271.517	Y 175.119 289.162 404.189 551.257 668.284 795.327 852.348 909.370 1022.454 1159.513 1260.560 1375.587	2 1 1 ak: 169 C-Term 16 15 14 13 12 11 10 9 8 7 6
11 12 Calculated STAGDTH N-Term. 1 2 3 4 5 6 7 8 9 10 11 12	I Mass	1169.664 es: STA DEDNR 8 60.044 161.092 232.129 289.151 404.178 505.225 642.284 755.368 812.390 869.411 996.454 1113.481	1197.659 b 88.039 189.087 260.124 317.146 432.173 533.220 670.279 783.363 840.385 897.406 1026.449 1141.476	74.060 44.049 30.034 88.039 74.060 110.071 86.096 30.034 30.034 102.055 88.039	a-17 43.018 144.066 215.103 272.124 387.151 488.199 625.258 738.342 795.363 852.385 981.427 1096.454	b-17 71.013 172.060 243.098 300.119 415.146 516.194 653.253 766.337 823.358 890.390 1009.422 1124.449	y 175.119 289.162 404.189 551.257 666.284 795.327 852.348 909.370 1022.454 1159.513 1260.560	2 1 1 ak: 169 C-Term 16 15 14 13 12 11 10 9 8 7 6 4 3

Fig. 5.11. (D) Analysis of Lift spectrum from peaks m/z 2022, 1215 and 1691.

E)

Heat shock cognate 70 kDa protein cognate: 21%

MAKAPAVGIDLGTTYSCVGVFQHGKVEIIANDQGNRTTPSYVAFTDTDRLIGD AAKNQVAMNPNNTIFDAKRLIGRKFEDATVQADMKHWPFEVVSDGGKPKIKV AYKGEDKTFPEEVSSMVLTKMKETAEAYLGKTVQNAVITVPAYFNDSQRQAT KDAGTISGLNVLRINEPTAAAIAYGLDKKGSGERNVLIFDLGGGTFDVSILTIED GIFEVKSTAGDTHLGGEDFDNRMVNHFVQEFKRKYKKDLTTNKRALRRLRTA CERAKRTLSSSTQASIEIDSLFEGIDFYTSITRARFEELNADLFRSTMEPVEKSLRD AKMDKSQIHDIVLVGGSTRIPKVQKLLQDFFNGKELNKSINPDEAVAYGAAVQAA ILHGDKSEEVQDLLLLDVTPLSLGIETAGGVMTTLIKRNTTIPTKQTQTFTTYSDN QPGVLIQVFEGERAMTKDNNLLGKFELTGIPPAPRGVPQIEVTFDIDANGILNVSA VEKSTNKENKITITNDKGRLSKEEIERMVNEAEKYRNEDEKQKETIQAKNALESY CFNMKSTMEDEKLKDKISDSDKQTILDKCNDTIKWLDSNQLADKEEYEHKQKEL

Fig. 5.11. (E).Heat shock 70 kDa protein cognate (HSP70 MANSE/Uniprot Acc. Q9U639) sequence. Red colour indicates the partial sequence coverage by various ions generated from spot 4 while blue box indicate the matching of *de novo* (m/z 2022, 1215 and 1691) sequence obtained from Biotools with one of the peptides identified by Mascot search engine.

Accession number	Protein name/ source	Sequence	Similarity (%)
Spot number xx (de	e novo sequence from PMF peak with m/z 2022)	TVQNAVITVPAYFNDSQR	100
OWR45261.1	Heat shock protein cognate 4/ Danaus plexippus plexippus	TVQNAVITVPAYFNDSQR	100
KPJ19257.1	Heat shock 70 kDa protein cognate 4 / Papilio machaon	TVQNAVITVPAYFNDSQR	100
KPJ05447.1	Heat shock 70 kDa protein cognate 4 / Papilio xuthus	TVQNAVITVPAYFNDSQR	100
AIZ00749.1	heat shock cognate 70 protein, partial/ Sesamia inferens	TVQNAVITVPAYFNDSQR	100
AGQ50301.1	heat shock cognate 70 / Leguminivora glycinivorella	TVQNAVITVPAYFNDSQR	100
AEG78288.1	heat shock protein 70/ Agrotis ipsilon	TVQNAVITVPAYFNDSQR	100
XP_021197880.1	heat shock 70 kDa protein cognate 4/ Helicoverpa armigera	TVQNAVITVPAYFNDSQR	100
XP_026745076.1	heat shock 70 kDa protein cognate 4/ Trichoplusia ni	TVQNAVITVPAYFNDSQR	100
AGQ50302.1	heat shock cognate 70 / Xestia c-nigrum	TVQNAVITVPAYFNDSQR ************	100

Fig. 5.11 F) Clustal alignment of *de novo* sequence from PMF peak (m/z 2022) with Heat shock protein cognate 4 complex identified in NCBI database.

Heat shock proteins (HSPs) are molecular chaperones present in all living organisms. They are highly conserved ubiquitous proteins expressed during temperature and other stresses such as heavy metal exposure, insecticides, desiccation and parasites (Yi et al., 2018). Hsp 70 is important for the survival and recovery of organisms at the time of stress. During metamorphosis, the heat shock gene Hsp 70 and the immune gene *Cecropin A* are expressed together, indicating that it might be a period of enhanced stress (Ekengren and Hultmark, 2001). Hsp 70 cognates are functionally linked to Hsp 70 and this association is required during normal development (Craig et al., 1982) as well as during stress response. Earlier studies showed that treatment with pesticides containing high fluoride content (Dutta et al. 2017) and pyrethroid (konus et al., 2013) downregulated the Hsp 70 cognate. Corroborating with these studies, feeding of T9BBI downregulated the Hsp 70 cognate in the midgut tissues to *A. janata* larvae in the present study (Figs. 5.6 and 5.7). Thus, at low levels of HSP 70 cognate, the T9BBI (8 μg/cm²) fed larvae might have failed to cope with the stress associated with metamorphosis and resulted in the emergence of abnormal larval-pupal intermediates (Fig. 5.5).

5.4.5. Identification of Spot 5 as protein Turandot:

Tryptic digestion of spot 5 followed by MALDI-TOF-TOF analysis showed a significant score of 89 with protein Turandot of *D. Pseudoobsura* in Mascot search engine (Fig. 5.12A). The PMF spectrum obtained was represented in Figure 5.12B. The following *de novo* sequence 'DDQYDTEKSR' was obtained for the lift spectrum (data not shown) by Biotools software when the PMF peak with m/z 1256 was ionized in MALDI-TOF-TOF, (Figs. 5.12C). Also, the various ions generated during MALDI-TOF-TOF studies showed partial sequence coverage of up to 75% with protein Turandot (Uniprot Acc No. Q299E6). Further, the *de novo* sequence obtained from PMF peak with m/z 1256 showed overlapping with the partial amino acid sequence recognised for protein Turandot (Fig. 5.12D). Furthermore, Clustal alignment of this *de novo* sequence with available sequences in NCBI database showed significant matching (90-100%) with protein Turandot from *D. persimilis*, *D. pseudoobscura* and *D. miranda* (Fig. 5.12E). These results confirm that protein Turandot

is down regulated by 2.3-fold when the *A. janata* larvae were exposed to the diet containing T9BBI.



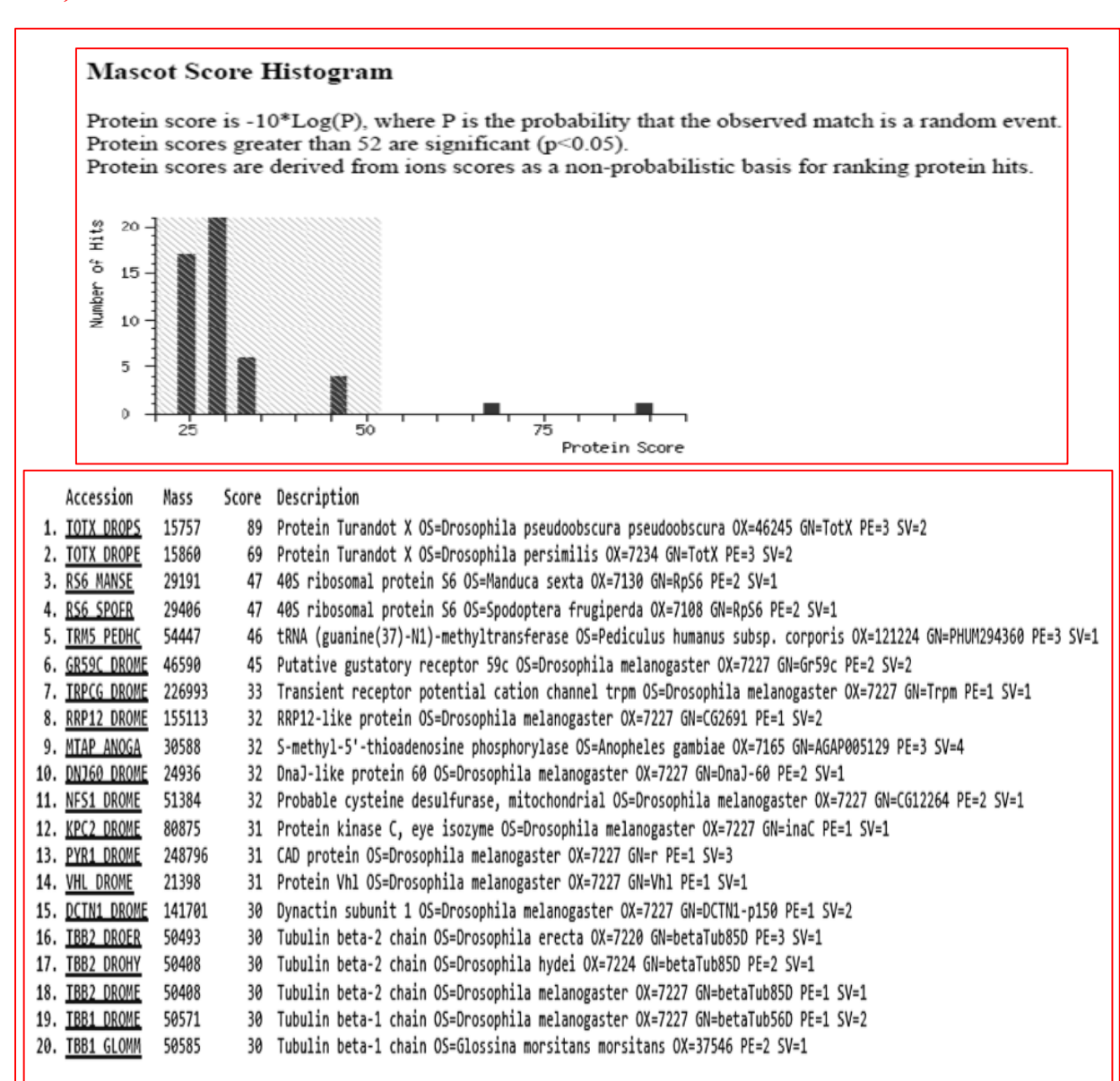
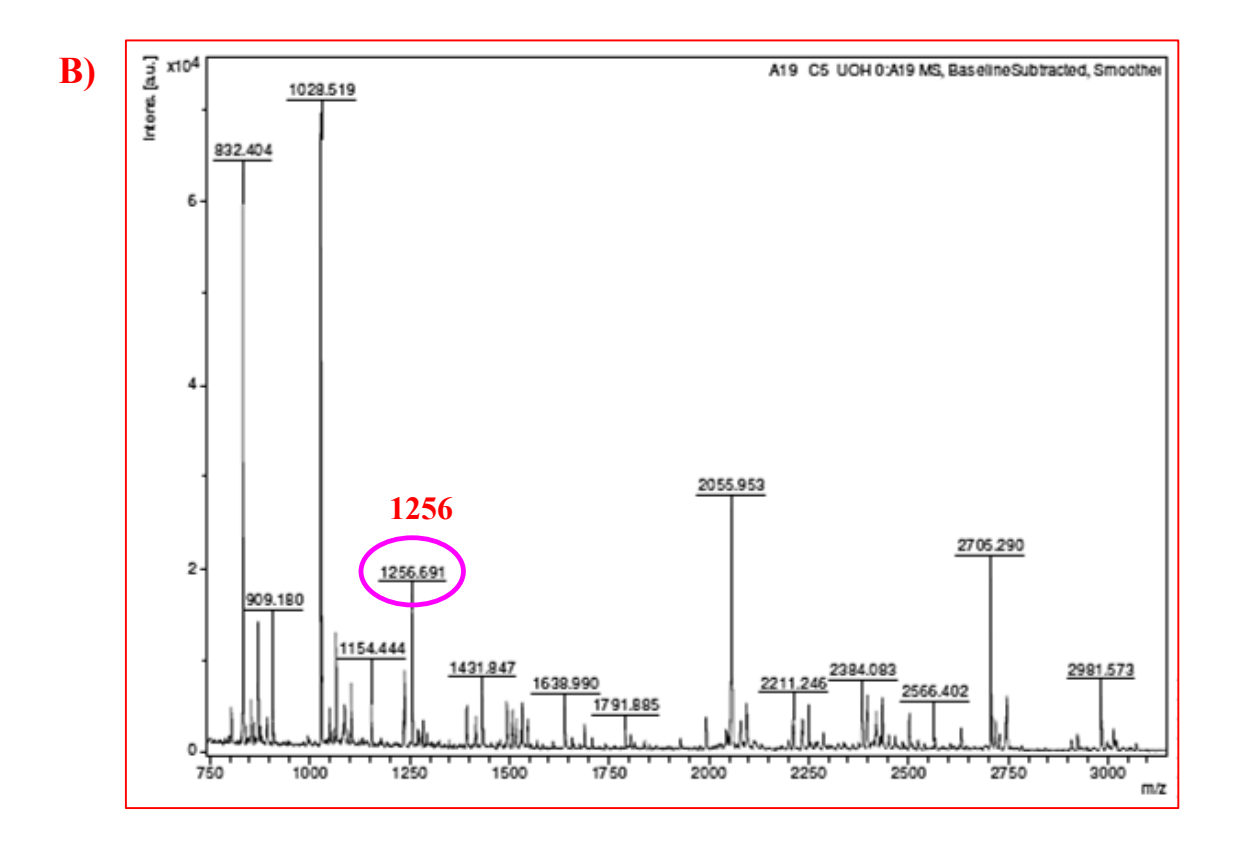


Fig. 5.12. Identification of spot 5 as protein Turandot, after tryptic digestion and MALDI-TOF-TOF analysis. (A) Histogram of MASCOT search results and corresponding protein hits.



C)

alculațe DQYDTE		6 S C	DDQYDTEKSR				Peak: 1256			
N-Term.	ion	а	b	1	a-17	b-17	٧	C-Term.	lor	
1	D	88.039	116.034	88.039	71.013	99.008	175.119	10	R	
2	D	203.066	231.061	88.039	186.040	214.035	262.151	9	8	
3	Q	331.125	359.120	101.071	314.098	342.093	390.246	8	K	
4	Y	494.188	522.183	136.076	477.162	505.157	519.289	7	Е	
5	D	609.215	637.210	88.039	592.189	620.183	620.336	6	T	
6	Т	710.263	738.258	74.060	693,236	721.231	735.363	5		
7	E	839.305	867.300	102.055	822.279	850.274	898.426	4	Y	
8	K	967.400	995.395	101.107	950.374	978.369	1026,485	3	0	
9	S	1054.432	1082.427	60.044	1037.406	1065.401	1141.512	2		
10	R	1210.533	1238.528	129.113	1193,507	1221.502	1256.539	1	D	

Fig. 5.12. (B) PMF spectra of spot 5 highlighting peak 1256 (m/z); **C)** Analysis of lift spectrum from peak m/z 1256 using Biotools.

D)

Sequence coverage: 75%

MRVPVFQLSCLLGLIVCLLCSVKAQKDDQYDTEKSR LEIYNNPAVDEFTKERNIPKLIEFYRRYPARIQ LPDADKRQWDEFVARYTESQTKLVDGLPAQGGWVGSVLSSTVGNLIAKFIFSLIRYDPTTPKPIGAP

Accession number	Protein name/ Source	Sequence	Similarity (%)
Spot number 5 (de novo s	sequence from PMF peak with m/z 1256)	DDQYDTEKSR	100
XP_026850667.1	protein Turandot X/ Drosophila persimilis	DDQYDTEKSR	100
XP_001358616.3	protein Turandot X/ Drosophila pseudoobscura	DDQYDTEKSR	100
XP_017139532.1	protein Turandot X/ Drosophila miranda	DDQYDTERSR ****** **	90

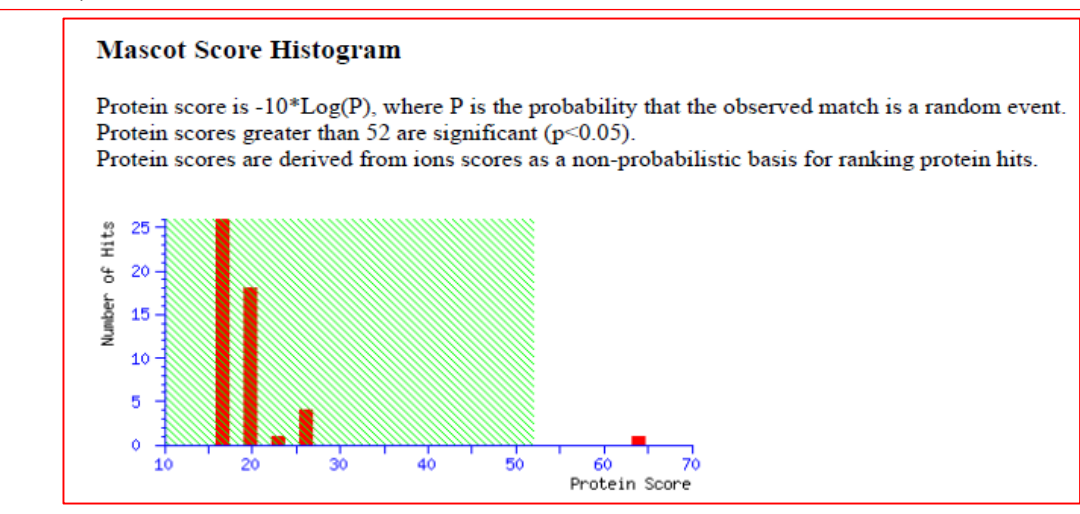
Fig. 5.12. (D): Protein Turandot (TOTX DROPS/Uniprot Acc. Q299E6) sequence. Red colour indicates the partial sequence coverage by various ions generated from spot 5 while blue box indicate the matching of *de novo* (m/z 1256) sequence obtained from Biotools with one of the peptides identified by Mascot search engine; **(E):** Clustal alignment of *de novo* sequence from PMF peak (m/z 1256) with Cyclin-C complex, identified in NCBI database.

Turandot X (Tot X) is a humoral factor which contributes to stress tolerance and it belongs to a poorly characterised class of secretory peptides. Turandot genes are expressed through the JAK-STAT signalling pathway in the fat body during stress conditions. It was also known to play a major role in the adaptation of (i) *Drosophila simulans* to daily fluctuating thermal conditions (Manenti et al., 2018), (ii) *D. melanogaster* to cold stress conditions (Salehipourshirazi et al., 2017), (ii) *Diatraea saccharalis* to microbial stress (Rocha et al., 2016) and (iv) *Drosophila* model to neurotoxicant Methyl mercury (MeHg) stress (Mahapatra et al., 2012). Also, paraquat-induced oxidative stress is known to activate Tot A, Tot X and Tot Z genes (Ekengren and Hultmark. 2001). Thus, the downregulation of protein Turandot X in the midgut tissue of *A. janata* larvae in the presence of T9BBI suggests its importance to cope up with nutritional stress caused possibly due to binding of T9BBI to its cognate proteases in the midgut, which eventually lead to the retardation in the growth of the larvae (Figs. 5.3-5.7 and 5.12).

5.4.6. Identification of Spot 6 as Pigment dispersing hormone (PDH) peptide:

Digestion of spot 6 with trypsin followed by MALDI-TOF-TOF showed matching to a PDH peptide of an insect *Romalea microptera* with a significant score of 64 in Mascot search analysis (**Fig. 5.13A**). The spectrum related to the PMF data was represented in Figure 5.13B. When the PMF peak with m/z 2387 was further ionized in MALDI-TOF-TOF, the resulting lift spectrum showed the following *de novo* sequence '**ELASWLAQLAHKNEP**' when analyzed using Biotools software (**Figs. 5.13C and D**). Also, the various ions generated during MALDI-TOF-TOF studies showed a partial sequence coverage up to 68% with a PDH peptide (Uniprot Acc No. P09929). Further, the *de novo* sequence obtained from PMF peak (m/z 2387) showed overlapping with the partial amino acid sequence recognised for pigment dispersing hormone peptide (**Fig. 5.13E**). Furthermore, Clustal alignment of this *de novo*

A)



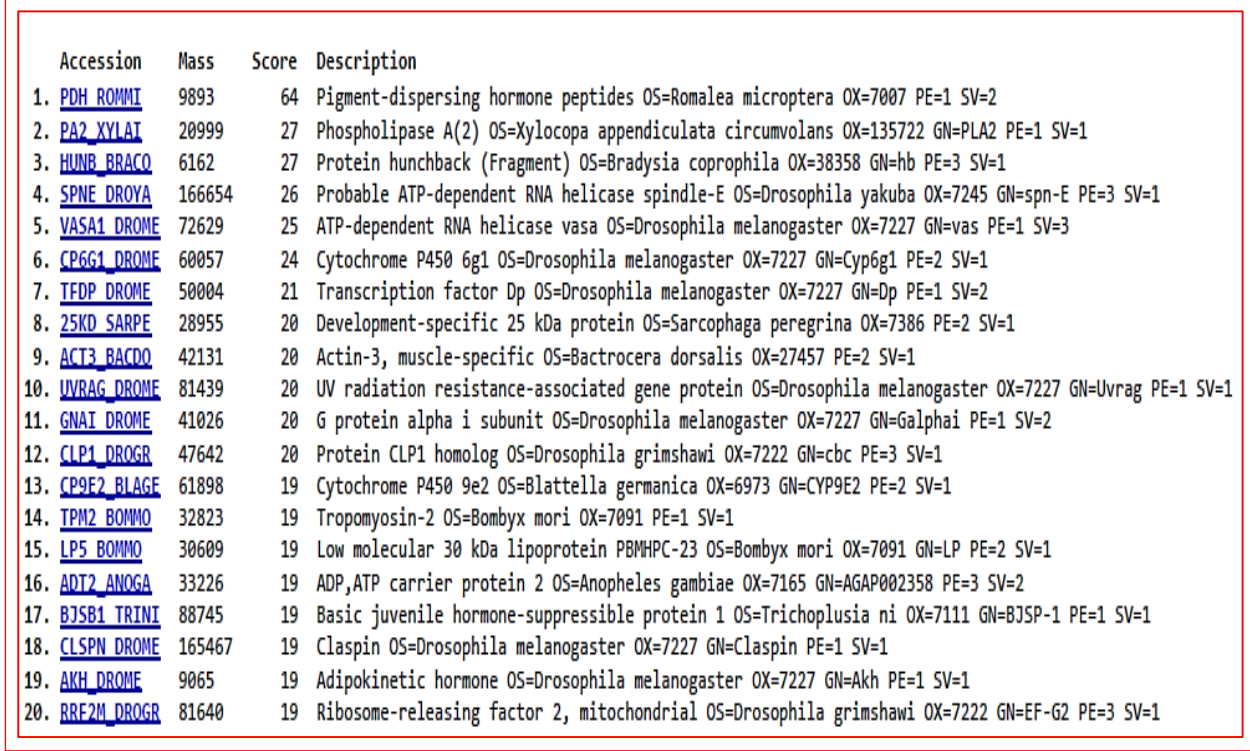
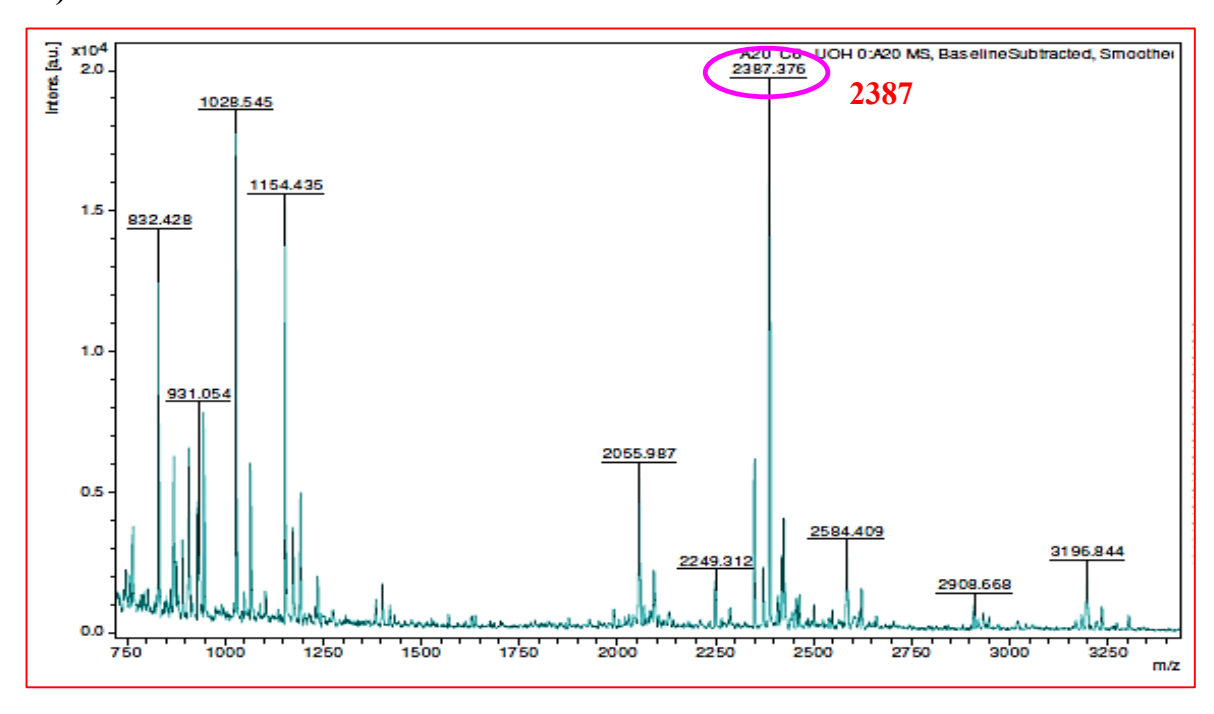


Fig. 5.13. Identification of spot 6 as Pigment dispersing hormone peptide and MALDI-TOF-TOF analysis. (A) Histogram of MASCOT search results and corresponding protein hits.

B)



C)

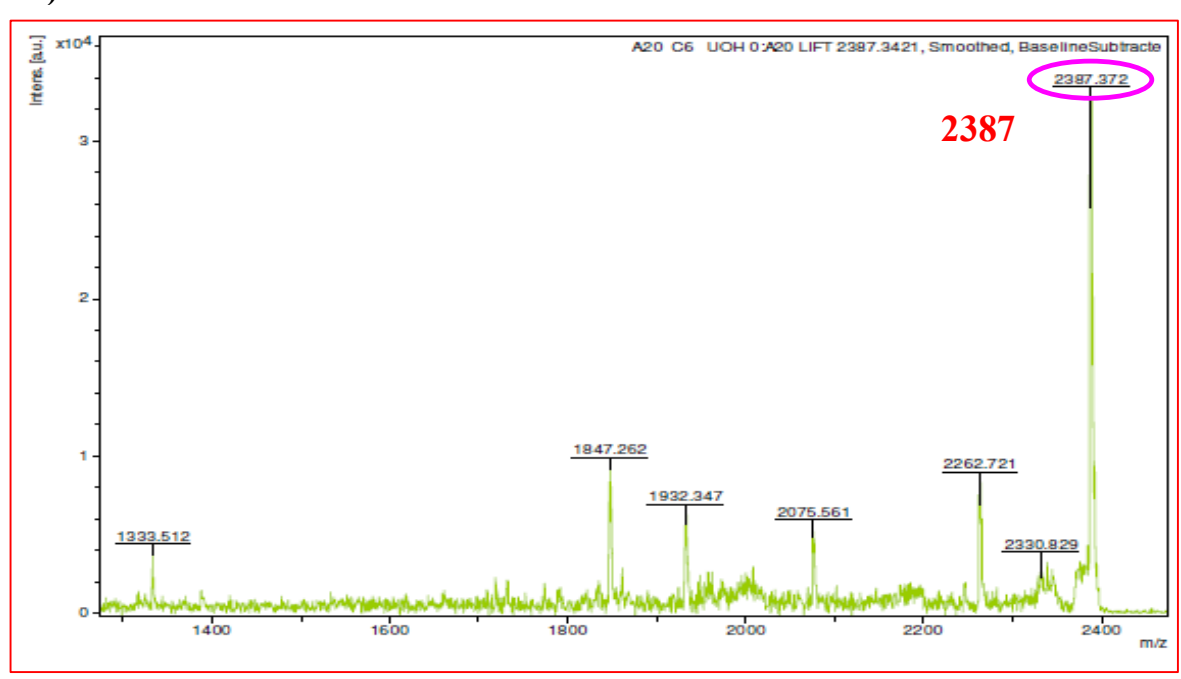


Fig. 5.13. (B): PMF spectrum of spot 6 highlighting peak 2387 (m/z); **(C)** Lift spectrum of PMF peak 2387 m/z.

D)

V-Term.	Ion	8	b	1	a-17	b-17	A	C-Term.	9
1	E	102.055	130.050	102.055	85.028	113.023	147.113	21	K
2	L	215.139	243.134	86.096	198.112	226.107	284.172	20	_
3	A	296.176	314.171	44.049	269.150	297.144	355.209	19	A
4	8	373.208	401.203	60.044	356.182	384.177	515.239	18	-
9	W	559.287	587.282	159.092	542.261	570.256	628.324	17	
6	L	672.372	700.366	86.096	655.345	683.340	699.361	16	*
7	A	743.409	771.404	44.049	726.382	754.377	796.413	15	
8	Q	871.467	899.462	101.071	854.441	882.436	925,456	14	
9	L	984.551	1012.546	86.096	967.525	995.520	1039,499	13	
10	A	1055.588	1083.583	44.049	1038.562	1066.557	1167.594	12	*
11	Н	1192.647	1220.642	110.071	1175.621	1203.616	1304,653	11	_
12	K	1320.742	1348.737	101.107	1303.716	1331.711	1375,690	10	A
13	N	1434.785	1462.780	87.055	1417.759	1445.754	1488.774	9	
14	Е	1563.828	1591.823	102.055	1546.801	1574.796	1616.833	8	9
15	P	1660.881	1688.875	70.065	1643.854	1671.849	1687,870	7	4
16	A	1731.918	1759.913	44.049	1714.891	1742.886	1800.954	6	L
17		1845.002	1872.997	86.096	1827.975	1855.970	1987.033	5	*
18	С	2005.032	2033.027	133.043	1988.006	2016.001	2074.065	4	99
19	A	2076.070	2104.064	44.049	2059.043	2087.038	2145.102	3	*
20	Н	2213.128	2241.123	110.071	2196.102	2224.097	2258.186	2	L
21	K	2341.223	2369.218	101.107	2324,197	2352.192	2387,229	1	

E)

Sequence coverage: 68%

MTAMAVSGKLLTALVLSTYILGLALTIQATQYEEDKYQENEVKYGR
ELASWLAOLAHKNEPAICAHKRNSEIINSLLGLPKLLNDAGRK

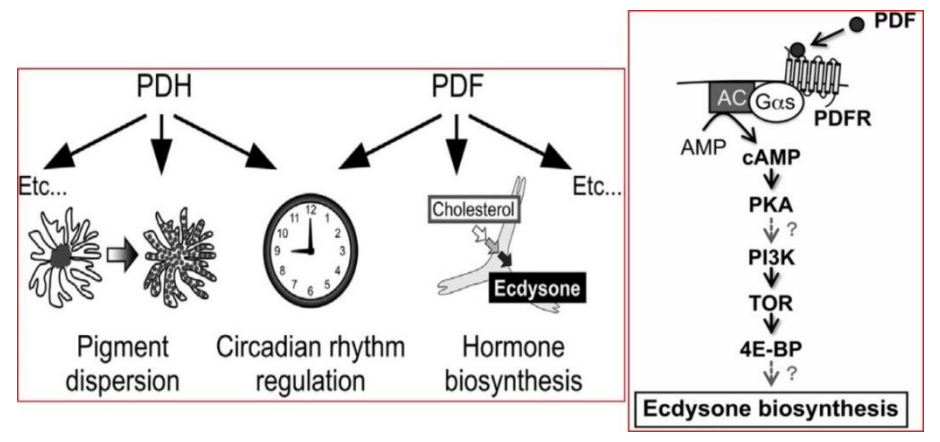
Fig. 5.13. (D): Analysis of Lift spectrum from peak m/z 2387 using Biotools; **(E)** Pigment dispersing hormone peptide (PDH_ROMMI/Uniprot Acc. P09929) sequence. Red colour indicates the partial sequence coverage by various ions generated from spot 6 while blue box indicate the matching of *de novo* (m/z 2387) sequence obtained from Biotools with one of the peptides identified by Mascot search engine.

F)

Accession	Protein name / Source	Sequence	Similarity
number			(%)
Spot number x	x (<i>de novo</i> sequence from PMF peak with m/z	ELASWLAQLAHKNEP	100
2387)			
P09929.2	Pigment-dispersing hormone peptide/ Romalea microptera	ELASWLAQLAHKNEP	100
AKN21252.1	pigment-dispersing factor, partial/ Locusta migratoria	ELA TL LAQLAHKNEP	87
ACY02888.1	pigment dispersing factor precursor/ Schistocerca gregaria	ELATILLAQLAHKNEP *** *** *** *** ***	87

Fig. 5.13. (**F**) Clustal alignment of *de novo* sequence from PMF peak (m/z 2387) with pigment dispersing hormone peptide, identified in NCBI database.

sequence with those available in NCBI database showed significant matching (87-100%) with several PDH peptides from the following insects: Romalea microptera, Locusta migratoria and Schistocerca gregaria (Fig 5.13F). These results confirm that PDH peptide is down regulated by 4.1-fold in the midgut tissue of the A. janata larvae upon feeding on a diet supplemented with T9BBI. PDH regulates the dispersion of retinal screening pigments and photo transduction process and the integumental chromatophores as well as crustacean circadian rhythms. Though insects do not have integumental chromatophores, PDH is known to be involved in the regulation of circadian rhythms, courtship behaviour, locomotor activity and male sex pheromone production in Drosophila. Also, PDH-like peptides are known to affect locomotion behaviour in nematodes (Janssen et al., 2009). On the other hand, the function of pigment dispersing factor (PDF), the orthologue of PDH peptide was reported in the B. mori larvae. It is known to influence the prothoracic gland, ecdysteroidogenic organs and biosynthesis of ecdysone, which stimulates metamorphosis and thereby regulates molting in B. mori (Iga et al., 2004). The matching of the spot 6 with PDH peptide in the present study suggests that feeding of the A. janata larvae with T9BBI has a significant influence on the synthesis of this peptide (Figs. 5.6. 5.7 and 5.13). Thus, down regulation of this peptide might have delayed the transition of the larva to pupa as well as negatively impacted the process of metamorphosis leading to the emergence of the abnormal larval-pupal intermediates when the larvae were fed upon the T9B BI (Figs. 5.3-5.7 and Table 5.1).

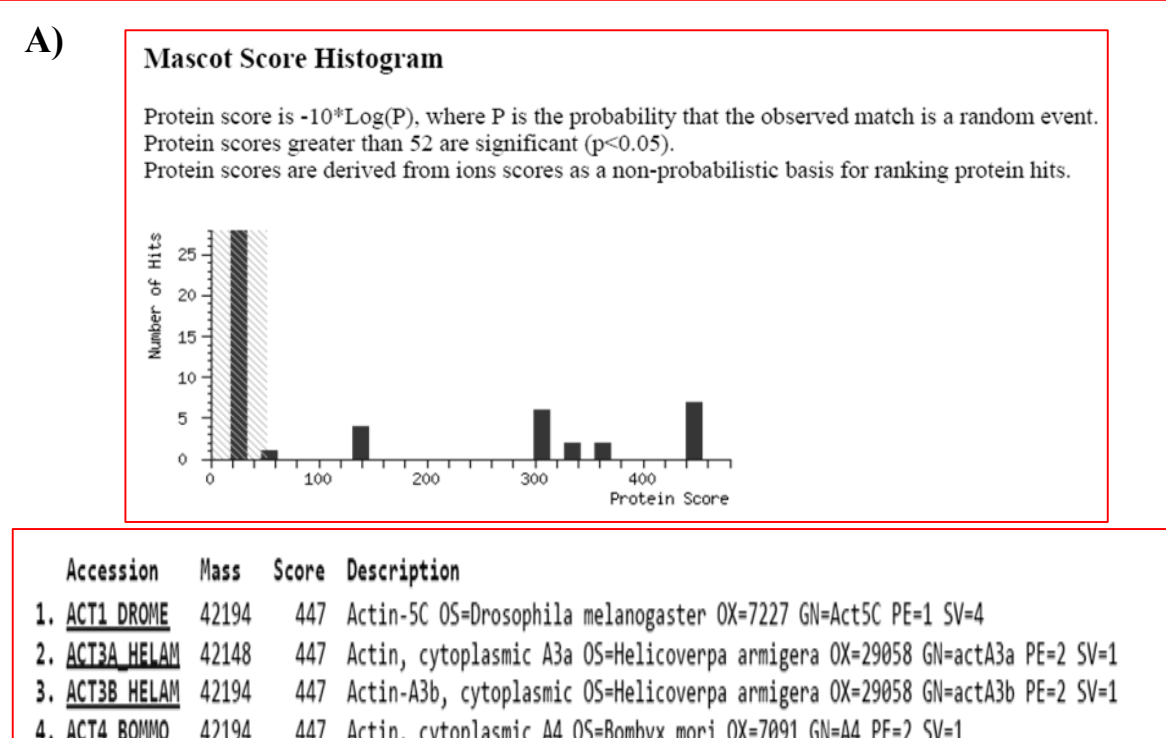


Supplementary Fig. 5.4. PDH/PDF function and signalling model (Adapted from Iga, M. 2016)

5.4.7. Identification of Spot 7 and Spot 8 as Actin-5C:

Digestion of the spot 7 and spot 8 with trypsin followed by MALDI-TOF-TOF analysis showed matching to Actin-5C of D. melanogaster with a significant score of 447 and 398, respectively, in the mascot search engine (Figs. 5.14A and 5.15A). The spectra for the corresponding PMF data was represented in the Figures 5.14B and 5.15B. The following de novo sequences 'TTGIVLDSGDGVHSTVPIYEGYALPHAILR' and 'AVFPSIVG', were derived from the lift spectra using bio tools software when the PMF peaks with m/z 3151 and m/z 1198 from spot 7 and spot 8 were further ionized by MALDI-TOF-TOF (Figs. 5.14C) and D; 5.15C and D). Also, the various ions generated from spot 7 and spot 8 during MALDI-TOF-TOF showed a partial sequence coverage of up to 58% and 51%, respectively with Actin-5C. Further, the de novo sequences derived from PMF peaks m/z 3151 and m/z 1198 also showed overlapping with the partial amino acid sequence(s) recognised for Actin-5C (Uniprot Acc No. Q299E6) (Fig. 5.14E and 5.15E). Furthermore, Clustal alignment of the de novo sequence from spot 7 with the available data in NCBI database showed 100% matching with Actin-5C from Bristowia sp. gabon, Sidusa sp. french guiana 2, D. mauritiana, Timema douglasi, S. litura, B. mori (Fig. 5.14F). In contrast, Clustal alignment of the de novo sequence from spot 8 with the available data in NCBI database showed 100% matching with Actin-5 from Pyricularia oryzae, Colletotrichum truncatum, C. coccodes, Paraphaeosphaeria, Malletia abyssorum, Phyllosticta citricarpa. These results confirm that Actin-5C is up-regulated by 6.8-fold (spot 7) and 5.7-fold (spot 8), respectively, in the midgut tissue of A. janata larvae upon feeding on a diet supplemented with T9BBI (Figs. 5.6, 5.7, **5.14 and 5.15**).

In general, actin which is ubiquitously expressed in all eukaryotic cells act as a critical element in cytoskeleton integrity and plays a main role in numerous cellular practices such as vesicle movement, cell motility, differentiation & cell proliferation and cell division (Kabsch and Vandekerckhove, 1992). As cytoskeletal elements communicate with cellular



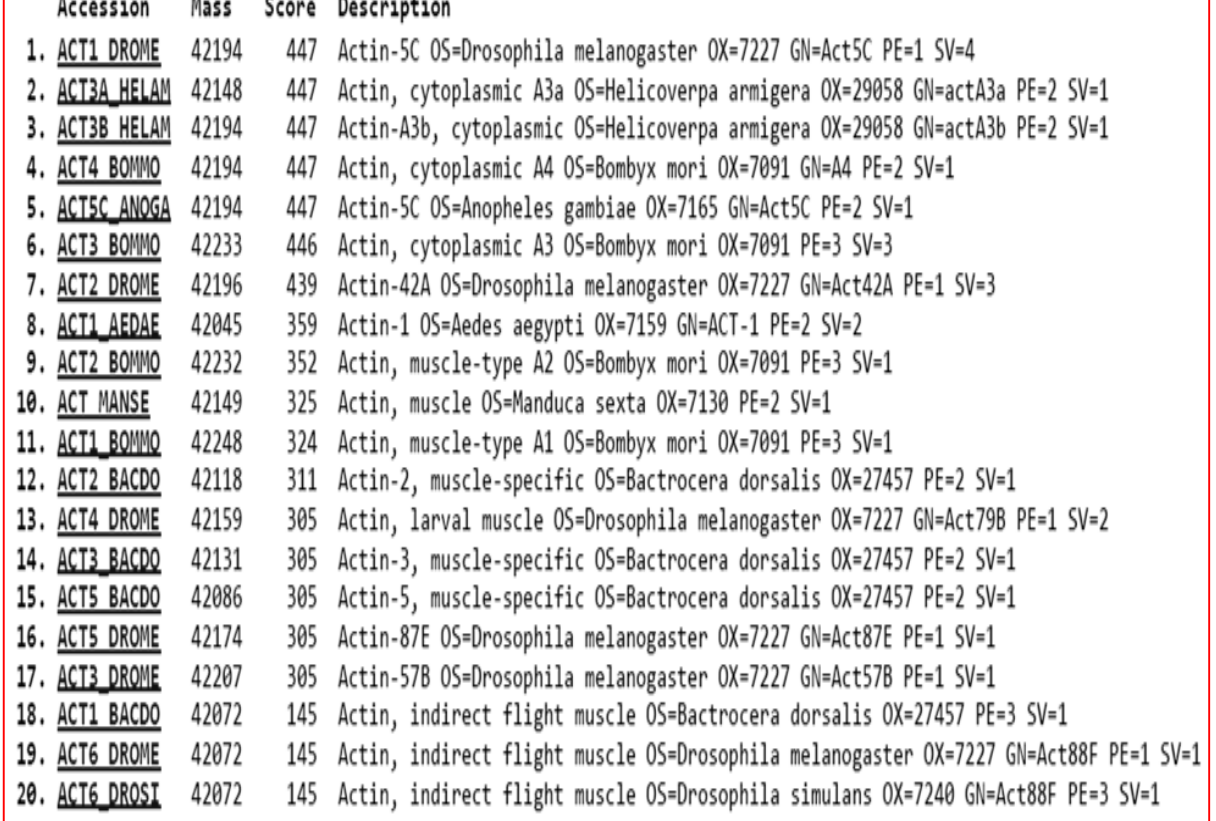
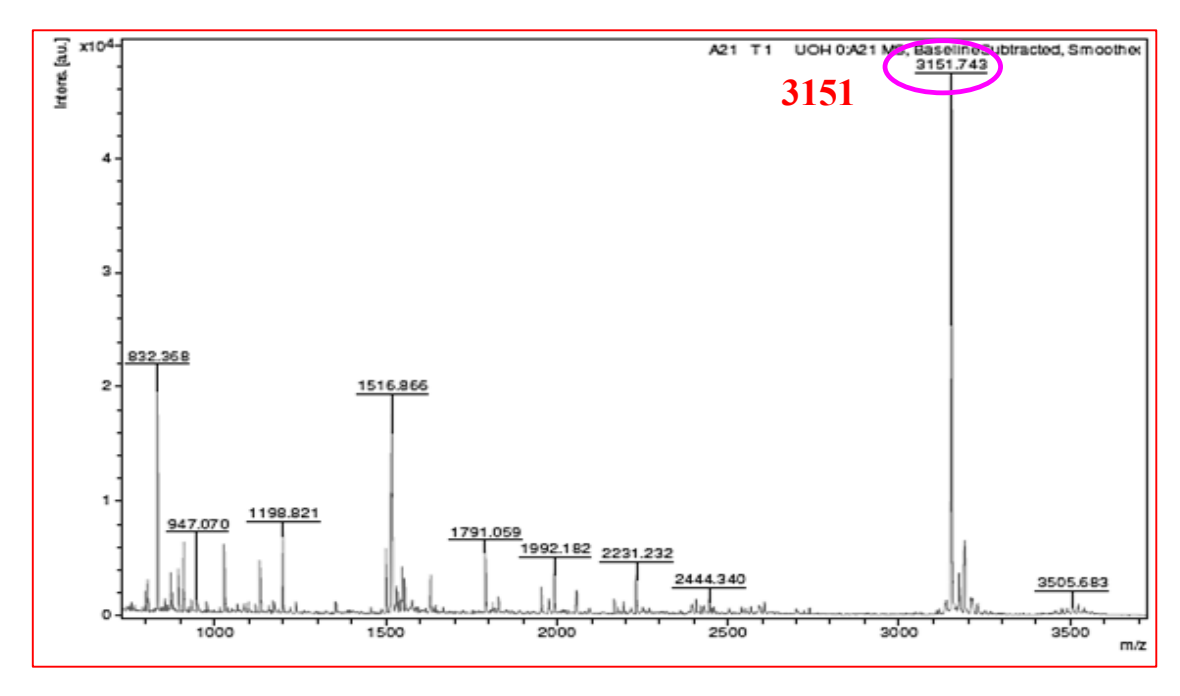


Fig. 5.14. Identification of spot 7 as Actin-5C after tryptic digestion and MALDI-TOF-TOF analysis. (A) Histogram of MASCOT search results and corresponding protein hits.

B)



C)

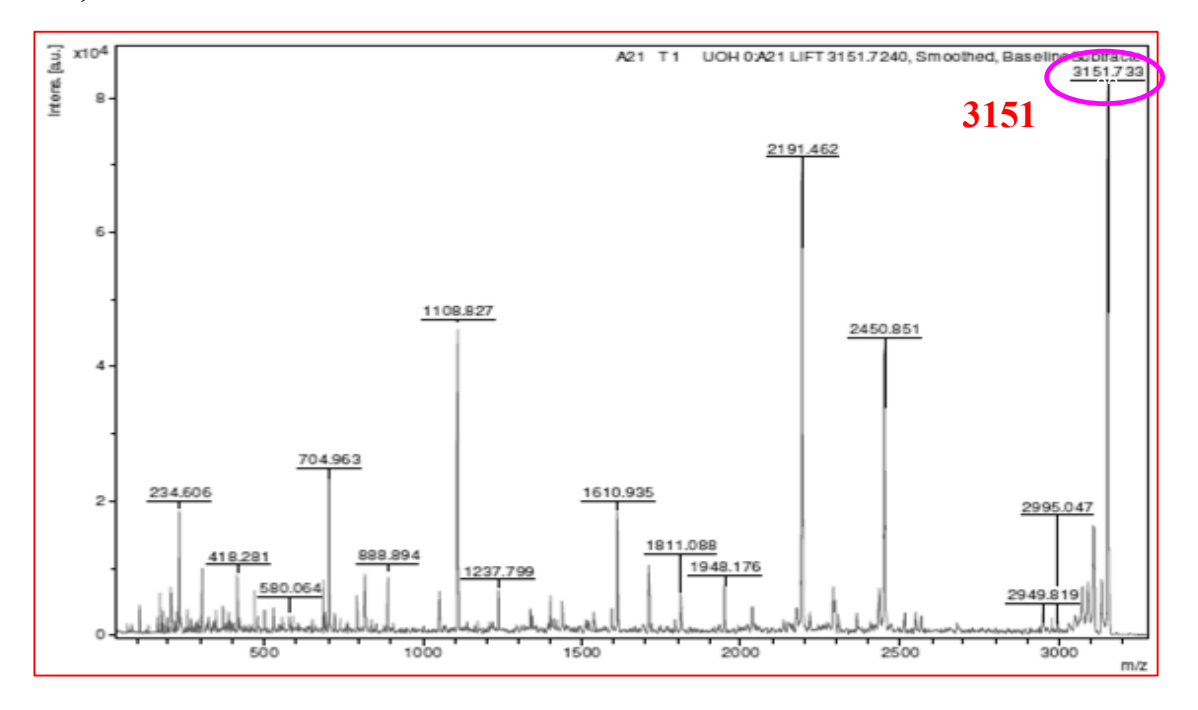


Fig. 5.14 (B) PMF spectra of spot 7 highlighting peak 3151 (m/z); **(C)** Lift spectrum of PMF peak with m/z 3151.

N-Term.	Ion	а	b	ı	a-17	b-17	y	C-Term.
1	T	74.060	102.055	74.060	57.033	85.028	175.119	30
2	Т	175.108	203.103	74.060	158.081	186.076	288.203	29
3	G	232.129	260.124	30.034	215.103	243.098	401.287	28
4	1	345.213	373.208	86.096	328.187	356.182	472.324	27
5	V	444.282	472.277	72.081	427.255	455.250	609.383	26
6	L	557.368	585.361	86.096	540.339	568.334	706,436	25
7	D	672.393	700.388	88.039	655.366	683.361	819.520	24
8	S	759,425	787.420	60.044	742,398	770.393	890.557	23
9	G	816,446	844.441	30.034	799,420	827.415	1053.620	22
10	D	931.473	969,468	88.039	914,447	942,441	1110.642	21
								,
11	G	988.495	1016.489	30.034	971.468	999.463	1239.684	
12	V	1087.563	1115.558	72.081	1070.536	1098.531	1402.748	
13	Н	1224.622	1252.617	110.071	1207.595	1235.590	1515.832	
14	S	1311.654	1339.649	60.044	1294.627	1322.622	1612.885	
15	T	1412.702	1440.697	74.060	1395.675	1423.670	1711.953	
16	V	1511.770	1539.765	72.081	1494.743	1522.738	1813.001	15
17	P	1608.823	1636.818	70.065	1591.796	1619.791	1900.033	
18		1721.907	1749.902	86.096	1704.880	1732.875	2037.092	13
19	Y	1884.970	1912.965	136.076	1867.944	1895.939	2136.160	12
20	E	2014.013	2042.008	102.055	1996.986	2024.981	2193.181	11
21	G	2071.034	2099.029	30.034	2054.008	2082.003	2308.208	10
22	Y	2234.098	2262.092	136.076	2217.071	2245.066	2365.230	9
23	A	2305.135	2333.130	44.049	2288.108	2316.103	2452.262	8
		2440.240	2445.214	86,096	2401,192	2429,187	2567.289	7
24	L	2418.219	2440.214	00.000	E-WILLIDE	E4E5.100	2001.200	
24	P	2515.271	2543.266	70.065	2498.245	2526.240	2680.373	
-	P							

86.096

86.096

129,113

E) **Sequence Coverage: 58%**

2836,452

2949.536

2864,446

2977.531

3133.632

MCDEEVAALVVDNGSGMCKAGFAGDDAPRAVFPSIVGRPRHQGVMVGMGQKDSYVGDE **AQSKRGILTLKYPIEHGIVTNWDDMEK**IWHHTFYNELRVAPEEHPVLLTEAPLNPKANREK MTQIMFETFNTPAMYVAIQAVLSLYASGR<mark>TTGIVLDSGDGVSHTVPIYEGYALPHAILR</mark>LDL AGRDLTDYLMKILTERGYSFTTTAERE VRDIKEKLCYVALDFEQEMIATAASSSSLEKSYE **LPDGQVITIGNERFR**CPEALFQPSFLGMEACGIHETTYNSIMKCDVDI**RKDLYANTVLSGGT TMYPGIADR**MQKEITALAPSTMKIK**IIAPPER**KYSVWIGGSILASLSTFQQMWISK**QEYDES GPSIVHRKCF**

2819,425

2932,509

3088.610

2847.420

2960.504

2949.547

3050.595

3151.642

G

Fig. 5.14. (D): Analysis of Lift spectrum from peak m/z 3151 using Biotools; (E) Actin-5C (ACT1 DSROME/Uniprot Acc. Q299E6) sequence. Red colour indicates the partial sequence coverage by various ions generated from spot 7 while blue box indicate the matching of de novo (m/z 3151) sequence obtained from Biotools with one of the peptides identified by Mascot search engine.

F)

Accession number	Protein name/ Source	Sequence	Similarity (%)
Spot number 7 (de no	ovo sequence from PMF peak with m/z 3151)	TTGIVLDSGDGVSHTVPIYEGYALPHAILR	100
AGJ82961.1	actin, partial / Bristowia sp. Gabon	TTGIVLDSGDGVSHTVPIYEGYALPHAILR	100
ADO15276.1	actin, partial / Oxytropis splendens	TTGIVLDSGDGVSHTVPIYEGYALPHAILR	100
AGJ82765.1	actin, partial/ Sidusa sp. French Guiana 2	TTGIVLDSGDGVSHTVPIYEGYALPHAILR	100
BAK64270.1	actin, partial/ Salix japonica	TTGIVLDSGDGVSHTVPIYEGYALPHAILR	100
ADQ58001.1	actin 5C, partial/ Drosophila mauritiana	TTGIVLDSGDGVSHTVPIYEGYALPHAILR	100
AAX54476.1	actin, partial/ Lolium multiflorum	TTGIVLDSGDGVSHTVPIYEGYALPHAILR	100
ADX66515.1	actin, partial/ Timema douglasi	TTGIVLDSGDGVSHTVPIYEGYALPHAILR	100
AQY03978.1	beta-actin, partial/ Spodoptera litura	TTGIVLDSGDGVSHTVPIYEGYALPHAILR	100
>AGR44787.1	actin-4/ Bombyx mori	TTGIVLDSGDGVSHTVPIYEGYALPHAILR ************************************	100

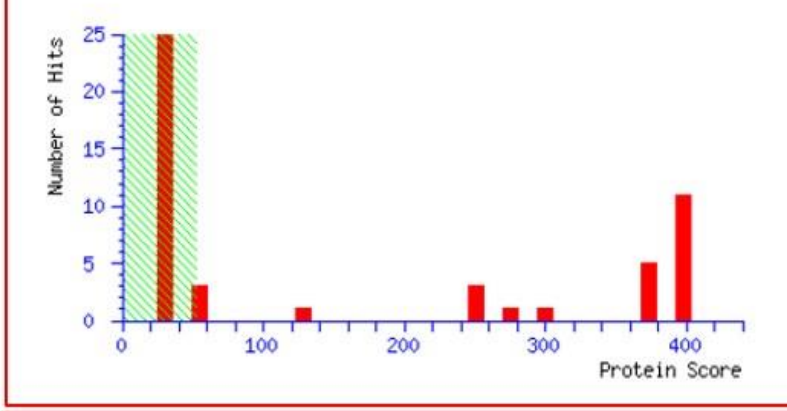
Fig. 5.14. (**F**): Clustal alignment of *de novo* sequence from PMF peak (m/z 3151) with Actin-5C, identified in NCBI database.

A)

Mascot Score Histogram

Protein score is -10*Log(P), where P is the probability that the observed match is a random event. Protein scores greater than 52 are significant (p<0.05).

Protein scores are derived from ions scores as a non-probabilistic basis for ranking protein hits.



	Accession	Mass	Score	Description
1.	ACT1 DROME	42194	398	Actin-5C OS=Drosophila melanogaster OX=7227 GN=Act5C PE=1 SV=4
1723	ACT3A HELAM	42148	398	Actin, cytoplasmic A3a OS=Helicoverpa armigera OX=29058 GN=actA3a PE=2 SV=1
222	ACT3B HELAM	42194	398	Actin-A3b, cytoplasmic OS=Helicoverpa armigera OX=29058 GN=actA3b PE=2 SV=1
4.	ACT4 BOMMO	42194	398	Actin, cytoplasmic A4 OS=Bombyx mori OX=7091 GN=A4 PE=2 SV=1
5.	ACTSC_ANOGA	42194	398	Actin-5C OS=Anopheles gambiae OX=7165 GN=Act5C PE=2 SV=1
6.	ACT3 BOMMO	42233	397	Actin, cytoplasmic A3 OS-Bombyx mori OX=7091 PE=3 SV=3
7.	ACT MANSE	42149	394	Actin, muscle OS=Manduca sexta OX=7130 PE=2 SV=1
8.	ACT1 BOMMO	42248	393	Actin, muscle-type A1 OS=Bombyx mori OX=7091 PE=3 SV=1
9.	ACT1 AEDAE	42045	388	Actin-1 OS=Aedes aegypti OX=7159 GN=ACT-1 PE=2 SV=2
10.	ACT2 BACDO	42118	386	Actin-2, muscle-specific OS=Bactrocera dorsalis OX=27457 PE=2 SV=1
11.	ACT3 DROME	42207	386	Actin-57B OS=Drosophila melanogaster OX=7227 GN=Act57B PE=1 SV=1
12.	ACT2 DROME	42196	371	Actin-42A OS=Drosophila melanogaster OX=7227 GN=Act42A PE=1 SV=3
13.	ACT3 BACDO	42131	370	Actin-3, muscle-specific OS=Bactrocera dorsalis OX=27457 PE=2 SV=1
14.	ACT5_BACDO	42086	370	Actin-5, muscle-specific OS=Bactrocera dorsalis OX=27457 PE=2 SV=1
15.	ACT5 DROME	42174	370	Actin-87E OS=Drosophila melanogaster OX=7227 GN=Act87E PE=1 SV=1
16.	ACT4 DROME	42159	369	Actin, larval muscle OS=Drosophila melanogaster OX=7227 GN=Act79B PE=1 SV=2
17.	ACT2_BOMMO	42232	297	Actin, muscle-type A2 OS=Bombyx mori OX=7091 PE=3 SV=1
18.	ACT MAYDE	42132	264	Actin OS=Mayetiola destructor OX=39758 PE=2 SV=1
19.	ACT1 BACDO	42072	248	Actin, indirect flight muscle OS=Bactrocera dorsalis OX=27457 PE=3 SV=1
20.	ACT6_DROME	42072	248	Actin, indirect flight muscle OS=Drosophila melanogaster OX=7227 GN=Act88F PE=1 SV=1

Fig. 5.15. Identification of spot 8 as Actin-5C after tryptic digestion and MALDI-TOF-TOF analysis. (A) Histogram of MASCOT search results and corresponding protein hits.

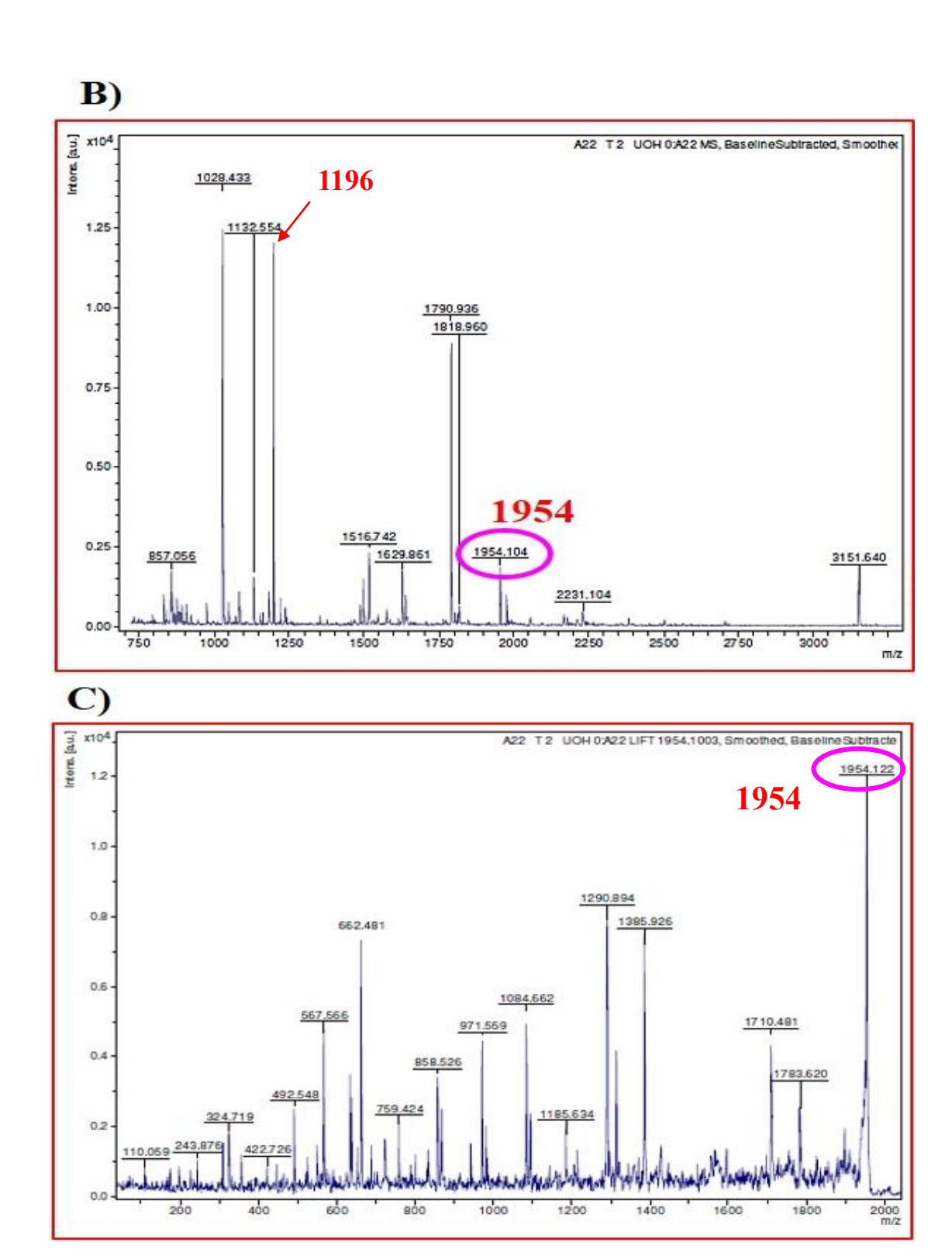


Fig. 5.15. (B) PMF spectra of spot 8 highlighting peaks 1196 and 1954 (m/z); **(C)** Lift spectrum of PMF peak with m/z 1954 m/z.

D)

VFPSIVG		AV		Peak: 1196					
N-Term.	Ion	a	b	1	a-17	b-17	٧	C-Term.	Ion
1	A	44.049	72044	44.049	27.023	55.018	175.119	11	R
2	٧	143.118	171.113	72.081	126.091	154.086	272.172	10	P
3	F	290.186	318.181	120.081	273.160	301.155	428.273	9	R
4	Р	387.239	415.234	70.065	370.213	398.207	485.294	8	G
5	S	474.271	502.266	60.044	457.245	485.239	584.363	7	٧
6		587.355	615.350	86.096	570.329	598.324	697.447	6	- 1
7	٧	686.424	714.418	72.081	669.397	697.392	784.479	5	S
8	G	743,445	771.440	30.034	726.418	754.413	881.532	4	P
9	R	899.546	927.541	129.113	882.520	910.515	1028.600	3	F
10	P	996.599	1024.594	70.065	979.572	1007.567	1127.668	2	٧
11	В	1152,700	1180,695	129,113	1135.673	1163,668	1198.708	1	A

E)

Sequence coverage: 51%

MCDEEVAALVVDNGSGMCKAGFAGDDAPRAVFPSIVGRPRHQGVMVGMGQKDSYVGDEAQSKRGILTLKYPIEHGIVT

NWDDMEKIWHHTFYNELRVAPEEHPVLLTEAPLNPKANREKMTQIMFETFNTPAMYVAIQAVLSLYASGRTTGIVLDSG

DGVSHTVPIYEGYALPHAILRLDLAGRDLTDYLMKILTERGYSFTTTAEREIVRDIKEKLCYVALDFEQEMATAASSSS

LEKSYELPDGQVITIGNERFRCPEALFQPSFLGMEACGIHETTYNSIMKCDVDIRKDLYANTVLSGGTTMYPGIADRMQK

EITALAPSTMKIKIIAPPERKYSVWIGGSILASLSTFQQMWISKQEYDESGPSIVHRKCF

Fig. 5.15. (D): Analysis of Lift spectrum from peak m/z 1196 using Biotools; **(E)** Actin-5C (ACT1_DSROME/Uniprot Acc. Q299E6) sequence. Red colour indicates the partial sequence coverage by various ions generated from spot 7 while blue box indicate the matching of *de novo* (m/z 1196) sequence obtained from Biotools with one of the peptides identified by Mascot search engine.

Accession number	Protein name/Source	Sequence	Similarity (%)
	de novo sequence from PMF peak with m/z 1196)	AVFPSIVGRPR	100
AHI17930.1	actin, partial/ Colletotrichum trifolii	AVFPSIVGRPR	100
AIC79005.1	actin, partial/ Verruconis gallopava	AVFPSIVGRPR	100
ARO35907.1	actin, partial/ Pyricularia oryzae	AVFPSIVGRPR	100
AGU13209.1	actin, partial/ Colletotrichum truncatum	AVFPSIVGRPR	100
API65521.1	actin, partial/ Colletotrichum coccodes	AVFPSIVGRPR	100
QHS64209.1	actin, partial/ Paraphaeosphaeria	AVFPSIVGRPR	100
QGW34938.1	actin, partial/Colletotrichum	AVFPSIVGRPR	100
AEM68335.1	actin, partial/Malletia abyssorum	AVFPSIVGRPR	100
ADY75810.1	actin, partial/Phyllosticta citricarpa	AVFPSIVGRPR ******	100

Fig. 5.15. (**F**): Clustal alignment of *de novo* sequence from PMF peak (m/z 1196) with Actin-5C, identified in NCBI database.

Table. 5.2: List of differentially expressed proteins in 2-DE (fig. 5.6) and their identification by MALDI-TOF-TOF analysis

Label of spots	Protein expression (C vs T)	Fold Change		M	S/MS analysis				
			Obtained protein Score	Identification of protein in the MASCOT search database	Mascot search/ Uniprot Acc. No	No. of peptides matched	Sequence coverage by matched peptides	Ref	
1	Down regulated	5.2	86*	COP9 signalosome complex subunit 3	CSN3_DROME /Q8SYG2	16	44%	Figs. 5.7 & 5.8	
2	Down regulated	3.4	92*	Protein SOEM-1	SOEM_CAEEL/ Q7YWN4	14	77%	Figs. 5.7 & 5.9	
3	Down regulated	5.2	66*	Cyclin-C	CCNC_DROPS/ Q29AI1	16	46%	Figs. 5.7 & 5.10	
4	Down regulated	5.5	354*	Heat shock 70 kDa protein cognate 4	HSP70_MANSE/ Q9U639.1	13	21%	Figs. 5.7 & 5.11	
5	Down regulated	2.3	89*	Protein Turandot X	TOTX_DROPS/ Q299E6	12	75%	Figs. 5.7 & 5.12	
6	Down regulated	4.1	64*	Pigment-dispersing hormone peptides	PDH_ROMMI/ P09929	9	68%	Figs. 5.7 & 5.13	
7	Up regulated	6.8	442*	Actin-5C	ACTI_DROME/ Q299E6	18	58%	Figs. 5.7 & 5.14	
8	Up regulated	5.7	398*	Actin-5C	ACTI_DROME/ Q299E6	17	58%	Figs. 5.7 & 5.15	

Note: * indicates obtained score is significant based on Histogram

membranes, they promote cellular responses including defensive mechanism. Actin filaments which form an ordered array to strengthen the apical surface of the brush border in the insect midgut was upregulated in the *H. armigera* larvae after Cry1Ac intoxication (Yuan et al., 2011). Several other studies also showed that actin act as the binding protein for Cry 1Ac in *H. armigera* (Chen et al., 2010), *Manduca sexta* larvae (Nall & Adang, 2003) and *Heliothis virescens* (Krishnamoorthy et al., 2007). Further, proteomic studies showed that actin was upregulated when beetle species *Tribolium castaneum* was treated with the insecticide diflubenzuron (Merzendorfer et al., 2012). In the present study, spot 7 and spot 8, which are possibly isoforms of Actin-5c are up-regulated by >5.0-fold when the larvae were fed upon T9BBI (Fig. 5.5, 5.7 and Table 5.2). Taken together the results from the present study and literature suggest that actin might play a significant role in retaining the normal shape of the cell by maintaining the cytoskeletal integrity during stress response such as intoxication by possibly binding to the toxin/insecticide injested by the larvae.

Thus, among the eight spots selected in the present study, six protein spots which were down-regulated are identified as CSN complex-3 subunit, SOEM-1, Cyclin-C, Heat shock 70 kDa protein cognate 4, Turandot and (PDH) peptide, respectively while other two protein spots which were Up-regulated are identified as isoforms of Actin-5C. A detailed summary of the results related to the MALDI-TOF-TOF analysis of the eight spots is revealed in **Table 5.2.**

Highlights of the Study:

- 1) T9BBI showed significant inhibitory potential against trypsin-like gut proteases of non-host pest *A. janata*.
- 2) Ingestion of T9BBI retarded the larval growth of *A. janata* up to 85% and showed mortality rate up to 80% at higher concentration (8µg/cm²).
- 3) T9BBI altered the midgut tissue proteome of *A. janata* significantly as evidenced by 2-D gel electrophoresis.
- 4) The proteins which showed altered expression are mainly involved in cell migration during larval growth and development (SOEM-1, CSN protein); metamorphosis (Cyc-C, PDH); to sustain stress and (HSP 70 cognate and Turandot) to maintain normal size and shape of the cell (Actins).

Chapter 6

Insecticidal Potential of T9BBI on Larval Growth and Development of a Host Insect Pest *Spodoptera litura*: Modulation in the Expression of Midgut Tissue Proteins

Chapter 6

Insecticidal Potential of T9BBI on Larval Growth and Development of a Host Insect Pest *Spodoptera litura*: Modulation in the Expression of Midgut Tissue Proteins

The armyworm, *Spodoptera litura* (Lepidoptera, Noctuidae) is a cosmopolitan polyphagous insect herbivore with a broad host spectrum covering over 44 families. It is a significant defoliator of castor, intrudes capsules and penetrates the stems at the time of huge outbreak or epidemics, leading to breakage and collapsing of castor plants (Lakshminarayana and Raoof 2005). A particular migratory capacity raises its population distribution all over the world (Rauf et al., 2019). In India, *S. litura* is mostly found in the fields of groundnut, tomato, chilli, bhendi and cotton (Elumalai et al., 2010). Also, *S. litura* is an economically important pest on *V. mungo* which is widely consumed all over India.

The studies of Prasad et al. (2010b) from our laboratory identified that PIs from *V. mungo* (TAU 1variety) were very effective in inhibiting the activity of *S. litura* trypsin-like midgut proteases (SGPs) and retarding the growth of larvae. These studies were limited by feeding the larvae with PI during the early stage of the third instar. These preliminary studies raised the following key questions such as: 1) Does all the domestic varieties of *V. mungo* possesses PIs which are active against SGPs; 2) If yes, what is their effect on larval and pupal growth when fed throughout their larval stage. Also, in general, the larvae are very well known for their dynamism to adapt to any new feeding habits. In this context, it would be interesting to monitor the changes that occur in the midgut tissue proteome of *S. litura* larvae upon feeding with T9BBI. This study also would pave the path to understand the biochemical/molecular strategies adapted by *S. litura* larvae to compensate for the loss in function of trypsin-like proteases in its midgut tissue.

Results and Discussion:

6.1. *In-vitro* inhibitory activity of T9BBI against *Spodoptera litura* trypsin-like midgut proteases (SGPs):

In the present study, the T9BBI purified (**Chapter 4**) from the seeds of black gram (*cv*. T9) showed significant inhibitory potential against SGPs (845±12 SGPI units/mg protein) and Bovine pancreatic trypsin (983±25 BPTI units/mg protein) when compared with crude protein (22±7 SGPI units/mg protein) as shown in **Fig. 6.1**. The reports from previous studies also indicated the potential of PIs isolated from seeds of *Archidendron ellipticum*, *Cajanus cajan*, *Murraya koenigii* and black gram (*cv*. TAU) in inhibiting the activity of trypsin-like midgut proteases of *S. litura* (Bhattacharya et al., 2006, Prasad et al., 2009, Gahloth et al., 2011). The crude extracts from *R. sublobata*, a wild-relative of *Cajanus cajan*, commonly called as pigeon pea showed <8.9 trypsin inhibitory units against *S. litura* midgut extracts (Prasad et al., 2009). Further, the PIs purified from black gram (24%) showed higher inhibitory potential than red gram (14%) against SGPs (Prasad et al., 2010b).

6.2. *In-vivo* evaluation of the insecticidal activity of T9BBI against *S. litura*:

The larvae of *S. litura* from first instar stage (average weight of 28±1.8 mg) were allowed to feed on an artificial diet containing a range of concentrations of T9BBI (0.01%, 0.025%, 0.05% and 0.1%) prepared in 50mM Tris-HCl (pH 8.0). The control larvae were allowed to feed on artificial diet containing 50mM Tris-HCl (pH 8.0) without T9BBI. With an increase in the concentration of T9BBI in the artificial diet, the mean weights of the larvae decreased from 2nd to 6th instar stage. Since major changes in the weight of the larvae were observed from the 4th instar larvae, comparative analysis in the weights of the larvae fed upon T9BBI and control larvae was shown from this specific stage.

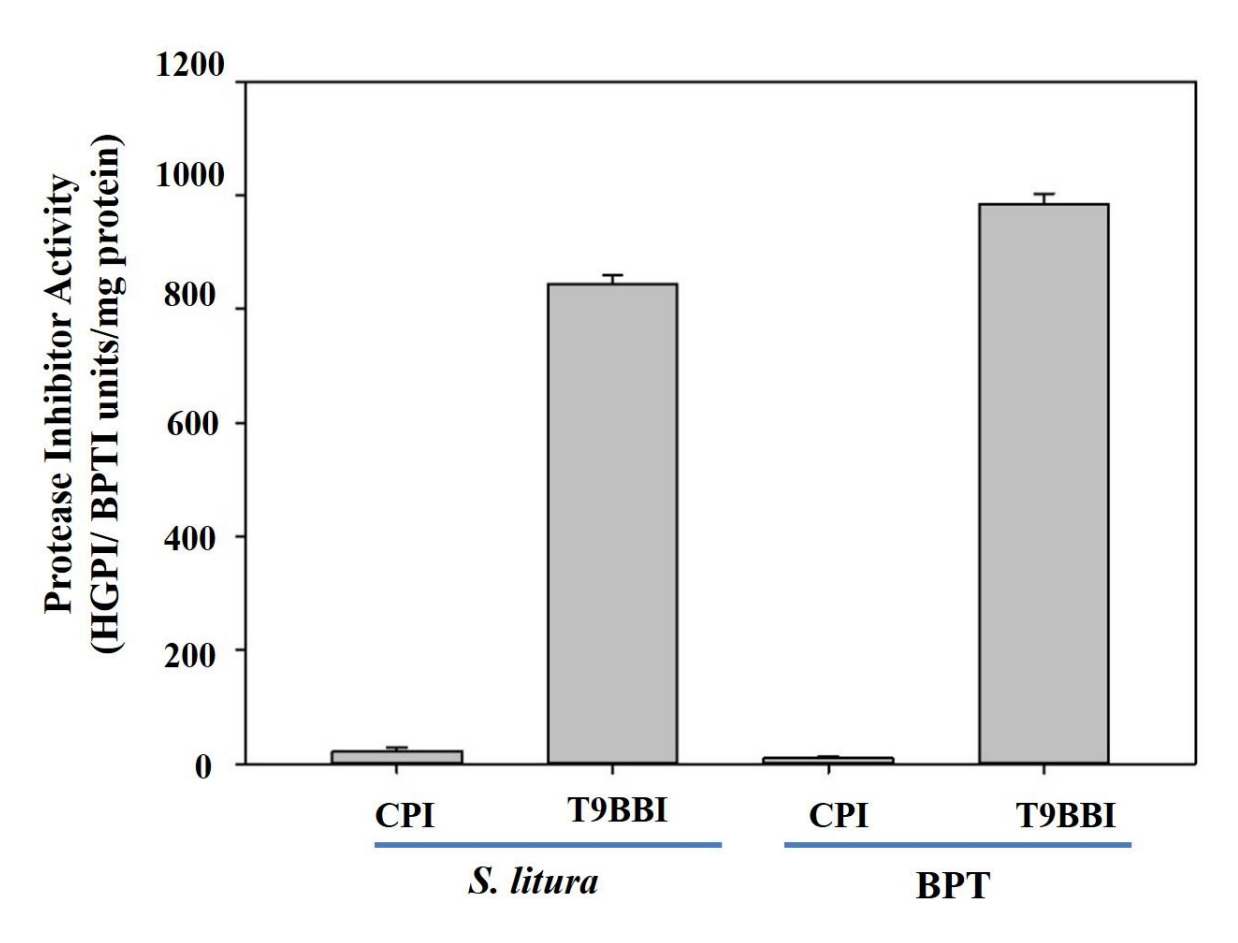


Fig. 6.1. A comparative inhibitory potential of crude proteinase inhibitor (CPI) extract and purified T9BBI from seeds of *V. mungo* (T9 variety) towards *S. litura* midgut trypsin-like proteases (SGPs) collected from 6th instar larvae and bovine pancreatic trypsin (BPT), which is used as a control. The specific activity of CPI and T9BBI was determined as the number of *S. litura* midgut trypsin-like proteinase inhibitor (SGPI) units mg⁻¹ protein and Bovine pancreatic trypsin inhibitor (BPTI) units mg⁻¹ protein, respectively. Further details were described in materials and methods.

The average weight of the control larvae in the early fourth instar stage actively feeding on an artificial diet without T9BBI for 9 days was 200±29 mg. The fourth instar larvae fed on T9BBI showed a remarkable reduction in its growth when compared with control larvae. The growth of the larvae was retarded by 5±0.49% (0.01% T9BBI), 15.4±2.9% (0.025% T9BBI), 30±2.7% (0.05% T9BBI) and 42±4.6% (0.1% T9BBI) of their respective control larvae with an increase in the concentration of T9BBI supplemented in the artificial diet (**Fig. 6.2A and B**).

Similarly, the average weight of the control larvae in the early fifth instar stage actively feeding on an artificial diet without T9BBI for 12 days was 444±59 mg. The growth of the *S. litura* larvae fed on an artificial diet supplemented with T9BBI was retarded by 3±0.27% (0.01% T9BBI), 8±1% (0.025% T9BBI), 27±2.6% (0.05% T9BBI) and 43.4±4.1% (0.1% T9BBI), respectively, when compared with the growth of their control larvae (**Fig. 6.3A and B**).

Further, the average weight of the control larvae in the early sixth instar stage, which is feeding on an artificial diet without T9BBI for 15 days was 844±96 mg. Similar to the earlier instar stages, the growth of the *S. litura* larvae fed on an artificial diet supplemented with T9BBI was inhibited by 5±0.3% (0.01% T9BBI), 10±1.6% (0.025% T9BBI), 37±3.5% (0.05% T9BBI) and 52±5.8% (0.1% T9BBI), respectively, when compared with the growth of control larvae (**Fig. 6.4A and B; Table 6.1**).

A mortality rate of ~20% was observed in the larvae fed upon diet containing T9BBI only at highest (0.1%) concentration used in the present study as compared to control larvae fed on a diet without T9BBI. The larvae which survived after feeding upon different concentrations of T9BBI were further converted into pupae. However, a delay (2-11 days) in the transformation of larvae to pupae was observed with an increase in the concentration of

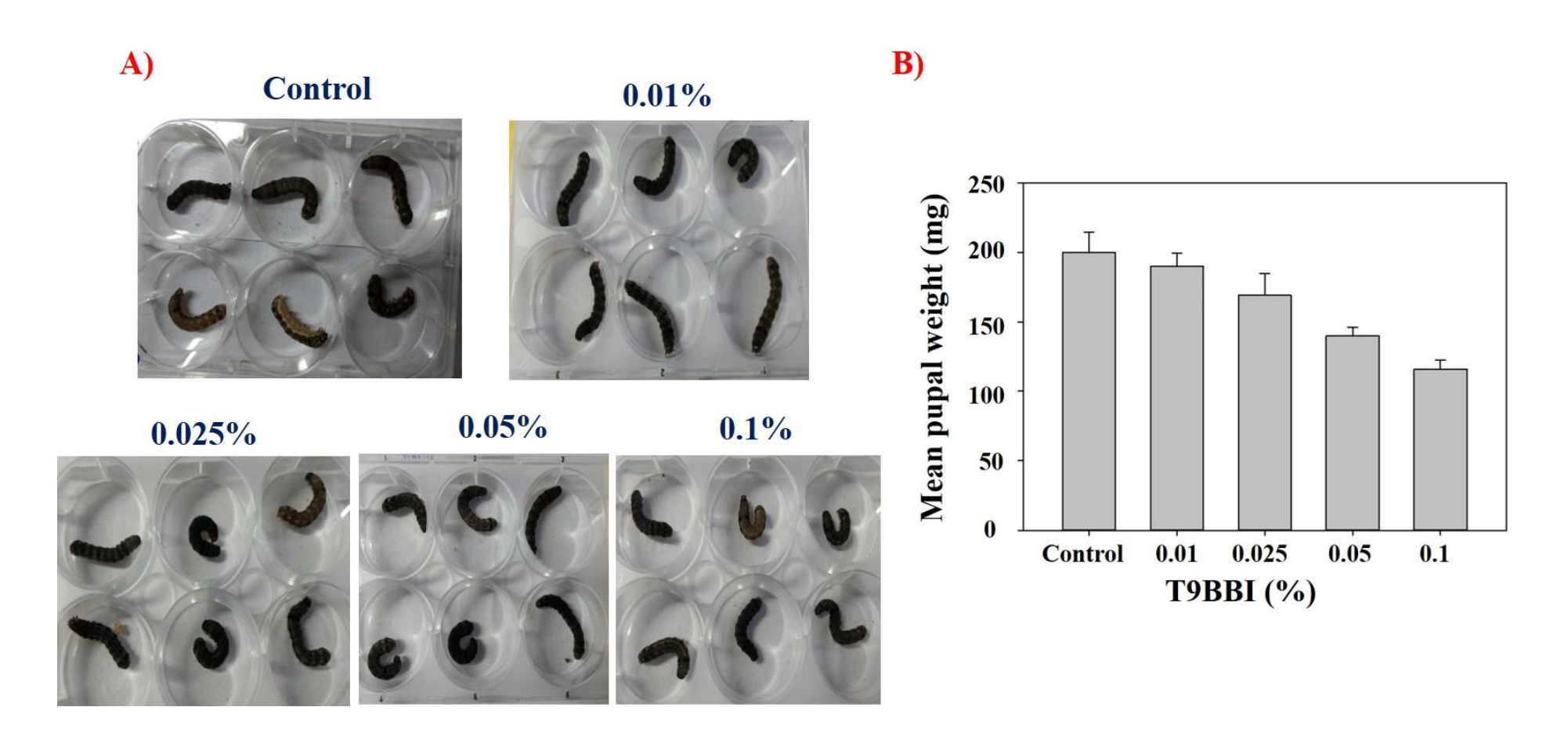


Fig. 6.2. Effect of T9BBI on the growth of 4th instar larvae of *S. litura*. (A) Pictorial depiction of larvae reared on castor leaf coated with buffer alone (control) and different concentrations of T9BBI (treated), and (B) Mean body weight of the corresponding larvae. Further details were described in materials and methods.

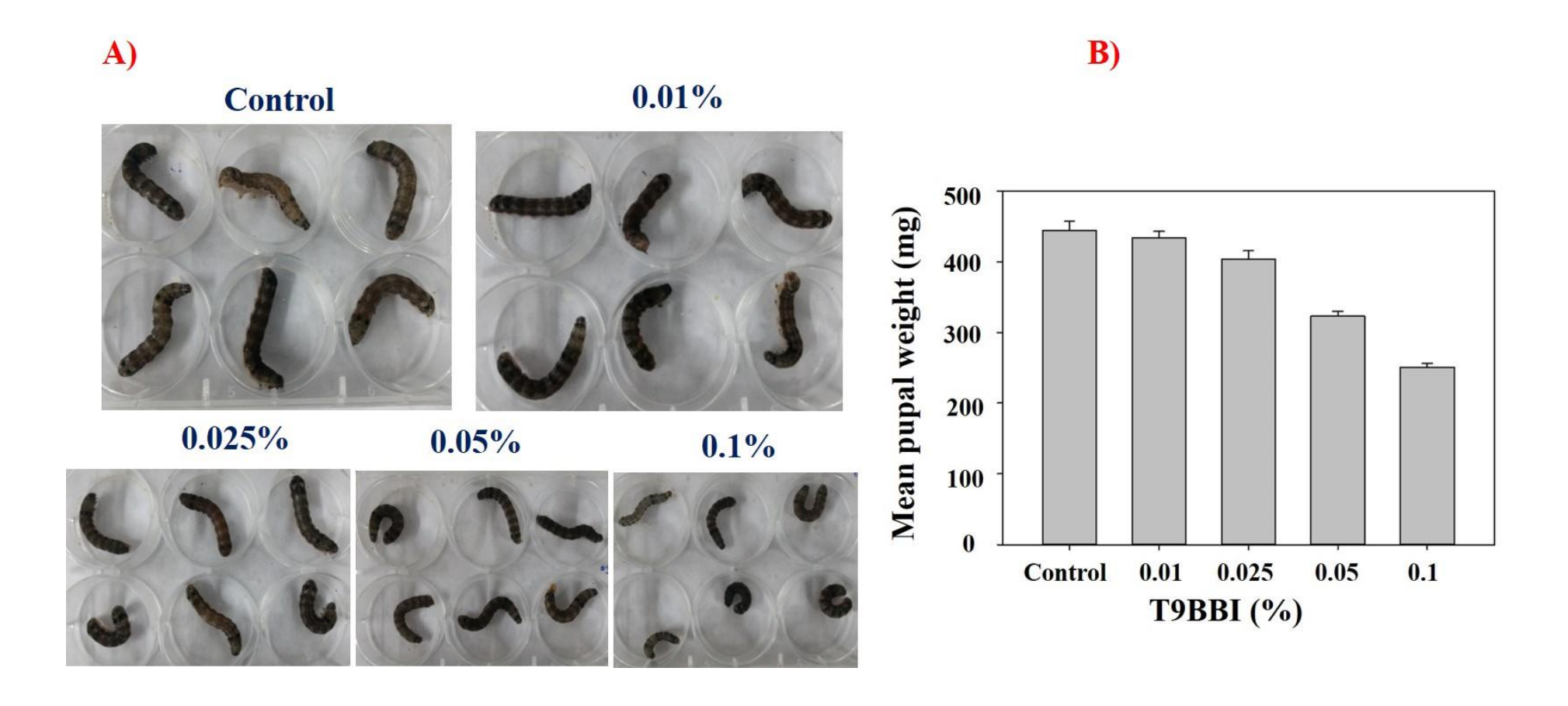


Fig. 6.3. Effect of T9BBI on the growth of 5th instar larvae of *S. litura*. (A) Pictorial depiction of larvae reared on castor leaf coated with buffer alone (control) and different concentrations of T9BBI (treated), and (B) Mean body weight of the corresponding larvae. Further details were described in materials and methods.

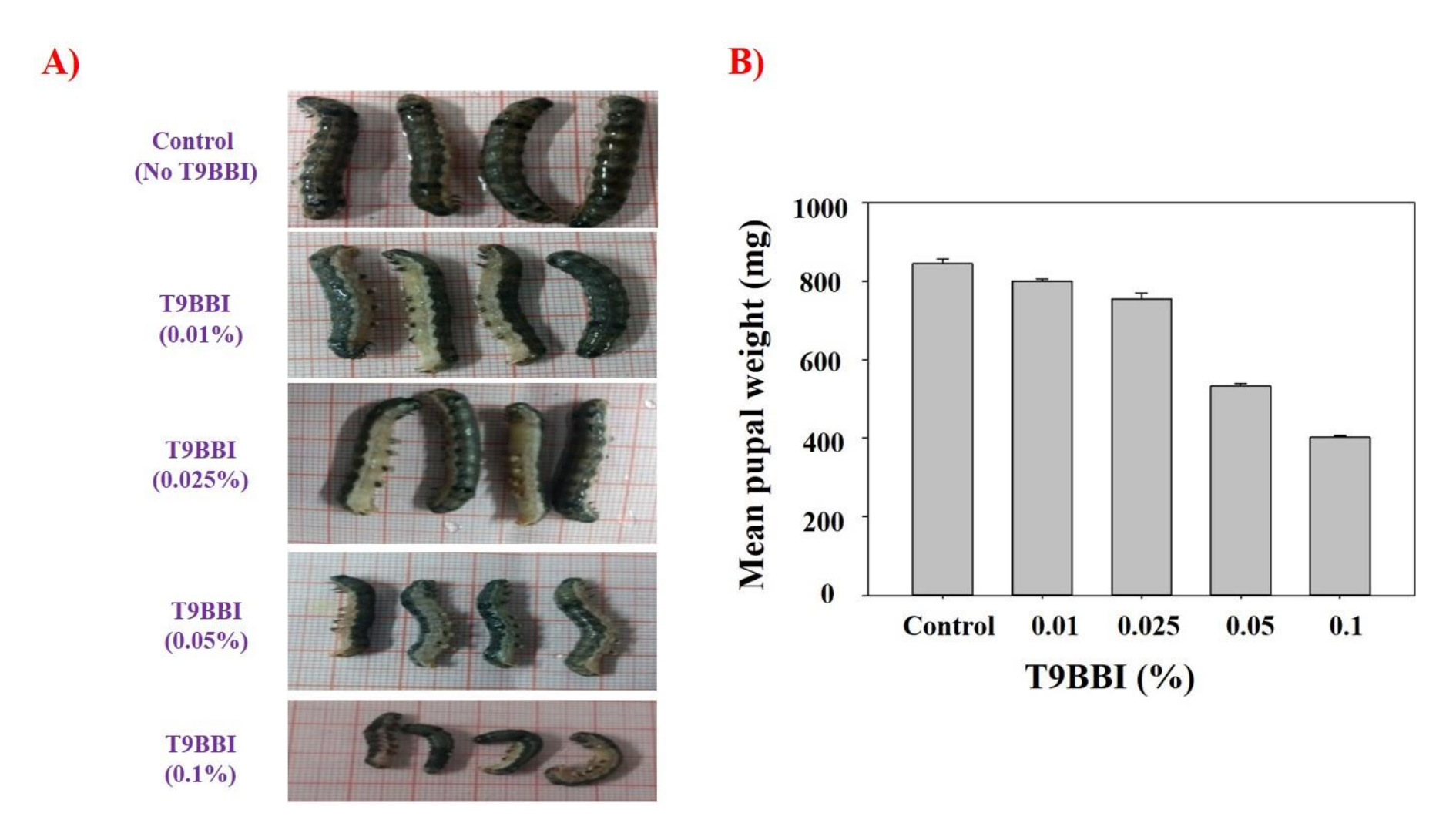


Fig. 6.4. Effect of T9BBI on the growth of 6th instar larvae of *S. litura*. (A) Pictorial depiction of larvae reared on castor leaf coated with buffer alone (control) and different concentrations of T9BBI (treated), and (B) Mean body weight of the corresponding larvae. Further details were described in materials and methods.

T9BBI in the artificial diet (**Table 6.1**). Concurrently, a reduction in the pupal weight was also observed when the larvae were fed upon T9BBI supplemented diet. The weight of the pupae was decreased by 7 to 60% when the concentration of T9BBI was increased from 0.01% to 0.1% in the diet (**Fig. 6.5A and B**). Subsequently, adults were emerged from pupae through metamorphosis. Nevertheless, the emergence of larval-pupal and pupal-adult intermediates was observed when the larvae were fed upon diet supplemented with high concentrations (0.05% and 0.1%) of T9BBI (**Fig. 6.5C**).

The PIs purified from red gram seeds showed larval growth retardation of 13% and 21% with 0.025% and 0.05% treatment and black gram seeds showed 28% and 39% when compared with the control of *S. litura*. Stunted growth was observed at higher concentration and the larval development period to the pupal stage was also extended when compared with their controls (Prasad et al., 2010b).

Earlier reports also showed that PIs isolated from different plants affected the growth and development of *S. litura* larvae. *Murraya koenigii* inhibited the larval growth and development of *S. litura*. At higher concentrations, the retardation in growth and mortality rate was observed up to 44% when compared with their control larvae. Further, along with the delay in larval period by 2 days, there was also a decrease in adult emergence and delay in total development up to 7 days when larvae were fed with PIs at higher concentration. Furthermore, malformed pupae and adult formation were observed at higher concentrations when compared to the controls (Gahloth et al., 2011). The PIs purified from *Glycine max* showed mortality rate of about 24% at higher concentration when compared to their control. A delay in larval development time and deformities were noticed up to 58% at 100 μg/ml concentration of PI along with defective fertility and fecundity when compared to the control (Vasudev et al., 2016).

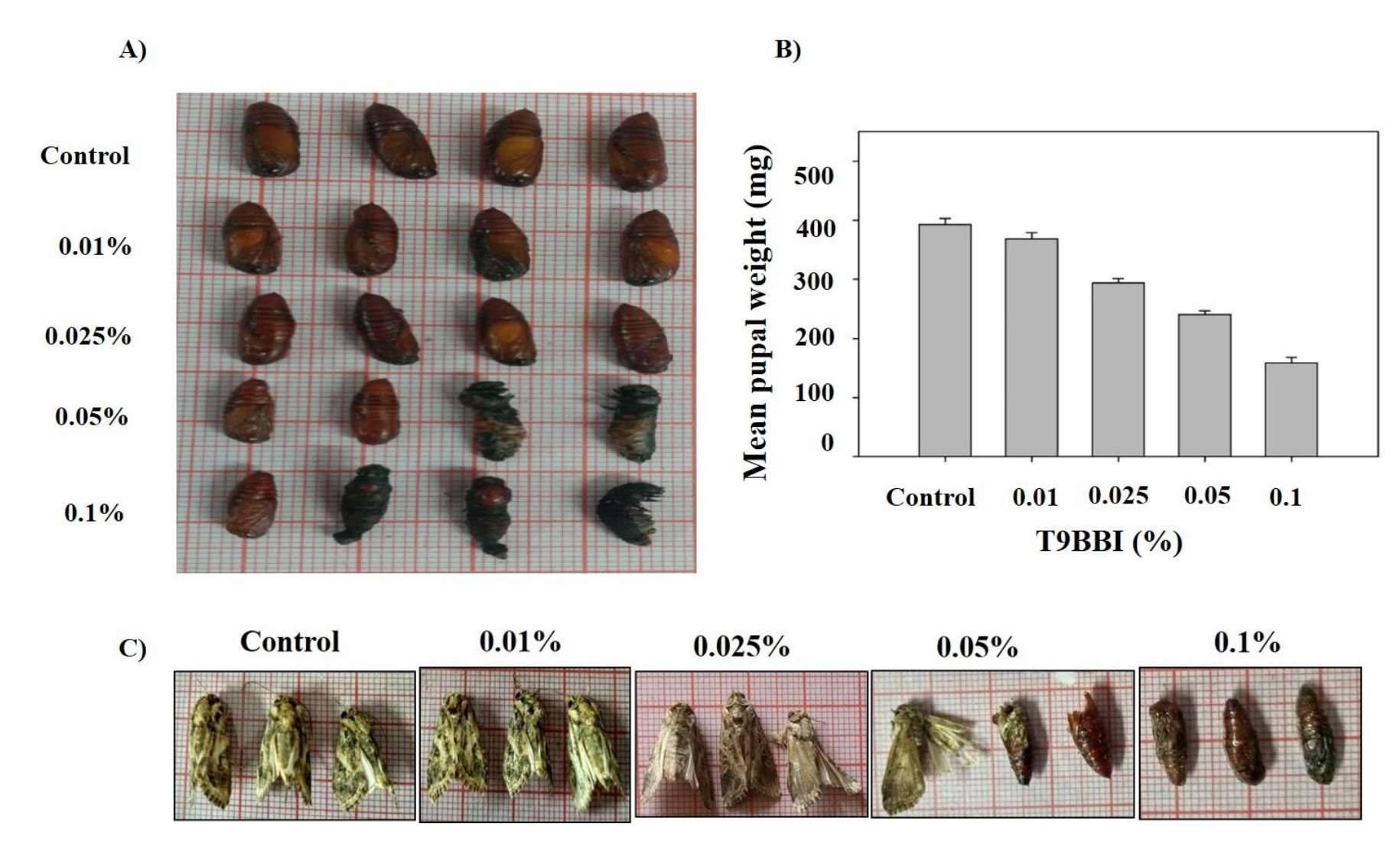


Fig. 6.5. Effect of T9BBI on development of *S. litura*. (A) Pictorial depiction of pupae formed from larvae reared on artificial diet without T9BBI (control) and T9BBI (treated), respectively; (B) Mean pupal weight and (C) Pictorial depiction of adults emerged from corresponding pupae. Further details were described in materials and methods.

Table. 6.1: Anti metabolic effect of T9BBI on larval growth and development of *S. litura*: Reduction in larval growth was represented after 5^{th} instar stage (15 days of feeding), while survival and mortality rate of larvae was represented after 6^{th} instar stage (18 days of feeding), respectively. Data shown here is the mean \pm SE values of three independent experiments (n=20). Further details were described in materials and methods.

Concentration of T9BBI on artificial diet (µg/cm ⁻²)	Reduction in larval growth (% control)	Survival rate (% control)	Mortality rate (% control)	Pupal formation time (days)	Intermediate	e formation	Adult emergence from pupa
					Larval-pupal	Pupal-adult	
0 (Control)	0	100	0	18-21	No	No	Yes
0.01%	5 ± 0.3%	100	0	19-23	No	No	Yes
0.025%	10±1.6%	100	0	20-23	No	No	Yes
0.05%	37±3.5%	100	0	22-26	Yes	Yes	Yes
0.1%	52±5.8%	81±5.6	19±4.4	24-30	Yes	Yes	No

The PIs purified from bitter gourd also showed 70% retardation in larval growth after 10 days of feeding. Larval-pupal intermediates formed are around 12%, the pupal formation was delayed by 3 days and emergence of malformed adults (14-20%) was observed. The fertility and fecundity was also found to be affected (Telang et al., 2003). Similar results were identified when *Momordica cochinchinensis* PIs was tested on *S. litura* larvae (Arimatsu et al., 2012). The cyclic peptides derived from Pin-II type PIs retarded the larval growth of *S. litura* by 50% when compared with the control (Saikhedkar et al., 2019). Corroborating with the literature cited above, the PIs purified from black gram retarded the larval growth, delayed the larval stage with concurrent larval-pupal intermediates, pupal weight reduction and pupal mortality etc. (Figs. 6.2-6.5 and Table 6.1).

However, transgenic tobacco plants overexpressing the *Solanum americanum* Pin-II PIs significantly retarded the growth of *S. litura* larvae than cited above. After 7 days of feeding, there was 80% reduction in their growth and mortality rate up to 87% when compared with their controls. This was followed by reduction in pupal formation rate (Luo et 1., 2009). Similarly, the cystatin gene from *Solanum pinnatisectum* retarded the larval and pupal weight of the *S. litura* (Zhu et al., 2019).

6.3. Differential expression of proteins in midgut tissue of *S. litura* larvae fed with T9BBI:

The protein extract prepared from midgut tissue of late 5th instar larvae feeding on a diet containing T9BBI (0.1%) and control diet were separated on IPG strips in the pH range from 4-7 followed by SDS-PAGE in the second dimension. The proteome profile from these tissues were compared for differentially expressed proteins by using image master platinum 7.0 software. A total of 110 protein spots were observed in 5 to 100 kDa range when

separated in the second dimension using SDS-PAGE (**Fig. 6.6**). Five protein spots which showed significant differences in their expression (> 1.5-fold), separated conspicuously and placed far off from other protein spots were considered for identification. The partial maps and 3-D views of the corresponding spots were represented in **Figure 6.7**. All the protein spots (Spot 1 to 5) were subjected to tryptic digestion followed by MALDI-TOF-TOF analysis to identify the molecular mechanisms by which *S.litura* larvae become adopted against T9BBI.

6.4. Mass spectrometric analysis of differentially expressed proteins:

6.4.1. Identification of Spot 1 as Zinc finger protein 271-like isoform X1:

Tryptic digestion of spot 1 followed by MALDI-TOF-TOF analysis showed matching to a Zinc finger protein 271-like isoform X1 from *Spodoptera litura* with 36 score in the Mascot score histogram (**Fig. 6.8A**). The mass spectrum corresponding to the PMF data was represented in **Figure 6.8B**. When the PMF peaks with m/z 1049 (lift spectrum not shown) and m/z 1198 (lift spectrum shown) were further ionized in MALDI-TOF-TOF, the following *de novo* sequences 'AFTRSDNMKK' and 'CSAKPTEEK' were derived when the lift spectra are analyzed using Biotools software (**Figs. 6.8C and D**). The various ions generated during MALDI-TOF-TOF studies showed partial sequence coverage up to 32% with Zinc finger protein 271-like isoform X1 (Uniprot Acc No. XP_022835582).

Further, the two *de novo* sequences obtained through Biotools showed overlapping with the partial amino acid sequences recognised for Zinc finger protein 271-like isoform X1 during MALDI-TOF-TOF analysis (**Fig. 6.8E**). Furthermore, Clustal alignment of the *de novo* sequence '**AFTRSDNMKK**' with available sequences in the NCBI database showed 100% matching to a Zinc finger protein 271-like isoform X1 from different insects such as *Operophtera brumata*, *Danaus plexippus*, *B. mori*, *Vanessa tameamea*, *Galleria mellonella*, *H. armigera*, *Trichoplusia ni*, *Ostrinia furnacalis and M. Sexta*, respectively (**Fig. 6.8F**)

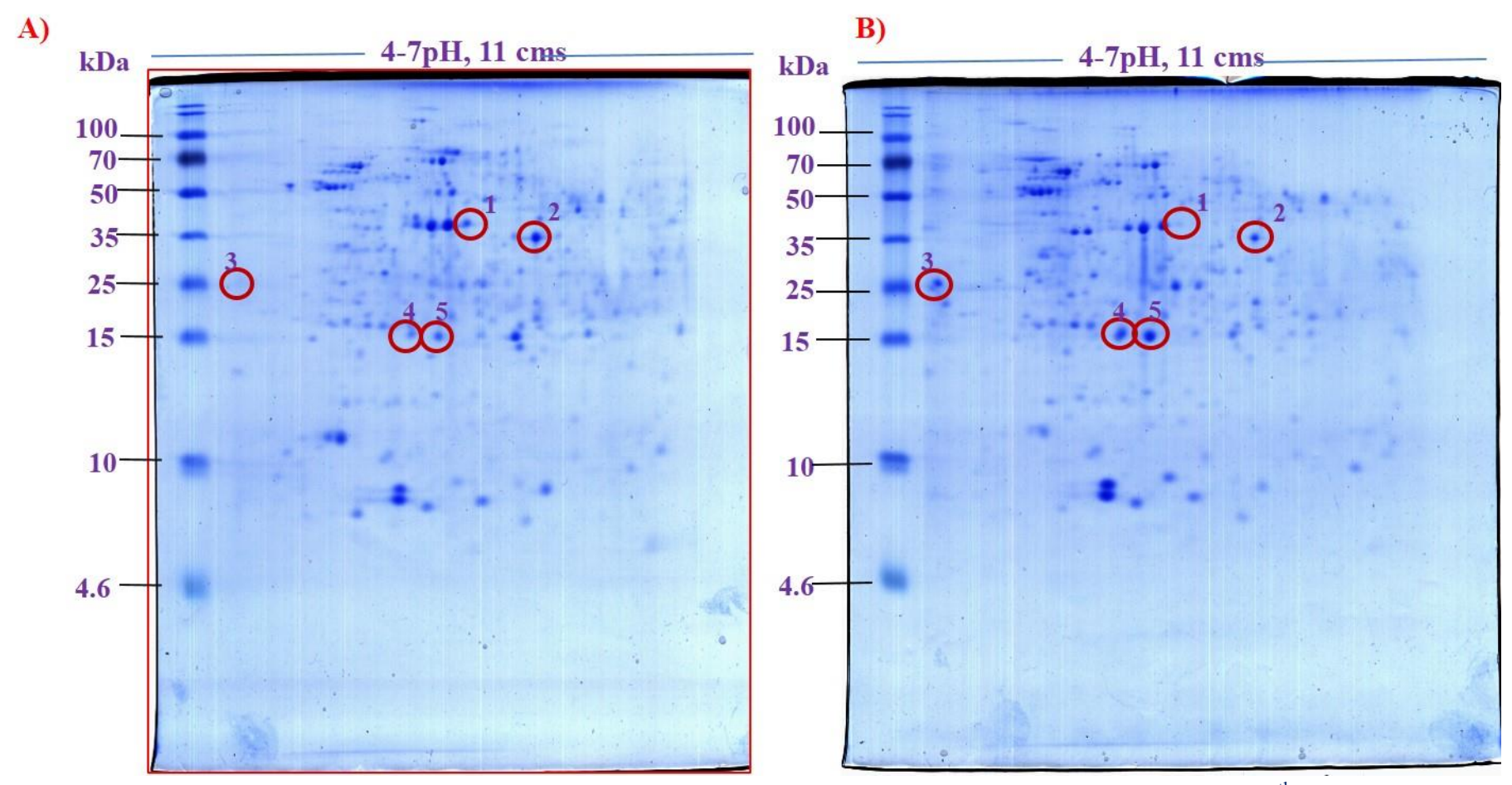


Fig. 6.6. Two dimensional gel electrophoresis of midgut tissue proteome from *S. litura* larvae (early 5th instar stage) fed up on **(A)** artificial diet with buffer (Control) and **(B)** artificial diet with T9BBI (0.1%), respectively. Among several spots which showed significant differences (> 2-fold), spots labelled as 1 to 5 (indicated with red circles) which are clearly separated from other spots are chosen for further studies, i.e., MALDI-TOF-TOF analysis. Further details were described in materials and methods.

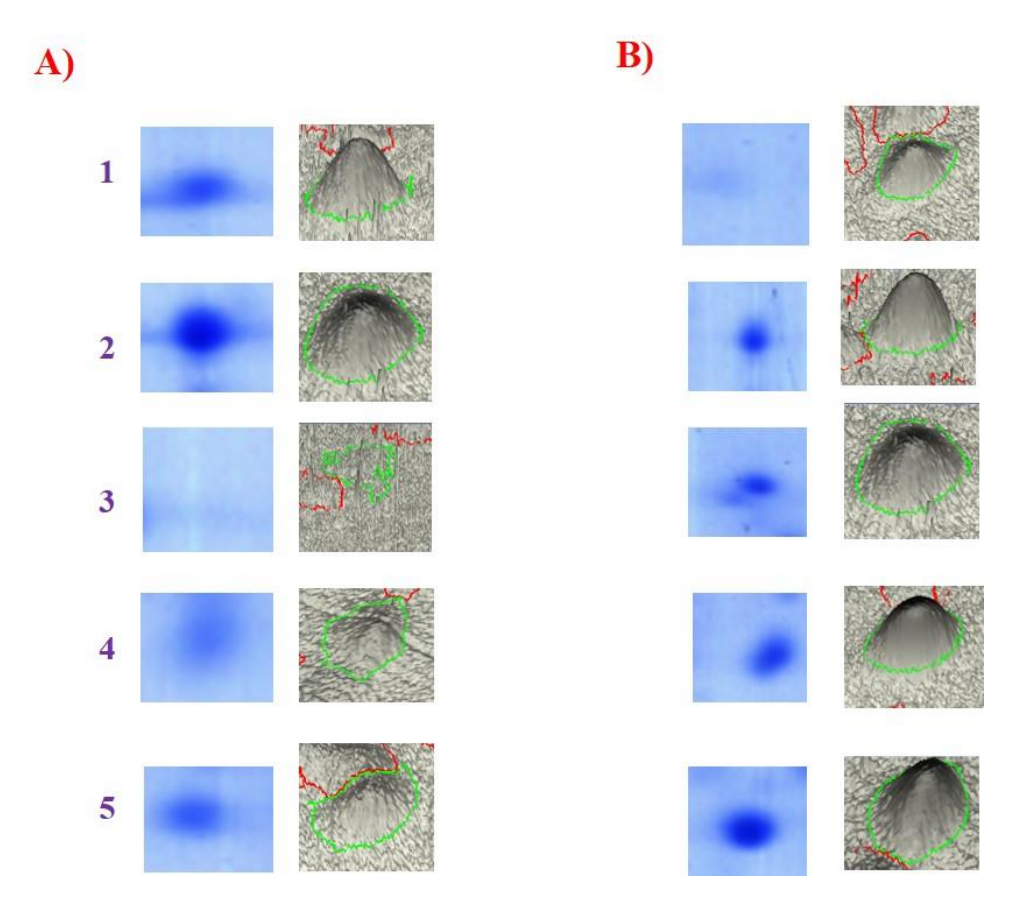


Fig. 6.7. Three-dimensional view of differentially expressed protein spots (1-5) labelled in 2-DE of fig 6.6 using Image Master Platinum software. Panels (A) and (B) represent protein spots from midgut proteome of *S. litura* larvae (early 5th instar stage) fed up on (A) artificial diet without T9BBI and (B) artificial diet with T9BBI (0.1%), respectively.

A)

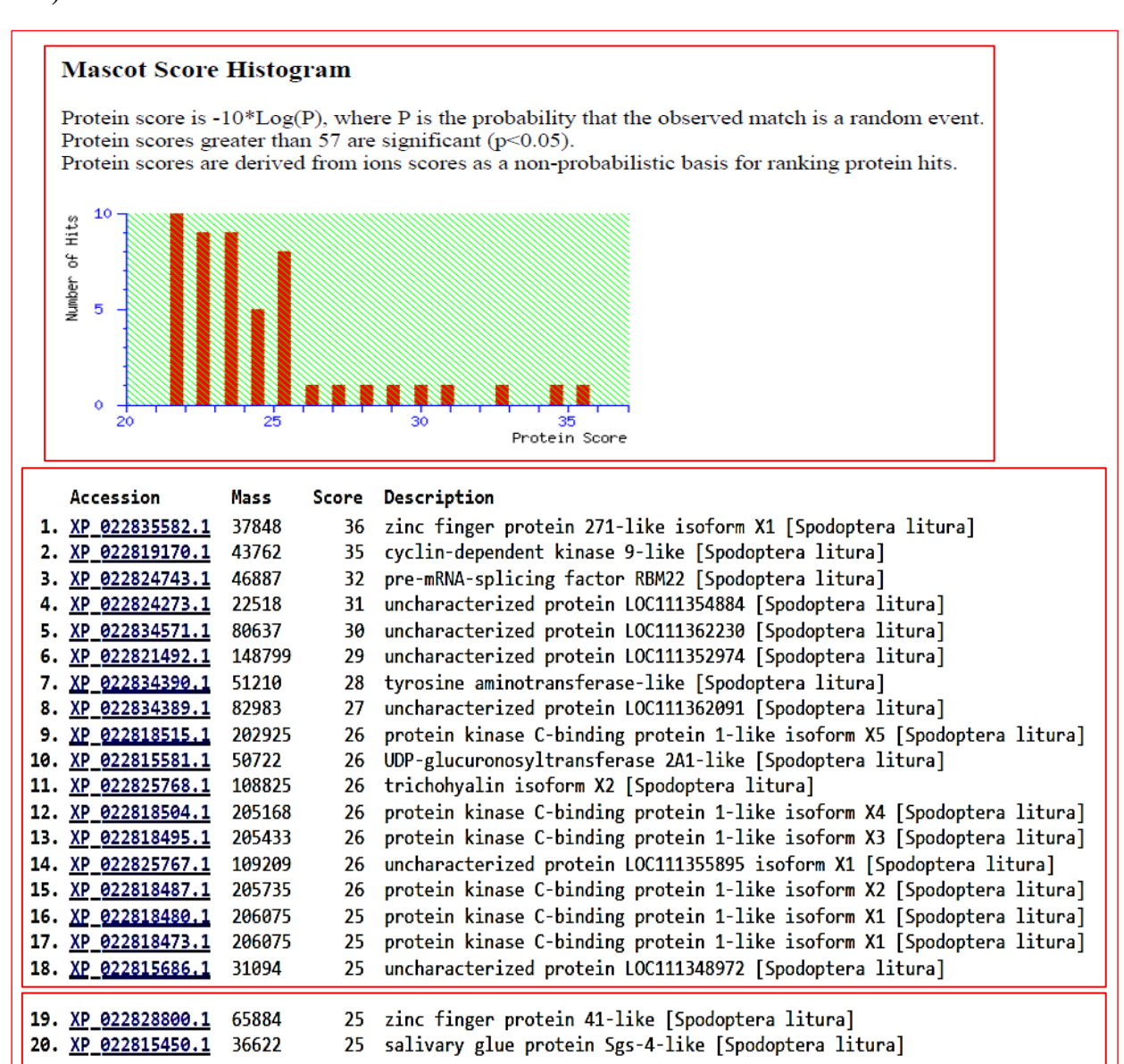
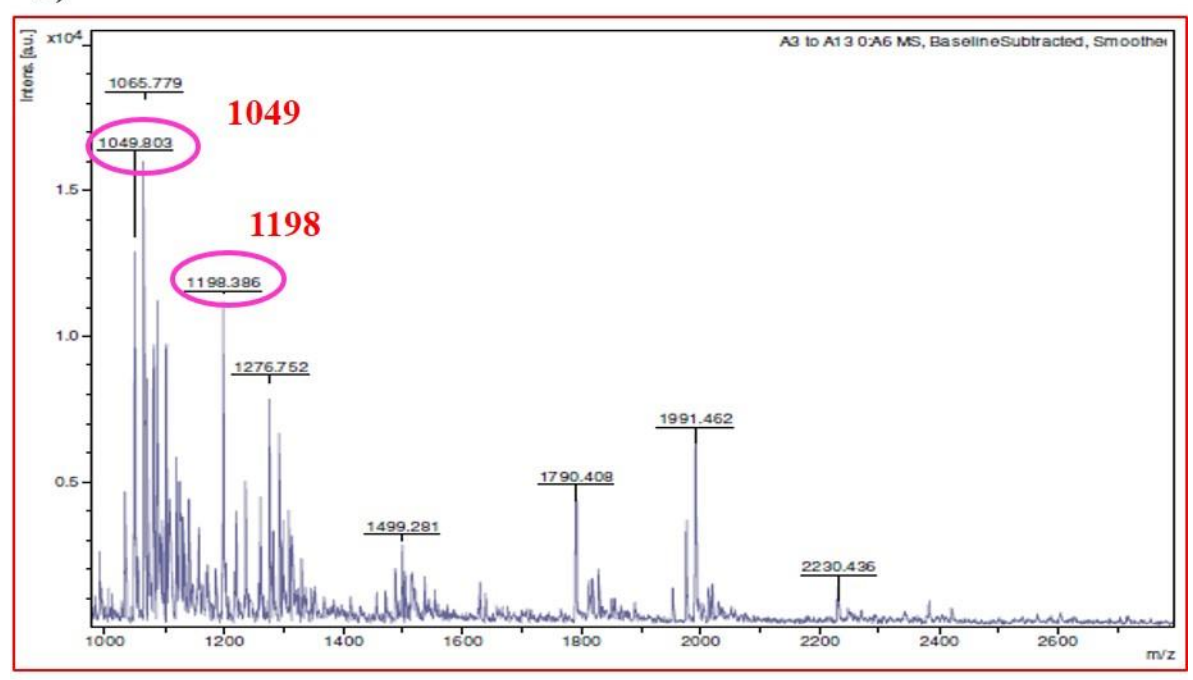


Fig. 6.8. Identification of spot 1 as Zinc-finger protein 271-like isoform X1 after tryptic digestion and MALDI-TOF-TOF analysis. (A) Histogram of MASCOT search results and corresponding protein hits.





C)

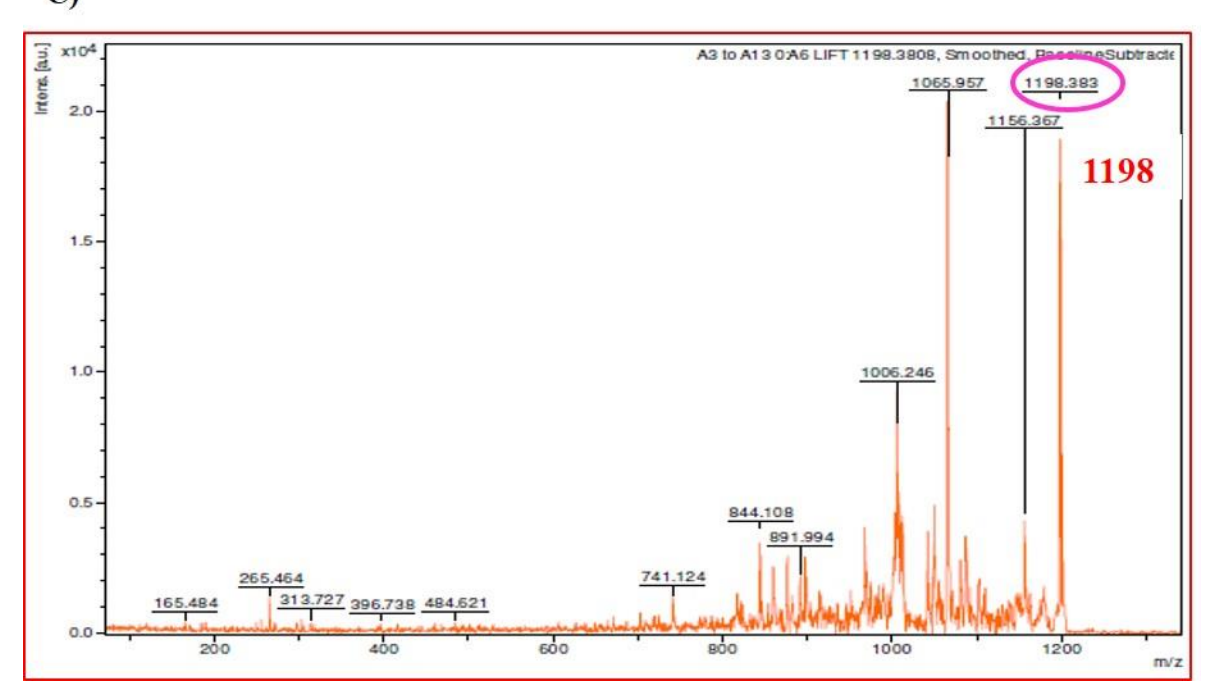


Fig. 6.8. (B): PMF spectrum of spot 1 highlighting peaks 1049 and 1198; **(C)** Lift spectrum of PMF peak with 1198 m/z.

D)

Calculated Masses: AFTRSDNMKK AFTRSDNMKK										Pe	eak: 1198		
N-Term.	Ion	8	b	1	a-17	a-18	b-17	b-18	b+18	V	y-17	C-Term.	lo
1	Α	44.049	72.044	44.049	27.023	26.039	55.018	54.034	90.055	147.113	130.110	10	K
2	F	191.118	219.113	120.081	174.091	173.107	202.096	201.102	237.123	275.208	258.205	9	K
3	T	292.166	320.160	74.060	275.139	274.155	303.134	302.150	338.171	406.248	389.246	8	N
4	R	448.267	476.262	129.113	431.240	430.256	459.235	458.251	494.272	520.291	503.288	7	١
5	S	535,299	563,294	60.044	518.272	517.288	546.267	545.283	581.304	635.318	618.315	6	1
6	D	650.326	678.321	88.039	633,299	632.315	661.294	660.310	696.331	722.350	705.347	5	4
7	N	764.369	792.363	87.055	747.342	746.358	775.337	774.353	810.374	878.451	861.449	4	F
8	M	895.409	923.404	104.053	878.383	877.398	906.377	905.393	941.415	979.499	962.496	3	
9	K	1023.504	1051.499	101.107	1006.477	1005,493	1034.472	1033.488	1069.510	1126.567	1109.565	2	1
10	K	1151,599	1179.594	101.107	1134.572	1133.588	1162,567	1161.583	1197,604	1197.604	1180,602	1	1

Juliu II	LIN I.	Carbamidometh	1,1(0)										
N-Term.	Ion	8	b	ı	a-17	a-18	b-17	b-18	b+18	у	y-17	C-Term.	lo
1	С	133.043	161.038	133.043	116.016	115.032	144.011	143.027	179.048	147.113	130.110	9	K
2	S	220.075	248.070	60.044	203.048	202.064	231.043	230.059	266.081	276.155	259,153	8	E
3	Α	291.112	319.107	44.049	274.086	273.102	302.081	301.097	337.118	405.198	388.195	7	E
4	K	419.207	447.202	101.107	402.181	401.197	430.175	429.191	465.213	506.246	489.243	6	T
5	Р	516.260	544.255	70.065	499.233	498.249	527.228	526.244	562.265	603.298	586.296	5	P
6	T	617.308	645.302	74.060	600.281	599.297	628.276	627.292	663.313	731.393	714.391	4	K
7	E	746.350	774.345	102.055	729.324	728.340	757.319	756.334	792.356	802.431	785.428	3	A
8	E	875.393	903.388	102.055	858.366	857.382	886.361	885.377	921.398	889.463	872.460	2	S
9	K	1003.488	1031.483	101.107	986,461	985.477	1014.456	1013.472	1049.493	1049.493	1032.490	1	C

E)

Sequence coverage: 32%

MQNNPQELSWQAIQAIVGVKLPPNVLRFDDIGFHLVNNTVSSAEDSDSDVEIVENDWESDNNVSSRP DHSDNE**KTTSPDRE**QSESPVLRLIEPDNNNTGKESLDY**REYVEKIDTKDISSRE**HMTQIQIDDADSS NGNVMSIENYLEVTLSTDSEASHTCNQCNQMFSNENSLASHK<mark>CSAKPTEEKKYPCHVCSEKF</mark>PSS WDLRKHLSSHFPGMLESKSSFCHLCQ**KDYTKTGFMNHLRKH**TGERPFVCELCHAFSQSSSLSIHM **KFHLNVRKHACTVCEKKFVTKSELSRH**MTVHTKQKSYYCGVCDKAFTRSDNMKKHEKTHG

Fig. 6.8. (D): Analysis of Lift spectrum from peaks m/z 1198 and 1049 using Biotools; **(E)** Zinc-finger protein 271-like isoform X1 (XP_022835582.1) sequence. Red colour indicates the partial sequence coverage by various ions generated from spot 1 while blue box indicate the matching of *de novo* (m/z 1198 and 1049) sequences obtained from Biotools with the peptides identified by Mascot search engine.

F)

Accession number	Protein name/ Source	Sequence	Similarity (%)
Spot number 1 (de nov	vo sequence from PMF peak with m/z 1198)	AFTRSDNMKK	100
KOB74681.1	Zinc finger and BTB domain-containing protein 17 / Operophtera brumata	AFTRSDNMKK	100
XP_032516611.1	Zinc finger protein 596-like isoform X1/ Danaus plexippus plexippus	AFTRSDNMKK	100
XP_012551354.1	Zinc finger protein 16 isoform X1/ Bombyx mori	AFTRSDNMKK	100
XP_026489825.1	Zinc finger protein 16 isoform X1/Vanessa tameamea	AFTRSDNMKK	100
XP_026748799.1	Gastrula zinc finger protein XlCGF28.1 isoform X1/ Galleria mellonella	AFTRSDNMKK	100
XP_021197220.1	Zinc finger protein 596-like isoform X1/ Helicoverpa armigera	AFTRSDNMKK	100
XP_026733611.1	Zinc finger protein 596-like/ Trichoplusia ni	AFTRSDNMKK	100
XP_028162969.1	Gastrula zinc finger protein XlCGF28.1 isoform X1/ Ostrinia furnacalis	AFTRSDNMKK	100
XP_030025489.1	Zinc finger protein 596-like/ Manduca sexta	AFTRSDNMKK *******	100

Fig. 6.8. (F): Clustal alignment of *de novo* sequence from PMF peak (m/z 1198) with Zinc-finger protein 271-like isoform X1, identified in NCBI database.

The *de novo* sequence 'CSAKPTEEK' also showed 100% similarity with the Zinc finger protein 271-like isoform X1 (Clustal alignment data not shown). These results confirm that Zinc finger protein 271-like isoform X1 is down-regulated by 3.24-fold in the midgut tissues of the *S. litura* larvae when fed upon a diet containing T9BBI.

Zinc finger protein is majorly involved in the regulation of transcription. Its extraordinary diverse functions include those of transcriptional activation, DNA recognition and RNA packaging, *etc.* (Laity et al., 2001). It has been confirmed from earlier studies that many zinc finger proteins are induced during stress conditions (Sakamoto et al., 2004; Ciftci-Yilmaz et al., 2007). Also, Zn-finger proteins play a significant role during developmental processes, for example, in wing development by regulating specific genes (Perea et al., 2013). Wings are developed from the wing imaginal disc, which is present inside the larval body. However, more morphological changes are required to develop larvae into an adult. In *Bombyx mori* Blimp-1 genes which are orthologous to the Zn-finger (C₂H₂ type) protein are up-regulated during metamorphosis. RNA interference of this gene resulted in abnormal development of wings (Wuetal., 2019).

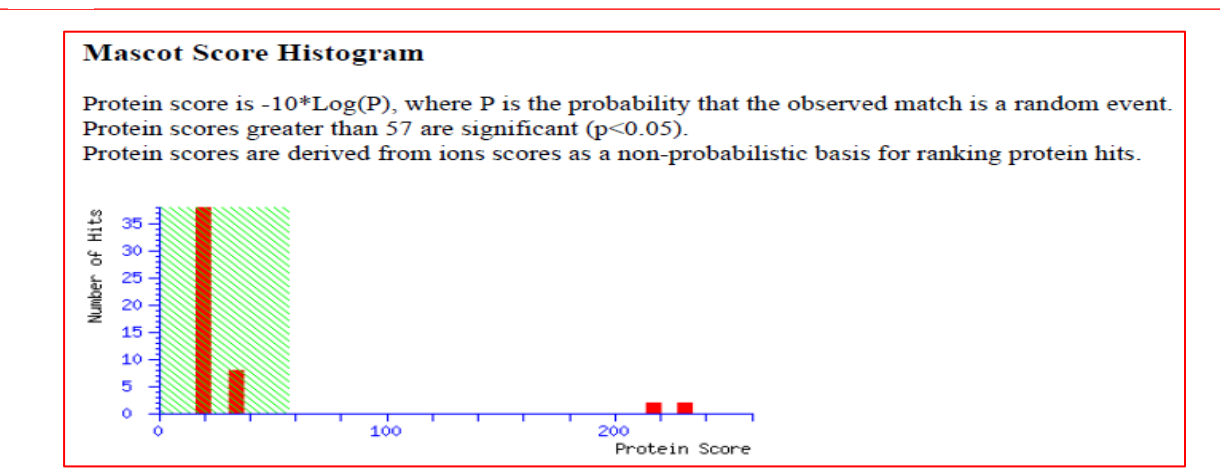
In insects, the synthesis and degradation of ecdysone (20 E- hydroxyecdysone) and juvenile hormones which are involved in insect larval molting and metamorphosis are regulated by transcriptional factors (King-Jones et al., 2005). Further, the studies of Zhao et al. (2018) demonstrated that Zinc finger transcriptional factors are down regulated in insecticide resistant strains of *Plutella xylostella* (Zhao et al., 2018). Nevertheless, the results from the present study demonstrated that feeding of T9BBI to *S. larvae* down regulated the expression of Zn-finger protein 271-like isoform X1 in its midgut tissue. This change in Zn-finger expression might have lead to delay in transformation of larvae to pupae as well as emergence of abnormal larval-pupal and pupal-adult intermediates, possibly due to disturbance in the levels of ecdysone and juvenile hormones. However, further experiments

need to be performed to understand the effect of T9BBI on ecdysone and juvenile hormone status in *S. litura* and their relation to the expression of zinc finger proteins (**Figs. 6.5-6.8 and Table 1**).

6.4.2. Identification of Spot 2 as Arginine kinase (AK) isoform X3:

Digestion of spot 2 with trypsin and subsequent MALDI-TOF-TOF analysis revealed the matching of this spot with Arginine kinase (AK) isoform X3 from S. litura with a significant score of 231 in the Mascot search engine (Fig. 6.9A). The mass spectrum corresponding to the PMF data was represented in Figure 6.9B. When the PMF peaks with m/z 1796 (lift spectrum shown), 2019 (lift spectrum not shown) were further ionized in MALDI-TOF-TOF, the following de novo sequences 'LGFLTFCPTNLGTTVR' and 'GTRGEHTEAEGGVYDISNK' were resulted when the corresponding lift spectra are analyzed using Biotools software (Figs. 6.9C and D). The various ions generated during MALDI-TOF-TOF studies showed partial sequence coverage up to 47.8% with AK isoform X3 (Uniprot Acc No. XP_022834762.1). Further, the two de novo sequences obtained through Biotools showed overlapping with the partial amino acid sequences recognised for AK isoform X3 during MALDI-TOF-TOF analysis (Fig. 6.9E). Furthermore, Clustal alignment of the de novo sequence 'LGFLTFCPTNLGTTVR' with available sequences in the NCBI database showed 100% matching to an AK isoform X3 from different insects such as Onthophagus taurus, Agrilus planipennis, Photinus pyralis, Asbolus verrucosus, Bicyclus anynana, Blattella germanica, Halyomorpha halys, Habropoda laboriosa, Zootermopsis nevadensis, and Osmia lignaria respectively (Fig. 6.9F). The de novo sequence 'GTRGEHTEAEGGVYDISNK' from PMF peak with m/z 2019 also showed 100% similarity with the AK isoform X3 (Clustal alignment data not shown). These results confirm that spot 2 belong to the AK isoform X3 and it is down-regulated by 1.8-fold in the midgut tissues of the S. litura larvae when fed upon a diet containing T9BBI (Figs. 6.6, 6.7 and 6.9).

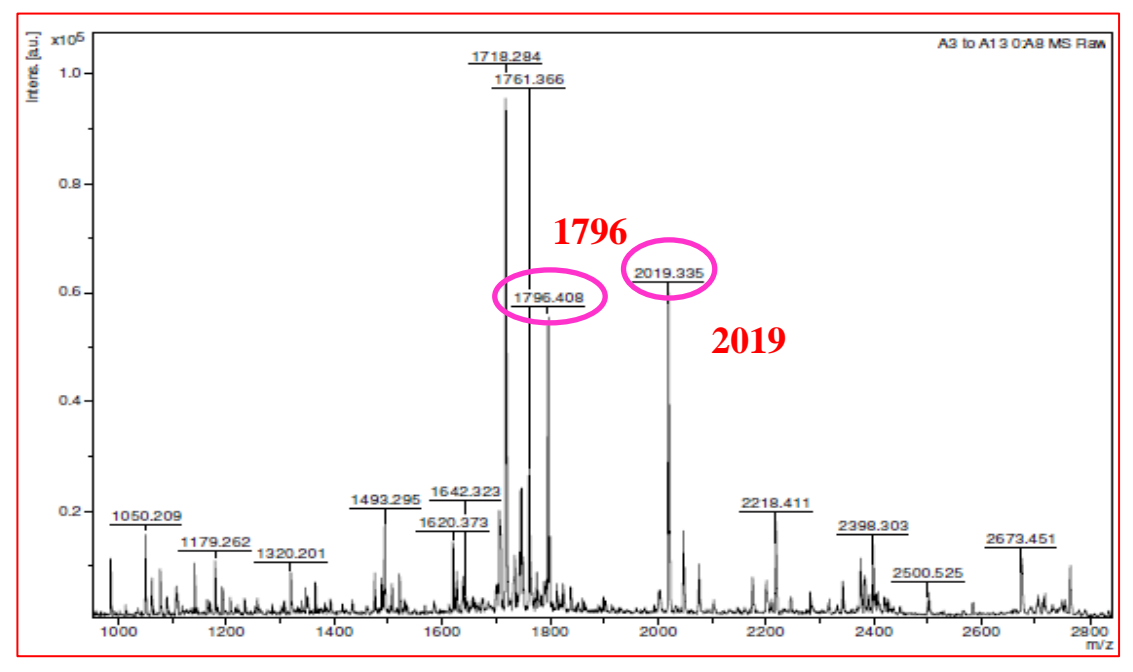
A)



	Accession	Mass	Score	Description
1.	XP_022834762.1	40225	231	arginine kinase isoform X3 [Spodoptera litura]
2.	ADW94627.1	40191	231	arginine kinase [Spodoptera litura]
3.	XP_022834761.1	43448	221	arginine kinase isoform X2 [Spodoptera litura]
4.	XP_022834760.1	43544	221	arginine kinase isoform X1 [Spodoptera litura]
5.	XP_022823305.1	126236	34	uncharacterized protein LOC111354196 isoform X1 [Spodoptera litura]
6.	XP_022814113.1	22679	33	protein phosphatase PTC7 homolog [Spodoptera litura]
7.	XP_022817671.1	38614	32	uncharacterized protein LOC111350349 [Spodoptera litura]
8.	XP_022817662.1	38614	32	uncharacterized protein LOC111350349 [Spodoptera litura]
9.	XP_022833899.1	34988	31	uncharacterized protein LOC111361733 [Spodoptera litura]
10.	XP_022835630.1	33583	29	protein phosphatase PTC7 homolog [Spodoptera litura]
11.	XP_022830959.1	35465	28	uncharacterized protein LOC111359599 [Spodoptera litura]
12.	XP_022816866.1	8505	27	FMRFamide-related neuropeptides [Spodoptera litura]
13.	XP_022818733.1	38823	27	uncharacterized protein LOC111351166 [Spodoptera litura]
14.	XP_022816705.1	34417	24	THUMP domain-containing protein 1 homolog [Spodoptera litura]
15.	AIS72935.1	19263	24	pheromone-binding protein 1 [Spodoptera litura]
16.	XP_022828187.1	16290	24	partner of bursicon [Spodoptera litura]
17.	XP_022817548.1	71847	23	TRAF3-interacting protein 1 [Spodoptera litura]
18.	XP_022823306.1	123034	23	uncharacterized protein LOC111354196 isoform X2 [Spodoptera litura]
19.	XP 022826511.1	20920	22	calcineurin subunit B type 2 isoform X1 [Spodoptera litura]
20.	XP_022819657.1	46269	22	serine-threonine kinase receptor-associated protein-like [Spodoptera litura]

Fig. 6.9. Identification of spot 2 as Arginine kinase isoform X3 after tryptic digestion and MALDI-TOF-TOF analysis. (A) Histogram of MASCOT search results and corresponding protein hits.







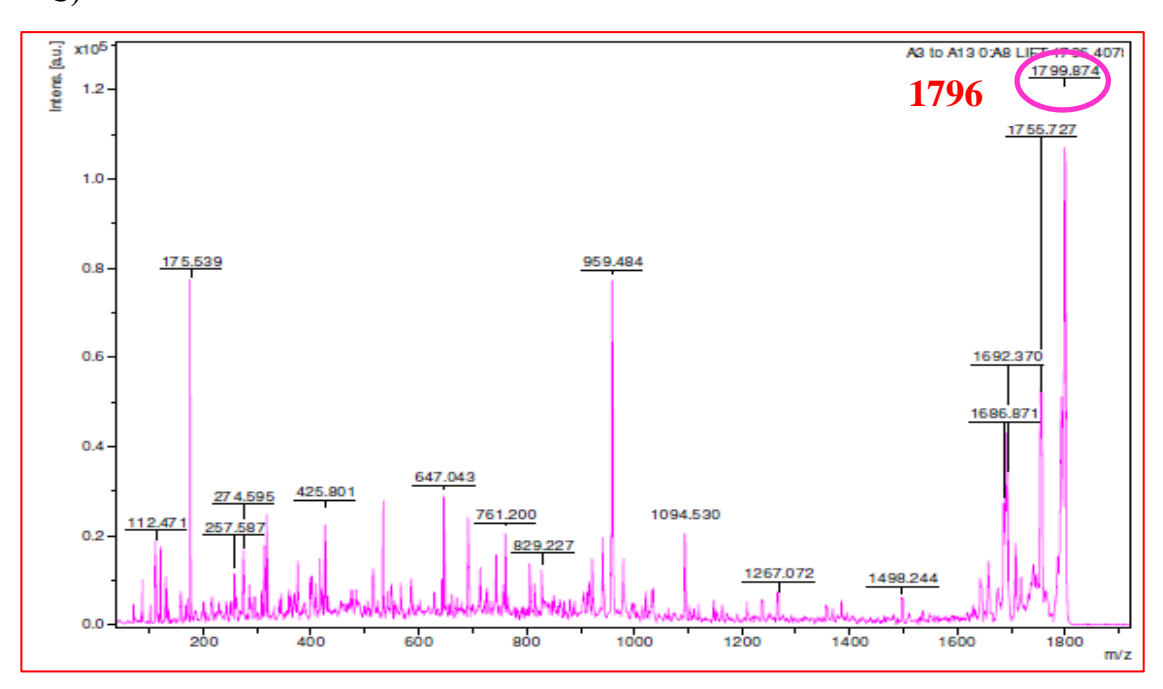


Fig. 6.9. (B): PMF spectrum of spot 2 highlighting peaks 1796 (m/z) and 2019 (m/z); **(C)** Lift spectrum of PMF peak with m/z 1796

SFLIFG	PTNLG	TTVR 7: Carba		Peak: 1796									
I-Term.	Ion	a	b	1	a-17	a-18	b-17	b-18	b+18	y	y-17	C-Term.	lo
1	L	86.096	114.091	86.096	69.070	68.086	97.065	96.081	132.102	175.119	158,116	16	F
2	G	143.118	171.113	30.034	126.091	125.107	154.088	153.102	189.123	274.187	257.185	15	١
3	F	290.186	318.181	120.081	273.160	272.176	301.155	300.171	336,192	375.235	358.232	14	Г
4	L	403.270	431.265	86.096	386.244	385.260	414.239	413.255	449.276	476.283	459.280	13	Г
5	T	504.318	532.313	74.060	487.291	486.307	515.286	514.302	550.324	533.304	516.301	12	(
6	F	651.386	679.381	120.081	634.360	633.376	662.355	661.371	697.392	646.388	629.386	- 11	П
7	C	811.417	839.412	133.043	794.391	793.407	822.385	821.401	857.423	760.431	743.428	10	П
8	Р	908.470	936.465	70.065	891.443	890.459	919.438	918.454	954.475	861.479	844.476	9	Г
9	T	1009.518	1037.512	74.060	992,491	991.507	1020.488	1019.502	1055.523	958.532	941.529	8	П
10	N	1123,560	1151.555	87.055	1106.534	1105.550	1134.529	1133.545	1169.566	1118.562	1101.560	7	
11	L	1236.645	1264.639	86.096	1219.618	1218.634	1247.613	1246.629	1282.650	1265.631	1248.628	6	П
12	G	1293.666	1321.661	30.034	1276.639	1275.655	1304.634	1303.650	1339.671	1366.678	1349.676	5	
13	T	1394.714	1422.709	74.060	1377.687	1376.703	1405.682	1404.698	1440.719	1479.762	1462.760	4	Г
14	T	1495.761	1523.756	74.060	1478.735	1477.751	1506.730	1505.746	1541.767	1626.831	1609.828	3	П
15	٧	1594.830	1622.825	72.081	1577.803	1576.819	1605.798	1604.814	1640.835	1683.852	1666.850	2	Т
16	R	1750.931	1778.926	129,113	1733,904	1732,920	1761.899	1760.915	1796,936	1796.936	1779,934	1	г

Calculated Masses: GTRGEHTEAEGGVYDISNK GTRGEHTEAEGGVYDISNK											Peak: 2019			
N-Term.	Ion	8	b	1	a-17	a-18	b-17	b-18	b+18	V	y-17	C-Term.	lor	
1	G	30.034	58.029	30.034	13.007	12.023	41.002	40.018	76.039	147.113	130.110	19	K	
2	T	131.082	159.076	74.060	114.055	113.071	142.050	141.066	177.097	261.156	244.153	18	N	
3	R	287.183	315.178	129.113	270.156	269.172	298.151	297.167	333.188	348.188	331.185	17	S	
4	G	344.204	372.199	30.034	327.178	326.194	355.172	354.188	390.210	461.272	444.269	16	١	
5	Е	473.247	501.242	102.055	456.220	455.236	484.215	483.231	519.252	576.299	559.296	15	0	
6	Н	610.306	638.300	110.071	593.279	592.295	621.274	620.290	656.311	739.362	722,359	14	Y	
7	T	711.353	739,348	74.060	694,327	693,343	722.322	721.338	757.359	838.431	821,428	13	١	
8	Е	840.396	868,391	102.055	823,369	822.385	851.364	850.380	896,401	895,452	878,449	12	G	
9	A	911,433	939,428	44,049	894,406	893,422	922,401	921,417	957,438	952,473	935,471	11	G	
10	Е	1040.476	1068.470	102.055	1023,449	1022,465	1051.444	1050.460	1095.481	1081.516	1064.513	10	E	
11	G	1097.497	1125.492	30.034	1080.470	1079.486	1108.465	1107.481	1143.503	1152.553	1135.550	9	A	
12	G	1154.518	1182.513	30.034	1137.492	1136.508	1165.487	1164.503	1200.524	1281.596	1264.593	8	E	
13	٧	1253.587	1281.582	72.081	1236,560	1235.576	1264.555	1263.571	1299.592	1382.643	1365.641	7	T	
14	Y	1416.650	1444.645	136.076	1399.624	1398.640	1427.619	1426.635	1462.656	1519.702	1502.700	6	Н	
15	D	1531.677	1559.672	88.039	1514.651	1513.667	1542.646	1541.662	1577.683	1648.745	1631.742	5	E	
16	1	1644.761	1672.756	86.096	1627.735	1626.751	1655.730	1654.746	1690.767	1705.766	1688.764	4	G	
17	S	1731.793	1759.788	60.044	1714.767	1713.783	1742.762	1741.778	1777.799	1861.867	1844.865	3	R	
18	N	1845.836	1873.831	87.055	1828.810	1827.826	1856.805	1855.821	1891.842	1962.915	1945.912	2	Т	
19	K	1973.931	2001.926	101,107	1956,905	1955,921	1984,900	1983,916	2019,937	2019.937	2002.934	1	G	

E)

Sequence coverage: 47.8%

MVDAATIEKLEAGFSKLQASDSKSLLKKYLTKEVFDALKNKKTSFGSTLLDCIQSGVENLDSGVGIYAPDAEAYT VFADLFDPIIEDYHNGFKKTDKHPPKNWGDVETLGNLDPAGEFVVSTRVRCGRSMEGYPFNPCLTEAQYKE MEEKVASTLSGLEGELKGTFYPLTGMSKETQQQLIDDHFLFKEGDRFLQAANACRFWPSGRGIYHNENKTFL VWCNEEDHLRLISMQMGGDLKQVYKRLVTAVNDIEKRIPFSHDDRLGFLTFCPTNLGTTVRASVHIKLPKL AADKAKLEEIASKYHLQVRGTRGEHTEAEGGVYDISNKRRMGLTEYDAVKEMYDGIAELIKIEKSL

Fig. 6.9. (D): Analysis of Lift spectrum from peaks m/z 1796 and 2019 using Biotools; **(E)** Arginine kinase isoform X3 (XP_022834762.1) sequence. Red colour indicates the partial sequence coverage by various ions generated from spot 2 while blue box indicate the matching of *de novo* (m/z 1796 & 2019) sequence obtained from Biotools with the peptides identified by Mascot search engine.

F)

Accession number	Protein name/ Source	Sequence	Similarity (%)
Spot number 2 (de novo	o sequence from PMF peak with m/z 1796)	LGFLTFCPTNLGTTVR	100
XP_022914844.1	Arginine kinase isoform X1 /Onthophagus taurus	LGFLTFCPTNLGTTVR	100
XP_018325550.1	Arginine kinase isoform X1/Agrilus planipennis	LGFLTFCPTNLGTTVR	100
XP_031335752.1	Arginine kinase isoform X1/ Photinus pyralis	LGFLTFCPTNLGTTVR	100
RZC33279.1	Arginine kinase/Asbolus verrucosus	LGFLTFCPTNLGTTVR	100
XP_023950045.1	Arginine kinase isoform X1/Bicyclus anynana	LGFLTFCPTNLGTTVR	100
PSN31172.1	Arginine kinase/Blattella germanica	LGFLTFCPTNLGTTVR	100
XP_014280926.1	Arginine kinase isoform X1/Halyomorpha halys	LGFLTFCPTNLGTTVR	100
KOC62125.1	Arginine kinase/Habropoda laboriosa	LGFLTFCPTNLGTTVR	100
XP_021917184.1	Arginine kinase isoform X1 /Zootermopsis nevadensis	LGFLTFCPTNLGTTVR	100
XP_034193506.1	Arginine kinase isoform X1/Osmia lignaria	LGFLTFCPTNLGTTVR ***********	100

Fig. 6.9. (F): Clustal alignment of *de novo* sequence from PMF peak (m/z 1796) with Arginine kinase isoform X3, identified in NCBI database.

In the present study, it was observed that the specific activity of the AK enzyme in larvae fed on the control diet and T9BBI containing diet were 0.0049245 units/mg protein and 0.0091248 units/mg protein, respectively (**Fig. 6.10**).

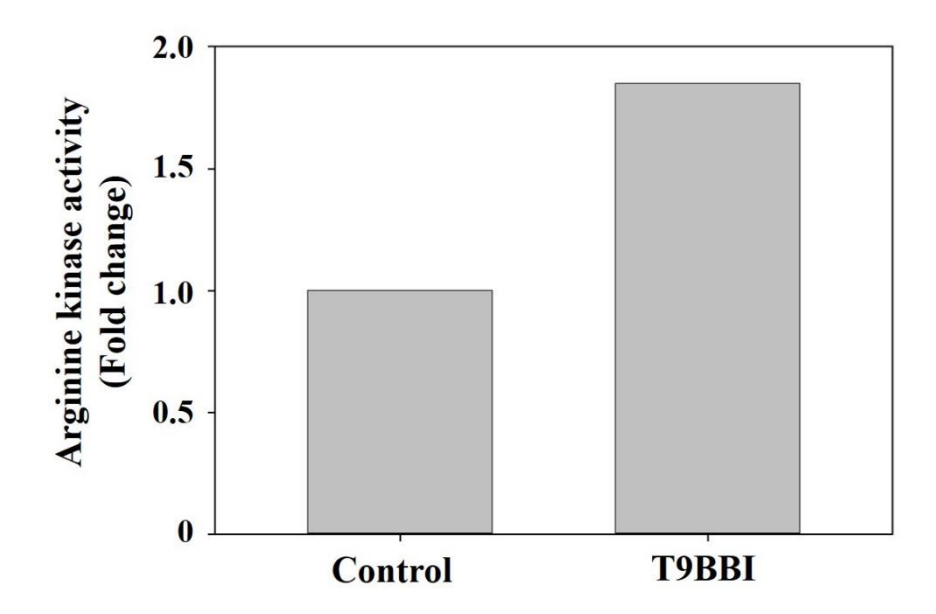


Fig.6.10. Arginine kinase enzyme activity in control and T9BBI (0.1%) gut extracts of *S. litura*

Arginine Kinase is directly linked with cell division, ATP regeneration, muscle contraction and energy transportation in cellular energy metabolism (Ai et al., 2018). Further, The laboratory of Qi et al. (2015) examined the levels of AK in *H. armigera* using RT-PCR under different conditions and derived the following conclusions: i) the peak expression levels of AK was identified in 5th instar larvae, (ii) the expression of AK was found to be down-regulated in *Bt*-resistant larvae. Corroborating with these results, in the present study, feeding of T9BBI to *S. litura* larvae also down-regulated the expression of AK protein as revealed by 2-D gel electrophoresis (**Figs. 6.6 and 6.7**). Further, targeting of AK gene in *H. armigera* using RNAi technology greatly enhanced the larval mortality rates and delayed the larval pupation (Qi et al., 2015). Also, in the present study, though larval mortality was not

observed, a significant delay in pupal development (7 to 9 days) and the emergence of larval-pupal and pupal-adult intermediates was observed when T9BBI was fed to *S. litura* larvae (**Table 6.1**). Further, in spite of the decrease in protein levels (spot 2) of AK in larvae fed upon T9BBI, its activity was increased significantly by >7.0 fold as compared to larvae fed on control (**Fig. 6.6, 6.7 and 6.13**). Possibly, this increase in activity of AK in larvae fed on T9BBI reflects the high energy requirement of midgut tissue to detoxify this biopesticide (**Fig. 6.10**)

6.4.3. Identification of Spot 3 as uncharacterized protein:

Spot 3, which is expressed in larvae upon feeding with T9BBI, was subjected to tryptic digestion and this was followed by MALDI-TOF-TOF analysis. The Mascot search results showed matching to an uncharacterized protein from S. litura with a prominent score of 46 (Fig. 6.11A). The mass spectrum corresponding to the PMF data was represented in Figure **6.11B.** When the PMF peaks with m/z 1493 (lift spectrum shown), 1234 (lift spectrum not shown) were further ionized in MALDI-TOF-TOF, the following de novo sequences 'SRENISRTMDLR' and 'ENISRTMDLR' have resulted from the corresponding lift spectra when analyzed using Biotools software (Figs. 6.11C and D). Also, the various ions generated during MALDI-TOF-TOF studies showed partial sequence coverage of up to 53% with an uncharacterized protein (Uniprot Acc No. XP_022819955.1). Further, the two de novo sequences obtained through Biotools showed overlapping with each other and also with the partial amino acid sequences recognised for uncharacterized protein during MALDI-TOF-TOF analysis (Fig. 6.11E). Furthermore, Clustal alignment of the de novo sequence 'SRENISRTMDLR' with available sequences in the NCBI database showed 92-100% matching to an 'Uncharacterized protein' from different insects such as M. sexta, Danus plexippus, Pieris rapae, Bicyclus anynana, Operophtera brumata and H. armigera, respectively (Fig. 6.11F).

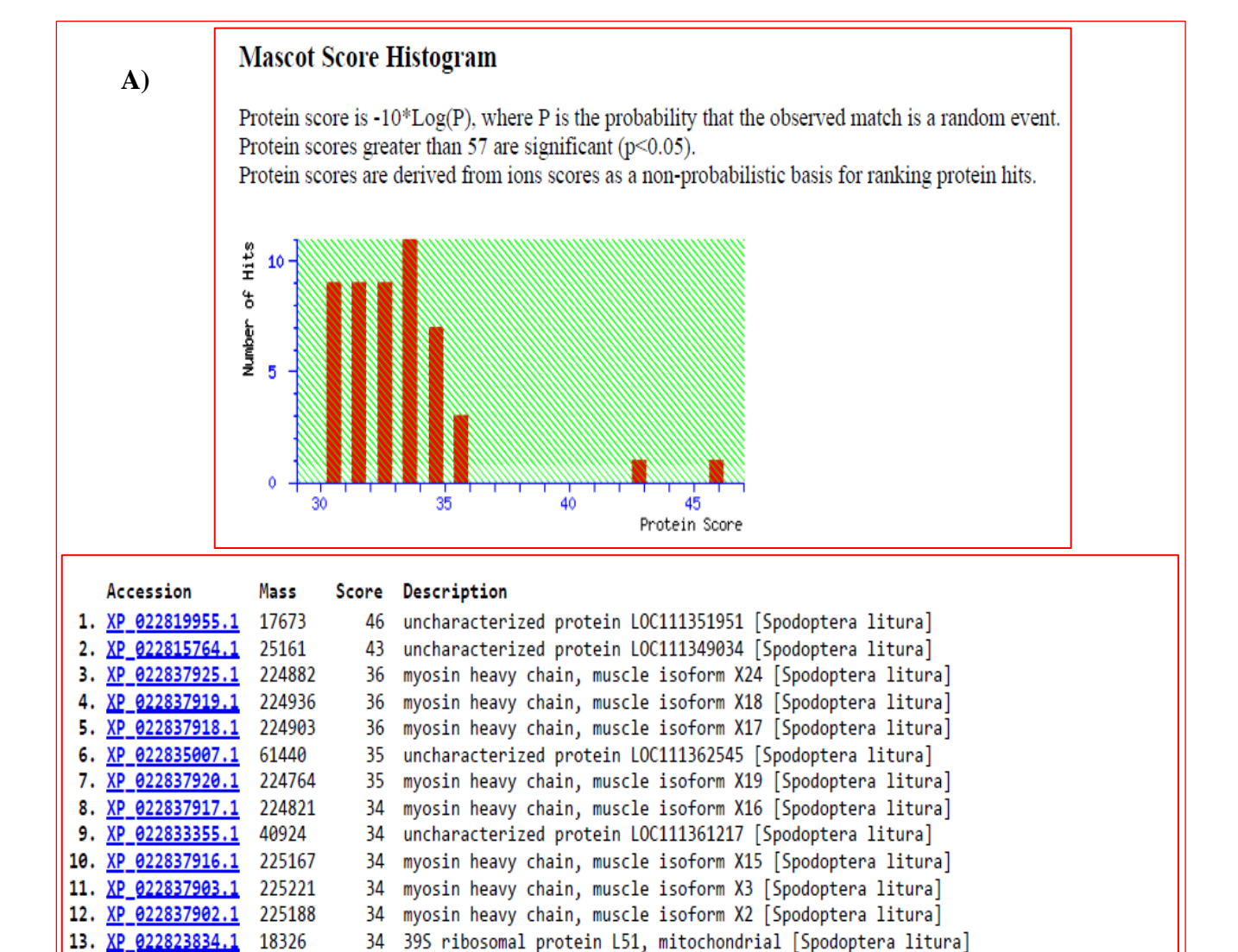


Fig. 6.11. Identification of spot 3 as uncharacterized protein, after tryptic digestion and MALDI-TOF-TOF analysis. (A) Histogram of MASCOT search results and corresponding protein hits.

33 histone H2A, sperm-like [Spodoptera litura]

34 transcription initiation factor TFIID subunit 4 isoform X7 [Spodoptera litura]

26S proteasome regulatory subunit 6B [Spodoptera litura]

myosin heavy chain, muscle isoform X26 [Spodoptera litura]

myosin heavy chain, muscle isoform X12 [Spodoptera litura]

myosin heavy chain, muscle isoform X39 [Spodoptera litura]

myosin heavy chain, muscle isoform X34 [Spodoptera litura]

80460

47161

224796

225184

222930

225003

14969

34

34

33

15. XP 022826943.1

16. XP 022837927.1

17. XP 022837913.1

18. XP 022837941.1

19. XP 022837936.1

20. XP_022816074.1

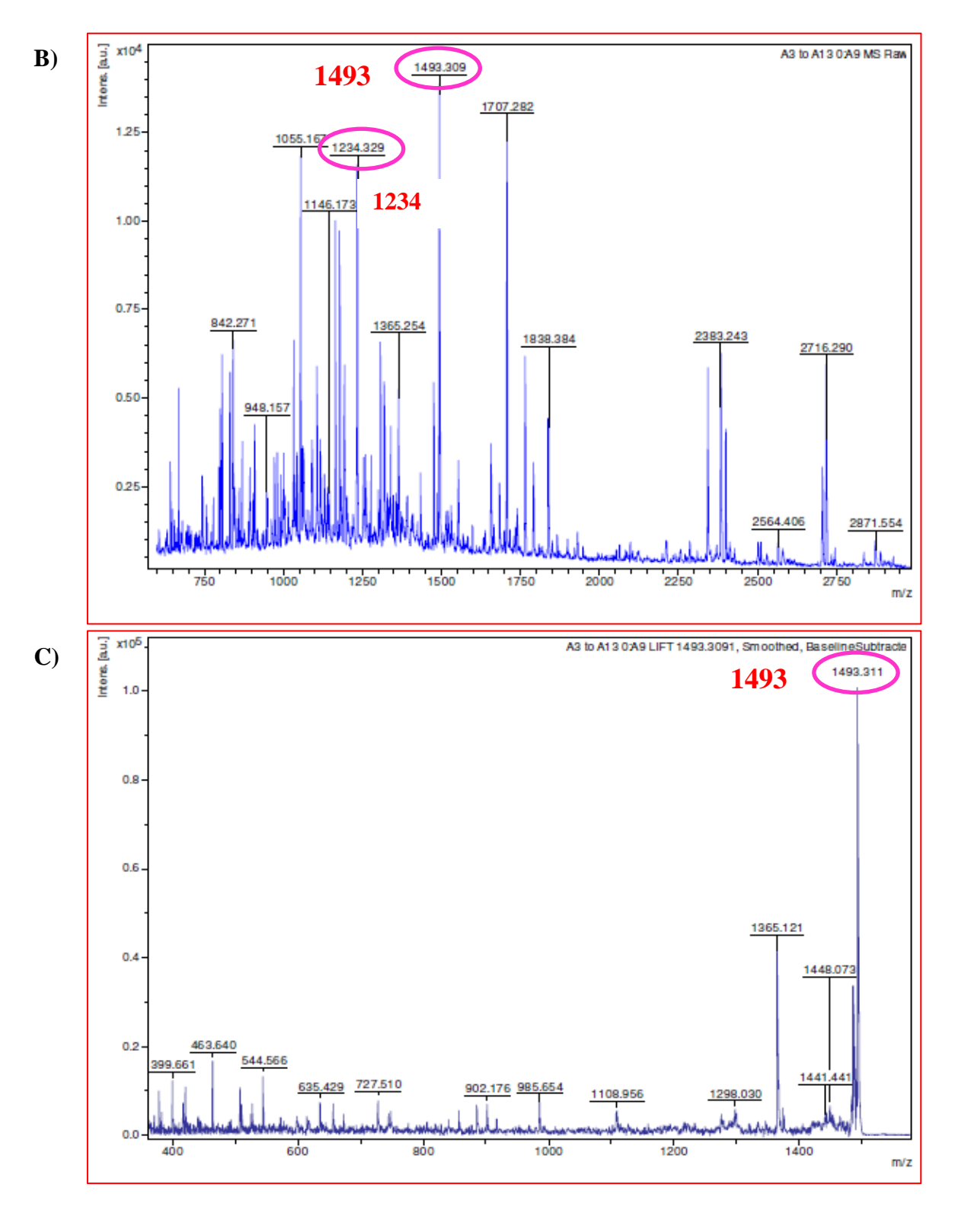


Fig. 6.11. (B): PMF spectrum of spot 3 highlighting peaks 1234 (m/z) and 1493 (m/z); **(C)** Lift spectrum of PMF peak with m/z 1493.

	d Mass	es: ? 9: Oxidation (1	M)	SRENISRTMDLR							Peak	: 1493	
N-Term.	Ion	a	b	I	a-17	a-18	b-17	b-18	b+18	y	y-17	C-Term.	loi
1	S	60.044	88.039	60.044	43.018	42.034	71.013	70.029	106.050	175.119	158.116	12	R
2	R	216.145	244.140	129.113	199.119	198.135	227.114	226.130	262.151	288.203	271.200	11	L
3	E	345.188	373.183	102.055	328.162	327.178	356.156	355.172	391.194	403.230	386,227	10	
4	N	459.231	487.226	87.055	442.204	441.220	470.199	469.215	505.236	550.265	533,263	9	M
5		572.315	600.310	86.096	555.289	554.305	583.283	582.299	618.321	651.313	634.310	8	1
6	S	659.347	687.342	60.044	642.321	641.337	670.315	669.331	705.353	807.414	790.411	7	ı
7	R	815.448	843.443	129.113	798.422	797.438	826.417	825.433	861.454	894.446	877.443	6	9
8	T	916.496	944.491	74.060	899.469	898.485	927.464	926.480	962.501	1007.530	990.527	5	
9	M*	1063.531	1091.526	120.048	1046.505	1045.521	1074.500	1073.516	1109.537	1121.573	1104.570	4	١
10	D	1178.558	1206.553	88.039	1161.532	1160.548	1189.527	1188.543	1224.564	1250.616	1233.613	3	E
- 11		1291.642	1319.637	86.096	1274.616	1273.632	1302.611	1301.627	1337.648	1406.717	1389.714	2	ı
12	R	1447.743	1475.738	129.113	1430.717	1429.733	1458.712	1457.728	1493.749	1493.749	1476.746	1	Ş
12 Calculated	1 Mass	1447.743 es:			1430.717	1429.733	1458.712	1457.728	1493.749	1493.749		1224	S
12 Calculated ENISRTMI	d Mass	1447.743	NISRTM							1493.749	Peak:		
12 Calculated	d Mass	1447.743	NISRTM	IDLR	a-17	a-18	b-17	b-18	b+18	y	Peak:	C-Term.	
Calculated ENISRTMI N-Term. 1	d Mass	1447.743 es: 11 E	NISRTM b 130.050	IDLR 102.055	a-17 85.028	a-18 84.044	b-17 113.023	b-18 112.039	b+18 148.060	y 175.119	Peak:	C-Term.	
Calculated ENISRTMI N-Term. 1 2	d Mass	1447.743 es: 11 E a 102.055 216.098	NISRTM b 130.050 244.093	IDLR 102.055 87.055	a-17 85.028 199.071	a-18 84.044 198.087	b-17 113.023 227.066	b-18 112.039 226.082	b+18 148.060 262.103	y 175.119 288.203	Peak: 9-17 158.116 271.200	C-Term. 10	
Calculated ENISRTMI N-Term. 1 2 3	I Mass	1447.743 PS: 102.055 216.098 329.182	b 130.050 244.093 357.177	IDLR 1 102.055 87.055 86.096	a-17 85.028 199.071 312.155	a-18 84.044 198.087 311.171	b-17 113.023 227.066 340.150	b-18 112.039 226.082 339.166	b+18 148.060 262.103 375.187	y 175.119 288.203 403.230	Peak: ¥-17 158.116 271.200 386.227	C-Term. 10 9	
Calculated ENISRTMI N-Term. 1 2 3	ION E N I S	1447.743 es: 102.055 216.098 329.182 416.214	b 130.050 244.093 357.177 444.209	IDLR 1 102.055 87.055 88.096 60.044	a-17 85.028 199.071 312.155 399.187	a-18 84.044 198.087 311.171 398.203	b-17 113.023 227.066 340.150 427.182	b-18 112.039 226.082 339.166 426.198	b+18 148.060 262.103 375.187 462.219	y 175.119 288.203 403.230 534.270	Peak: y-17 158.116 271.200 386.227 517.268	C-Term. 10 9 8 7	
Calculated ENISRTMI N-Term. 1 2 3 4 5	I Mass	1447.743 PS: 102.055 216.098 329.182 416.214 572.315	b 130.050 244.093 357.177 444.209 600.310	IDLR 1 102.055 87.055 86.096 60.044 129.113	a-17 85.028 199.071 312.155 399.187 555.289	8-18 84.044 198.087 311.171 398.203 554.305	b-17 113.023 227.066 340.150 427.182 583.283	b-18 112.039 226.082 339.166 426.198 582.299	b+18 148.060 262.103 375.187 462.219 618.321	y 175.119 288.203 403.230 534.270 635.318	Peak: y-17 158.118 271.200 386.227 517.268 618.315	C-Term. 10 9 8 7	
Calculated ENISRTMI N-Term. 1 2 3	d Massa DLR en Ion E N I S R	1447.743 PS: 102.055 216.098 329.182 416.214 572.315 673.363	b 130,050 244,093 357,177 444,209 600,310 701,358	IDLR 1 102.055 87.055 88.096 60.044 129.113 74.060	a-17 85.028 199.071 312.155 399.187 555.289 656.336	8-18 84.044 198.087 311.171 398.203 554.305 655.352	b-17 113.023 227.066 340.150 427.182 583.283 684.331	b-18 112.039 226.082 339.166 426.198 582.299 683.347	b+18 148.050 262.103 375.187 462.219 618.321 719.368	y 175.119 288.203 403.230 534.270 635.318 791.419	Peak: y-17 158.118 271.200 386.227 517.268 618.315 774.416	C-Term. 10 9 8 7 6	
12 Calculate ENISRTMI N-Term. 1 2 3 4 5 6 7	I Masson DLR en Ion E N I S R	1447.743 BS: 102.055 216.098 329.182 416.214 572.315 673.363 804.403	D 130.050 244.093 357.177 444.209 600.310 701.358 832.398	IDLR 1 102.055 87.055 88.096 60.044 129.113 74.060 104.053	a-17 85.028 199.071 312.155 399.187 555.299 656.336 787.377	8-18 84.044 198.087 311.171 399.203 554.305 655.352 796.393	b-17 113.023 227.066 340.150 427.182 583.283 684.331 815.372	b-18 112.039 226.082 339.166 426.198 582.299 683.347 814.388	b+18 148.060 262.103 375.187 462.219 618.321 719.368 850.409	y 175.119 288.203 403.230 534.270 635.318 791.419 878.451	Peak: y-17 158.116 271.200 386.227 517.268 618.315 774.416 861.449	C-Term. 10 9 8 7 6 5	
12 Calculate CENISRTMI N-Term. 1 2 3 4 5 6 7 8	d Massa DLR en Ion E N I S R	1447.743 BES: 102.055 216.098 329.182 416.214 572.315 673.363 804.403 919.430	D 130.050 244.093 357.177 444.209 600.310 701.358 832.398 947.425	IDLR 1 102.055 87.055 88.096 60.044 129.113 74.060 104.053 88.039	a-17 85.028 199.071 312.155 399.187 555.299 656.336 787.377 902.404	8-18 84.044 198.087 311.171 398.203 554.305 655.352 786.393 901.420	b-17 113.023 227.066 340.150 427.182 583.283 684.331 815.372 930.399	b-18 112.039 226.082 339.166 426.198 582.299 683.347 814.388 929.415	b+18 148.060 262.103 375.187 462.219 618.321 719.368 850.409 965.436	y 175.119 288.203 403.230 534.270 635.318 791.419 878.451 991.535	Peak: y-17 158.116 271.200 386.227 517.268 618.315 774.416 861.449 974.533	C-Term. 10 9 8 7 6 5 4	
12 Calculate ENISRTMI N-Term. 1 2 3 4 5 6 7	I Masson DLR en Ion E N I S R	1447.743 BS: 102.055 216.098 329.182 416.214 572.315 673.363 804.403	D 130.050 244.093 357.177 444.209 600.310 701.358 832.398	IDLR 1 102.055 87.055 88.096 60.044 129.113 74.060 104.053	a-17 85.028 199.071 312.155 399.187 555.299 656.336 787.377	8-18 84.044 198.087 311.171 399.203 554.305 655.352 796.393	b-17 113.023 227.066 340.150 427.182 583.283 684.331 815.372	b-18 112.039 226.082 339.166 426.198 582.299 683.347 814.388	b+18 148.060 262.103 375.187 462.219 618.321 719.368 850.409	y 175.119 288.203 403.230 534.270 635.318 791.419 878.451	Peak: y-17 158.116 271.200 386.227 517.268 618.315 774.416 861.449	C-Term. 10 9 8 7 6 5 4	

E) Sequence coverage: 53%

MLSKFIRSTYKSNVGLLLTRKVIPKILNVRYADMIPPTQYDVPFPSRLKFGCIIRERWEII PLFIATGVALSFMFYSIVYACQNKVDVVFTSR<mark>SRENISRTMDLR</mark>CPTIHKLIIINQKYPP WPEMQSVLDKMRMAEKRAL MRLQTCAHP

Fig. 6.11. (D): Analysis of Lift spectrum from peaks m/z 1493 and 1234 using Biotools; **(E)** Uncharacterized protein (XP_022819955.1) sequence. Red colour indicates the partial sequence coverage by various ions generated from spot 3 while blue box indicate the matching of *de novo* (m/z 1493 and 1234) sequences obtained from Biotools with the peptides identified by Mascot search engine.

F)

Accession number	Protein name/ Source	Sequence	Similarity (%)
Spot number 3, (de nov	o sequence from PMF peak with m/z 1493)	SRENISRTMDLR	100
XP_030034601.1	uncharacterized protein LOC115450672/ Manduca sexta	SRENISRTMDLR	100
XP_032513462.1	uncharacterized protein LOC116767314/ Danaus plexippus plexippus	SR D NISRTMDLR	92
XP_022124386.1	uncharacterized protein LOC110999577/ Pieris rapae	SR D NISRTMDLR	92
XP_023947670.1	uncharacterized protein LOC112052721/ Bicyclus anynana	SR D NISRTMDLR	92
KOB69896.1	Uncharacterized protein OBRU01_15437/ Operophtera brumata	SR S NISRTMDLR	92
XP_021188456.1	uncharacterized protein LOC110374876/ Helicoverpa armigera	SR Q NISRTMDLR ** *******	92

Fig. 6.11. F): Clustal alignment of *de novo* sequence from PMF peak (m/z 1493) with uncharacterized protein identified in NCBI database.

Thus, this study reveal that a new uncharacterized protein was expressed in *S. litura* larvae fed upon T9BBI to cope with the nutritional stress posed by this biopesticide (**Figs. 6.4**, **6.6** and **6.7**).

6.4.4. Identification of Spot 4 and Spot 5 as Actin-5C:

Digestion of the spot 4 and spot 5 with trypsin followed by MALDI-TOF-TOF analysis showed matching to an isoform of Actin of S. litura with a significant score of 64 and 216, respectively, in the mascot search engine (Figs. 6.12A and 6.13A). The spectra for the corresponding PMF data was represented in the Figures 6.12B and 6.13B. following de novo sequences 'GYSFTTTAER' and 'SYELPDGQVITIGNER' (lift from and spectrum 4 'SYELPDGQVITIGNER' not shown) spot and 'DLYANTVLSGGTTMVP' (lift spectrum not shown) from spot 5 were derived from the lift spectra using Biotools software when the PMF peaks related to spot 4 (m/z 1132, 1790) and spot 5 (m/z 1790, 2230) were further ionized by MALDI-TOF-TOF (Figs. 6.12C and D; **6.13C and D**). Also, the various ions generated from spot 4 and spot 5 during MALDI-TOF-TOF showed a partial sequence coverage of up to 15% and 44%, respectively with Actin, muscle-type A2 and Actin-5C from S. litura. Further, the de novo sequences derived from PMF peaks related to (m/z 1132, 1790) spot 4 and (m/z 1790, 2230) spot 5 also showed overlapping with the partial amino acid sequence(s) recognised for Actin, muscle-type A2 (Uniprot Acc No. XP_022837900.1) and Actin-5C (Uniport Acc No. XP_022831297.1), respectively (Fig. 6.12E and 6.13E). Furthermore, Clustal alignment of the *de novo* sequence 'GYSFTTTAER' from spot 4 with the available data in NCBI database showed 100% matching with Actin, muscle-type A2 from Necator americanus, Trichenella pseudospiralis, Bos taurus, Mus spretus, Carassius auratus, Stylophora pistillata and T. Patagoniensis (Fig. **6.12F**). In contrast, Clustal alignment of the *de novo* sequence 'SYELPDGQVITIGNER' from spot 5 with the available data in NCBI database showed 100% matching with Actin-5C from Coregonus lavaretus, Channa gachua, Chiloscyllium punctatum, Bemisia tabaci, Schizophyllum commune, Onnia tomentosa, Pseudodiamesa branickii and Moesziomyces antarcticus (Fig. 6.13F). These results confirm that Actin, muscle-type A2 is also expressed parallel to Actin-5C and they are up-regulated by 2.44-fold (spot 4) and 1.69-fold (spot 5), respectively, in the midgut tissue of *S. litura* larvae upon feeding on a diet supplemented with T9BBI (Figs. 6.6, 6.7, 6.12 and 6.13).

As discussed in Chapter 5, different forms of actin which are critical in maintaining cytoskeletal integrity and thereby cell shape, cell motility and cell division etc. might play a significant defensive role in the brush border of the midgut tissue by binding to the various toxins injested by the insect pest (Kabsch and Vandekerckhove, 1992, Yuan et al., 2011). Thus, in the present study, these actin isoforms may bind to the injested T9BBI and thereby protect the *S. litura* from nutritional stress as demonstrated in the case of Cry1Ac intoxication by *H. armigera* (Yuan et al., 2011), *M. sexta* larvae (Nall and Adang, 2003) and Cry4Ba by *A. aegypti* (Bayyareddy et al., 2009). Also, the proteomic studies of Merzendorfer et al. (2012) revealed an up-regulation of actin protein when *T. castaneum* was fed with diflubenzuron insecticide.

Thus, among the five spots selected in the present study, two protein spots which were down-regulated in *S. litura* larvae fed with T9BBI are identified as Zinc finger protein 271 like isoform X1 and AK isoform X3. Further, the literature suggests that the third spot which is newly expressed is an uncharacterized protein. On the other hand, 4th and 5th spots which were up-regulated in T9BBI fed larvae are identified as isoforms of Actin such as Actin, muscle-type A2 and Actin-5C. A detailed summary of the results related to the MALDI-TOF-TOF analysis of the five spots is revealed in **Table 6.2.**

19. XP 022828580.1

20. XP 022828578.1

113871

115002

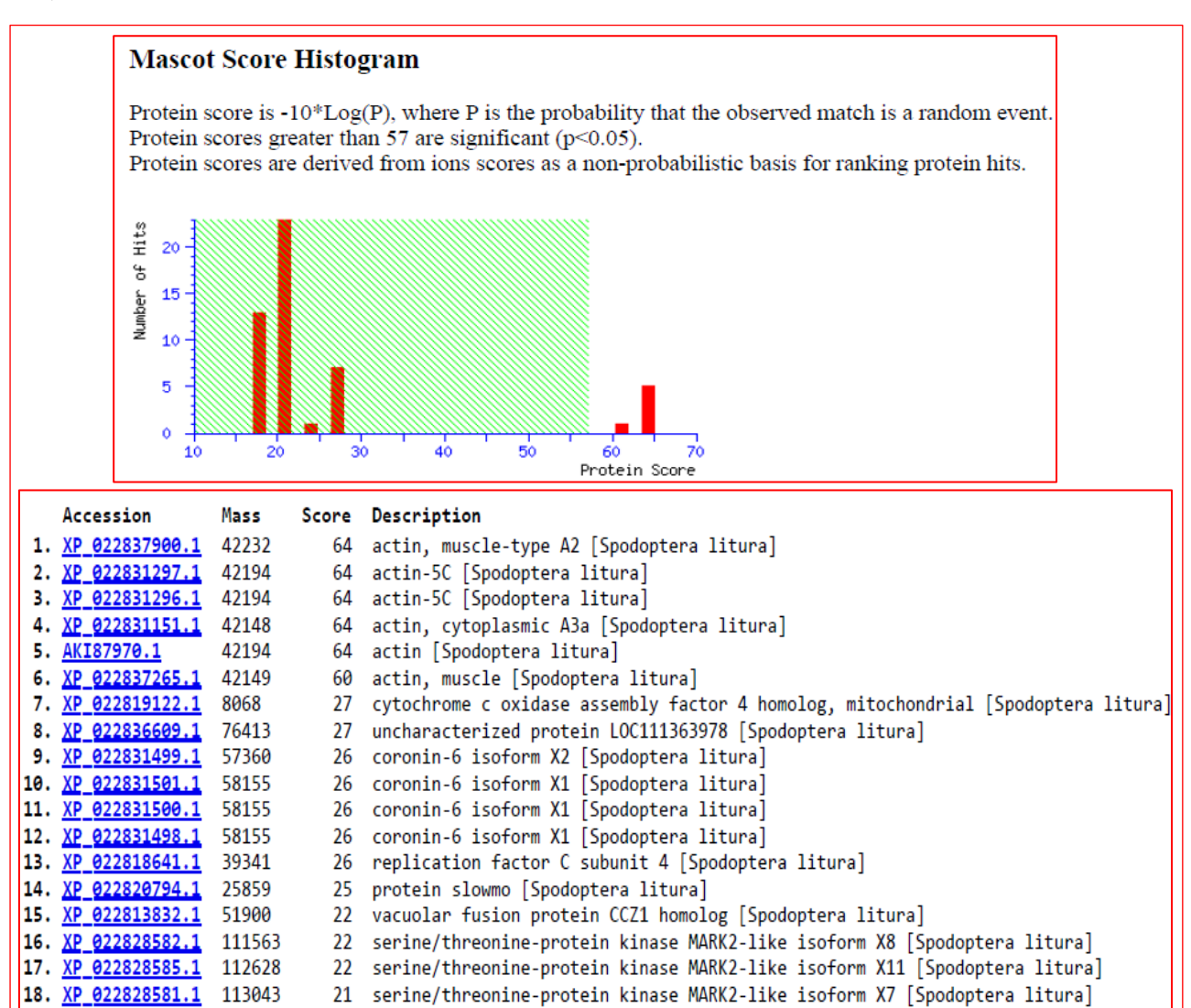
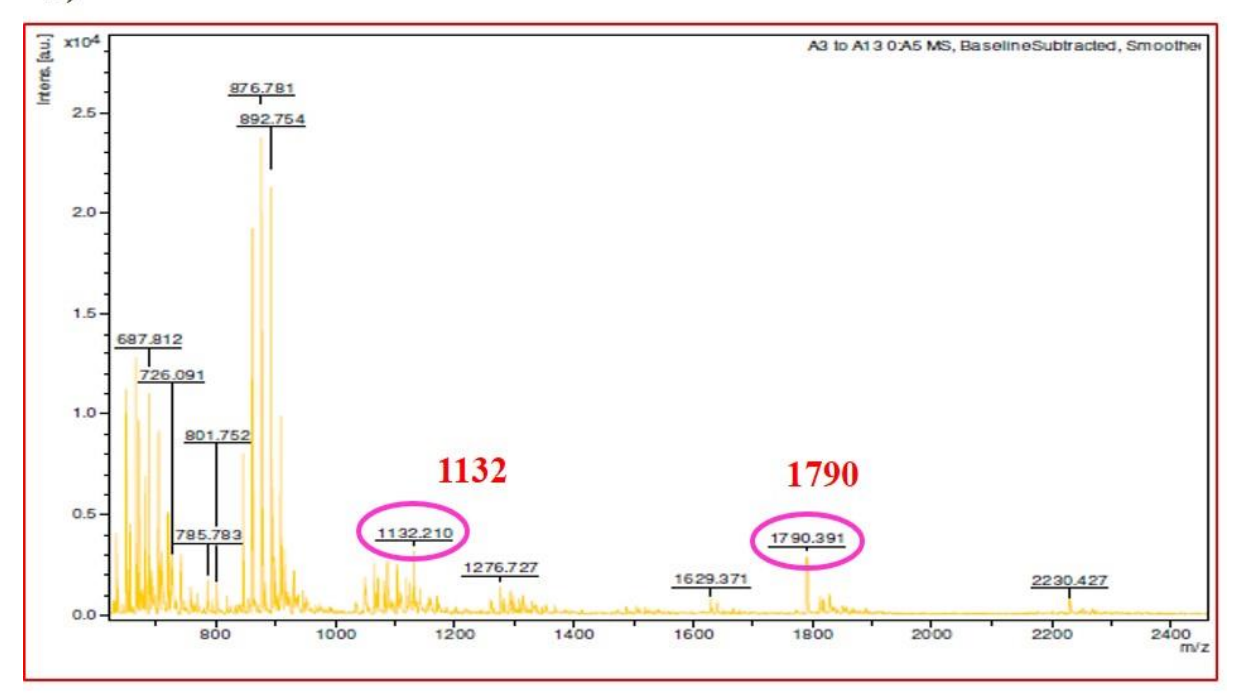


Fig. 6.12. Identification of spot 4 as Actin, muscle-type A2, after tryptic digestion and MALDI-TOF-TOF analysis. (A) Histogram of MASCOT search results and corresponding protein hits.

serine/threonine-protein kinase MARK2-like isoform X6 [Spodoptera litura]

serine/threonine-protein kinase MARK2-like isoform X5 [Spodoptera litura]

B)



C)

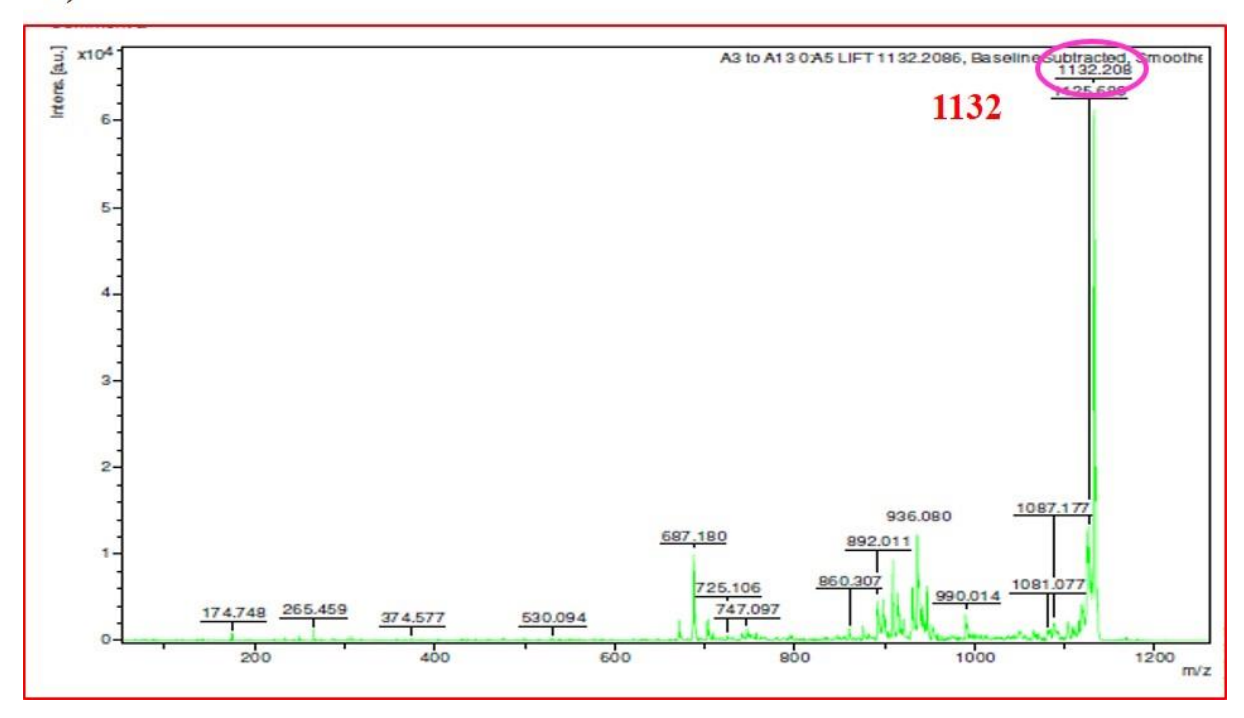


Fig. 6.12. (B): PMF spectrum of spot 4 highlighting peaks 1132 (m/z) and 1790 (m/z); **(C)** Lift spectrum of PMF peak with m/z 1132.

D)

Calculated Masses: GYSFTTTAER GYSFTTTAER									Peak:	Peak: 1132			
N-Term.	Ion	a	b	I	a-17	a-18	b-17	b-18	b+18	V	y-17	C-Term.	lor
1	G	30.034	58.029	30.034	13.007	12.023	41.002	40.018	76.039	175.119	158.116	10	R
2	Υ	193.097	221.092	136.076	176.071	175.087	204.066	203.082	239.103	304.162	287.159	9	E
3	S	280.129	308.124	60.044	263.103	262,119	291.098	290.114	326.135	375.199	358,196	8	A
4	F	427.198	455.193	120.081	410.171	409.187	438.166	437.182	473.203	476.246	459.244	7	1
5	T	528.245	556.240	74.060	511.219	510.235	539.214	538.230	574.251	577.294	560.291	6	1
6	T	629.293	657.288	74.060	612.266	611.282	640.261	639.277	675.298	678.342	661.339	5	1
7	T	730.341	758.336	74.060	713,314	712.330	741.309	740.325	776.346	825.410	808.407	4	F
8	Α	801.378	829.373	44.049	784.351	783.367	812.346	811.362	847.383	912.442	895,439	3	5
9	E	930.420	958.415	102.055	913.394	912.410	941.389	940.405	976.426	1075.505	1058.503	2	١
10	R	1086.521	1114.516	129.113	1069,495	1068.511	1097.490	1096.506	1132.527	1132.527	1115.524	1	(

YELPDG			SYELF	שליUGQVI	TIGNER	(Peak: 1			
N-Term.	Ion	а	b	1	a-17	a-18	b-17	b-18	b+18	V	y-17	C-Term.	Ion
1	S	60.044	88.039	60.044	43.018	42.034	71.013	70.029	106.050	175.119	158.116	16	R
2	Y	223.108	251.103	136.076	206.081	205.097	234.076	233.092	269.113	304.162	287.159	15	E
3	E	352.150	380.145	102.055	335.124	334.140	363.119	362.135	398.156	418.204	401.202	14	N
4	L	465.234	493.229	86.096	448.208	447.224	476.203	475.219	511.240	475.228	458.223	13	G
5	Р	562.287	590.282	70.065	545.261	544.277	573.258	572.271	608.293	588.310	571.307	12	1
6	D	677.314	705.309	88.039	660.288	659.304	688.282	687.298	723.320	689.358	672.355	11	Т
7	G	734.336	762.330	30.034	717.309	716.325	745.304	744.320	780.341	802.442	785.439	10	- 1
8	Q	862.394	890.389	101.071	845.368	844.384	873.362	872.378	908.400	901.510	884.507	9	V
9	V	961.463	989.457	72.081	944.436	943.452	972.431	971.447	1007.468	1029.569	1012.566	8	Q
10	1	1074.547	1102.542	86.096	1057.520	1056.536	1085.515	1084.531	1120.552	1086.590	1069.587	7	G
11	T	1175.594	1203.589	74.060	1158.568	1157.584	1186.563	1185.579	1221.600	1201.617	1184.614	6	D
12	1	1288.678	1316.673	86.096	1271.652	1270.668	1299.647	1298.663	1334.684	1298.670	1281.667	5	P
13	G	1345.700	1373.696	30.034	1328.673	1327.689	1356.668	1355.684	1391.705	1411.754	1394.751	4	L
14	N	1459.743	1487.738	87.055	1442.716	1441.732	1470.711	1469.727	1505.748	1540.797	1523.794	3	E
15	E	1588.785	1616.780	102.055	1571.759	1570.775	1599.754	1598.770	1634.791	1703.860	1686,857	2	Y
16	R	1744.886	1772.881	129.113	1727.860	1726.876	1755.855	1754.871	1790.892	1790.892	1773.889	1	S

Fig. 6.12. (D): Analysis of Lift spectrum from peaks m/z 1132 & 1790 using Biotools.

 \mathbf{E})

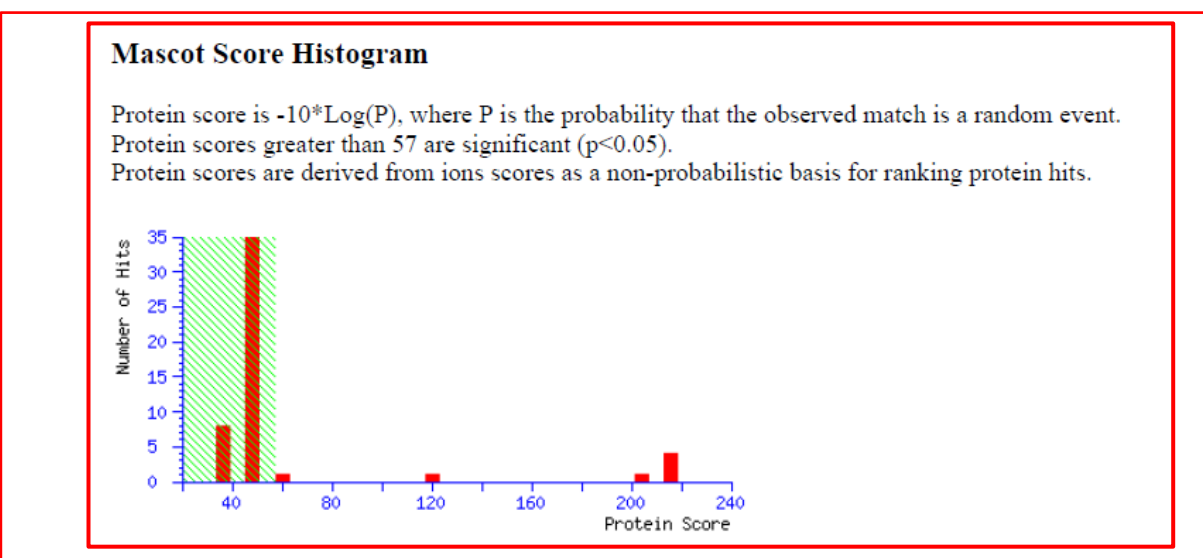
Actin-Muscle type A2: 15% Coverage:

MCDEEVAALVVDNGSGMCKAGFAGDDAPRAVFPSIVGRPRHQGVMVGMGQKDSYVGDEAQSKRGILTL KYPIEHGIVTNWDDMEKIWHHTFYNELRVAPEEHPVLLTEAPLNPKANREKMTQIMFETFNTPAMYVAIQ AVLSYASGRTTGIVLDSGDGVSHTVPIYEGYALPHAILRLDLAGRDLTDYLMKILTERGYSFTTTAEREIVR DIEKLCYVALDFEQEMATAASSSSLEKSYELPDGQVITIGNERFR CPEALFQPSFLGMEACGIHETTYNS IMKCDVDIR KDLYAN VLS GGTTMYPGIADRMQKETALAPSTMKIKIIAPPERKYSVWIGGSILASLSTF QQMWISQEYDESGPSIVHRKCF

Fig. 6.12. (E) Actin, muscle-type A2 (XP_022837900.1) sequence. Red colour indicates the partial sequence coverage by various ions generated from spot 4 while blue box indicate the matching of *de novo* (m/z 1132 & 1790) sequences obtained from Biotools with one of the peptides identified by Mascot search engine.

Accession number	Protein name/ Source	Sequence	Similarity (%)
Spot number 4 (de novo sequ	ence from PMF peak with m/z 1132)	GYSFTTTAER	100
XP_013298257.1	Actin/ Necator americanus	GYSFTTTAER	100
KRY74818.1	Actin-5C/ Trichinella pseudospiralis	GYSFTTTAER	100
AAZ32296.1	beta-actin, partial/ Bos Taurus	GYSFTTTAER	100
AAQ55830.1	Beta-actin, partial/ Mus spretus	GYSFTTTAER	100
ADZ44595.1	Beta-actin, partial/ Carassius auratus	GYSFTTTAER	100
PFX33495.1	Actin, nonmuscle/ Stylophora pistillata	GYSFTTTAER	100
KRY07999.1	Actin, acrosomal process isoform / Trichinella patagoniensis	GYSFTTTAER ********	100

Fig. 6.12. (F): Clustal alignment of *de novo* sequence from PMF peak (m/z 1132) with Actin, muscle-type A2, identified in NCBI database.



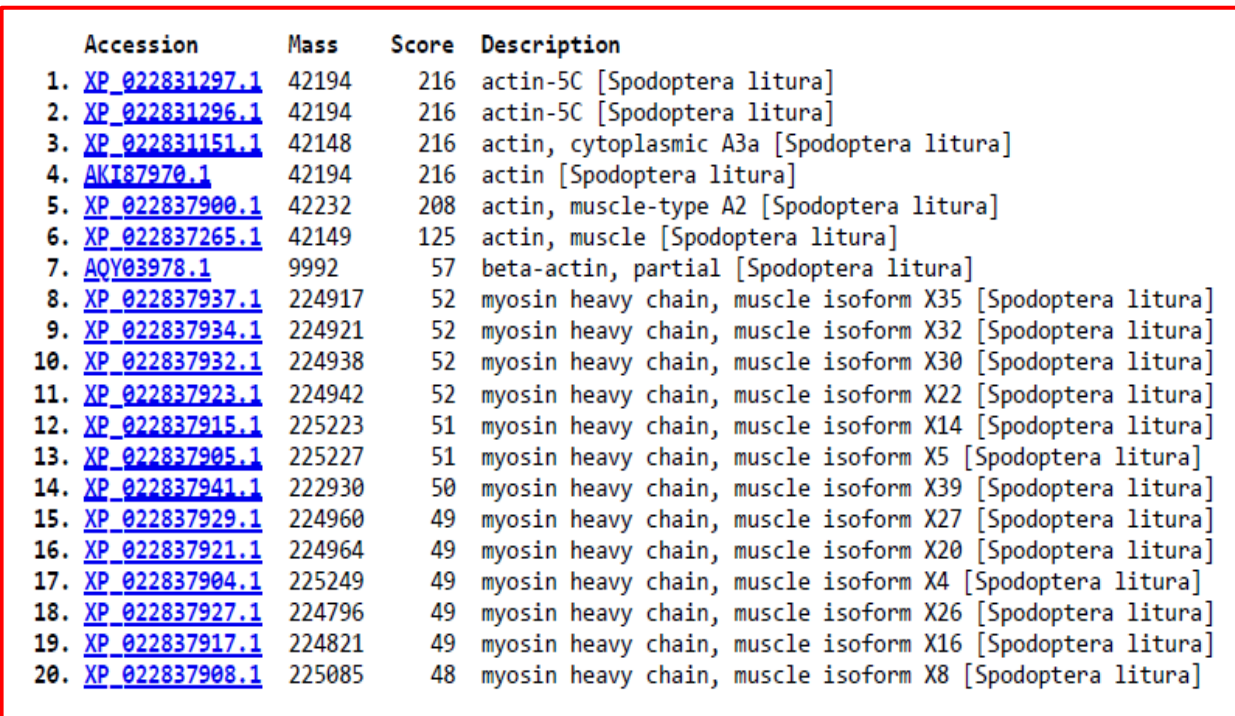
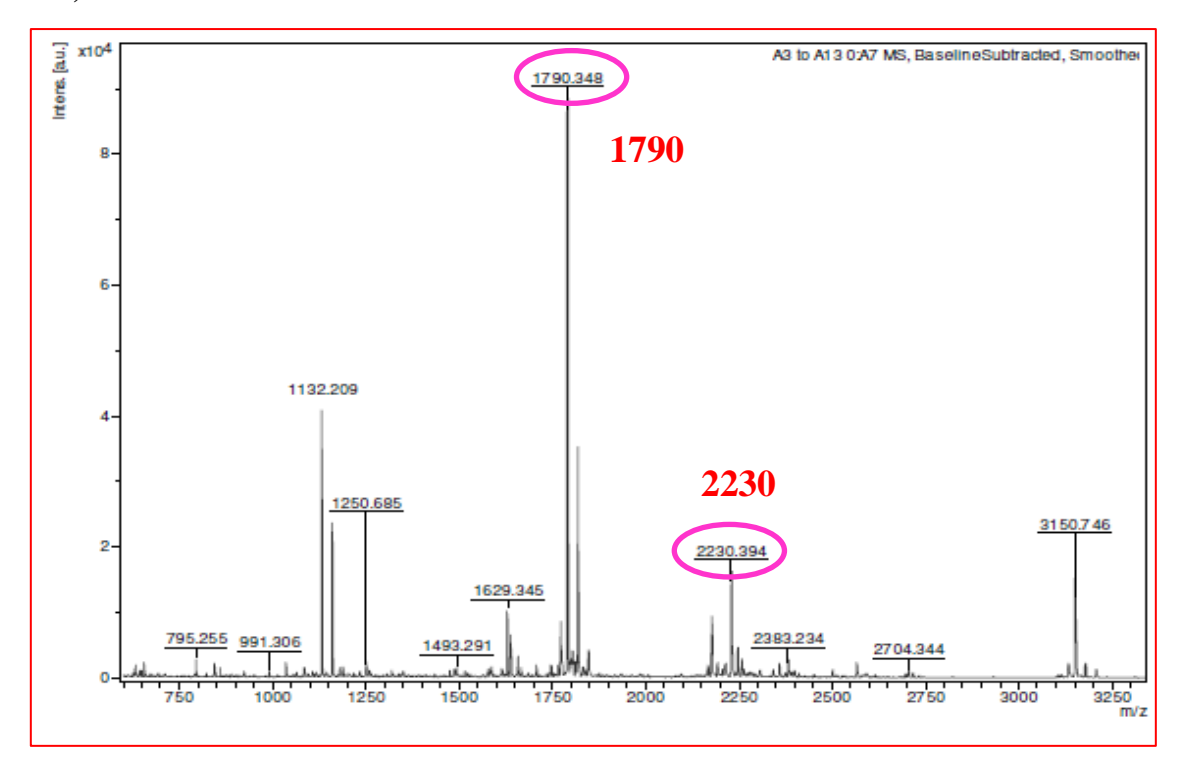


Fig. 6.13. Identification of spot 5 as Actin-5C, after tryptic digestion and MALDI-TOF-TOF analysis. (A) Histogram of MASCOT search results and corresponding protein hits.

B)



C)

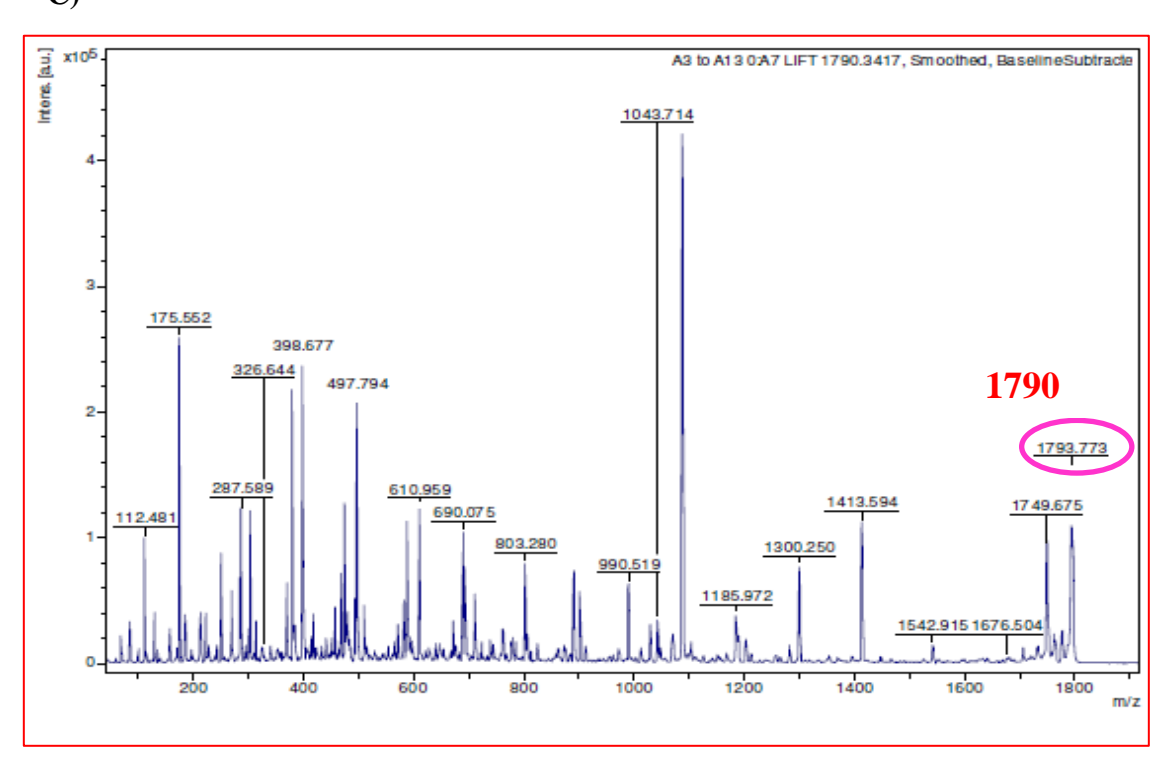


Fig. 6.13. (B): PMF spectrum of spot 5 highlighting peaks m/z 1790 and 2230 (m/z); **(C)** Lift spectrum of PMF peak with m/z 1790

				5	SYELPD	GQVIT	IGNER				Peak: 17	90	
-Term. I	on	a	b	1	a-17	a-18	b-17	b-18	b+18	v	y-17	C-Term	ı. T
1	S	60.044	88.039	60.044	43.018	42.034	71.013	70.029	106.050	175.11			✝
2	Y	223.108	251.103	136.076	206.081	205.097	234.076	233.092	269.113	304.16		9 15	ℸ
3	E	352.150	380.145	102.055	335.124	334.140	363,119	362.135	398.156	418.20	401.20	2 14	┪
4	L	465.234	493,229	86.096	448.208	447.224	476.203	475.219	511.240	475.22		3 13	┪
5	Р	562.287	590.282	70.065	545.261	544.277	573.256	572.271	608.293	588.31	0 571.30	7 12	┪
6	D	677.314	705.309	88.039	660.288	659.304	688.282	687.298	723.320	689.35		5 11	┪
7	G	734.336	762.330	30.034	717.309	716.325	745.304	744.320	780.341	802.44	2 785.43	9 10	┪
8	Q	862.394	890.389	101.071	845,368	844.384	873.362	872.378	908.400	901.51			┪
	V	961,463	989.457	72.081	944.436	943,452	972.431	971.447	1007.468	1029.56			┪
10		1074.547	1102.542	86.096	1057.520	1056.536	1085.515	1084.531	1120.552	1086.59	0 1069.58	7 7	┪
11	T	1175,594	1203.589	74.060	1158.568	1157.584	1186,563	1185.579	1221.600	1201.61			7
12	T	1288.678	1316.673	86.096	1271.652	1270.668	1299.647	1298.663	1334.684	1298.67			┪
	Ġ	1345.700	1373.695	30.034	1328.673	1327.689	1356.668	1355.684	1391.705	1411.75			7
	Ň	1459.743	1487.738	87.055	1442.716	1441.732	1470.711	1469.727	1505.748	1540.79			┪
	E	1588.785	1616.780	102.055	1571.759	1570,775	1599.754	1598,770	1634,791	1703.86			┪
	R	1744.886	1772.881	129,113	1727.860	1726.876	1755.855	1754.871	1790.892	1790.89			\dashv
DLYANTVI	LSGG	TTMYPGIADR	14: Oxidation (N		DLYAN	FVLSG(GTTMY	P			Peak: 2	2230	
				d)	<u> </u>				h.18	v			lor
DLYANTVI N-Term.	Ion	а	b	d)	a-17	a-18	b-17	b-18	D+18	y 175.119	y-17	C-Term. I	
N-Term. 1		a 88.039	b 116.034	I 88.039	a-17 71.013	a-18 70.029	b-17 99.008	b-18 98.024	134.045	175.119	y-17 158.116	C-Term. I	R
	Ion	а	b 116.034 229.118	I 88.039 86.096	a-17 71.013 184.097	a-18 70.029 183.113	b-17	b-18		175.119 290.146	y-17 158.116 273.143	C-Term. I	R D
N-Term. 1 2	lon D L	88.039 201.123	b 116.034	I 88.039	a-17 71.013	a-18 70.029	b-17 99.008 212.092	b-18 98.024 211.108	134.045 247.129	175.119	y-17 158.116	C-Term. I 21 20 19	R D
N-Term. 1 2 3	D L Y	88.039 201.123 364.187	b 116.034 229.118 392.182	88.039 86.096 136.076	a-17 71.013 184.097 347.160	a-18 70.029 183.113 346.176	b-17 99.008 212.092 375.155	b-18 98.024 211.108 374.171	134.045 247.129 410.192	175.119 290.146 361.183	y-17 158.116 273.143 344.180	C-Term. I 21 20 19 18	D A
N-Term. 1 2 3 4 5	D L Y A N	8 88,039 201,123 364,187 435,224 549,267 650,314	b 116.034 229.118 392.182 463.219 577.262 678.309	88.039 88.096 136.076 44.049 87.055 74.060	a-17 71.013 184.097 347.160 418.197 532.240 633.288	a-18 70.029 183.113 346.176 417.213 531.256 632.304	b-17 99.008 212.092 375.155 446.192 560.235 681.283	b-18 98.024 211.108 374.171 445.208 559.251 680.299	134.045 247.129 410.192 481.229 595.272 696.320	175.119 290.146 361.183 474.267 531.289 628.341	y-17 158.116 273.143 344.180 457.264 514.286 611.339	C-Term. I 21 20 19 18 17 16	A G P
N-Term. 1 2 3 4 5 6 7	D L Y	88.039 201.123 364.187 435.224 549.267 650.314 749.383	b 116.034 229.118 392.182 463.219 577.262 678.309 777.378	88.039 88.096 138.076 44.049 87.055 74.060 72.081	a-17 71.013 184.097 347.160 418.197 532.240 633.288 732.358	a-18 70.029 183.113 346.176 417.213 531.256 632.304 731.372	b-17 99.008 212.092 375.155 446.192 560.235 681.283 780.351	b-18 98.024 211.108 374.171 445.208 559.251 600.299 759.367	134,045 247,129 410,192 481,229 595,272 696,320 795,388	175.119 290.146 361.183 474.267 531.289 628.341 791.405	y-17 158.116 273.143 344.180 457.264 514.286 611.339 774.402	C-Term. 1 21 20 19 18 17 16	A G P
N-Term. 1 2 3 4 5 6 7	Ion D L Y A N T V L	8 88.039 201.123 364.187 435.224 549.267 650.314 749.383 862.467	b 116.034 229.118 392.182 463.219 577.262 678.309 777.378 890.462	88.039 88.096 138.076 44.049 87.055 74.060 72.081 86.096	a-17 71.013 184.097 347.160 418.197 532.240 633.288 732.356 845.440	a-18 70.029 183.113 346.176 417.213 531.256 632.304 731.372 844.456	b-17 99.008 212.092 375.155 446.192 560.235 681.283 780.351 873.435	b-18 98.024 211.108 374.171 445.208 559.251 680.299 759.367 872.451	134,045 247,129 410,192 481,229 595,272 696,320 795,388 908,472	175.119 290.146 361.183 474.267 531.289 628.341 791.405 938.440	y-17 158.116 273.143 344.180 457.264 514.286 611.339 774.402 921.437	C-Term. 1 21 20 19 18 17 16 15	A I G
N-Term. 1 2 3 4 5 6 7 8	Ion D L Y A N T V L	8 88.039 201.123 364.187 435.224 549.267 650.314 749.383 862.467 949.499	b 116.034 229.118 392.182 463.219 577.262 678.309 777.378 890.462 977.494	88.039 88.096 138.076 44.049 87.055 74.060 72.081 88.096 60.044	a-17 71.013 184.097 347.160 418.197 532.240 633.288 732.356 845.440 932.472	a-18 70.029 183.113 346.176 417.213 531.256 632.304 731.372 844.456 931.488	b-17 99.008 212.092 375.155 446.192 560.235 681.283 780.351 873.435 980.467	b-18 98.024 211.108 374.171 445.208 559.251 680.299 759.367 872.451 959.483	134.045 247.129 410.192 481.229 595.272 696.320 795.388 908.472 995.504	175.119 290.146 361.183 474.267 531.269 628.341 791.405 938.440 1039.488	y-17 158.116 273.143 344.180 457.264 514.286 611.339 774.402 921.437 1022.495	C-Term. 1 21 20 19 18 17 16 15 14	R D A I G P Y M'
N-Term. 1 2 3 4 5 6 7 8 9	D L Y A N T V L S G	8 88.039 201.123 354.187 435.224 549.267 650.314 749.383 862.467 949.499	b 116.034 229.118 392.182 463.219 577.262 678.309 777.378 890.462 977.494	88.039 88.099 88.096 138.076 44.049 87.055 74.060 72.081 88.096 60.044 30.034	a-17 71.013 184.097 347.160 418.197 532.240 633.288 732.356 845.440 932.472 989.494	a-18 70.029 183.113 346.176 417.213 531.256 632.304 731.372 844.456 931.488 988.510	b-17 99.008 212.092 375.155 445.192 560.235 661.283 760.351 873.435 980.467 1017.489	b-18 98.024 211.108 374.171 445.208 559.251 680.299 759.367 872.451 959.483 1016.505	134.045 247.129 410.192 481.229 595.272 696.320 795.388 908.472 995.504 1052.526	175.119 290.146 361.183 474.267 531.269 628.341 791.405 938.440 1039.488 1140.535	y-17 158.116 273.143 344.180 457.264 514.286 611.339 774.402 921.437 1022.485 1123.533	C-Term. 1 21 20 19 18 17 16 15 14 13	R D A I G P Y M'T T
N-Term. 1 2 3 4 5 6 7 8 9 10 11	Ion D L Y A N T V L	8 88.039 201.123 354.187 435.224 549.267 650.314 749.383 962.467 949.499 1006.520 1063.542	b 116.034 229.118 392.182 463.219 577.262 678.309 777.378 890.462 977.494 1034.515 1091.537	88.039 88.096 136.076 44.049 87.055 74.060 72.081 88.096 60.044 30.034	a-17 71.013 184.097 347.160 418.197 532.240 633.288 732.356 845.440 932.472 989.494 1046.515	a-18 70.029 183.113 346.176 417.213 531.256 632.304 731.372 844.456 931.488 988.510 1045.531	b-17 99.008 212.092 375.155 446.192 560.235 681.283 780.351 873.435 980.467 1017.489 1074.510	b-18 98.024 211.108 374.171 445.208 559.251 680.299 759.367 872.451 959.483 1016.505 1073.526	134.045 247.129 410.192 481.229 595.272 696.320 795.388 908.472 995.504 1052.526 1109.547	175.119 290.146 361.183 474.267 531.289 628.341 791.405 938.440 1039.488 1140.535 1197.557	y-17 158.116 273.143 344.180 457.264 514.286 611.339 774.402 921.437 1022.485 1123.533 1180.554	C-Term. 1 21 20 19 18 17 16 15 14 13 12	R D A I G P Y M'T T G
N-Term. 1 2 3 4 5 6 7 8 9 10 11 12	D L Y A N T V L S G	8 88.039 201.123 364.187 435.224 549.267 650.314 749.383 862.467 949.499 1006.520 1063.542 1164.590	b 116.034 229.118 392.182 463.219 577.262 678.309 777.378 890.462 977.494 1034.515 1091.537	88.039 88.096 136.076 44.049 87.055 74.060 72.081 88.096 60.044 30.034 74.060	a-17 71.013 184.097 347.160 418.197 532.240 633.288 732.356 845.440 932.472 989.494 1046.515 1147.563	a-18 70.029 183.113 346.176 417.213 531.256 632.304 731.372 844.456 931.488 988.510 1045.531 1146.579	b-17 99.008 212.092 375.155 446.192 560.235 661.263 760.351 873.435 980.467 1017.489 1074.510 1175.558	b-18 98.024 211.108 374.171 445.208 559.251 660.299 759.367 872.451 959.483 1016.505 1073.526 1174.574	134.045 247.129 410.192 481.229 595.272 696.320 795.388 908.472 995.504 1052.526 1109.547 1210.595	175.119 290.146 361.183 474.267 531.289 628.341 791.405 938.440 1039.488 1140.535 1197.557	y-17 158.116 273.143 344.180 457.264 514.288 611.339 774.402 921.437 1022.485 1123.533 1180.554 1237.576	C-Term. 1 21 20 19 18 17 16 15 14 13 12 11	P Y M' T G
N-Term. 1 2 3 4 5 6 7 8 9 10 11 12 13	D L Y A N T V L S G G T T T	8 88.039 201.123 364.187 435.224 549.267 650.314 749.383 862.467 949.499 1006.520 1063.520 1164.590 1265.637	b 116.034 229.118 392.182 463.219 577.262 678.309 777.378 890.462 977.494 1034.515 1091.537 1192.584 1293.632	88.039 88.096 138.076 44.049 87.055 74.060 72.081 88.096 60.044 30.034 74.060 74.060	a-17 71.013 184.097 347.160 418.197 532.240 633.288 732.356 845.440 932.472 989.494 1046.515 1147.563 1248.611	a-18 70.029 183.113 346.176 417.213 531.256 632.304 731.372 844.456 931.488 988.510 1045.531 1146.579 1247.627	b-17 99.008 212.092 375.155 446.192 560.235 661.283 780.351 873.435 960.467 1017.489 1074.510 1175.558 1276.806	b-18 98.024 211.108 374.171 445.208 559.251 600.299 759.367 872.451 959.483 1016.505 1073.526 1174.574 1275.622	134.045 247.129 410.192 481.229 595.272 696.320 795.388 908.472 995.504 1052.526 1109.547 1210.595 1311.643	175.119 290.146 361.183 474.267 531.289 628.341 791.405 938.440 1039.488 1140.535 1197.557 1254.578 1341.610	y-17 158.116 273.143 344.180 457.264 514.286 611.339 774.402 921.437 1022.485 1123.533 1180.554 1237.576 1324.608	C-Term. 1	R D A I G P Y M'T T G G S
N-Term. 1 2 3 4 5 6 7 8 9 10 11 12 13 14	Ion D L Y A N T V L S G G T T M*	8 88.039 201.123 354.187 435.224 549.267 650.314 749.383 862.467 949.499 1006.520 1063.542 1164.590 1265.637 1412.673	b 116.034 229.118 392.182 463.219 577.262 678.309 777.378 890.462 977.494 1034.515 1091.537 1192.584 1293.632 1440.668	88.039 88.096 138.076 44.049 87.055 74.060 72.081 88.096 60.044 30.034 74.060 74.060 120.048	a-17 71.013 184.097 347.160 418.197 532.240 633.288 732.356 845.440 932.472 989.494 1046.515 1147.563 1248.611	a-18 70.029 183.113 346.176 417.213 531.256 632.304 731.372 844.456 931.488 989.510 1045.531 1146.579 1247.627 1394.662	b-17 99.008 212.092 375.155 446.192 560.235 681.283 780.351 873.435 980.467 1017.489 1074.510 1175.558 1276.606 1423.641	b-18 98.024 211.108 374.171 445.208 559.251 660.299 759.367 872.451 959.483 1016.505 1073.526 1174.574 1275.622 1422.657	134.045 247.129 410.192 481.229 595.272 696.320 795.388 908.472 995.504 1062.526 1109.547 1210.595 1311.643 1458.678	175.119 290.146 361.183 474.267 531.289 628.341 791.405 938.440 1039.488 1140.535 1197.557 1254.578 1341.610	y-17 158.116 273.143 344.180 457.264 514.286 611.339 774.402 921.437 1022.485 1123.533 1180.554 1237.576 1324.608 1437.692	C-Term. 1 21 20 19 18 17 16 15 14 13 12 11 10 9	R D A I G P Y M'T T G G S L
N-Term. 1 2 3 4 5 6 7 8 9 10 11 12 13 14 15	Ion D L Y A N T V L S G G T T M Y	8 88.039 201.123 354.187 435.224 549.267 650.314 749.383 862.467 949.499 1006.520 1063.542 1164.593 1265.637 1412.673	b 116.034 229.118 392.182 463.219 577.262 678.309 777.378 890.462 977.494 1034.515 1091.537 1192.584 1293.632 1440.668 1603.731	88.039 88.039 88.096 136.076 44.049 87.055 74.060 72.081 86.096 60.044 30.034 74.060 74.060 120.048 136.076	a-17 71.013 184.097 347.160 418.197 532.240 633.288 732.356 845.440 932.472 989.494 1046.515 1147.563 1248.611 1395.646	a-18 70.029 183.113 346.176 417.213 531.256 632.304 731.372 844.456 931.488 988.510 1045.531 1146.579 1247.627 1394.662 1557.725	b-17 99.008 212.092 375.155 446.192 560.235 661.283 760.351 873.435 980.467 1017.489 1074.510 1175.588 1276.808 1423.541 1586.704	b-18 98.024 211.108 374.171 445.208 559.251 680.299 759.367 872.451 959.483 1016.505 1073.526 1174.574 1275.622 1422.657 1585.720	134.045 247.129 410.192 481.229 595.272 696.320 795.388 908.472 995.504 1052.526 1109.547 1210.596 1311.643 1458.678 1621.741	175.119 290.146 361.183 474.267 531.269 628.341 791.405 938.440 1039.488 1140.535 1197.557 1254.578 1341.610 1454.694 1553.763	y-17 158.116 273.143 344.180 457.264 514.286 611.339 774.402 921.437 1022.485 1123.533 1180.554 1237.576 1324.608 1437.692 1536.760	C-Term. 1 21 20 19 18 17 16 15 14 13 12 11 10 9	R D A I G P Y M'T T G G S L V
N-Term. 1 2 3 4 5 6 7 8 9 10 11 12 13 14 15 16	Ion D L Y A N T V L S G G T T M* Y	8 88.039 201.123 354.187 435.224 549.267 650.314 749.383 862.467 949.499 1006.520 1063.542 1164.590 1265.637 1412.673 1672.789	b 116.034 229.118 392.182 463.219 577.262 678.309 777.378 890.462 977.494 1034.515 1091.537 1192.584 1293.632 1440.668 1603.731 1700.784	88.039 88.096 138.076 44.049 87.055 74.060 72.081 86.096 60.044 30.034 74.060 74.060 120.048 138.076 70.065	8-17 71.013 184.097 347.160 418.197 532.240 633.288 732.356 845.440 932.472 989.494 1046.515 1147.563 1248.611 1395.646 1558.709	a-18 70.029 183.113 346.176 417.213 531.256 632.304 731.372 844.456 931.488 988.510 1045.531 1146.579 1247.627 1394.662 1557.725 1654.778	b-17 99.008 212.092 375.155 446.192 560.235 681.283 780.351 873.435 980.467 1017.489 1074.510 1175.558 1276.606 1423.641 1596.704 1683.757	b-18 98.024 211.108 374.171 445.208 559.251 680.299 759.367 872.451 959.483 1016.505 1073.526 1174.574 1275.622 1422.657 1585.720 1682.773	134.045 247.129 410.192 481.229 595.272 696.320 795.388 908.472 995.504 1052.526 1109.547 1210.595 1311.643 1458.678 1621.741 1718.794	175.119 290.146 361.183 474.267 531.289 628.341 791.405 938.440 1039.488 1140.535 1197.557 1254.578 1341.610 1454.694 1553.763 1654.810	y-17 158.116 273.143 344.180 457.264 514.286 611.339 774.402 921.437 1022.485 1123.533 1180.554 1237.576 1324.608 1437.692 1536.760 1637.808	C-Term. 1 21 20 19 18 17 16 15 14 13 12 11 10 9 8 7 6 6	R D A I G P Y M'T T G G S L V T
N-Term. 1 2 3 4 6 7 8 9 10 11 12 13 14 15 16 17	Ion D L Y A N T V L S G G T T M Y	8 88.039 201.123 364.187 435.224 549.267 650.314 749.383 962.467 949.499 1006.520 1063.542 1164.590 1265.637 1412.673 1575.738 1575.738 1729.810	b 116.034 229.118 392.182 463.219 577.262 678.309 777.378 890.462 977.494 1034.515 1091.537 1192.584 1293.632 1440.668 1603.731 17700.784 1757.805	88.039 88.096 138.076 44.049 87.055 74.060 72.081 88.096 60.044 30.034 74.060 74.060 120.048 138.076 70.065	a-17 71.013 184.097 347.160 418.197 532.240 633.288 732.356 845.440 932.472 989.494 1046.515 1147.563 1248.611 1395.646 1558.709 1655.762 1712.784	a-18 70.029 183.113 346.176 417.213 531.256 632.304 731.372 844.456 931.488 988.510 1045.531 1146.579 1247.627 1394.662 1557.725 1654.778 1711.800	b-17 99.008 212.092 375.155 446.192 560.235 681.283 780.351 873.435 980.467 1017.489 1074.510 1175.558 1276.806 1423.641 1586.704 1683.757 1740.779	b-18 98.024 211.108 374.171 445.208 559.251 680.299 759.367 872.451 959.483 1016.505 1073.526 1174.574 1275.622 1422.657 1585.720 1682.773 1739.795	134.045 247.129 410.192 481.229 595.272 696.320 795.388 908.472 995.504 1052.526 1109.547 1210.596 1311.643 1458.678 1621.741 1718.794 1775.816	175.119 290.146 361.183 474.267 531.289 628.341 791.405 938.440 1039.488 1140.535 1197.557 1254.578 1341.610 1454.694 1553.763 1654.810 1768.853	y-17 158.116 273.143 344.180 457.264 514.286 611.339 774.402 921.437 1022.495 1123.533 1180.554 1237.576 1324.608 1437.692 1536.760 1637.808 1751.851	C-Term. 1 21 20 19 18 17 16 15 14 1 13 12 11 10 9 8 7 6 5 6 5	R D A I G P Y M T T G G S L V T N
N-Term. 1 2 3 4 5 6 7 8 9 10 11 12 13 14 15 16 17	Ion D L Y A N T V L S G G T T M Y P G I	8 88.039 201.123 364.187 435.224 549.267 650.314 749.383 862.467 949.499 1006.520 1063.542 1164.590 1265.637 1412.673 1575.736 1672.789 1729.810 1842.894	b 116.034 229.118 392.182 463.219 577.262 678.309 777.378 890.462 977.494 1034.515 1091.537 1192.584 1293.632 1440.668 1603.731 1700.784 1757.805	88.039 88.096 136.076 44.049 87.055 74.060 72.081 88.096 60.044 30.034 74.060 74.060 120.048 136.076 70.065 30.034 88.096	a-17 71.013 184.097 347.160 418.197 532.240 633.288 732.356 845.440 932.472 989.494 1046.515 1147.563 1248.611 1395.646 1558.709 1655.762 1712.784 1825.868	a-18 70.029 183.113 346.176 417.213 531.256 632.304 731.372 844.456 931.488 988.510 1045.531 1146.579 1247.627 1394.662 1567.725 1654.778 1711.800 1824.884	b-17 99.008 212.092 375.155 446.192 560.235 661.263 760.351 873.435 960.467 1017.489 1074.510 1175.558 1276.606 1423.541 1586.704 1683.757 1853.863	b-18 98.024 211.108 374.171 445.208 559.251 680.299 759.367 872.451 959.483 1016.505 1073.526 1174.574 1275.622 1422.657 1585.720 1682.773 1739.795 1852.879	134.045 247.129 410.192 481.229 595.272 696.320 795.388 908.472 995.504 1052.526 1109.547 1210.595 1311.643 1458.678 1621.741 1718.794 1775.816 1888.900	175.119 290.146 361.183 474.267 531.289 628.341 791.405 938.440 1039.488 1140.535 1197.557 1254.578 1341.610 1454.694 1553.763 1654.810 1768.853 1839.891	y-17 158.116 273.143 344.180 457.264 511.339 774.402 921.437 1022.485 1123.533 1180.554 1237.576 1324.608 1437.692 1536.760 1637.898 1751.885 1822.888	C-Term. 1	R D A I G P Y M'T T G G S L V T N A
N-Term. 1 2 3 4 6 7 8 9 10 11 12 13 14 15 16 17	Ion D L Y A N T V L S G G T T M* Y	8 88.039 201.123 364.187 435.224 549.267 650.314 749.383 962.467 949.499 1006.520 1063.542 1164.590 1265.637 1412.673 1575.738 1575.738 1729.810	b 116.034 229.118 392.182 463.219 577.262 678.309 777.378 890.462 977.494 1034.515 1091.537 1192.584 1293.632 1440.668 1603.731 17700.784 1757.805	88.039 88.096 138.076 44.049 87.055 74.060 72.081 88.096 60.044 30.034 74.060 74.060 120.048 138.076 70.065	a-17 71.013 184.097 347.160 418.197 532.240 633.288 732.356 845.440 932.472 989.494 1046.515 1147.563 1248.611 1395.646 1558.709 1655.762 1712.784	a-18 70.029 183.113 346.176 417.213 531.256 632.304 731.372 844.456 931.488 988.510 1045.531 1146.579 1247.627 1394.662 1557.725 1654.778 1711.800	b-17 99.008 212.092 375.155 446.192 560.235 681.283 780.351 873.435 980.467 1017.489 1074.510 1175.558 1276.806 1423.641 1586.704 1683.757 1740.779	b-18 98.024 211.108 374.171 445.208 559.251 680.299 759.367 872.451 959.483 1016.505 1073.526 1174.574 1275.622 1422.657 1585.720 1682.773 1739.795	134.045 247.129 410.192 481.229 595.272 696.320 795.388 908.472 995.504 1052.526 1109.547 1210.596 1311.643 1458.678 1621.741 1718.794 1775.816	175.119 290.146 361.183 474.267 531.289 628.341 791.405 938.440 1039.488 1140.535 1197.557 1254.578 1341.610 1454.694 1553.763 1654.810 1768.853	y-17 158.116 273.143 344.180 457.264 514.286 611.339 774.402 921.437 1022.495 1123.533 1180.554 1237.576 1324.608 1437.692 1536.760 1637.808 1751.851	C-Term. 1 21 20 19 18 17 16 15 14 1 13 12 11 10 9 8 7 6 5 4 3 3	R D A I G P Y M T T G G S L V T N

Fig. 6.13. (D): Analysis of Lift spectrum from peaks m/z 1790 & 2230 using Biotools

E)

Sequence coverage: 44%

MCDEEVAALVVDNGSGMCKAGFAGDDAPRAVFPSIVGRPRHQGVMVGMGQKDSYVGDEAQSKRGIL TLKYPIEHGIVTNWDDMEKIWHHTFYNELRVAPEEHPVLLTEAPLNPKANREKMTQIMFETFNTPAMYVAI QAVLSLYASGRTTGIVLDSGDGVSHTVPIYEGYALPHAILRLDLAGRDLTDYLMKILTERGYSFTTTAE REIVRDIKEKLCYVALDFEQEMATAASSSSLEKSYELPDGQVITIGNERFRCPEALFQPSFLGMEACGIH ETTYNSIMKCDVDIRKDLYANTVLSGGTTMYPGIADRMQKEITALAPSTMKIKIIAPPERKYSVWIGGSI LASL STFQQMWISKQEYDESGPSIVHRKCF

Fig. 6.13. (E) Actin-5C (XP_022831297.1) sequence. Red colour indicates the partial sequence coverage by various ions generated from spot 5 while blue box indicate the matching of *de novo* (m/z 1790 & 2230) sequences obtained from Biotools with the peptides identified by Mascot search engine.

F)

Accession number	Protein name/ Source	Sequence	Similarity (%)
Spot number 5 (de n	ovo sequence from PMF peak with m/z 1790)	SYELPDGQVITIGNER	100
ABB22794.1	beta-actin, partial/ Coregonus lavaretus	SYELPDGQVITIGNER	100
ACR25275.1	beta-actin, partial/ Channa gachua	SYELPDGQVITIGNER	100
AHA84099.1	beta-actin, partial / Chiloscyllium punctatum	SYELPDGQVITIGNER	100
ACT78447.1	actin, partial/ Bemisia tabaci	SYELPDGQVITIGNER	100
AMT75487.1	actin, partial /Schizophyllum commune	SYELPDGQVITIGNER	100
AAW82382.1	actin, partial/ Onnia tomentosa	SYELPDGQVITIGNER	100
ADQ43334.1	actin, partial /Pseudodiamesa branickii	SYELPDGQVITIGNER	100
BBI93157.1	Actin/ Moesziomyces antarcticus	SYELPDGQVITIGNER ************	100

Fig. 6.13. (F): Clustal alignment of *de novo* sequence from PMF peak (m/z 1790) with Actin-5C, identified in NCBI database.

Table. 6.2: List of differentially expressed proteins and their identification by MALDI-TOF-TOF analysis

Label of	Protein	Fold		Ŋ	MS/MS analysis			
spots	expression	change						
	(C vs T)				<u> </u>	-		
			Obtained	Identification of protein in the	NCBI	No. of	Sequence	Ref
			protein score	MASCOT search database	Accession No	peptides matched	coverage	
1	Down	3.24	36	Zinc finger protein 271-like	XP_022835582.1	16	32%	Fig.
	regulated			isoform X1	*****			6.7.& 6.8
2	Down	1.8	231*	Arginine kinase isoform-3	XP_022834762.1	16	48%	Fig.
	regulated							6.7.& 6.9
3	Newly		46	Uncharacterized protein	XP_022819955.1	4	52%	Fig.
	expressed							6.7.&
								6.10
4	Up	2.44	64*	Actin-Muscle type A2	XP_022837900.1	16	15%	Fig.
	regulated							6.7.&
								6.11
5	Up	1.69	216*	Actin 5C	XP_022831297.1	14	44%	Fig.
	regulated							6.7.&
	rogulated							6.12

Note: * indicates the obtained score is significant based on Histogram

High lights of the Study:

- 1. T9BBI showed moderate inhibitory activity against trypsin-like gut proteases of host pest *S. litura*
- 2. Ingestion of T9BBI retarded the larval growth of *S. litura* up to 52% at higher concentration (0.1%).
- 3. Feeding with T9BBI altered the expression of midgut tissue proteome of *S. litura* larvae as evident by 2-dimensional gel electrophoresis.
- 4. Proteins which showed altered expression pattern are involved in transcription (Zincfinger protein), energy metabolism (Arginine kinase), structural stability and integrity (Actin) related proteins functions.

Chapter 7

Insecticidal Potential of T9BBI on Larval Growth and Development of a Host Insect Pest *Helicoverpa armigera*: Modulation in the Expression of Midgut Tissue Proteins

Chapter 7

Insecticidal Potential of T9BBI on Larval Growth and Development of a Host Insect Pest *Helicoverpa armigera*: Modulation in the Expression of Midgut Tissue Proteins

In general, *H. armigera* acquires resistance to insecticides much faster as compared to other polyphagous pests. The free amino acids formed by the action of digestive enzymes on dietary proteins in insect midgut play a crucial role in contributing to insect growth, development and reproductive phenomena. Hence, these enzymes are mainly targeted in insect pest management. Almost 30% of the pesticides used worldwide are targeted to overcome the insect pest *H. armigera*. Due to its high polyphagy and wide distribution across the globe, this insect pest has developed resistance against various insecticides and adapted towards various cropping systems (Rajapakse and Walter, 2007). In this context, usage of possible provide improved solution in controlling insect pests without harming human beings and non-target organisms (Andow, 2008).

The *in vitro* studies demonstrated by Prasad et al. (2010b) from our laboratory indicated that PIs from *V. mungo* (TAU 1 variety) were more effective in inhibiting the activity of *H. armigera* trypsin-like midgut proteases (HGPs). With these preliminary studies, we intended to test the efficacy of PIs from T9 variety of black gram chosen in the present study on the larval growth and development of *H. armigera*. As examined in the earlier chapters 5 and 6, in this chapter, we monitored the changes in the proteins from midgut tissue of *H. armigera* larvae fed upon T9BBI as compared to the larvae fed on a normal diet.

Results and discussion:

7.1. *In-vitro* inhibitory activity of T9BBI against *H. armigera* trypsin-like midgut proteases (HGPs):

In the present study, the T9BBI purified from the seeds of black gram (chapter 4) has shown an inhibitory potential of 436±9.24 HGPI units/mg protein and 983±25 BPTI units/mg

protein against *H. armigera* midgut trypsin-like (HGPs) and bovine pancreatic trypsin (BPT), respectively which is 27-fold and 115-fold higher than the activity shown by crude protein extract against HGPs and BPT, respectively (**Figure 7.1**). The specific activity of T9BBI obtained in the present study was comparable with the TAU1 variety of *V. mungo* which showed approximately 1000 TI units/mg protein (Prasad et al., 2010 b). Also, the present study demonstrates that the T9BBI purified from *V. mungo* possesses the remarkable potential to inhibit the trypsin-like proteases present in the midgut of *H. armigera*.

Several reports from previous studies also indicated the potential of PIs in inhibiting the activity of trypsin-like midgut proteases of *H. armigera*. The PIs isolated from various host plants such as pigeon pea (Lomate et al., 2012), *Capsicum annuum* (Joshi et al., 2014), *Acacia nilotica* (babu et a., 2012), *Eugenia jambolona* (singh et al., 2014), *Murraya koeningii* (Gahloth et al., 2011), non-host PIs from *Datura albaness* (Parde et al., 2010) and Caffeic acid extract also (Joshi et al., 2014) showed inhibitory activity against trypsin-like midgut proteinases of *H. armigera*. The PIs from *Madhuca indica* seeds inhibited 76% (Jamal et al., 2014), pigeon pea inhibited 21% and *V. mungo* TAU1 inhibited 48% activity of the trypsin-like midgut proteases of *H. armigera* (Prasad et al., 2010b) The crude protein extract isolated from the pigeon pea wild relative *R. sublobata* seeds have shown 62 HGPI units/mg protein while the Kunitz inhibitors purified from it showed 15000 HaGPI units/mg protein and an IC₅₀ of 59 ng against HaGPs (Mohanraj et al., 2018, 2019).

7.2. Insecticidal activity of BBIs against *H. armigera*:

The larvae of H. armigera from first instar stage (average weight of 24 ± 1.9 mg) were allowed to feed on an artificial diet containing a range of concentrations of T9BBI (0.01%, 0.025%, 0.05% and 0.1%) prepared in 50 mM Tris-HCl (pH 8.0). The control larvae were allowed to feed on an artificial diet containing 50mM Tris-HCl (pH 8.0) without T9BBI. With an increase in the concentration of T9BBI in the artificial diet, the mean

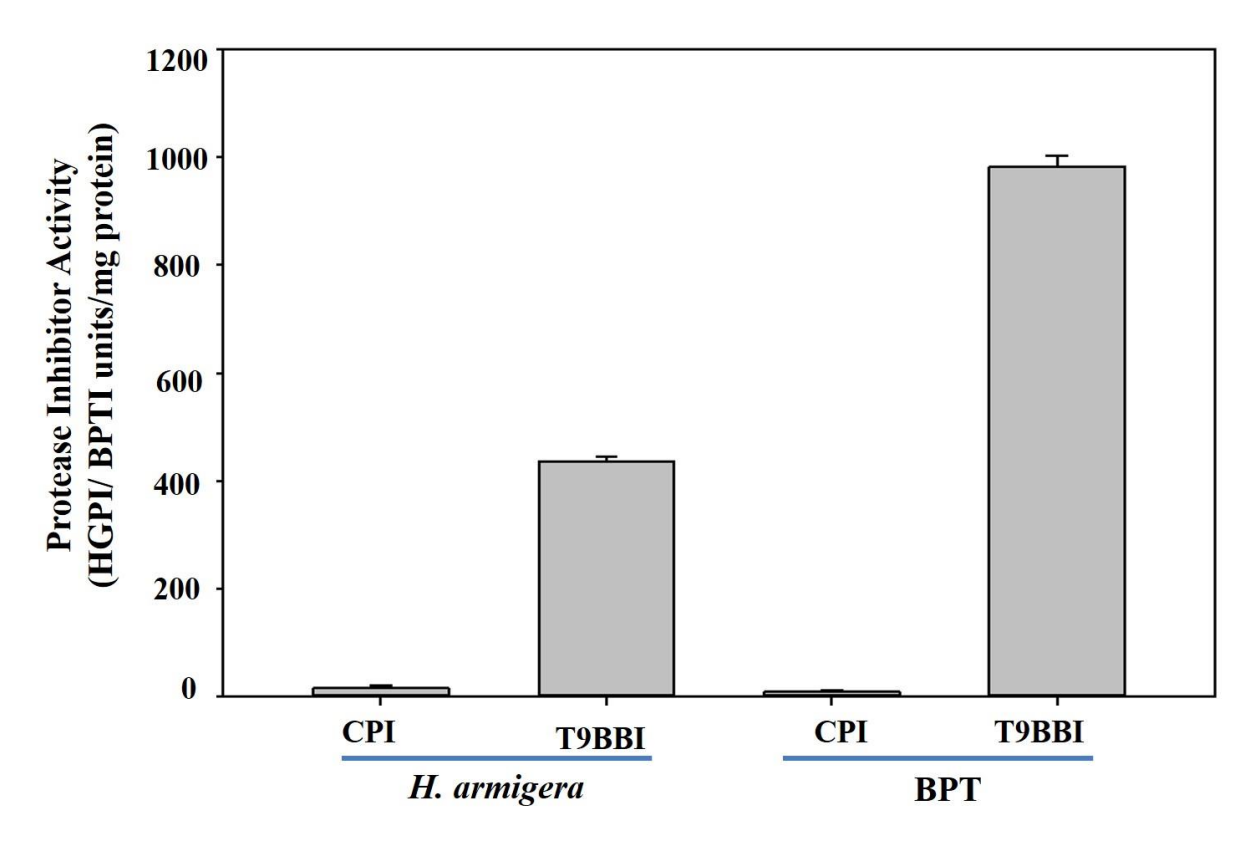


Fig. 7.1. A comparative inhibitory potential of crude proteinase inhibitor (CPI) extract and purified T9BBI from seeds of *V. mungo* (T9 variety) towards *H. armigera* midgut trypsin-like proteases (HGPs) collected from 5th instar larvae and bovine pancreatic trypsin (BPT), which is used as a control. The specific activity of CPI and T9BBI was determined as the number of *H. armigera* midgut trypsin-like proteinase inhibitor (HGPI) units mg⁻¹ protein and Bovine pancreatic trypsin inhibitor (BPTI) units mg⁻¹ protein, respectively. Further details were described in materials and methods.

weights of the larvae decreased from 2^{nd} to 6^{th} instar stage. However, a comparative analysis of the data on the weight gain of the larvae fed upon T9BBI with control larvae were shown from the 3^{rd} instar stage.

The average weight of the control larvae in the early third instar stage actively feeding on an artificial diet without T9BBI for 6 days was 56 ± 10 mg. The growth of the T9BBI fed larvae was retarded by $7.3\pm1\%$ (0.01%), $25\pm2.4\%$ (0.025%), $41\pm3.7\%$ (0.05%) and $51\pm6.4\%$ (0.1%), respectively, when compared with the growth of control larvae (**Fig. 7.2A**).

The average weight of the control larvae in the early fourth instar stage actively feeding on an artificial diet without T9BBI for 9 days was 98 ± 14 mg. The growth of the T9BBI fed larvae was retarded by $27\pm2.6\%$ (0.01%), $46\pm4.9\%$ (0.025%), $57\pm4.1\%$ (0.05%) and $62\pm5.3\%$ (0.1%), respectively, when compared with the growth of control larvae (**Fig. 7.2B**).

The average weight of the control larvae in the early fifth instar stage actively feeding on an artificial diet without T9BBI for 12 days was 218 ± 39 mg. The growth of the T9BBI fed larvae retarded by $11\pm1.6\%$ (0.01%), $27\pm3.8\%$ (0.025%), $37\pm2.9\%$ (0.05%) and $44\pm5.2\%$ (0.1%), respectively, when compared with the growth of control larvae (**Fig. 7.3A and B**).

Further, the average weight of the control larvae in the early sixth instar stage, which is feeding on an artificial diet without T9BBI for 15 days was 330±51 mg. Similar to the earlier instar stage, the growth of the *H. armigera* larvae fed on an artificial diet supplemented with T9BBI was inhibited by 13±2.8% (0.01% T9BBI), 27±3.3% (0.025% T9BBI), 39±3.8 (0.05% T9BBI) and 44±4.9% (**0.1% T9BBI**), respectively, when compared with the growth of control larvae (**Fig. 7.3C and D**).

The T9BBI fed larvae did not show any mortality though growth was retarded significantly. The larvae developed on the control diet and T9BBI supplemented diet were further converted into pupae. But, a delay (2-11 days) in the transformation of the larva to

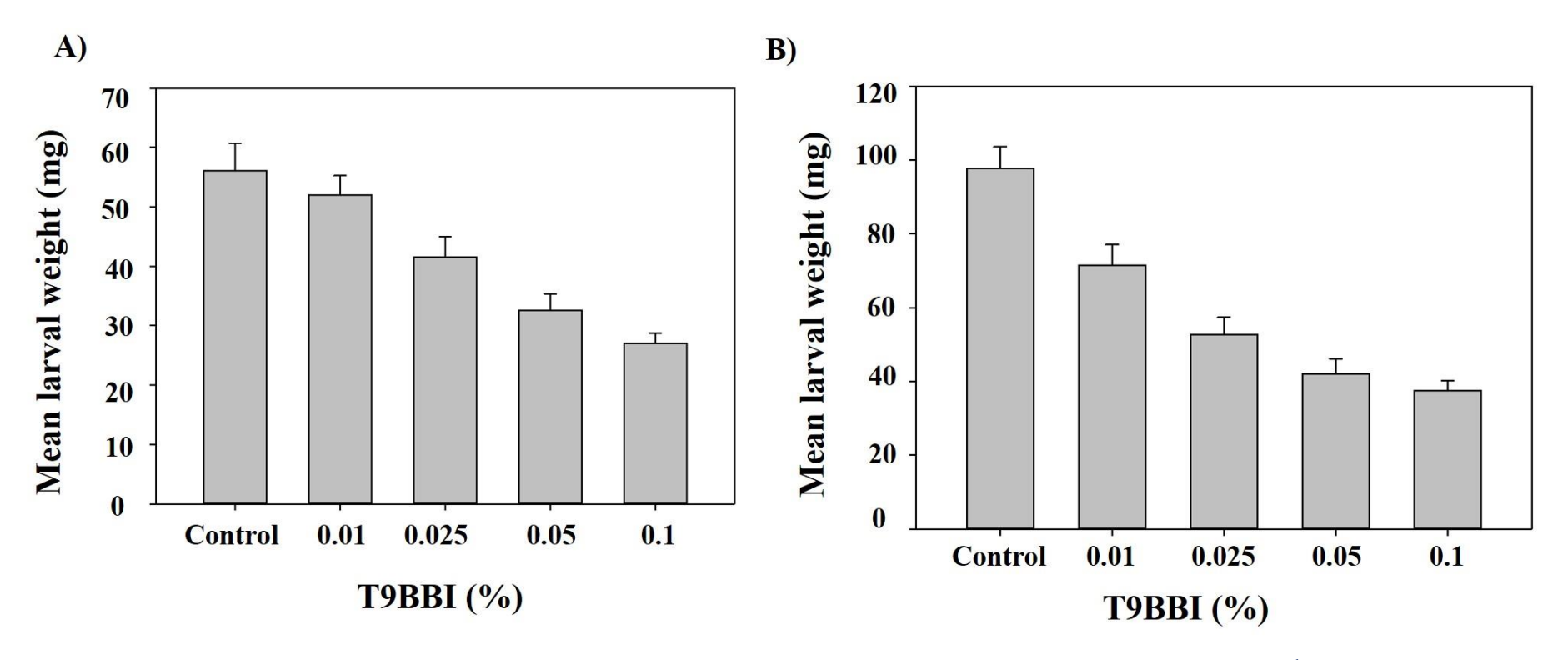


Fig. 7.2. Effect of T9BBI on the growth of *H. armigera* larvae (A) Mean body weight of the 3rd instar larvae reared on artificial diet alone (Control) and different concentrations of T9BBI (treated). (B) Mean body weight of the 4th instar larvae reared on artificial diet alone (Control) and different concentrations of T9BBI (treated). Further details were described in materials and methods.

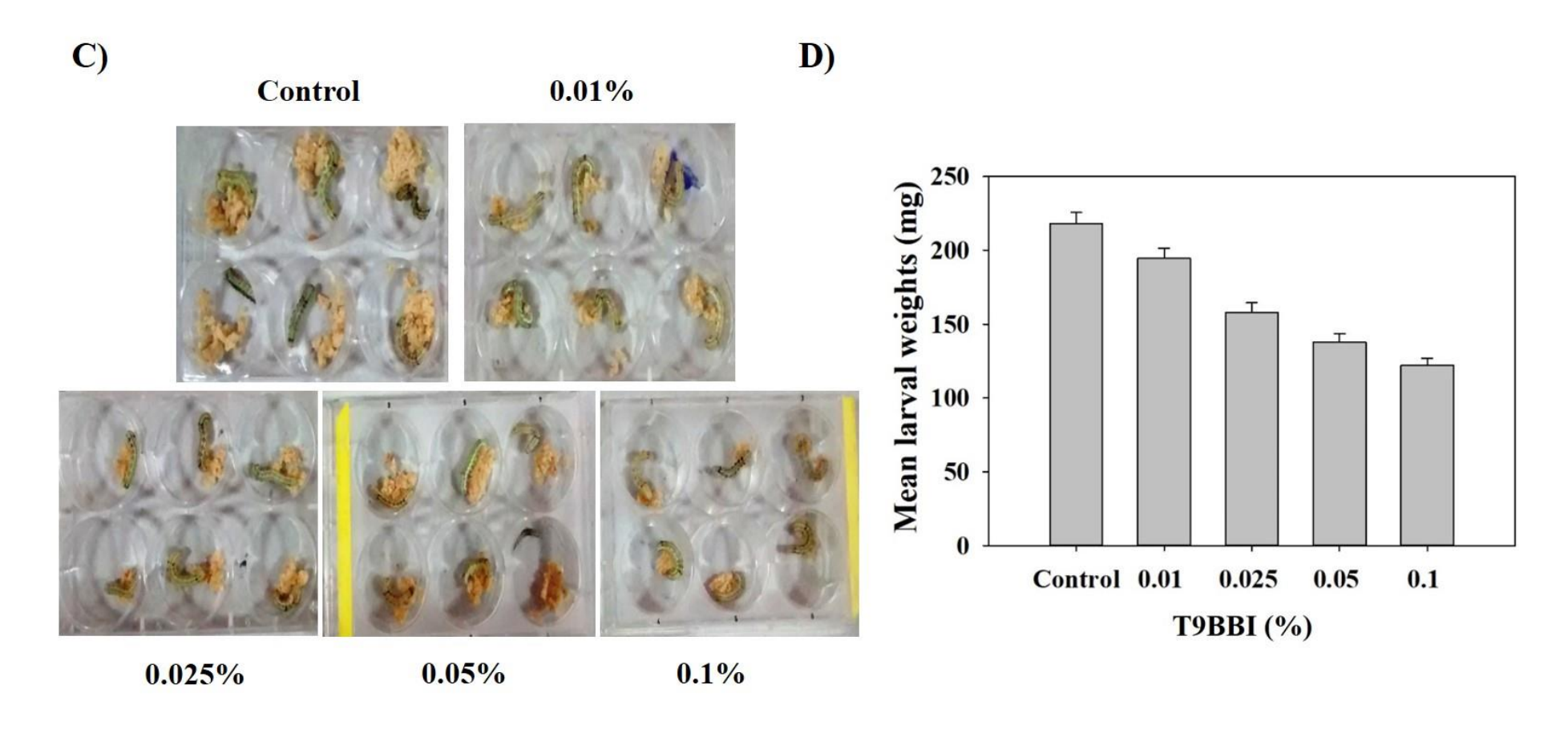


Fig. 7.2. Effect of T9BBI on the growth of 5th instar larvae of *H. armigera*. (C) Pictorial depiction of larvae reared on castor leaf coated with buffer alone (control) and different concentrations of T9BBI (treated), and (D) Mean body weight of the corresponding larvae. Further details were described in materials and methods.

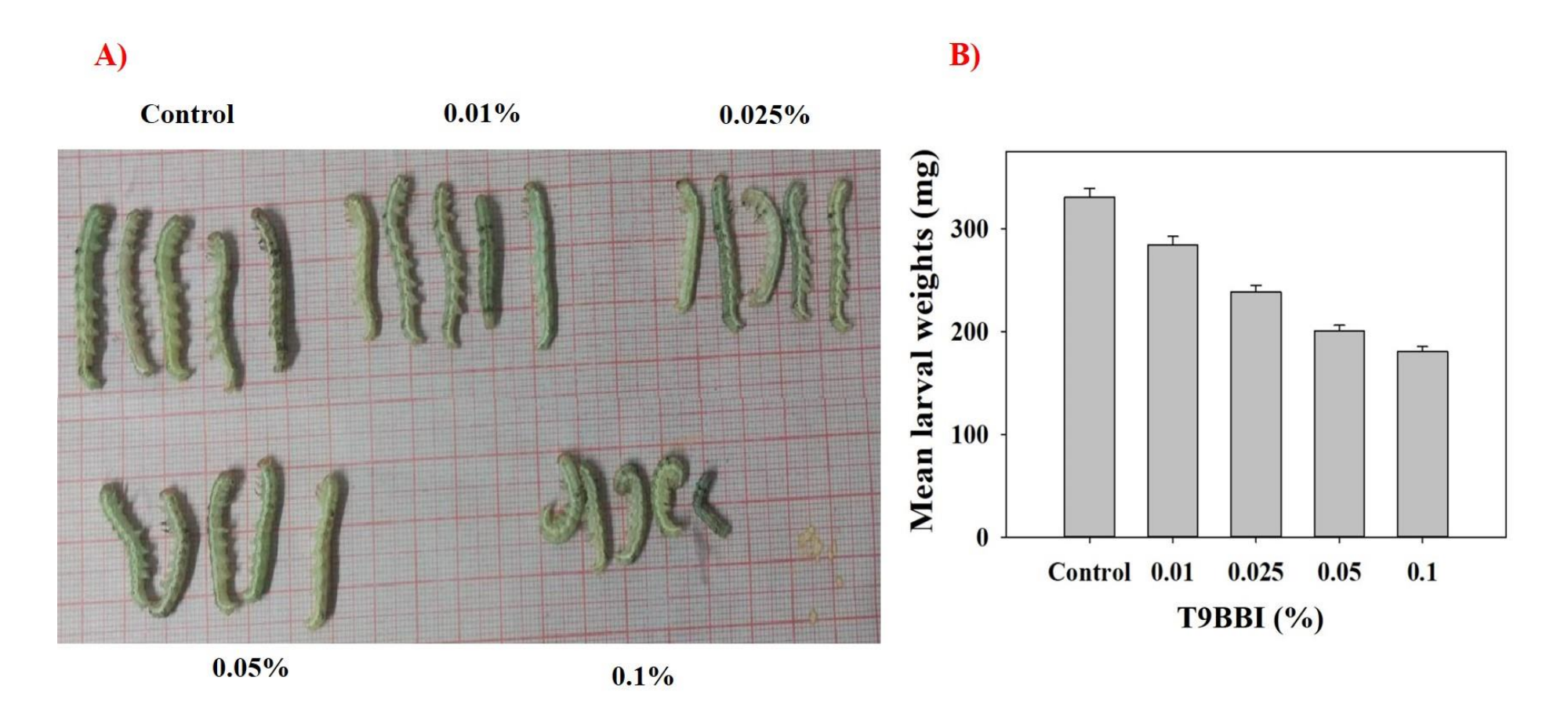


Fig. 7.3. Effect of T9BBI on the growth of 6th instar larvae of *H. armigera*. (A) Pictorial depiction of larvae reared on castor leaf coated with buffer alone (control) and different concentrations of T9BBI (treated), and (B) Mean body weight of the corresponding larvae. Further details were described in materials and methods.

pupa was observed with an increase in the concentration of T9BBI in the artificial diet (Table.7.1). Further, a reduction in the pupal weight was observed when the larvae were fed upon T9BBI supplemented diet. The weight of the pupa was decreased by 7 to 55% when the concentration of T9BBI was increased from 0.01% to 0.1% in the diet (Fig. 7.4A and B). Subsequently, adults have emerged from pupae through metamorphosis. However, the formation of transient larval-pupal and pupal-adult intermediates was observed when the larvae were fed upon diet supplemented with high concentrations (0.05% and 0.1%) of T9BBI (Fig. 7.4C).

The reports from previous studies indicated that the PI purified from *Eugenia jambolana* seeds showed significant inhibitory activity against *H. armigera*. Feeding experiments with different concentration (0.05, 0.15 and 0.45% w/w) of PI on 4th instar larvae showed significant growth retardation up to 71%. Parallel to increase in larval mortality up to 51%, the formation of larval-pupal and pupal-adult intermediates was observed, while 24% of larvae pupated and adult emergence decreased up to 28% (Singh et al., 2014).

Similarly, trypsin/ chymotrypsin inhibitors from the winged bean showed growth retardation in *H. armigera* at about 12, 27 and 49%, respectively by the end of 14, 16 and 18 days of feeding. Larval mortality was observed to be 72% in PI fed larvae when compared with their respective control larvae (Banerjee et al., 2017).

Similarly, PIs purified from *Acacia nilotica* seeds showed inhibitory activity against *H. armigera*. The larval weights were decreased at higher concentrations (0.5 & 1%) when compared with control. While the larval period was extended by one day, the mean pupal weight was reduced. Also, 10-20% malformation was observed during metamorphosis when compared with their control studies (Babu et al., 2012).

The combined effect of Cry1 Ac toxin (Bt) and PI has shown significant larval growth retardation when compared with control sets and treatment with Cry1Ac and PI independently. Moreover, a higher mortality rate was recorded when fed on a diet containing a combination of Cry1Ac and PI. Further, the larvae showed stunted growth at all the given treatments when compared with their respective control studies (Lomate et al., 2013).

Non-host PI purified from *Madhuca indica* seeds also showed significant growth retardation by 50% and development in *H. armigera* larvae at different concentrations (0.5, 1.0 and 1.5% w/w) when compared with their control larvae. Further, larval development was delayed by 6 days while the developmental time period for pupa was also increased by 3 days. A reduction in pupal weight (67%) was observed along with malformation (Jamal et al., 2014).

Retardation in larval growth, delay in pupal formation and emergence of larval-pupal and pupal-adults in the presence of T9BBI correlated with several previous studies. However, the effect of T9BBI was found to be greater at the early instar (3rd and 4th) stages when compared with the late instar (5th & 6th) stages (**Table 7.1**). The molecular mechanism by which the late instar larvae are adapted to T9BBI was revealed by closely monitoring the expression pattern of midgut tissue proteins from control and T9BBI fed larvae through 2D electrophoresis followed by MALDI-TOF-TOF studies.

7.3. Differential expression of proteins in midgut tissue of *H. armigera* larvae fed with T9BBI:

The protein extract prepared from midgut tissue of late 5th instar larvae feeding on a diet containing T9BBI (0.1%) and control diet were separated on IPG strips in the pH range from 4-7 followed by SDS-PAGE in the second dimension. The proteome profile of midgut tissues were compared for differentially expressed proteins by using image master platinum

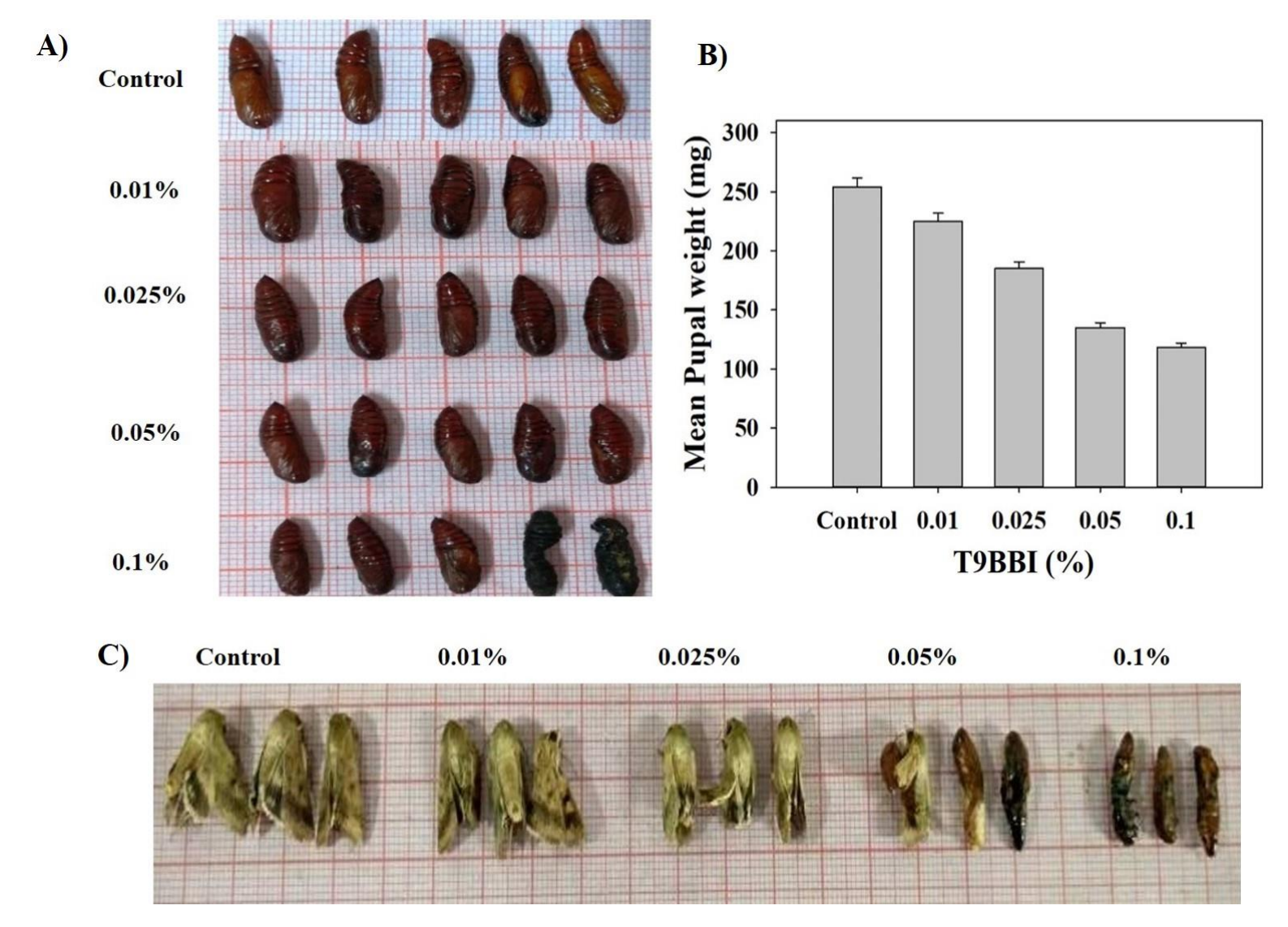


Fig. 7.4. Effect of T9BBI on development of *H. armigera*. (A) Pictorial depiction of pupae formed from larvae reared on artificial diet without T9BBI (control) and T9BBI (treated), respectively; (B) Mean pupal weight and (C) Pictorial depiction of adults emerged from corresponding pupae. Further details were described in materials and methods.

Table. 7.1: Anti metabolic effect of T9BBI on larval growth and development of *H. armigera*: Reduction in larval growth was represented after 5^{th} instar stage (15 days of feeding), while survival and mortality rate of larvae was represented after 6^{th} instar stage (18 days of feeding), respectively. Data shown here is the mean \pm SE values of three independent experiments (n=20). Further details were described in materials and methods.

Concentration of T9BBI on artificial diet	Reduction in larval growth	Survival rate (% control)	Mortality rate (% control)	Pupal formation time	Intermediate formation		Adult emergence from pupa
(μg/cm ⁻²)	(% control)		(70 control)	(days)	Larval-pupal	Pupal-adult	
0					No	No	Yes
(Control)	0	100	0	18-19			
0.01%	13±2.8	100	0	21-25	No	No	Yes
0.025%	27±3.3	100	0	23-28	No	No	Yes
0.05%	39±3.8	100	0	24-30	No	No	Yes
0.1%	45±4.9	100	0	30-35	Yes	Yes	Yes

7.0 software. A total of 204 protein spots were observed in 5 to 100 kDa range when separated in the second dimension using SDS-PAGE (**Fig. 7.5**). Seven protein spots which showed significant differences in their expression (> 2.0 -fold), separated conspicuously and placed distantly from other protein spots were considered for identification. The partial maps and 3-D views of the corresponding spots were represented in **Figure 7.6**.

All the protein spots (Spot 1 to 7) were subjected to tryptic digestion followed by MALDI-TOF-TOF analysis to identify the molecular mechanisms by which *H. armigera* larvae are adopted to T9BBI.

7.4. Mass spectrometric analysis of differentially expressed proteins:

7.4.1. Identification of Spot 1 as Hdd23-like protein:

Mascot search results for various ions generated from spot 1 on subjecting to tryptic digestion and MALDI-TOF-TOF showed a significant score of 102 with Hdd23-like protein of *H. armigera* (Fig. 7.7A). The spectrum corresponding to peptide mass fingerprint (PMF) data was represented in Figure 7.7B. When the peak with m/z 1369 from PMF spectrum was further ionized in MALDI-TOF-TOF, the resulting lift spectrum showed the following *de novo* sequence 'QVLLLLDEPSSR' when analyzed using Biotools software (Figs. 7.7C and D). Further, the various ions generated during MALDI-TOF-TOF studies showed 91% identity with the amino acid sequence of Hdd23-like protein (Uniprot Acc No. V5KZ60). Also, the *de novo* sequence obtained from PMF peak with m/z 1369 showed over-lapping with one of the internal amino acid sequence recognised for Hdd 23-like protein during MS/MS ion search (Fig. 7.7E). Furthermore, clustal alignment of this *de novo* sequence with sequences available in the NCBI database showed significant (100%) matching with the Hdd 23-like protein of *H. armigera* species (Fig. 7.7F). These results confirm that Hdd 23-like

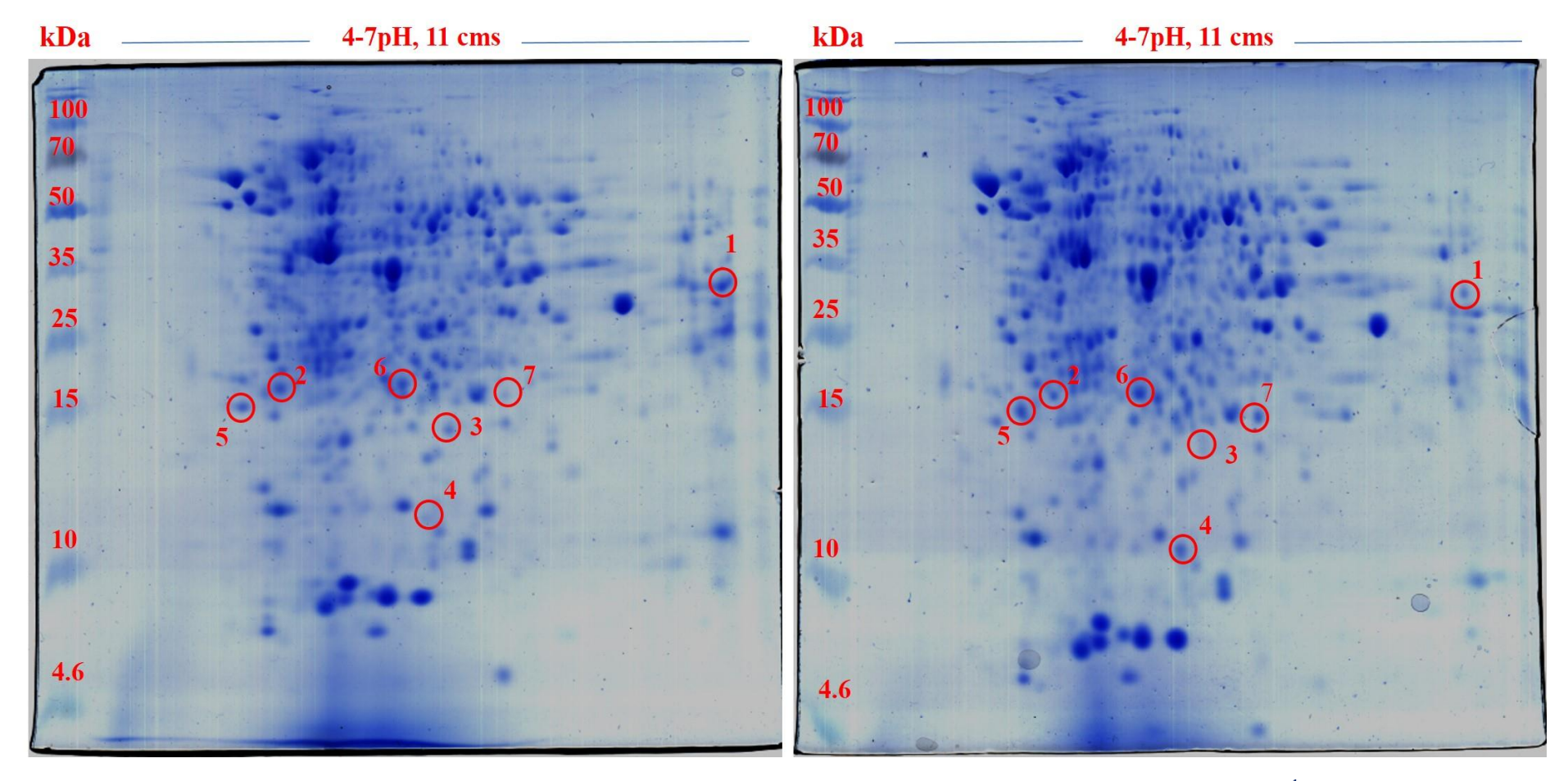


Fig. 7.5. Two dimensional gel electrophoresis of midgut tissue proteome from H. armigera larvae (early 5^{th} instar stage) fed up on **(A)** artificial diet without T9BBI (Control) and **(B)** artificial diet with T9BBI (0.1%), respectively. Among several spots which showed significant differences (> 2-fold), spots labelled as 1 to 7 (indicated with red circles) which are clearly separated from other spots are chosen for further studies, i.e., MALDI-TOF-TOF analysis. Further details were described in materials and methods.

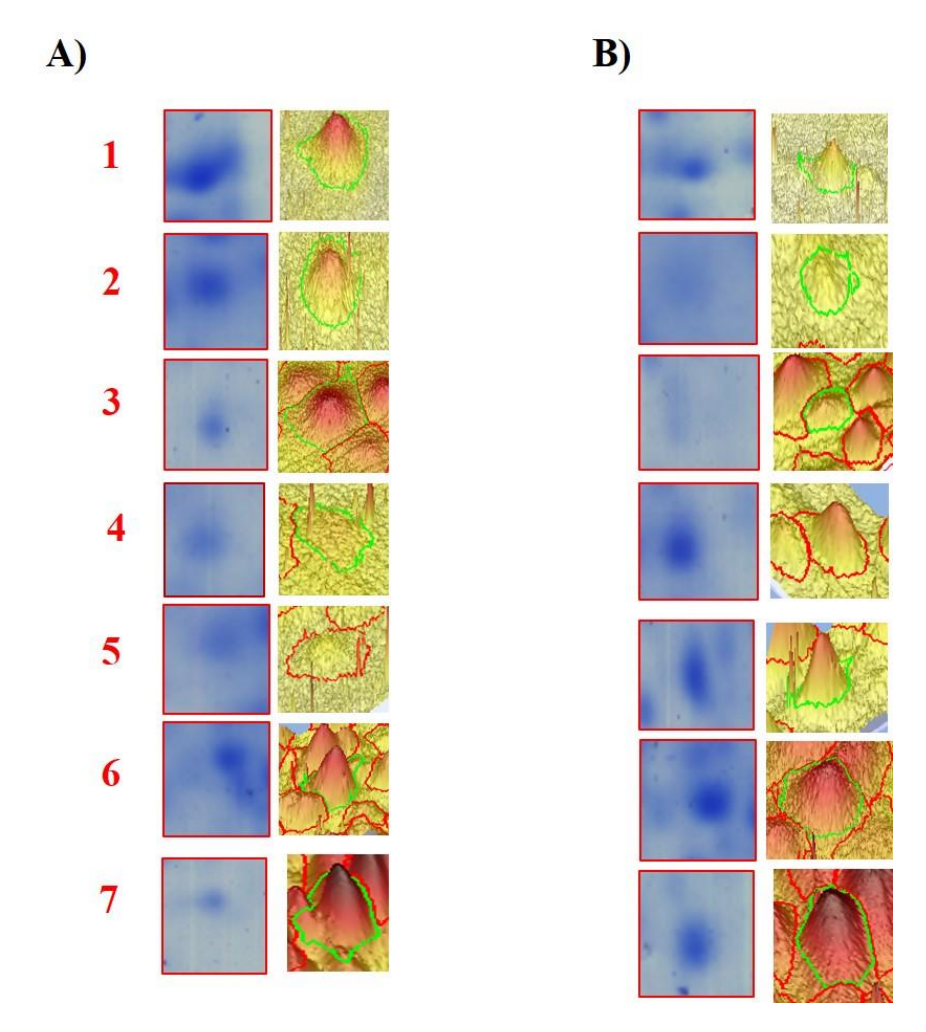
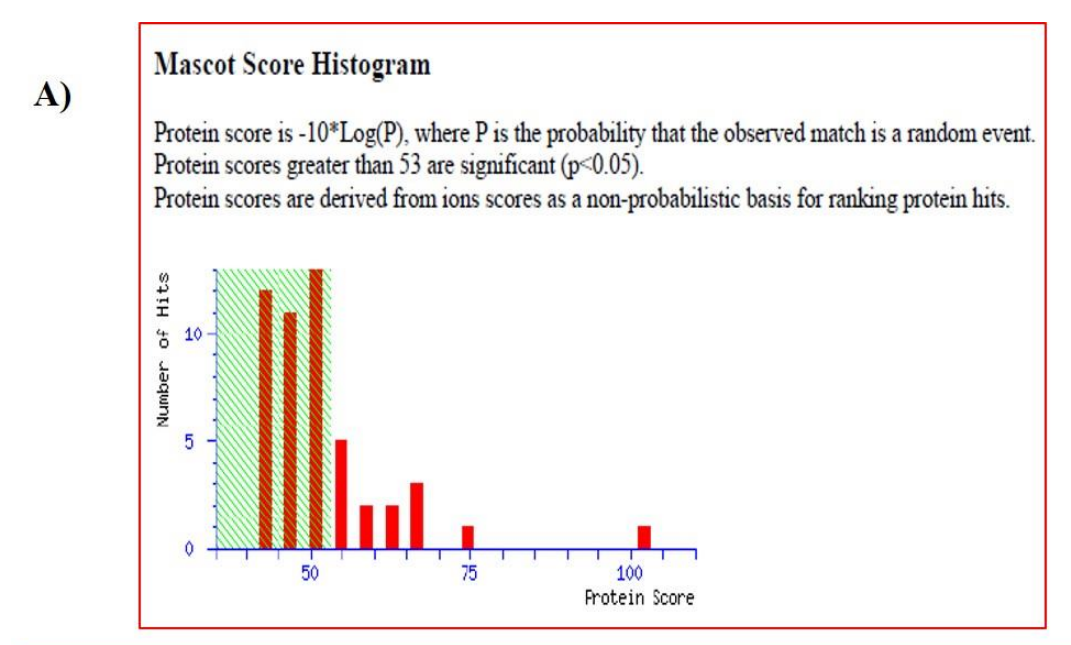


Fig. 7.6. Three-dimensional view of differentially expressed protein spots (1-7) labelled in 2-DE of fig 7.5 using Image Master Platinum software. Panels (A) and (B) represent protein spots from midgut proteome of *H. armigera* larvae (early 5th instar stage) fed up on (A) artificial diet without T9BBI and (B) artificial diet with T9BBI (0.1%), respectively.



	Accession	Mass	Score	Description
1.	V5KZ60 HELAM	13141	102	Hdd23-like protein OS=Helicoverpa armigera OX=29058 PE=2 SV=1
2.	A0A2W1BLQ7 HELAM	456415	73	Uncharacterized protein OS=Helicoverpa armigera OX=29058 GN=HaOG207647 PE=4 SV=1
3.	A0A2W1BIP6 HELAM	477240	66	Uncharacterized protein OS=Helicoverpa armigera OX=29058 GN=HaOG209998 PE=4 SV=1
4.	A0A2W1BK91 HELAM	38466	65	Uncharacterized protein OS=Helicoverpa armigera OX=29058 GN=HaOG206033 PE=4 SV=1
5.	A0A2W1BPS9_HELAM	19524	65	Uncharacterized protein OS=Helicoverpa armigera OX=29058 GN=HaOG200708 PE=4 SV=1
6.	A0A2W1BEX5 HELAM	52629	64	Uncharacterized protein OS=Helicoverpa armigera OX=29058 GN=HaOG208995 PE=4 SV=1
7.	A0A2W1BQ80 HELAM	135000	61	Uncharacterized protein OS=Helicoverpa armigera OX=29058 GN=HaOG203702 PE=4 SV=1
8.	A0A2W1BMH5_HELAM	37988	59	Uncharacterized protein OS=Helicoverpa armigera OX=29058 GN=HaOG206032 PE=4 SV=1
9.	A0A2W1BSE1_HELAM	39404	57	Uncharacterized protein OS=Helicoverpa armigera OX=29058 GN=HaOG204463 PE=4 SV=1
10.	A0A2W1BDN2 HELAM	40222	55	Uncharacterized protein OS=Helicoverpa armigera OX=29058 GN=HaOG214453 PE=4 SV=1
11.	A0A2W1C0Z2_HELAM	86323	54	Katanin p80 WD40 repeat-containing subunit B1 OS=Helicoverpa armigera OX=29058 GN
12.	A0A2W1BL24 HELAM	70677	54	Phosphodiesterase OS=Helicoverpa armigera OX=29058 GN=HaOG206852 PE=3 SV=1
13.	A0A2W1BGQ1 HELAM	134860	53	Uncharacterized protein OS=Helicoverpa armigera OX=29058 GN=HaOG214777 PE=4 SV=1
14.	A0A2W1B7A9_HELAM	61326	53	Uncharacterized protein OS=Helicoverpa armigera OX=29058 GN=HaOG212445 PE=4 SV=1
15.	A0A2W1BT77 HELAM	68695	52	Uncharacterized protein OS=Helicoverpa armigera OX=29058 GN=HaOG202331 PE=4 SV=1
16.	D5G3D5 HELAM	62282	52	Carboxylic ester hydrolase OS=Helicoverpa armigera OX=29058 PE=2 SV=1
17.	A0A2W1BMR8 HELAM	34623	52	Uncharacterized protein OS=Helicoverpa armigera OX=29058 GN=HaOG204716 PE=4 SV=1
18.	A0A2W1BGT5 HELAM	159306	52	Uncharacterized protein OS=Helicoverpa armigera OX=29058 GN=HaOG208126 PE=4 SV=1
19.	A0A2W1BTR2_HELAM	48450	50	Uncharacterized protein OS=Helicoverpa armigera OX=29058 GN=HaOG202123 PE=4 SV=1
20.	A0A2W1BCQ7_HELAM	47748	50	Uncharacterized protein OS=Helicoverpa armigera OX=29058 GN=HaOG212893 PE=4 SV=1

Fig. 7.7. Identification of spot 1 as Hdd23-like protein after tryptic digestion and MALDI-TOF-TOF analysis. (A) Histogram of MASCOT search results and corresponding protein hits.

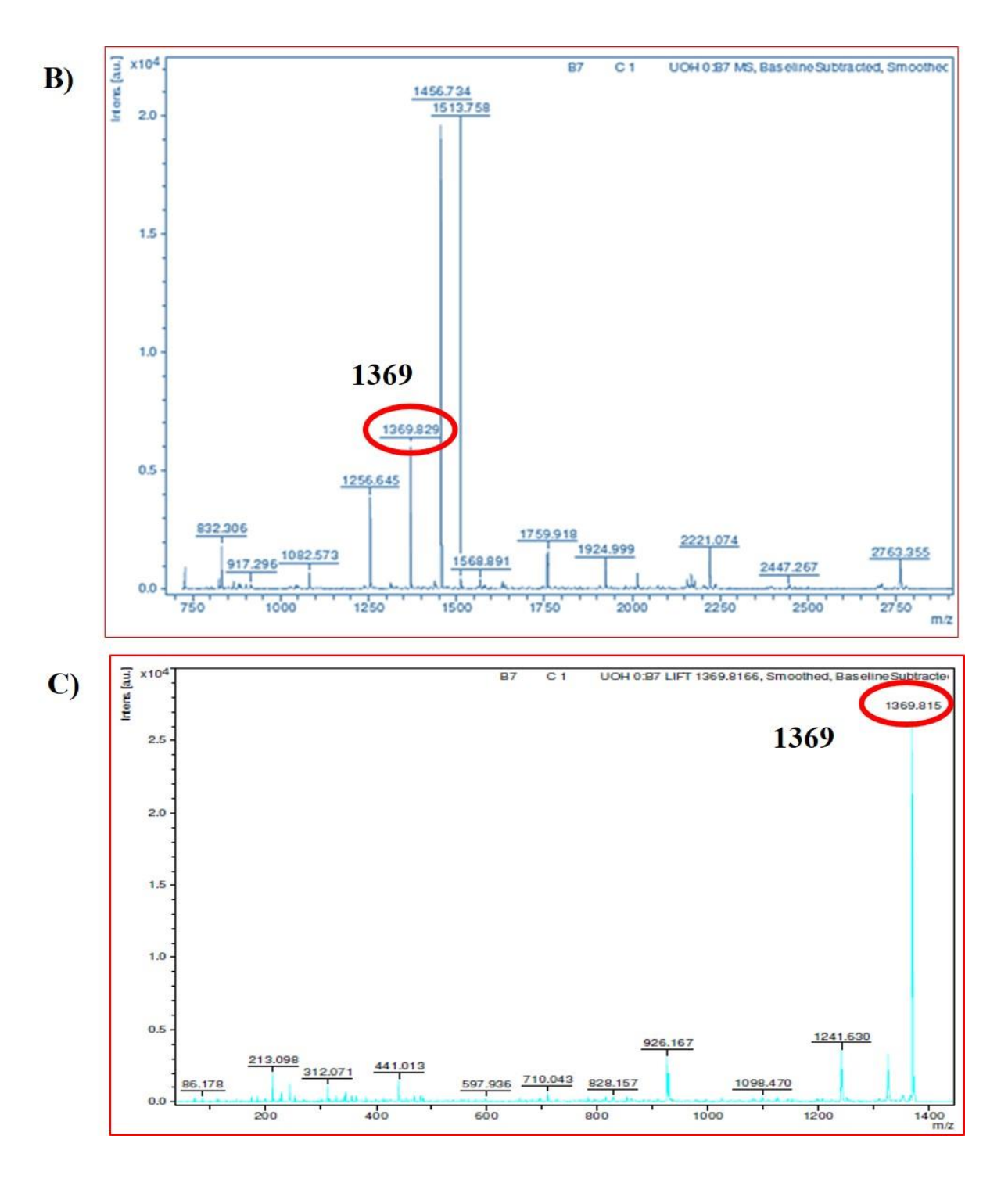


Fig. 7. 7. **(B)** PMF spectra of spot 1 highlighting peak 1369 (m/z); **C)** Lift spectrum of PMF peak with m/z 1369

D) Calculated Masses:

QVLLLLDEPSSR

N-Term.	Ion	a	b		a-17	b-17	γ	C-Term.	lon
1	O	101.071	129.066	101.071	84.044	112.039	175.119	12	Ħ
2	٧	200.139	228.134	72.081	183.113	211.108	262.151	11	ŝ
3	L	313.223	341.218	86.096	296.197	324.192	349.183	10	8
4	L	426.307	454.302	86.096	409.281	437.276	446.236	9	P
5	L	539.392	567.386	86.096	522.365	550.360	575.278	8	E
6	L	652.476	680.471	86.096	635.449	663.444	690.305	7	D
7	D	767.503	795.497	88.039	750.476	778.471	803.389	6	L
8	E	896.545	924.540	102.055	879.519	907.514	916.473	5	L
9	P	993,598	1021.593	70.065	976.571	1004.566	1029.557	4	
10	S	1080.630	1108.625	60.044	1063.603	1091.598	1142.642	3	L
11	S	1167.662	1195.657	60.044	1150.635	1178.630	1241.710	2	٧
12	R	1323.763	1351.758	129.113	1306.737	1334.731	1369.769	1	O

E) Sequence coverage: 91%

 $MYTNMCVKIAVCLALVVSIDSHILKHHEVPLSPEGMVVEITVKNKGNEHPVSSMKIDVDE\\ KDKQVLLLLDEPSSRVPRKTGDSSTEVVPTIGSRHNIRVGACPAGYTRTGGFCFPDDY$

Fig. 7.7. (D): Analysis of Lift spectrum from peak m/z 1369 using Biotools; **(E)** Hdd 23-like protein (V5KZ60_HELAM/ Uniprot Acc. V5KZ60) sequence. Red colour indicates the partial sequence coverage by various ions generated from spot 1, while blue box indicate the matching of *de novo* (m/z 1369) sequence obtained from Biotools with one of the peptides identified by Mascot search engine.

Accession number	Protein name/Source	Sequence	Similarity (%)
Spot number 1, (de novo	sequence from PMF peak with m/z 1369	QVLLLLDEPSSR	100
AHA43054.1	Hdd23-like protein /Helicoverpa armigera	QVLLLLDEPSSR *******	100

Fig. 7.7. F): Clustal alignment of *de novo* sequence from PMF peak (m/z 1369) with Hdd23-like protein, identified in NCBI database.

protein is down-regulated by 3.6-fold in *H. armigera* larvae upon feeding on a diet supplemented with T9BBI (Figs. 7.5-7.7, Table 7.2).

In *Hyphantria cunea*, the injection of bacterial (*E.coli & M. luteus*) strains into the hemocoel of 5th instar larvae resulted in induction of several genes (Hdd 1, 2, 3, 11, 15, 17, 23, 106 and 302). However, injection of double distilled water also slightly up-regulated the mRNA levels of these immune-related genes (Shin et al., 1998). In *B. mori* Hdd 1 is known to be expressed during molting and metamorphosis stages under normal physiological conditions and during bacterial injection (Zhang et al., 2017). In the present study, the morphological changes or abnormalities caused by T9BBI might be due to the down regulation of the Hdd 23-like immune-related protein.

7.4.2. Identification of Spot 2 and 3 as uncharacterized proteins:

The protein spots 2 and 3 are identified as uncharacterized proteins when the ions generated from the corresponding spots are subjected to tryptic digestion and Mascot-ion search. The same results was confirmed when the ions generated during MALDI-TOF-TOF showed partial sequence coverage with an uncharacterized protein in the Uniprot (Accession no's are A0A2W1BAL7 and A0A2W1C0A5) database. These results confirm that two uncharacterized proteins are down-regulated up to 2.8 and 4.1-fold, respectively, in the midgut tissue when fed upon T9BBI diet and they might play a significant role in the sustenance of growth and development of *H. armigera* larvae (**Table 7.2**).

7.4.3. Identification of Spot 4 as Thioredoxin peroxidase:

Digestion of spot 4 with trypsin and subsequent MALDI-TOF-TOF analysis revealed the matching of this spot with Thioredoxin peroxidase (Tpx) from *H. armigera* with a significant score of 348 in the Mascot search engine (**Fig. 7.8A**). The mass spectrum corresponding to the PMF data was represented in **Figure 7.8B**. When the PMF peaks with m/z 1431 (lift spectrum not shown) and 1595 (lift spectrum shown) were further ionized in

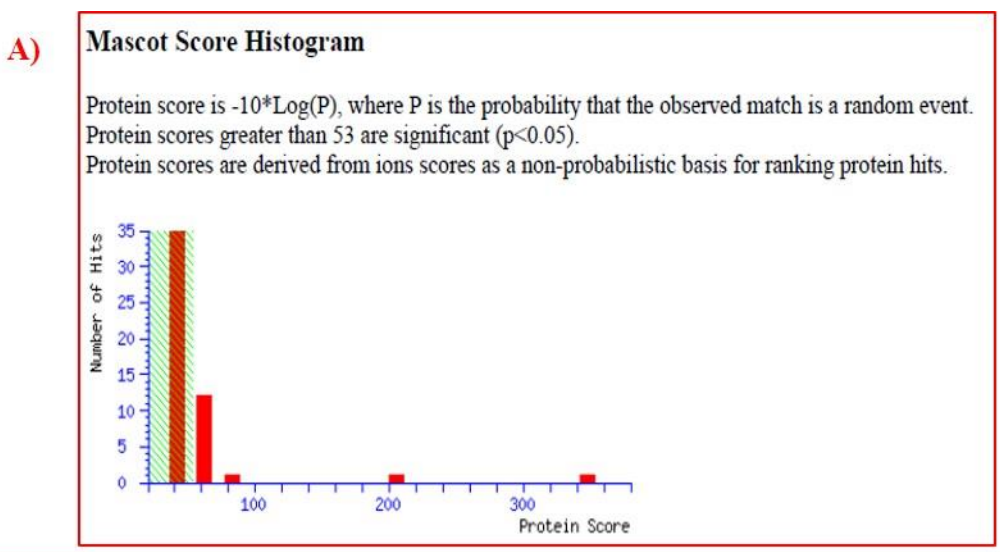
MALDI-TOF-TOF, the following *de novo* sequences 'GLFIIDDKQNLR' and 'DYGVLNEESGIPFR' were resulted when the corresponding lift spectra are analyzed using Biotools software (Figs. 7.8C and D). Also, the various ions generated during MALDI-TOF-TOF studies showed partial sequence coverage up to 67% with Thioredoxin peroxidase (Uniprot Acc No. B2KSE9). Further, the two *de novo* sequences obtained through Biotools showed overlapping with the partial amino acid sequences recognised for Thioredoxin peroxidase during MALDI-TOF-TOF analysis (Fig. 7.8E). Furthermore, Clustal alignment of the *de novo* sequence 'DYGVLNEESGIPER' with available sequences in the NCBI database showed 100% matching to a Tpx from *H. armigera* and *Heortia vitessoides*, respectively (Fig. 7.8F). The *de novo* sequence 'GLFIIDDKQNLR' from PMF peak with m/z 1431 also showed 100% similarity with the Tpx (Clustal alignment data not shown). These results confirm that spot 4 belong to the Tpx and it is upregulated by 3.4-fold in the midgut tissues of the *H. armigera* larvae when fed upon a diet containing T9BBI (Figs. 7.5, 7.6 and 7.8, Table 7.2).

Thioredoxins are found almost in all known organisms. Thioredoxin proteins act as important antioxidant enzymes by reducing the disulfide bonds of other proteins through the cysteine thiol-disulfide exchange. Toxic chemicals, thermal stress, UV radiation, heavy metals, pesticides and microbial invasion are different types of xenobiotic inducers which cause accumulation of reactive oxygen species (Fan et al., 2014; Shafeeq et al., 2017). To scavenge the excess ROS levels and to protect against oxidative damage, organisms have developed an efficient antioxidant enzyme such as Tpx (Yan et al., 2014). Five Tpx's have been identified in *D. melanogaster*, to combat oxidative stress (Radyuk et al., 2001). The Tpx genes expression was upregulated in the *Apis cerana* due to many stressors such as insecticides, hydrogen peroxide and UV light. Further, knockdown of Tpx genes by RNAi technology in *H. armigera*, *S. litura and Acyrthosiphon pisum* increased the larval mortality rate (Zhang et

Table. 7.2: List of differentially expressed proteins and their identification by MALDI-TOF-TOF analysis

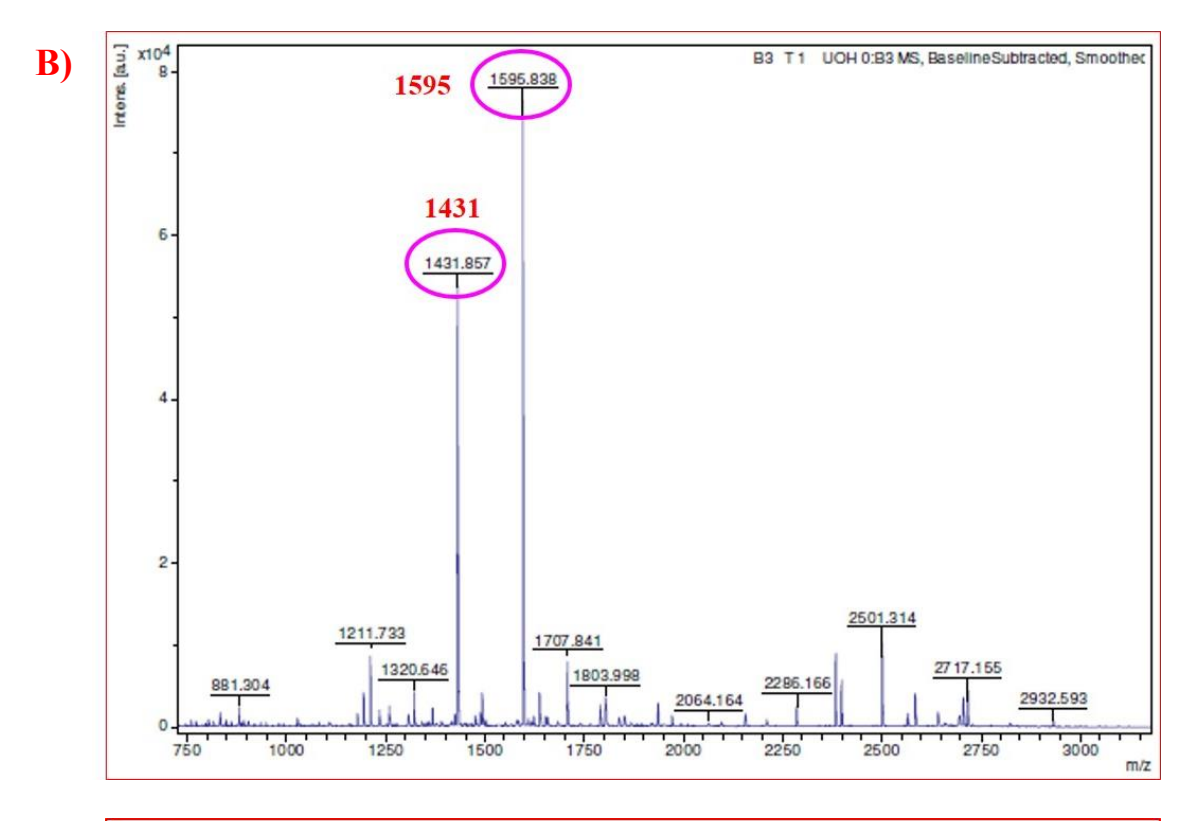
Label of spots	Significance (C vs T)	Fold			MS/MS analysis			
			Obtained protein Score	Identified proteins in MASCOT search data base	Mascot search/ Uniprot accession number	No. of peptides matched	Sequence Coverage by matched peptides	Ref
1	Down regulated	3.6	102*	Hdd (Hyphantria differentially displayed) 23-like protein	V5KZ60_HELAM/ V5KZ60	12	32	Fig. 7.6 & 7.7
2	Down regulated	2.8	100*	Un characterized protein	A0A2W1BAL7_HELAM/ A0A2W1BAL7	18	49	Fig. 7.6 & 7.8
3	Down regulated	4.1	65*	Un characterized protein	A0A2W1C0A5_HELAM/ A0A2W1C0A5	4	27	Fig. 7.6 & 7.9
4	Up regulated	3.4	348*	Thioredoxin peroxidase	B2KSE9_HELAM/ B2KSE9	12	64	Fig. 7.6 & 7.10
5	Up regulated	4.6	62*	Carboxylic ester hydrolase	D5KX86_HELAM/ D5KX86	22	59	Fig. 7.6 & 7.11
6	Up regulated	5.3	150*	Glutathione S-transferase	A0A0D3M5T8_HELAM/ A0A0D3M5T8	11	62	Fig. 7.6 & 7.12
7	Up regulated	3.7	89*	Cytochrome p-450	Q6PY59_HELAM/ Q6PY59	32	52	Fig. 7.6 & 7.13

Note: * indicates the obtained score is significant based on Histogram



	Accession	Mass	Score	Description
1.	B2KSE9 HELAM	22122	348	Thioredoxin peroxidase OS=Helicoverpa armigera OX=29058 PE=2 SV=1
2.	A0A2W1BUMO HELAM	40506	196	Uncharacterized protein OS=Helicoverpa armigera OX=29058 GN=HaOG204500 PE=4 SV=1
3.	A0A2W1BEL6 HELAM	190552	84	Uncharacterized protein OS=Helicoverpa armigera OX=29058 GN=HaOG209401 PE=4 SV=1
4.	A0A2W1BKD1_HELAM	201142	71	Uncharacterized protein OS=Helicoverpa armigera OX=29058 GN=HaOG211825 PE=4 SV=1
5.	A0A2W1BSN9 HELAM	423625	69	Uncharacterized protein OS=Helicoverpa armigera OX=29058 GN=HaOG202604 PE=4 SV=1
6.	A0A2W1AZIO HELAM	541179	69	Uncharacterized protein (Fragment) OS=Helicoverpa armigera OX=29058 GN=HaOG215825
7.	A0A2W1BHV7 HELAM	39081	64	Uncharacterized protein OS=Helicoverpa armigera OX=29058 GN=HaOG209716 PE=4 SV=1
8.	A0A2W1BJA7 HELAM	713603	62	ATP-dependent DNA helicase OS=Helicoverpa armigera OX=29058 GN=HaOG206881 PE=3 SV
9.	A0A2W1B918 HELAM	78734	62	Uncharacterized protein (Fragment) OS=Helicoverpa armigera OX=29058 GN=HaOG215377
10.	A0A2W1BSN6 HELAM	86569	60	Uncharacterized protein OS=Helicoverpa armigera OX=29058 GN=HaOG203510 PE=4 SV=1
11.	A0A2W1BAS6 HELAM	77425	60	Uncharacterized protein OS=Helicoverpa armigera OX=29058 GN=HaOG215703 PE=4 SV=1
12.	A0A2W1AYN2_HELAM	11111	56	Uncharacterized protein (Fragment) OS=Helicoverpa armigera OX=29058 GN=HaOG202343
13.	A0A2W1BGP9_HELAM	92594	53	Uncharacterized protein OS=Helicoverpa armigera OX=29058 GN=HaOG210375 PE=4 SV=1
14.	A0A2W1BXV7_HELAM	42715	52	Uncharacterized protein OS=Helicoverpa armigera OX=29058 GN=HaOG202602 PE=4 SV=1
15.	A0A2W1BRH7 HELAM	108541	52	Uncharacterized protein OS=Helicoverpa armigera OX=29058 GN=HaOG203146 PE=4 SV=1
16.	A0A2W1BMZ6 HELAM	98901	51	Uncharacterized protein OS=Helicoverpa armigera OX=29058 GN=HaOG206819 PE=4 SV=1
17.	A0A2W1BB13 HELAM	93536	51	Uncharacterized protein OS=Helicoverpa armigera OX=29058 GN=HaOG215541 PE=4 SV=1
18.	A0A2W1BZ92 HELAM	151731	50	Uncharacterized protein OS=Helicoverpa armigera OX=29058 GN=HaOG202026 PE=4 SV=1
19.	A0A2W1BSJ3 HELAM	111633	50	Uncharacterized protein OS=Helicoverpa armigera OX=29058 GN=HaOG202641 PE=4 SV=1
20.	A0A2W1BWT3 HELAM	72068	50	Uncharacterized protein OS=Helicoverpa armigera OX=29058 GN=HaOG202619 PE=4 SV=1

Fig. 7.8. Identification of spot 4 as Thioredoxin peroxidase after tryptic digestion and MALDI-TOF-TOF analysis. (A) Histogram of MASCOT search results and corresponding protein hits.



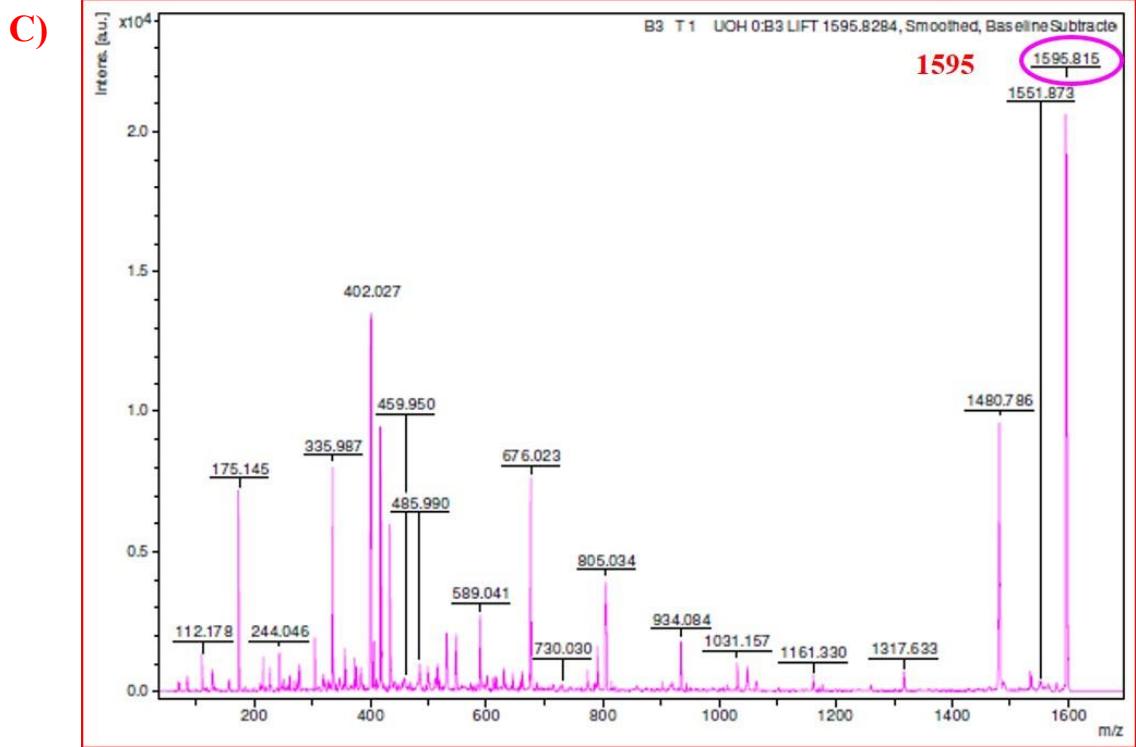


Fig. 7.8. (B): PMF spectrum of spot 4 highlighting peaks 1431 (m/z) and 1595 (m/z); **(C)** Lift spectrum of PMF peak with m/z 1595

D)

alculate (e <u>s:</u>	GLFIIDDK	QNLR		Peak: 1431					
N-Term.	Ion	а	b	1	a-17	b-17	у	C-Term.	lon		
1	G	30.034	58.029	30.034	13.007	41.002	175.119	12	R		
2	L	143.118	171.113	86.096	126.091	154.086	288.203	11	L		
3	F	290.186	318.181	120.081	273.160	301.155	402.246	10	N		
4	1	403.270	431.265	86.096	386.244	414.239	530.305	9	Q		
5		516.354	544.349	86.096	499.328	527.323	658.399	8	K		
6	D	631.381	659.376	88.039	614.355	642.350	773.426	7	D		
7	D	746.408	774.403	88.039	729.382	757.377	888.453	6	D		
8	K	874.503	902.498	101.107	857.477	885.472	1001.537	5	- 1		
9	Q	1002.562	1030.557	101.071	985.535	1013.530	1114,621	4			
10	N	1116.605	1144.600	87.055	1099.578	1127.573	1261.690	3	F		
11	L	1229.689	1257.684	86.096	1212.662	1240.657	1374.774	2	L		
12	R	1385,790	1413,785	129,113	1368,763	1396,758	1431.795	1	G		

DYGVLNE			GVLNEESO	GIPFR	Peak: 1595						
N-Term.	Ion	а	b	1	a-17	b-17	V	C-Term.	lon		
1	D	88.039	116.034	88.039	71.013	99.008	175.119	14	R		
2	Y	251.103	279.098	136.076	234.076	262.071	322.187	13	Т		
3	G	308.124	336.119	30.034	291.098	319.092	419.240	12	D.		
4	V	407.193	435.187	72.081	390.166	418.161	532.324	11	1		
5	L	520.277	548.271	86.096	503.250	531.245	589.346	10	G		
6	N	634.320	662.314	87.055	617.293	645.288	676.378	9	S		
7	E	763.362	791.357	102.055	746.336	774.330	805.420	8	Е		
8	E	892.405	920.400	102.055	875.378	903.373	934.463	7	E		
9	S	979.437	1007.432	60.044	962.410	990.405	1048.508	6	N		
10	G	1036.458	1064.453	30.034	1019.432	1047.427	1161.590	5	L		
11	ı	1149.542	1177.537	86.096	1132.516	1160.511	1260.658	4	٧		
12	Р	1246.595	1274.590	70.065	1229.568	1257.563	1317.680	3	G		
13	F	1393.663	1421.658	120.081	1376.637	1404.632	1480.743	2	Y		
14	R	1549.765	1577.759	129.113	1532.738	1560.733	1595.770	1	D		

E)

Sequence coverage: 67%

MPLQLTKPAPQFKTTAVVNGEFKDIALSDYKGKYVVLFFYPLDFTFVCPTEIIAFSERADDF RKIGCEIIGASTDSHFTHLAWINTPRKQGGLGPMNIPLLSDKSHRIARDYGVLNEESGIPFR GLFIIDDKQNLRQITVNDLPVGRSVEETLRLVQAFQYTDKFGEVCPANWQPGSKTIKPDTK AAQEYFIDAN

Fig. 7.8. (D): Analysis of Lift spectrum from peaks m/z 1431 & 1595 using Biotools; **(E)** Thioredoxin peroxidase (B2KSE9_HELAM/Uniprot Acc. B2KSE9) sequence. Red colour indicates the partial sequence coverage by various ions generated from spot 4 while blue box indicate the matching of *de novo* (m/z 1431 & 1595) sequences obtained from Biotools with the peptides identified by Mascot search engine.

Accession number	Protein name/ Source	Sequence	Similarity (%)
Spot number 4 1595)	(de novo sequence from PMF peak with m/z	DYGVLNEESGIPFR	100
ABW96360.1	Thioredoxin peroxidase/ Helicoverpa armigera	DYGVLNEESGIPFR	100
AVC05622.1	Thioredoxin peroxidase / Heortia vitessoides	DYGVINEESGIPFR *********	100

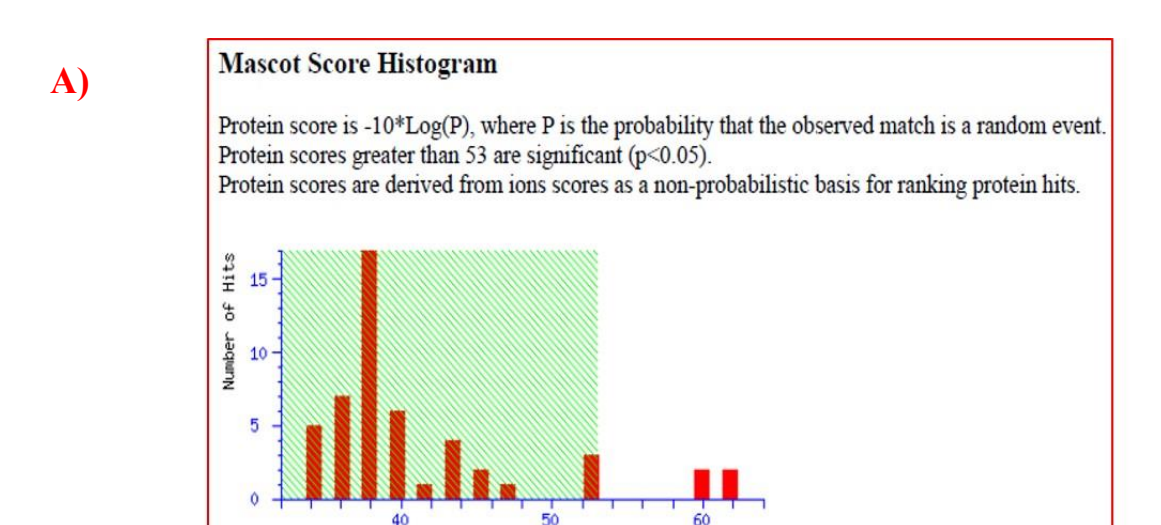
Fig. 7.8. F): Clustal alignment of *de novo* sequence from PMF peak (m/z 1595) with Thioredoxin peroxidase in NCBI database.

al., 2015). The results from the present study suggest that Tpx play a significant role in detoxifying the T9BBI in the midgut tissues of *H. armigera* larvae.

7.4.4. Identification of Spot 5 as Carboxylic ester hydrolase:

Mascot search results for various ions generated from spot 5 after tryptic digestion followed by MALDI-TOF-TOF analysis showed a significant score of 62 with carboxylic ester hydrolase of *H. armigera* (Fig. 7.9A). The spectrum corresponding to peptide mass fingerprint (PMF) data was represented in Figure 7.9B. When the peak with m/z 1607 from PMF spectrum was ionized further in MALDI-TOF-TOF, the resulting lift spectrum showed the following de novo sequence 'VIPESGGNLAALAIQR' when analyzed using Biotools software (Figs. 7.9C and D). Further, the various ions generated during MALDI-TOF-TOF studies showed 60% identity with the amino acid sequence of Carboxylic ester hydrolase (Uniprot Acc No. D5KX86). Also, the de novo sequence obtained from PMF peak with m/z 1607 showed over-lapping with one of the internal amino acid sequence recognised for Carboxylic ester hydrolase during MS/MS ion search (Fig. 7.9E). Furthermore, clustal alignment of this de novo sequence with available sequences in the NCBI database showed significant (100%) matching with the Carboxylic ester hydrolase of *H. armigera* (Fig. 7.9F). These results confirm that Carboxylic ester hydrolase is up-regulated by 4.6-fold in H. armigera larvae upon feeding on a diet supplemented with T9BBI (Figs. 7.5, 7.6 and 7.9, **Table 2**).

Esterases belong to a group of hydrolase enzymes which can hydrolyse the ester bond present in the compounds. Esterases react with the water and split the esters into alcohol and an acid. Carboxyl esterases are sub-group of esterases, involved in the conversion of a carboxylic ester to carboxylate and alcohol. They are known to provide insect resistance against carbamates, organophosphates and pyrethroids by overexpression or mutation in coding sequence or conjugation of these processes (Li et al., 2007). Previous reports



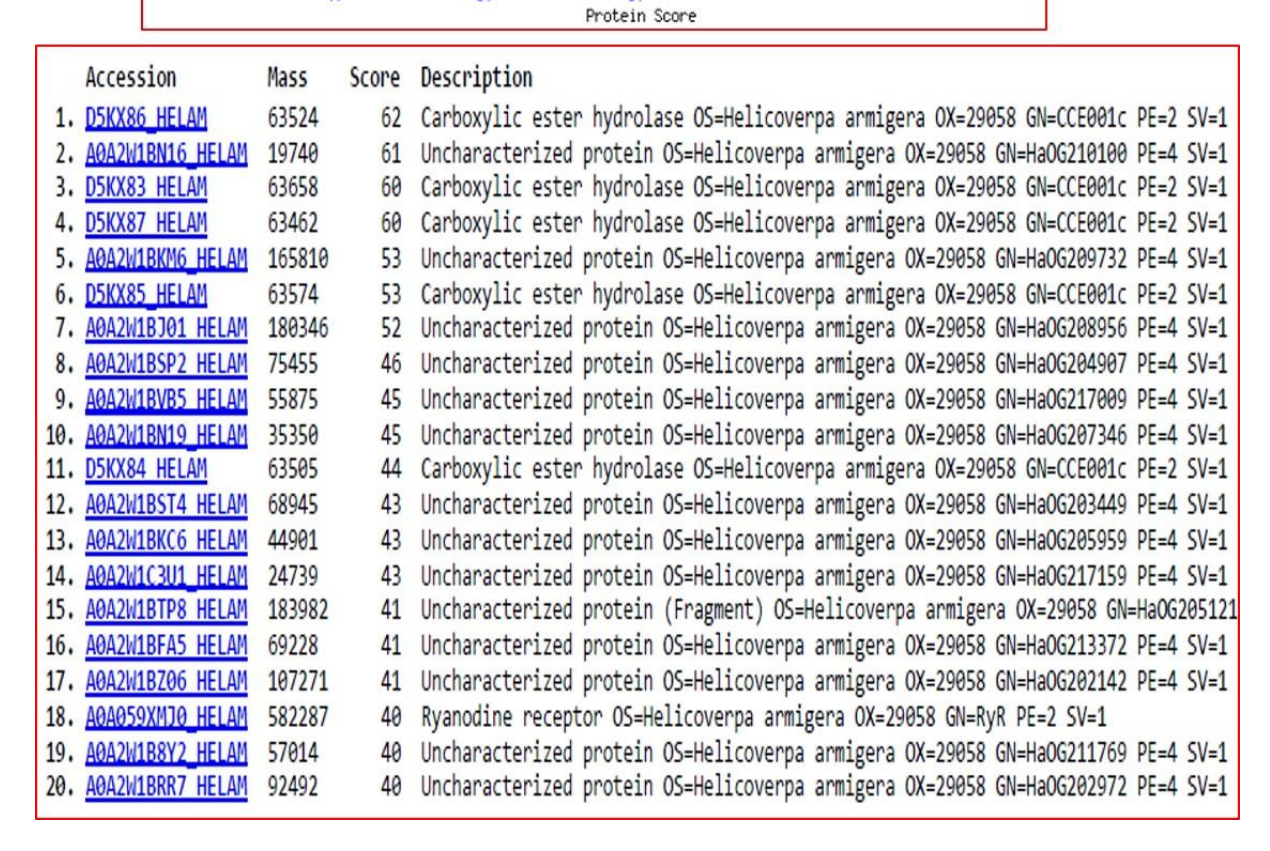


Fig. 7.9. Identification of spot 5 as Carboxylic ester hydrolase after tryptic digestion and MALDI-TOF-TOF analysis. (A) Histogram of MASCOT search results and corresponding protein hits.

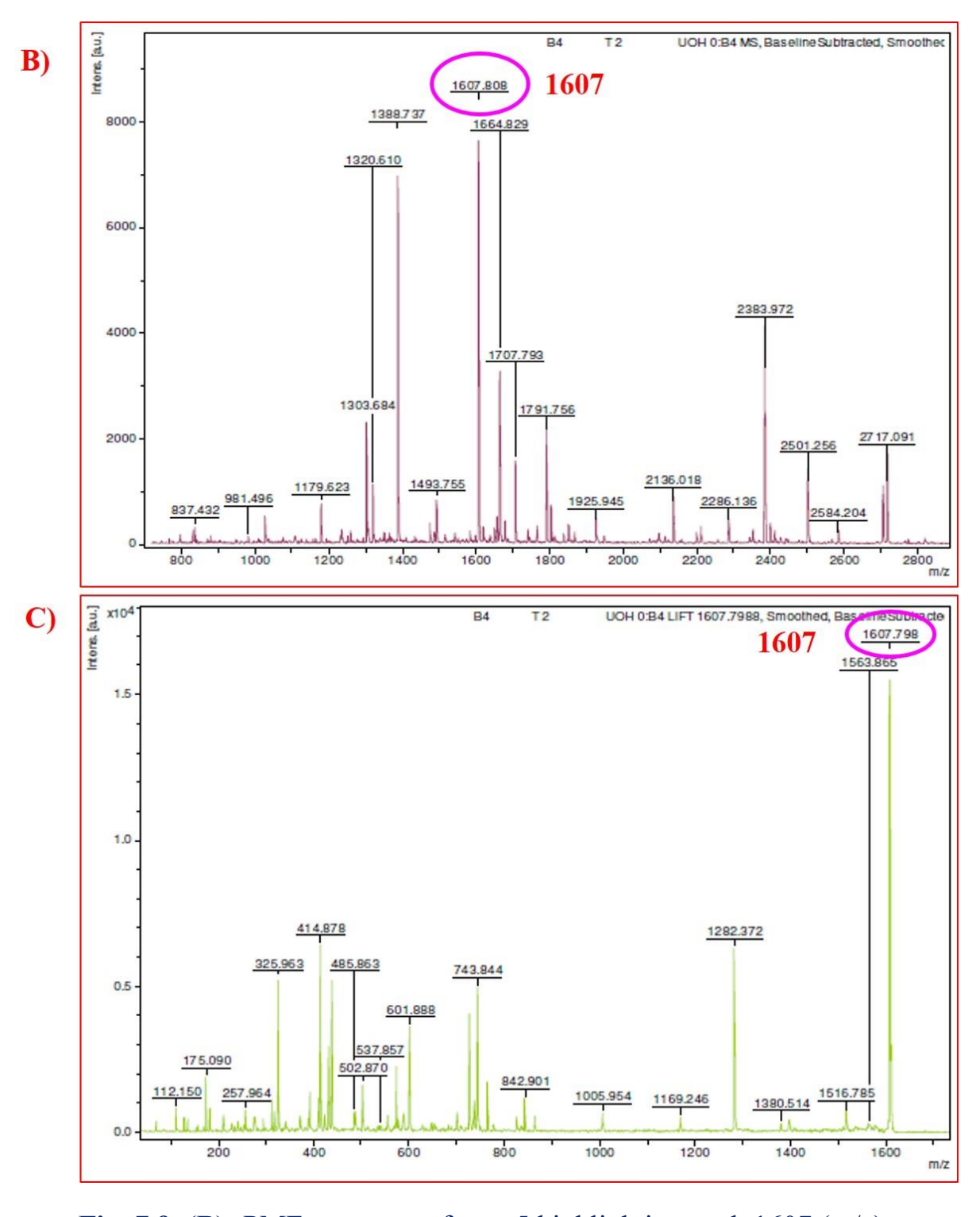


Fig. 7.9. (B): PMF spectrum of spot 5 highlighting peak 1607 (m/z); (C) Lift spectrum of PMF peak with m/z 1607

D)

alculate (VIPESGGNI	LAALAIQ	R	Peak: 1607				
N-Term.	Ion	а	b	1	a-17	b-17	у	C-Term.	lor	
1	V	72.081	100.076	72.081	55.054	83.049	175.119	16	R	
2	1	185.165	213.160	86.096	168.138	196.133	303.178	15	Q	
3	P	282.218	310.213	70.065	265.191	293.186	416.262	14	- 1	
4	E	411.260	439.255	102.055	394.234	422.229	487.299	13	Α	
5	S	498.292	526.287	60.044	481.266	509.261	600.383	12	L	
6	G	555.314	583.309	30.034	538.287	566.282	671.420	11	Α	
7	G	612.335	640.330	30.034	595.309	623.304	742.457	10	Α	
8	N	726.378	754.373	87.055	709.352	737.346	855.541	9	L	
9	L	839.462	867.457	86.096	822.436	850.431	969.584	8	N	
10	A	910.499	938.494	44.049	893.473	921.468	1026.605	7	G	
11	A	981.536	1009.531	44.049	964.510	992.505	1083.627	6	G	
12	L	1094.620	1122.615	86.096	1077.594	1105.589	1170.659	5	S	
13	A	1165.658	1193.652	44.049	1148.631	1176.626	1299.702	4	E	
14		1278.742	1306.737	86.096	1261.715	1289.710	1396.754	3	P	
15	Q	1406.800	1434.795	101.071	1389.774	1417.769	1509.838	2	1	
16	R	1582,901	1590.896	129,113	1545.875	1573.870	1608.907	1	V	

E)

Sequence coverage: 60%:

MTKWWTCVVFMCAAVLADDEWREVRTAQGPVRGRKRPTEDIYTFYNIPYATAPT
GKDKFKAPLPPPVWSETFDAVDEFVICPQAKSPWDMLMPKNRVVKENCLIANVYV
PNTKEKNLSVLVIVHGGAFLMGSGEQLKGTKFMNTKDFIIVTFNYRLGIHGFLCLG
TEDAPGNAGMKDQVALLRWVQKNIASFGGNPDDVTIDGYSAGSVSVDLLMLSKS
AEGLFQVIPESGGNLAALAIQRDPVEIAKTHARKLNFTNVDDIYALEDFYRKAPLE
LLLTPDDLFDRTDSIFKFSPCVERDTGDGAFLTESPLTILKSGNYRKVPLLYGFANME
GLLRIGFFDIWKHKMNEKFSDFLPPDLKFDSDEEREEVANKIKKFYFGDKPVDNDN
ILKYVDSFSDVIFAYPMLRAVKLHAEAGNDQVYLYEYSFVDEDIPLVPHTNVRGAD
HCAQSMALFDGKNLTQSDESQATPEYQ NMMKIIRETWHNFLKTGTPVPEGSWLPA
WPAAGADRAPHMSLGERLELRGALLAERTRFWDDIYQRYYRDAVPPPKPPPRRN
EL

Fig. 7.9. (D): Analysis of Lift spectrum from peak m/z 1607 using Biotools; **(E)** Carboxylic ester hydrolase (D5KX86_HELAM/Uniprot Acc. D5KX86) sequence. Red colour indicates the partial sequence coverage by various ions generated from spot 5 while blue box indicate the matching of *de novo* (m/z 1607) sequence obtained from Biotools with one of the peptides identified by Mascot search engine.

Accession number	Protein name/ Source	Sequence	Similarity (%)
Spot number 5	(de novo sequence from PMF peak with m/z 1607)	VIPESGGNLAALAIQR	100
ADD97155.1	Carboxyl esterase / Helicoverpa armigera	VIPESGGNLAALAIQR *******	100

Fig. 7.9. F): Clustal alignment of *de novo* sequence from PMF peak (m/z 1607) with Carboxylic ester hydrolase, identified in NCBI database.

indicated that overproduction of esterase isozymes resulted in the development of resistance against pyrethroid insecticides in *H. armigera* (Gunning et al., 1999; Konus et al., 2014).

Corroborating with these studies, the up-regulation of carboxylic ester hydrolase by 4.6-fold in the present study suggests its role to detoxify the bio-insecticide T9BBI.

7.4.5. Identification of Spot 6 as Glutathione S-transferase GSTS4:

Tryptic digestion of spot 6 followed by MALDI-TOF-TOF analysis showed matching to a Glutathione S-transferase GSTS4 from *H. armigera* with a significant score of 150 in the Mascot score histogram (Fig. 7.10A). The mass spectrum corresponding to the PMF data was represented in Figure 7.10B. When the PMF peaks with m/z 1170 (lift spectrum is shown) and m/z 3109 (lift spectrum not shown) were further ionized in MALDI-TOF-TOF, the following *de novo* sequences 'QYAQSYAIAR' and 'LLLSYGGQEFEDHRVSQDDWQSFKPK' were derived when the lift spectra are analyzed using Biotools software (Figs. 7.10C and D). The various ions generated during MALDI-TOF-TOF studies showed partial sequence coverage up to 75% with Glutathione S-transferase GSTS4 (Uniprot Acc No. A0A0D3M5T8).

Further, the two *de novo* sequences obtained through Biotools showed overlapping with the partial amino acid sequences recognised for Glutathione S-transferase GSTS4 during MALDI-TOF-TOF analysis (Fig. 7.10E). Furthermore, Clustal alignment of the *de novo* sequence 'QYAQSYAIAR' with available sequences in the NCBI database showed 100% matching to a Glutathione S-transferase from different insects such as *H. armigera*, *Choristoneura fumiferana* and *Platynota idaeusalis*, respectively (Fig. 7.10F). The other *de novo* sequence 'LLLSYGGQEFEDHRVSQDDWQSFKPK' also showed 100% similarity with the Glutathione S-transferase GSTS4 (Clustal alignment data not shown). These results confirm that Glutathione S-transferase GSTS4 is up-regulated by 5.3-fold in the midgut

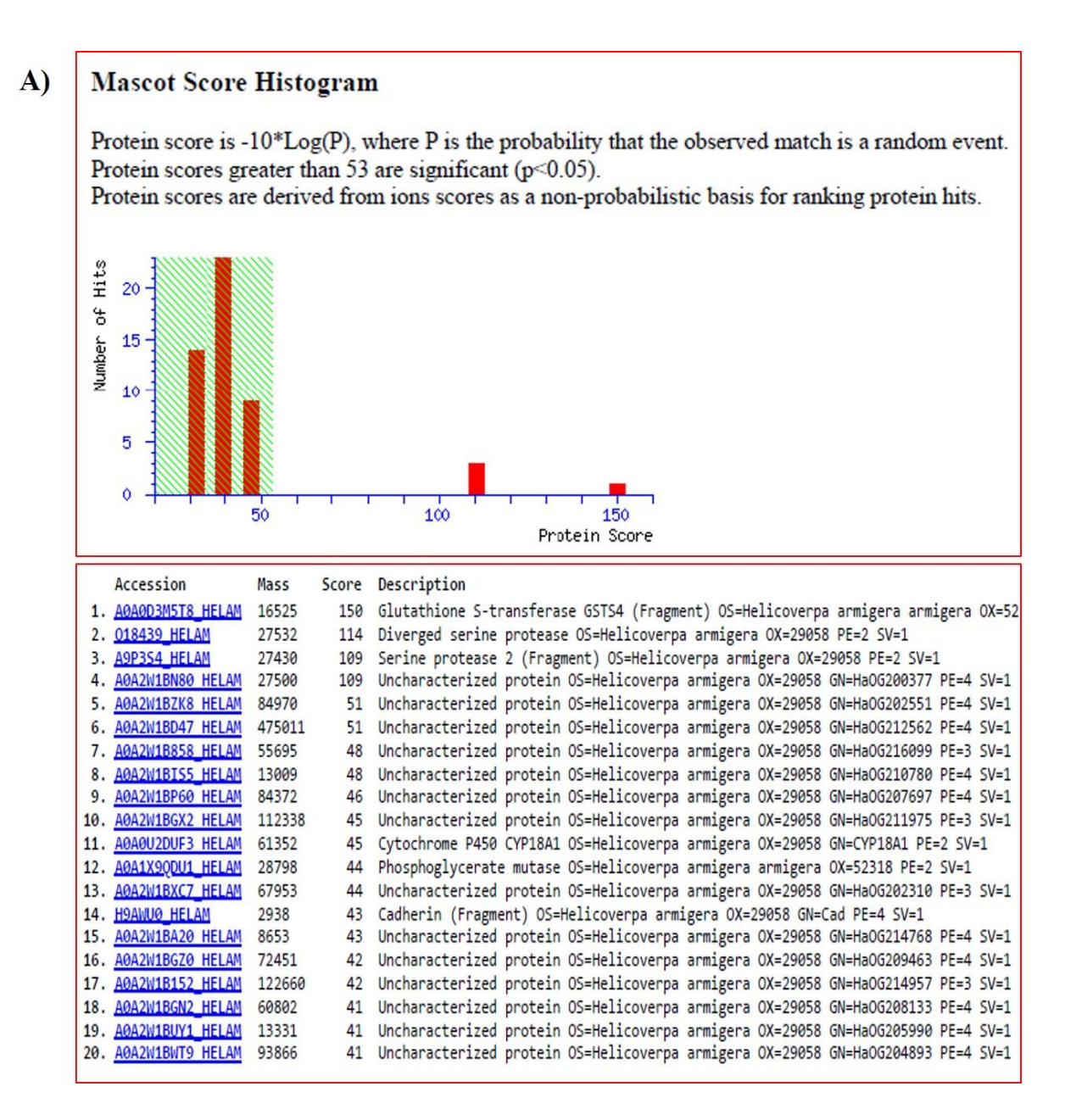


Fig. 7.10. Identification of spot 6 as Glutathione S-transferase GST4 after tryptic digestion and MALDI-TOF-TOF analysis. (A) Histogram of MASCOT search results and corresponding protein hits.

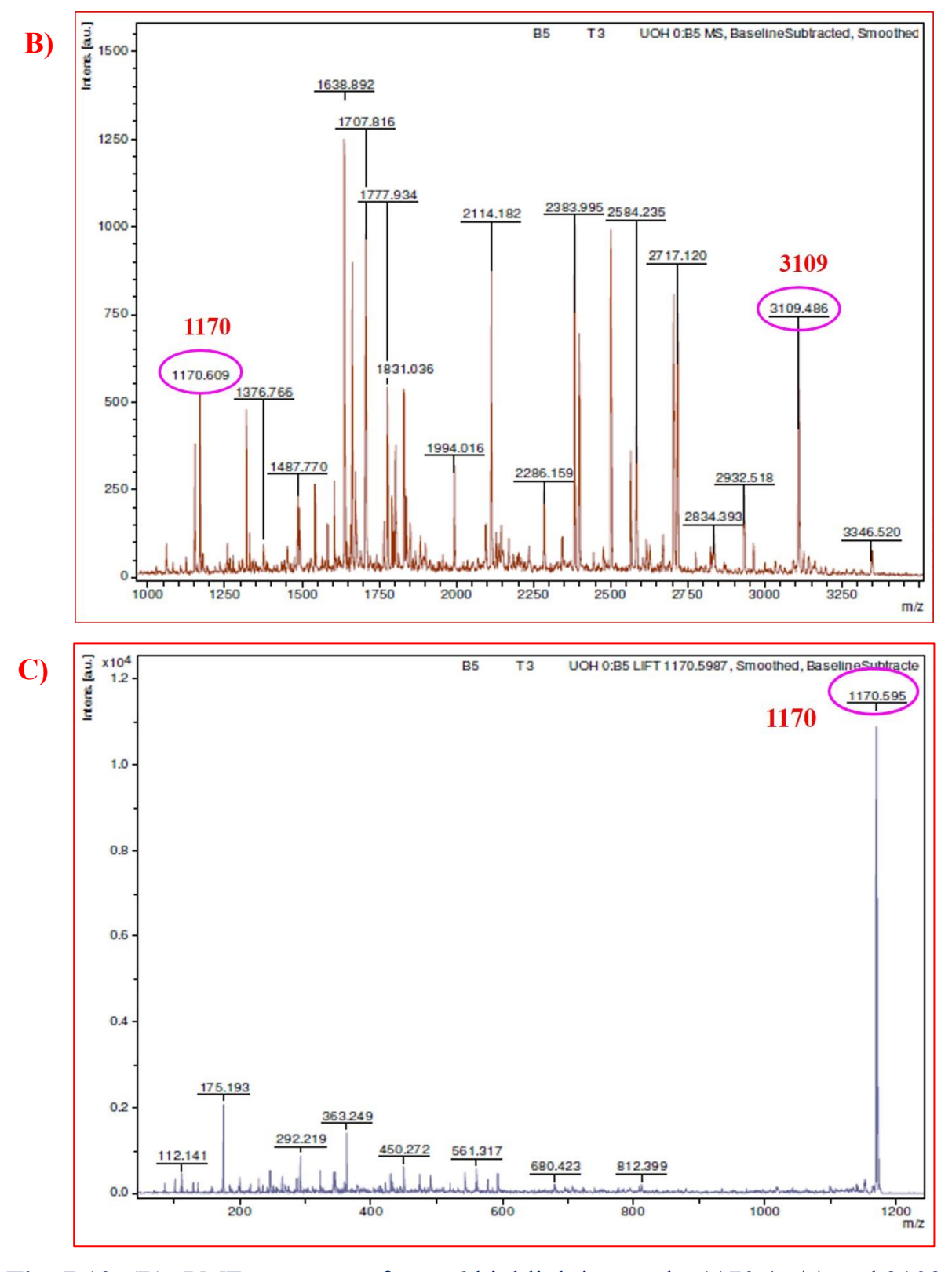


Fig. 7.10. (B): PMF spectrum of spot 6 highlighting peaks 1170 (m/z) and 3109 (m/z); **(C)** Lift spectrum of PMF peak with m/z 1170

Calculated Masses: QYAQSYAIAR			QYAQSYA	IAR	Peak: 1170						
N-Term.	Ion	а	b	I	a-17	b-17	у	C-Term.	lon		
1	Q	101.071	129.066	101.071	84.044	112.039	175.119	10	B		
2	Y	264.134	292.129	136.076	247.108	275.103	246.156	9	Α		
3	Α	335.171	363.166	44.049	318.145	346.140	359.240	8	-		
4	Q	463.230	491.225	101.071	446.203	474.198	430.277	7	A		
5	S	550.262	578.257	60.044	533.235	561.230	593.341	6	Y		
6	Y	713.325	741.320	136.076	696.299	724.294	680.373	5	S		
7	Α	784.362	812.357	44.049	767.336	795.331	808.431	4	C		
8	1	897.446	925.441	86.096	880.420	908.415	879.468	3	Α		
9	Α	968.484	996.479	44.049	951.457	979.452	1042.532	2	Y		
10	R	1124.585	1152,580	129.113	1107.558	1135.553	1170.590	1	C		

N-Term.	Ion	8	b	-	a-17	b-17	٧	C-Term.	lon
1	L	86.096	114.091	86.096	69.070	97.065	147.113	26	K
2	L	199.180	227.175	86.096	182.154	210.149	244.166	25	Р
3	L	312.265	340.259	86.096	295.238	323.233	372.261	24	K
4	S	399.297	427.291	60.044	382.270	410.265	519,329	23	F
5	Y	562,360	590.355	136.076	545.333	573.328	606.361	22	S
6	G	619.381	647.376	30.034	602.355	630.350	734.420	21	C
7	G	676.403	704.398	30.034	659.376	687.371	920,499	20	W
8	Q	804.461	832.456	101.071	787.435	815.430	1035,526	19	
9	E	933,504	961,499	102.055	916,477	944,472	1150.553	18	
10	F	1080.572	1108.567	120.081	1063.546	1091.541	1278.611	17	C
11	E	1209,615	1237.610	102.055	1192.588	1220.583	1365,643	16	S
12	D	1324.642	1352.637	88.039	1307.615	1335.610	1464.712	15	٧
13	Н	1461.701	1489.696	110.071	1444.674	1472.669	1620.813	14	H
14	R	1617.802	1645.797	129.113	1600.775	1628.770	1757.872	13	Н
15	V	1716.870	1744.865	72.081	1699.844	1727.839	1872.899	12	
16	S	1803.902	1831.897	60.044	1786.876	1814.871	2001.941	11	E
17	Q	1931.961	1969.956	101.071	1914.934	1942.929	2149.010	10	F
18	D	2046.988	2074.983	88.039	2029.961	2057.956	2278.052	9	E
19	D	2162.015	2190.010	88.039	2144.988	2172.983	2406.111	8	C
20	W	2348.094	2376.089	159.092	2331.068	2359.063	2463,132	7	G
21	Q	2476.153	2504.148	101.071	2459.126	2487.121	2520.154	6	G
22	S	2563.185	2591.180	60.044	2546.158	2574.153	2683.217	5	Y
23	F	2710.253	2738.248	120.081	2693.227	2721.222	2770.249	4	S
24	K	2838.348	2866.343	101.107	2821.322	2849.317	2883.333	3	L
25	Р	2935.401	2963,396	70.065	2918.374	2946.369	2996,417	2	
26	K	3063,496	3091.491	101.107	3046,469	3074,464	3109.501	1	1

E) Sequence coverage: 75%

MPKVVFYYFPVKALGEASR LSYGGQEFEDHRVSQDDWQSFKPK TPFGQMPV LVIDGKQYAQSYAIARYLGRKYGLVGETLEDSLEIDQNVDLIDDLRAKAALVD YEPDEAVKEKKYAEYVKTVFPDGKLNAIIVKNNGHVAL

Fig. 7.10. (D): Analysis of Lift spectrum from peak m/z 1170 & 3109 using Biotools; **(E)** Glutathione S-transferase GST4 (A0A0D3M5T8_HELAM/Uniprot Acc. A0A0D3M5T8) sequence. Red colour indicates the partial sequence coverage by various ions generated from spot 6 while blue box indicate the matching of *de novo* (m/z 1170 & 3109) sequences obtained from Biotools with peptides identified by Mascot search engine.

Accession number	Protein name/ Source	Sequence	Similarity (%)
Spot number 6 (de n	novo sequence from PMF peak with m/z 1170)	QYAQSYAIAR	100
XP_021186024.1	Glutathione S-transferase 2-like/ Helicoverpa armigera	QYAQSYAIAR	100
ACK75952.1	Glutathione S-transferase 4/ Choristoneura fumiferana	QYAQSYAIAR	100
AAC34097.1	Glutathione transferase/ Platynota idaeusalis	QYAQSYAIAR *****	100

Fig. 7.10. F): Clustal alignment of *de novo* sequence from PMF peak (m/z 1170) with Glutathione S-transferase GST4, identified in NCBI database.

tissues of the *H. armigera* larvae when fed upon a diet containing T9BBI (**Figs. 7.5, 7.6 and 7.10, Table-2**).

Insects use many enzymes for the detoxification of xenobiotic compounds such as glutathione S-transferase (GST), esterases and cytochrome oxidases and thioredoxins. They degrade the chemicals before they reach their molecular target sites (Bogwitz et al., 2005). GST enzymes catalyse the conjugation of reduced (sulfur substituted) glutathione to electrophilic centres on a broad range of substrates through a sulfhydryl group (Douglas, 1987). GST catalytic reactions transform xenobiotics (carcinogens, herbicides, insecticides and therapeutic drugs) to more water-soluble compounds for further metabolism and excretion (Allocati et al., 2009). GST levels have increased in *H. armigera* after microbial infection (Bilal et al., 2018). High GST activity was detected in some resistant insect strains (Ottea and Plapp, 1984). The present study corroborates with these studies in up-regulating the GSTS4 in the presence of T9BBI possibly to eliminate it from the larval body.

7.4.6. Identification of Spot 7 as Cytochrome-P450 (Cyt-P450):

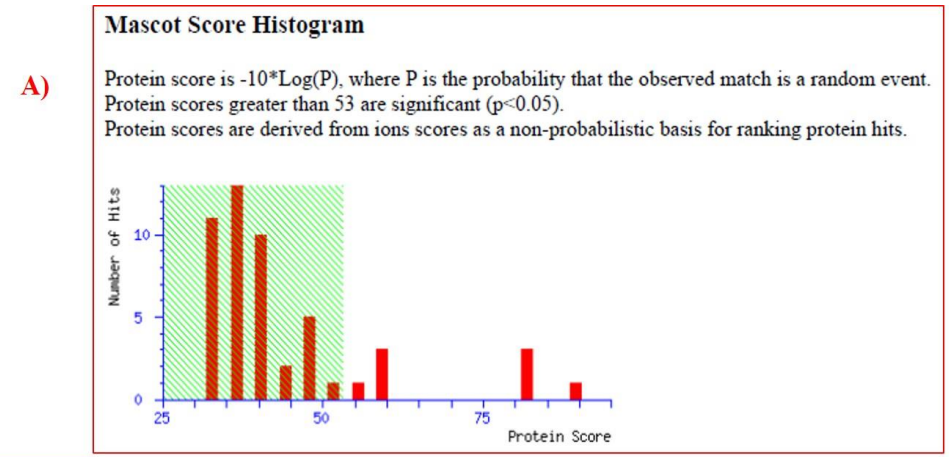
Tryptic digestion of spot 7 followed by MALDI-TOF-TOF analysis showed matching to a Cyt-P450 from *H. armigera* with 89 score in the Mascot score histogram (**Fig. 7.11A**). The mass spectrum corresponding to the PMF data was represented in **Figure 7.11B**. When the PMF peaks with m/z 2182 (lift spectrum shown) and m/z 2383 (lift spectrum not shown) were further ionized in MALDI-TOF-TOF, the following *de novo* sequences 'KNIGIVMEEIYNQFPDEK' and 'NDFMDLILELRQMGEVTSNK' were derived when the lift spectra are analyzed using Biotools software (**Figs. 7.11C and D**). The various ions generated during MALDI-TOF-TOF studies showed partial sequence coverage up to 43% with Cytochrome P450 (Uniprot Acc No. Q6PY59).

Further, the two *de novo* sequences obtained through Biotools showed overlapping with the partial amino acid sequences recognised for Cyt-P450 during MALDI-TOF-TOF

analysis (**Fig. 7.11E**). Furthermore, Clustal alignment of the *de novo* sequence '**KNIGIVMEEIYNQFPDEK**' with available sequences in the NCBI database showed 100% matching to a Cyt-P450 from different insects such as *H. armigera* and *H. zea* (**Fig. 7.11F**). The *de novo* sequence '**NDFMDLILELRQMGEVTSNK**' also showed 100% similarity with the Cyt-P450 (Clustal alignment data not shown). These results confirm that Cyt-P450 is up-regulated by 3.7-fold in the midgut tissues of the *H. armigera* larvae when fed upon a diet containing T9BBI (**Figs. 7.5, 7.6 and 7.11, Table-2**).

Resistance to synthetic and natural toxins in insects has evolved in many ways and multiple levels. These biochemical adaptations are mainly of two types 1) Target site resistance (involves protein level variations), 2) Catabolic resistance (Involves gene, transcript, protein level). The enzymes which are involved in toxin catabolism are Cyt-P450, Glutathione S-transferase (GST) and Esterases (Schuler et al., 2012). Consumption of allelochemicals increased the activities of GSTs, carboxylesterase and Cyt-P450 in the midgut and fat body of *H. armigera* (Chen et al., 2019). Most Cyt-P450 enzymes have been involved in the oxidation of organic substances to perform many essential tasks ranging from the synthesis to degradation of natural or synthetic xeno-biotic substances and formation of lipid metabolic intermediates (Feyereisen, 1999). It is well known that many instances of insecticide metabolic resistance resulted from elevated concentrations of Cyt-P450 (Agosin, 1985). In the RNA interference (RNAi) studies of Cyt-P450 transcripts in H. armigera impaired the tolerance to gossypol and reduce the larval growth (Mao et al., 2011). Cantharidin bio insecticide also overexpressed the Cyt-P450 in H. armigera (Rashid et al., 2013). Corroborating with these studies, feeding of the bioinsecticide T9BBI elevated the levels of Cyt-P450 in the midgut tissues of *H. armigera* larvae.

In the present study, the resistance against the bioinsecticide T9BBI might be due to the upregulation of the Cyt-P450



	Accession	Mass	Score	Description
1.	Q6PY59 HELAM	58504	89	Cytochrome P450 OS=Helicoverpa armigera OX=29058 PE=3 SV=1
2.	D7R771 HELAM	58454	82	Cytochrome P450 OS=Helicoverpa armigera OX=29058 GN=CYP6B7 PE=3 SV=1
3.	A0A0K0YD48 HELAM	58564	81	Cytochrome P450 monooxygenase CYP6B7 OS=Helicoverpa armigera OX=29058 GN=CYP6B7 PE=2 SV=1
4.	Q6J663_HELAM	58488	81	Cytochrome P450 CYP6B7 OS=Helicoverpa armigera OX=29058 GN=CYP6B7 PE=2 SV=1
5.	A0A2W1BRI6 HELAM	124048	61	Uncharacterized protein OS=Helicoverpa armigera OX=29058 GN=HaOG203092 PE=3 SV=1
6.	A0A2W1BD47 HELAM	475011	59	Uncharacterized protein OS=Helicoverpa armigera OX=29058 GN=HaOG212562 PE=4 SV=1
7.	CP6B7 HELAM	58580	57	Cytochrome P450 6B7 OS=Helicoverpa armigera OX=29058 GN=CYP6B7 PE=2 SV=1
8.	I3PL64 HELAM	23819	56	Small GTPase Rab4b OS=Helicoverpa armigera OX=29058 PE=2 SV=1
9.	A0A2W1BXU0 HELAM	13130	50	Uncharacterized protein OS-Helicoverpa armigera OX=29058 GN=HaOG203138 PE=4 SV=1
10.	A0A2W1BHW2 HELAM	89483	49	Uncharacterized protein OS=Helicoverpa armigera OX=29058 GN=HaOG208738 PE=4 SV=1
11.	A0A2W1BS21 HELAM	256218	48	DNA polymerase epsilon catalytic subunit OS=Helicoverpa armigera OX=29058 GN=HaOG202959 PE=3 SV=1
12.	A0A2W1BFG4 HELAM	32109	47	Uncharacterized protein OS=Helicoverpa armigera OX=29058 GN=HaOG212227 PE=4 SV=1
13.	A0A2W1BFW3 HELAM	128016	47	Uncharacterized protein OS-Helicoverpa armigera OX=29058 GN=HaOG208488 PE=4 SV=1
14.	A0A2W1BGK3_HELAM	90175	46	Uncharacterized protein OS=Helicoverpa armigera OX=29058 GN=HaOG212243 PE=4 SV=1
15.	M1RNR1 HELAM	89463	44	Very-high-density lipoprotein receptor OS=Helicoverpa armigera OX=29058 GN=VHDL-R PE=2 SV=1
16.	A0A2W1BZA1 HELAM	181842	43	Uncharacterized protein OS=Helicoverpa armigera OX=29058 GN=HaOG203687 PE=4 SV=1
17.	A0A2R4RM56 HELAM	89899	42	E3 ubiquitin-protein ligase OS=Helicoverpa armigera OX=29058 PE=2 SV=1
18.	A0A2W1C1Q6_HELAM	20137	42	Uncharacterized protein OS=Helicoverpa armigera OX=29058 GN=HaOG217090 PE=4 SV=1
19.	A0A2W1BGZ7_HELAM	623284	42	Uncharacterized protein OS=Helicoverpa armigera OX=29058 GN=HaOG210326 PE=4 SV=1
20.	A0A2W1BN97_HELAM	252598	41	Histone acetyltransferase OS=Helicoverpa armigera OX=29058 GN=HaOG208190 PE=3 SV=1

Fig. 7.11. Identification of spot 7 as Cytochrome P450 after tryptic digestion and MALDI-TOF-TOF analysis. (A) Histogram of MASCOT search results and corresponding protein hits.

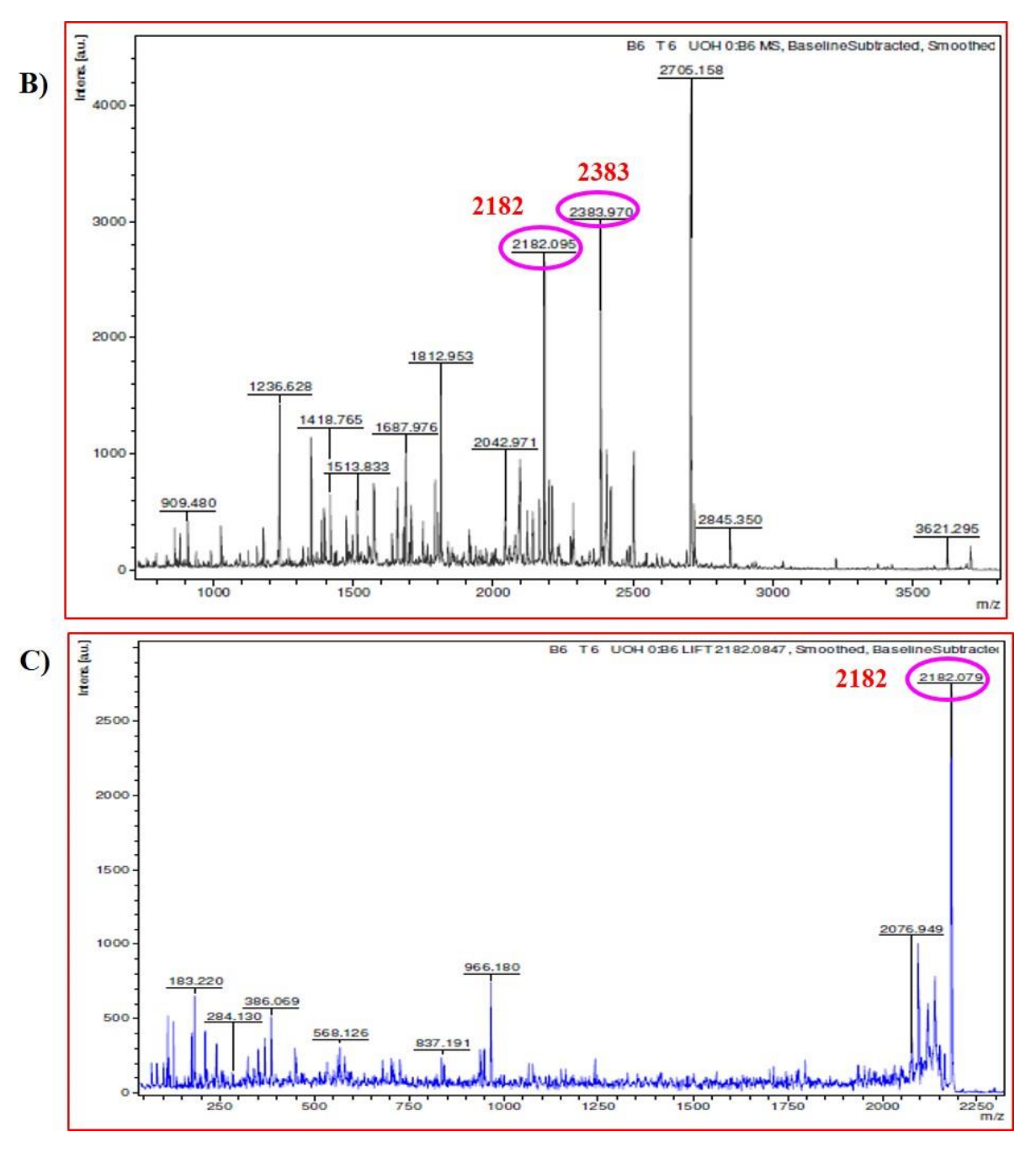


Fig. 7.11. (B): PMF spectrum of spot 7 highlighting peaks 2182 (m/z) and 2383 (m/z); **(C)** Lift spectrum of PMF peak with m/z 2182

D)

Calculated Masses: KNIGIVMEEIYNQFPDEK 7: Oxidation (M)				KNIGIVMEEIYNQFPDEK				Peak: 2182		
N-Term.	Ion	a	b	1	a-17	b-17	V	C-Term.	lo	
1	K	101.107	129.102	101.107	84.081	112.076	147.113	18	K	
2	N	215.150	243.145	87.055	198.124	226.119	276.155	17	E	
3	1	328.234	356.229	86.096	311.208	339.203	391.182	16	1	
4	G	385.256	413.251	30.034	368.229	396.224	488.235	15	-	
5	1	498.340	526.335	86.096	481.313	509.308	635.304	14	-	
6	V	597.408	625.403	72.081	580.382	608.377	763.362	13	(
7	M*	744.444	772.439	120.048	727.417	755.412	877.405	12		
8	E	873.486	901.481	102.055	856.460	884.455	1040.468	11	7	
9	E	1002.529	1030.524	102.055	985.502	1013.497	1153.552	10	П	
10		1115.613	1143.608	86.096	1098.586	1126.581	1282.595	9		
11	Y	1278.676	1306.671	136.076	1261.650	1289.645	1411.638	8		
12	N	1392.719	1420.714	87.055	1375.693	1403.688	1558,673	7	ħ	
13	Q	1520.778	1548.773	101.071	1503.751	1531.746	1657.741	6	١	
14	F	1667.846	1695.841	120.081	1650.820	1678.815	1770.825	5		
15	Р	1764.899	1792.894	70.065	1747.872	1775.867	1827.847	4	(
16	D	1879.926	1907.921	88.039	1862.899	1890.894	1940.931	3		
17	E	2008.968	2036.963	102.055	1991.942	2019.937	2054.974	2	1	
18	K	2137.063	2165.058	101,107	2120.037	2148.032	2183.069	1	ŀ	

Calculated Masses: NDFMDLILELROMGEVTSNK 4: Ox				DLILELE 3. Oxidation (N	Peak: 2383				
N-Term.	Ion	a	b	1	a-17	b-17	V	C-Term.	lor
1	N	97.055	115.050	87.055	70.029	98.024	147.113	20	K
2	D	202.082	230.077	88.039	185.056	213.051	261.156	19	N
3	F	349.151	377.146	120.081	332.124	360.119	348.188	18	S
4	M*	496.186	524.181	120.048	479.159	507.154	449.235	17	Т
5	D	611.213	639.208	88.039	594.186	622,181	548.304	16	٧
6	L	724.297	752.292	86.096	707.271	735.265	677.346	15	E
7	1	837.381	865.376	86.096	820.355	848.349	734.368	14	G
8	L	950.465	978.460	86.096	933,439	961.434	881.403	13	M'
9	E	1079.508	1107.503	102.055	1062.481	1090.476	1009.462	12	Q
10	L	1192.592	1220.587	86.096	1175.565	1203.560	1165,563	11	R
11	R	1348.693	1376.688	129,113	1331.666	1359.661	1278.647	10	L
12	Q	1476.752	1504.746	101.071	1459.725	1487.720	1407.690	9	Ε
13	M*	1623.787	1651.782	120.048	1606.760	1634.755	1520.774	8	L
14	G	1680.808	1708.803	30.034	1663.782	1691.777	1633.858	7	1
15	E	1809.851	1837.846	102.055	1792.824	1820.819	1746.942	6	L
16	ν	1908.919	1936.914	72.081	1891.893	1919.888	1861.969	5	D
17	T	2009.967	2037.962	74.060	1992.941	2020.935	2009.004	4	M'
18	S	2096.999	2124.994	60.044	2079.973	2107.967	2156.073	3	F
19	N	2211.042	2239.037	87.055	2194.015	2222.010	2271.100	2	D
20	K	2339.137	2367.132	101,107	2322,110	2350.105	2385.142	1	N

E)

Sequence coverage: 43%

MWVLYLPAVLSVLIVTLYLYFTRTFNYWKKRNVRGPEPTVFFGNLKDSTLRKKNIGIVMEEIYNQFPDEK

VVGMYRMTTPCLLVRDLDVIKHIMIKDFEAFRDRGVEFSKEGLGQNLFHADGETWRALRNRFTPIFTSG

KLKNMFYLMHEGADNFIDHVSKECEKKQEFEVHSLLQTYTMSTISSCAFGVSYNSISDKVQTLEIVDKIIS

EPSYAIELDYMYPKLLAKLNLSIIPTPVQHFFKSLVDSIISQRNGKPAGRNDFMDLILELRQMGEVTSNKY

LDGVTSLEITDEVICAQAFVFYVAGYETSATTMSYFTLFFCS

Fig. 7.11. (D): Analysis of Lift spectrum from peaks m/z 2182 & 2383 using Biotools; **(E)** Cytochrome P450 (Q6PY59_HELAM/ Uniprot Acc.Q6PY59) sequence. Red colour indicates the partial sequence coverage by various ions generated from spot 7 while blue box indicate the matching of *de novo* (m/z 2182 & 2383) sequences obtained from Biotools with peptides identified by Mascot search engine.

Accession number	Protein name/ Source	Sequence	Similarity (%)
Spot number 7	(de novo sequence from PMF peak with m/z 2182)	KNIGIVMEEIYNQFPDEK	100
AAT01211.1	Cytochrome-P450 / Helicoverpa armigera	KNIGIVMEEIYNQFPDEK	100
AAL89656.1	Cytochrome-P450 monooxygenase / Helicoverpa zea	KNIGIVMEEIYNQFPDEK **********	100

Fig. 7.11. (F): Clustal alignment of *de novo* sequence from PMF peak (m/z 2182) with Cytochrome-P450 in NCBI database.

Taken together with the results in the present study and literature, we suggest that inspite of up-regulation in the various enzymes such as Tpx, carboxylic ester hydrolase, GSHS4 and Cyt-P450 related to antioxidant and xenobiotic activities, a remarkable effect of T9BBI on the growth and development of the *Helicoverpa* larvae was observed. Further, a significant effect of the T9BBI on the larval growth at early instar (3rd and 4th) stages and development of delay in pupal formation suggest that it can be applied as a biopesticide.

Highlights of the Study:

- 1. T9BBI possessed moderate inhibitory potential against trypsin like gut proteases of host pest *H. armigera*.
- 2. Ingestion of T9BBI at higher concentration (0.1%) retarded the larval growth of *H. armigera* up to 65% at early instar (3rd and 4th) stages and 45% at late instar stages (5th and 6th), respectively.
- 3. T9BBI altered the midgut proteome of *H. armigera* significantly as evidenced by 2-D gel electrophoresis.
- 4. Proteins which showed altered expression pattern are involved in the functions associated with immune system (Hdd23 like protein) and detoxification (GST, Tpx, Carboxyl ester hydrolase and Cyt- P450).

Chapter 8

Cloning of *T9BBI1* from the seeds of *V. mungo* (*cv.*T9) and its expression in *E.coli* shuffle cells using pET-32a vector

Chapter 8

Cloning of *T9BBI1* from the seeds of *V. mungo* (*cv.*T9) and its expression in *E.coli* shuffle cells using pET-32a vector

Constitutive expression of PI(s) helps the plants to overcome the insect pests and pathogens. However, in recent years transgenic plants are generated with specific PI genes using recombinant DNA technology to reduce the attack of insect pests (Srinivasan et al., 2009). But to generate a transgenic plant which is resistant to insect pests, it is necessary to have prior information on PI(s). Such as (i) The family to which PI belongs and (ii) its potential insecticidal activity under both in vitro and in vivo conditions. Identification of PIs from legume seeds and their expression using recombinant DNA technology is well reported in the literature. For instance, BBI from Rhynchosia sublobata seeds both in native and recombinant forms showed significant inhibitory activity against A. janata midgut proteases (Mohanraj et al., 2018, 2019). PIs isolated from *Capsicum annum* inhibited the larval growth of Chilo partellus (Jadhav et al., 2016). Also, two recombinant PIs purified from Bauhinia bauhinioides exhibited inhibitory activity against Nasutitermes corniger gut enzymes (Ferreira et al., 2019). Similarly, as we observed the significant insecticidal potential for T9BBI against the three lepidopteran insects, A. janata, S. litura and H. armigera in the earlier chapters (5-7), it was intended to clone, express and purify the recombinant T9BBI (rT9BBI) to evaluate its function using a bacterial system.

8.1. Cloning of *T9BBI1* from mature seeds of *V. mungo* T9 variety

The total RNA isolated from the mature seeds of V. mungo was quantified by using Nanodrop spectrophotometer. The obtained $A_{260/280}$ ratio of 2.09 indicated the purity of RNA, which was further converted into complementary DNA by using Verso cDNA synthesis kit (Thermo Fisher Scientific). The oligonucleotide primers were designed based on the

sequence of protease inhibitor from *Vigna radiata* (NCBI Accession no. AY713305.2) mentioned in **Figure 8. 1A**. The PCR amplification of T9BBI gene (cDNA template) was carried out by using the *V. radiata* PI specific primers (FP- 5' ATG ATG GTG CTA AAG GTG TGT G 3' and RP- 5' GGT TTG TAA CAG AAA TCA TCA GTG TCA AGG C 3'). The thermal cycling conditions are used as follows: initial denaturation at 98°C for 30 sec followed by 35 cycles of amplification consisting of denaturation (98°C for 30 sec), annealing (54°C for 15 sec) and extension (72°C for 15 sec) followed by a final extension of 10 min at 72°C. The amplified gene product was visualized on 1% agarose gel (**Fig. 8. 1B**) and purified using the Qiagen gel extraction kit.

The purified PCR product was subjected to 3' adenylation by incubating for 30 min in the presence of Taq DNA polymerase and ATPs. The mixture containing the adenylated gene of interest and pTZ57R/T vector was subjected to ligation and transformed into *E.coli* DH5α cells. The positive colonies were identified by using the method of Blue-white screening and the colonies were confirmed by colony PCR and the recombinant plasmid was used for clone confirmation by restriction digestion using EcoRI and PstI (Figs. 8. 1C & D). Further, the recombinant plasmid was subjected to Sanger's sequencing by using M13 forward primer. The sequence (complete cds 416 bp) obtained was submitted to GenBank with the accession no: KP966296.1 and translated with Expasy to obtain amino acid sequence (Fig. 8.1E). The alignment of accepted Genbank sequence with the known Bowman birk and proteinase inhibitor sequences obtained from NCBI database confirmed that it belongs to BBI gene, hence named as "rT9BBII" (Fig. 8. 2).

Construction of recombinant T9BBI1-pET32a vector

For the expression of *rT9BBI1*, The 342 bp (Open reading frame of clone product with restriction sites) was amplified with the *T9BBI1* primers designed for the cloned gene

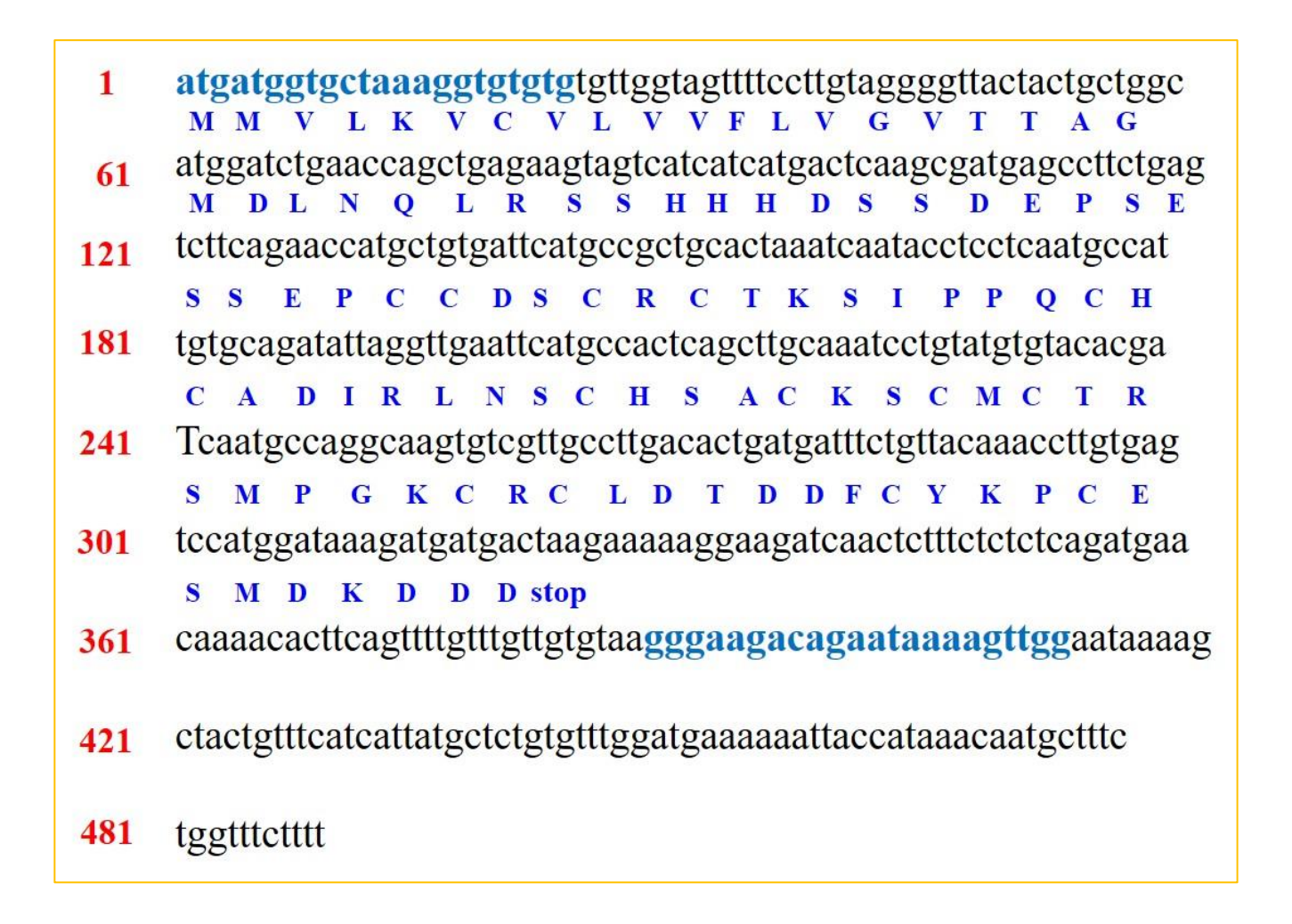


Fig. 8.1 (A) *Vigna radiata var. radiata* proteinase inhibitor mRNA, complete CDS (491 bp) with the accession number AY713305.2. This sequence is used as a standard for designing the primers for cloning of BBI gene from *Vigna mungo*. Forward and reverse primer sequences are in blue colour.

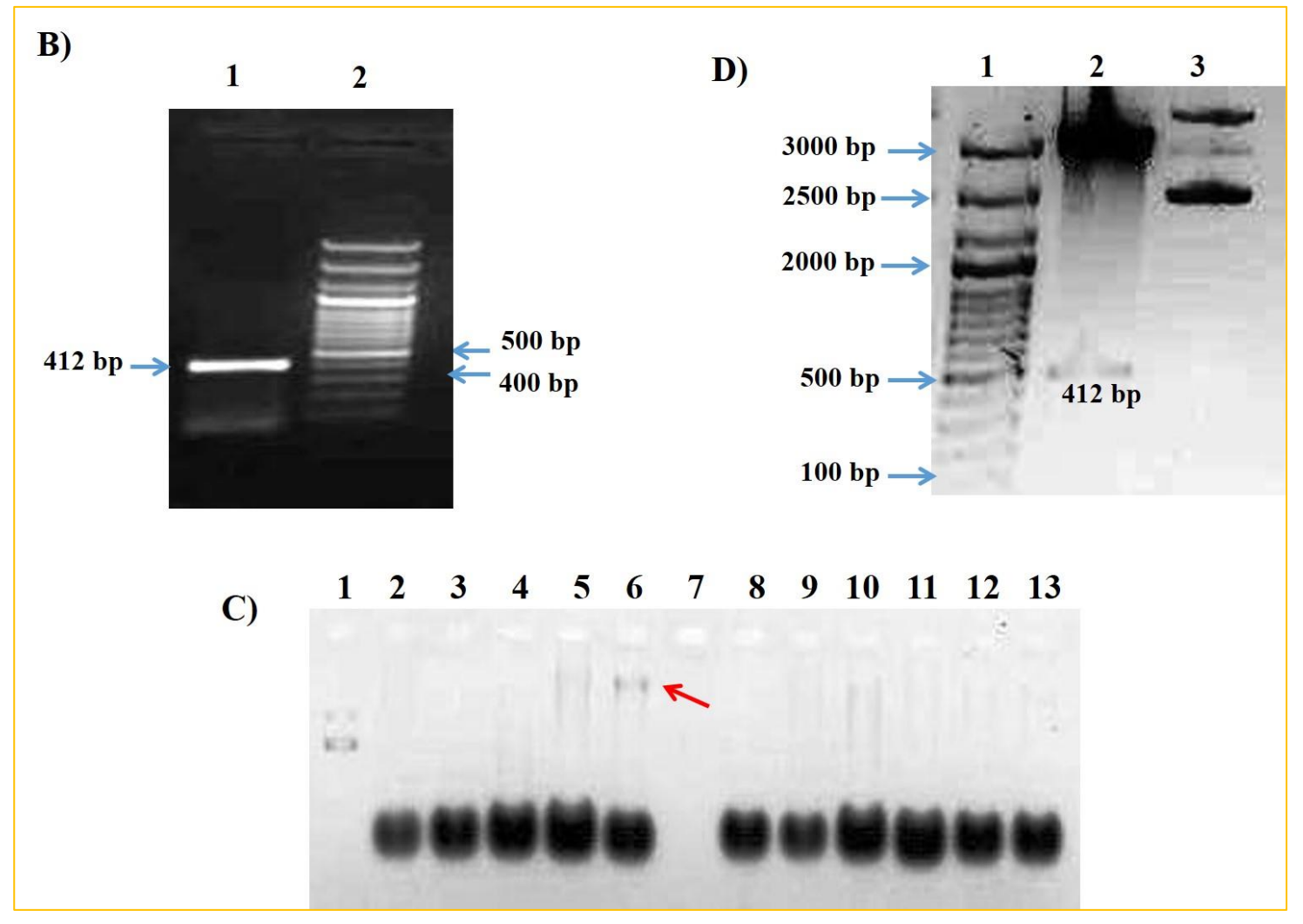


Fig. 8.1 (B-D). Cloning and confirmation of *T9BBI*1. (B) Agarose gel electrophoresis (1.5%): Lane 1, amplified gene product and Lane 2, 50 bp DNA ladder; (C) Colony PCR: Lane 1, pTZ57R/T vector control (2887 bp), Lanes 2-13: plasmid isolated from different colonies while Lane 6 represented confirmed colony for T9BBI gene (indicated by arrow mark) and (D) Restriction digestion: Lane 1, 100 bp DNA ladder, Lane 2, plasmid digested with EcoRI and PstI and Lane 3, undigested plasmid.

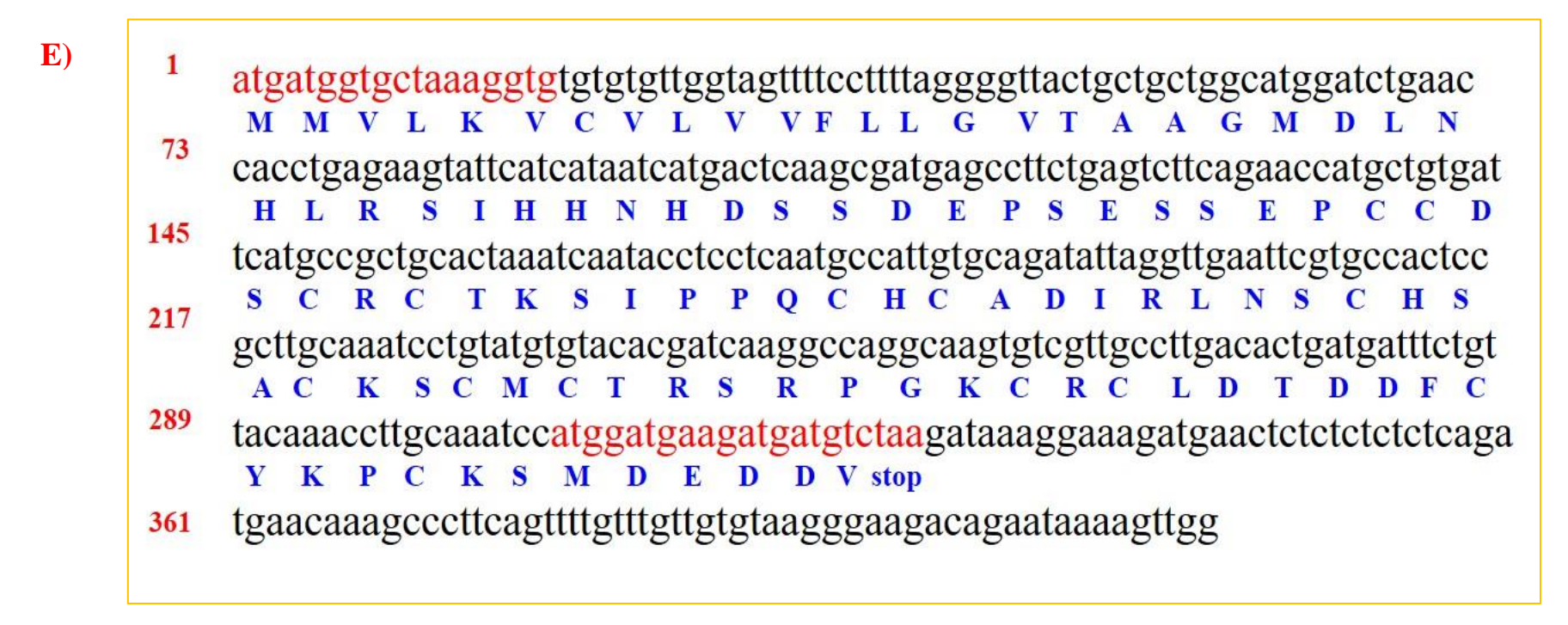


Fig 8.1. (E): Complete cds (416 bp) of *V. mungo T9BBI*1 and it's *in silico* translated amino acid sequence. Forward and reverse Primers designed for expression of *T9BBI1* are indicated in red colour.

Accession number	Description/ source of PIs	Amino acid sequence	Residue No.
KP966296.1 (Query sequence)	Proteinase inhibitor/Vigna mungo	MMVLKVCVLVVFLLGVTAAGMDL NHLRSIHHNHDSSDEPSESSEPCCDSCRC	52
ANH58933.1	Serine type protease inhibitor/ V. mungo	MMVLKVCVLVVFLLGVTAAGMDL NHLRSIHHNHDSSDEPSESSEPCCDSCRC	52
XP_017406861	Bowman Birk type proteinase inhibitors/ <i>V. angularis</i>	MMVLKVCVLVLFLVGVTAAGMDL KHLRSVHH-HDSSDEPSESSEPCCDLCLC	51
ADG29119.1	Bowman Birk type protease-inhibitor/ V. radiata	TTAGMDL NQLRSSHH-HDSSDEPSESSEPCCDSCRC	35
AEW50186.1	Bowman Birk type protease-inhibitor/ Cicer arietinum	MMVLKVCVLVVFLLGVTAAGMDL NHLRSIHHNHDSSDEPSESSEPCCDSCRC	52
AAK97766.1	Double headed Bowman Birk inhibitor, partial/ <i>V. mungo</i>	MVVLKVCLMLLFLLGTCAASLKQ SELEQLIKSGRHHESTDEPSESSKPCCDQCAC	55
ABD97865.1	Serine proteinase inhibitor/ V. mungo	MVVLKVCLMLLFLLGTCAASLKQ SELEQLIKSGRHHESTDEPSESSKPCCDQCAC	55
AHY03235.1	Bowman Birk inhibitor/ Macroptilium lathyroides	- MVLKVCFMLLFLLGS S TA SLKLSELGQLFKSGHHHHSTDEPSELSKPCCDQCAC	54
XP_003534064.1	Bowman Birk type proteinase-inhibitor/ <i>Glycine max</i>	MVVLKVCFLVLFLVGVTNARMEL NLFKSDN SSSDDESSKPCCDLCMC	47
CAO82009.1	Serine proteinase inhibitor/ Phaseolus oligospermus	MMVLKVCLLLVFLVGVTTARMDL NHLIRSNH-HDSSDEPSESSEPCCDHCMC	51
		* :	

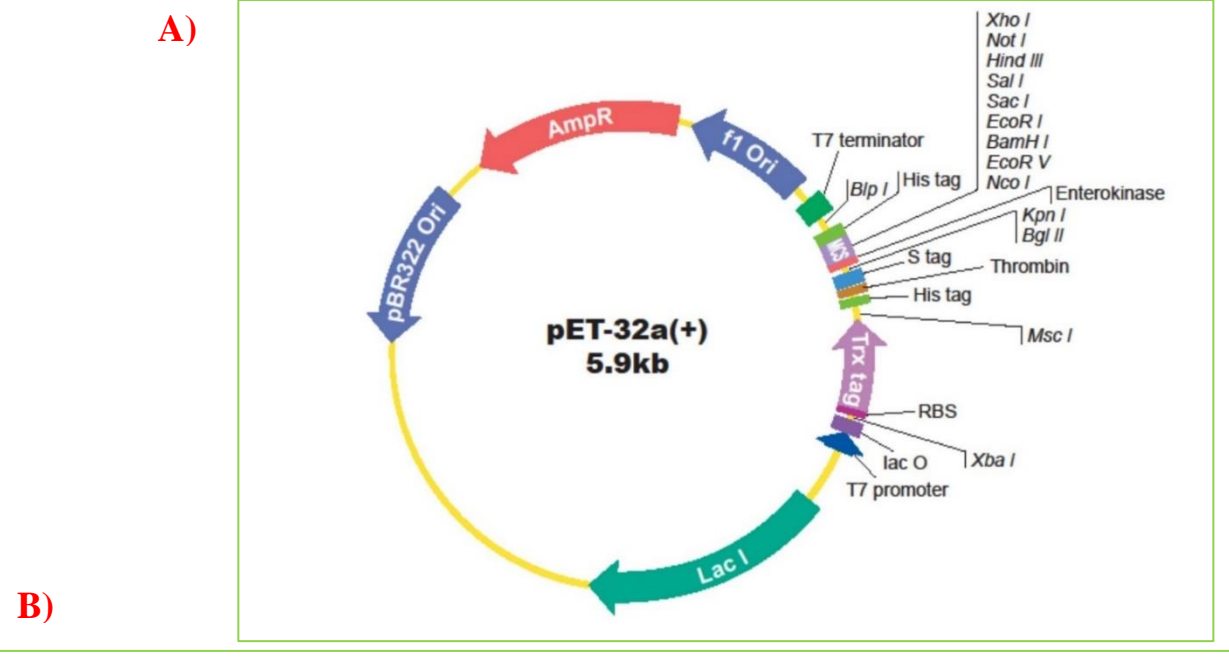
KP966296.1	Proteinase inhibitor/Vigna mungo	TKSIPPQCHCADIRLNSCHSACKSCMC TRSRPGK CRCLDTDDFCYKPCKSMDEDDV	108
(Querysequence)			
ANH58933.1	Serine type protease inhibitor/ <i>V. mungo</i>	TKSIPPQCHCADIRLNSCHSACKSCMC TRSRPGK CRCLDTDDFCYKPCKSMDKDD-	107
XP_017406861	Bowman Birk type proteinase-inhibitors/ <i>V. angularis</i>	TKSIPPQCQCADIRLNSCHSACKSCMC TRSMPGQ CRCLDTHDFCHKPCKSRDKDDV	107
ADG29119.1	Bowman Birk type protease-inhibitor/ V. radiata	TKSIPPQCHCADVRLNSCHSACKSCMCTRSMPGK CRCLDIDDFCYKPCESMDKDD-	90
AEW50186.1	Bowman Birk type protease inhibitor/ <i>C. arietinum</i>	TKSIPPQCHCADIRLNSCHSACKSCMC TRSRPGK CRCLDTDDFCYKPCKSMDKDD-	107
AAK97766.1	Double headed Bowman Birk inhibitor, partial/ V. mungo	TKSIPPKCRCSDLRLNSCHSACKSCAC TYSIPAQ CYCADINDFCYEPCK	104
ABD97865.1	Serine proteinase inhibitor/ V. mungo	TKSIPPKCRCSDLRLNSCHSACKSCAC TYSIPAQ CYCADINDFCYEPCKSSHDDD-	110
AHY03235.1	Bowman-Birk-inhibitor/ Macroptilium-lathyroides	TMSIPPQCRCTDIRLNSCHSGCESCMC TFSHPAK CVCTDIMDFCYGPCKSSHDDD-	109
XP_003534064.1	Bowman-Birk-type-proteinase-inhibitor/ <i>Glycine max</i>	TASMPPQCHCADIRLNSCHSACDRCAC TRSMPGQ CRCLDTTDFCYKPCKSSDEDD-	102
CAO82009.1	Serine-proteinase-inhibitor/ Phaseolus oligospermus	TDSIPPICQCTDIRLNSCHSACKSCMC TRSMPGK CRCLDTTDFCYKSCKSSGEDD-	106
		* * * * * * * * * * * * * * * * * * * *	

Fig. 8. 2. Multiple sequence alignment of query sequence (*V. mungo* Proteinase inhibitor with the accession number KP966296.1) with other legume sources of PIs from NCBI-BLASTp search. The amino acid residues of trypsin and chymotrypsin binding loop were highlighted in yellow colour. Identical residues are indicated by asterisks '*' and conserved residues are indicated by a colon ':' and less conserved residues are indicated by period '.'

(*T9BBI1*) sequence was tagged with restriction sites of BamHI-HF and Sac I HF (FP- 5' TCG GAT CCG ATG ATG GTG CTA AAG GTG 3' and RP- 5' CCT GAG CTC TTA GAC ATC ATC TTC ATC CAT 3') of pET32a vector (Figs. 8.1E & 8.3). The following conditions were applied to amplify the gene: initial denaturation at 98°C for 30 sec followed by 35 cycles of amplification consisting of denaturation (98°C for 30 sec), annealing (59°C for 15 sec) and extension (72°C for 15 sec), and a final extension of 10 min at 72°C (Fig 8.4A). The ligated product was transformed into *E. coli* shuffle cells and further confirmed by using colony PCR and restriction digestion (Figs. 8.4B & C).

8.2. Expression and purification of recombinant T9BBI1:

The shuffle cells containing the recombinant plasmid are grown at 37°C and induced with 1mM IPTG (0.5 OD at 600 nm) at 16°C. The induced cell pellet was dissolved in lysis buffer (100 mM Tris-HCl and 120 mM NaCl) and sonicated at 35% amplitude with 15 seconds pulse for duration of 15 minutes. After sonication, the cell extract was centrifuged twice at 10,000 rpm. After induction, T9BBI was identified in the supernatant fraction as evident in 12.5% non-denaturing SDS-PAGE (**Fig. 8.5A**). Further, the supernatant enriched with rT9BBI was subjected to Ni-NTA purification. The elution fractions contained *rT9BBI1* with a molecular mass of ~18.2 kDa, which is evident as a single band in 12.5% non-denaturing SDS-PAGE (**Fig. 8.5B**). The purified rT9BBI was further confirmed by western blot analysis using anti-His tag IgG antibody (**Fig. 8.5C**).



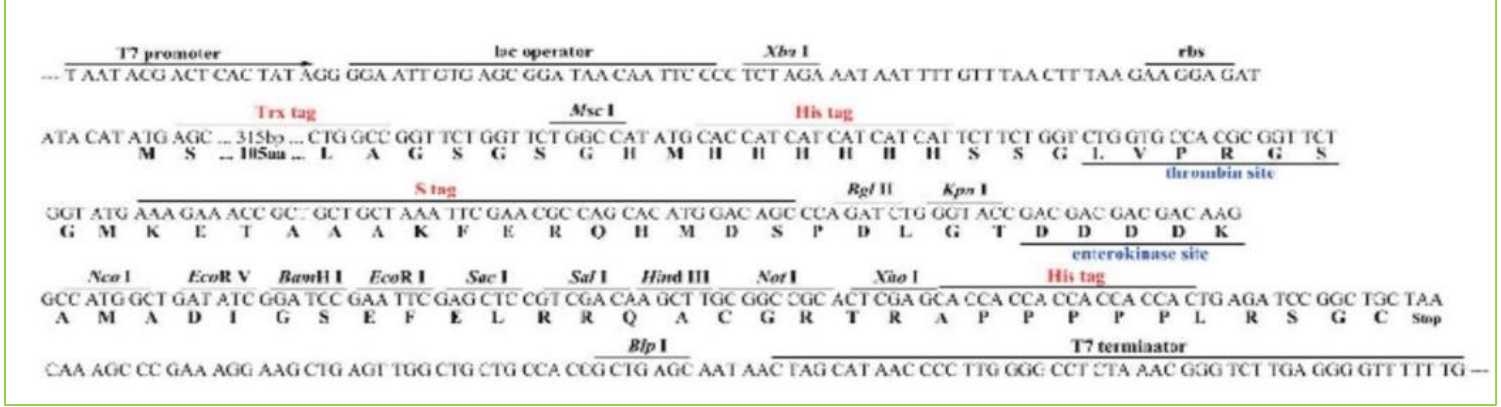


Fig. 8.3. **(A)** pET-32a vector circular map and its cloning sites **(B)** Linear map of the pET-32a vector. Cloning sites "BamH1" and "Sac1" are used for expression of *T9BBI1* gene.

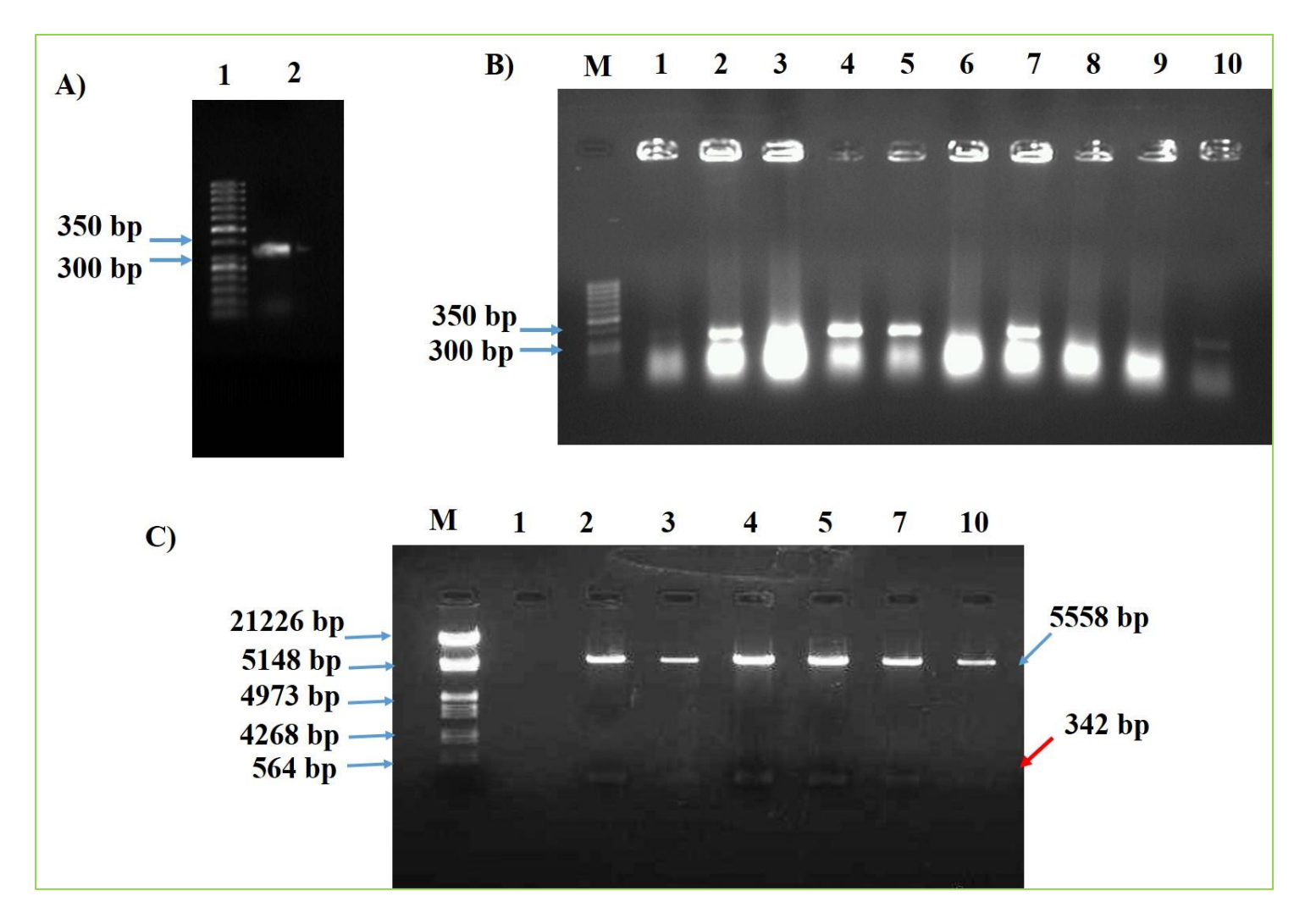


Fig. 8. 4. Confirmation of *T9BBI1* **in pET-32a vector. (A)** Agarose gel electrophoresis (1.5%): Lane 1, 50 bp DNA ladder and Lane 2, amplified *T9BBI1* **(B)** Colony PCR: M, 50 bp ladder; Lanes 1-10; plasmid isolated from different colonies, where lane 6, 8 and 9 are confirmed colonies for *T9BBI1* and **(C)** Restriction digestion of the plasmid with SacI HF and BamHI HF enzymes; M, 100 bp DNA ladder.

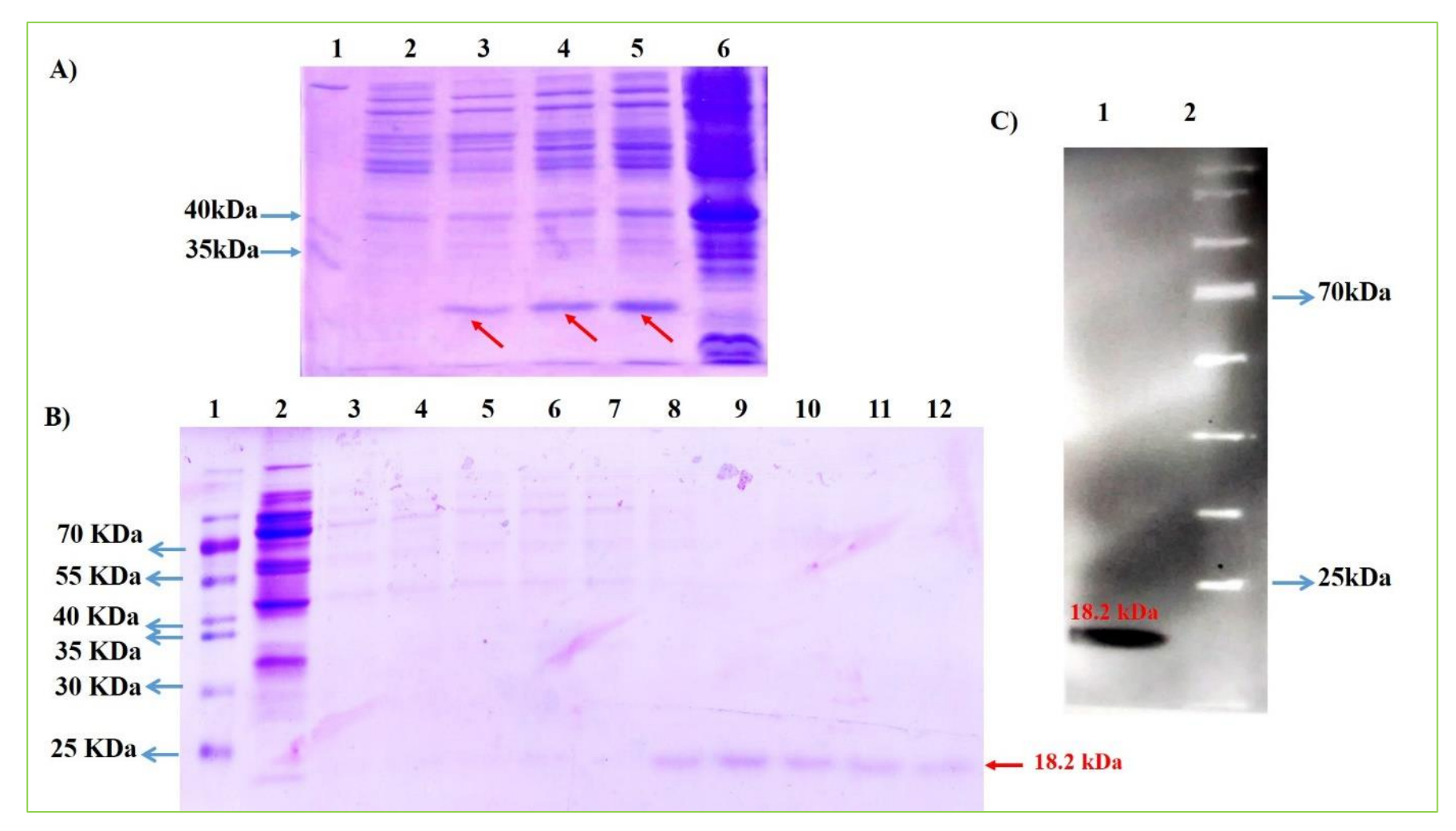


Fig. 8.5. Induction and Purification of rT9BBI1 and its confirmation by western blotting. (A) SDS-PAGE (12.5%): Lane 1, protein marker; Lane 2, Uninduced supernatant; Lanes 3-5, IPTG induced supernatant, Lane 6: IPTG induced pellet, (B) SDS-PAGE (12.5%); Lane 1, protein marker; Lane 2, flow through fractions, Lanes 3-7, wash fractions; Lanes 8-12, elution fractions (red arrow indicates the rT9BBI1 protein ~18.2kDa) and (C) Western blot analysis of the purified rT9BBI using anti-His tag antibody: Lane 1, rT9BBI1 and Lane 2, 100kDa protein ladder.

The molecular mass of the purified native T9BBI was 8.2 kDa (chapter 4, Fig. 4.3) while, the molecular mass of the rT9BBI obtained was ~18.2 kDa (Fig. 5B). This discrepancy in molecular masses might be due to the expression of 58 amino acids (6.38kDa) in the vector which are placed before the *V. mungo* BBI gene (108 amino acids =11.8 kDa, Figs. 3B, 4C). The inhibitory activity of rT9BBI1 was determined by *in vitro* inhibition assays (data not shown). However, the rT9BBI1 showed less inhibitory potential towards both bovine pancreatic trypsin and lepidopteran insect midgut trypsin-like proteases as compared to native T9BBI. This could be possibly due to the existence of purified rT9BBI1 in the unfolded state because of the hindrance caused by S-Tag and His-Tag expressed along with the BBI gene (Fig. 3B, 4C, 5B). Further, the different molecular masses observed for native T9BBI (8 kDa) and rT9BBI (11.2 kDa) in the present study suggests that *V. mungo* possesses more than one gene coding for BBI.

Highlights of the study:

- 1) *V. mungo* proteinase inhibitor gene (T9BBI1) was successfully cloned by using the *V. radiata* sequence in *E. coli*, DH5α bacterial cells.
- 2) The cloned gene was uploaded in the Genbank with the accession number KP966296.1
- 3) pET32a vector was used for the expression of the cloned gene in the *E. coli* shuffle cells.
- 4) The expressed protein was purified by using the Ni-NTA affinity column and confirmed by western blot analysis.

Based on these studies, it is proposed to use pET-23a vector with cloning sites Nde1 and Xho1 in place of pET-32a with BamH1 and Sac1 to avoid additional tags present before the cloning sites to get the expressed protein in the properly folded state.

Chapter 9 Summary and Conclusion

Chapter 9 Summary and Conclusion

The results from **chapter 4** reveals the purification of T9BBI from the mature seeds of *V. mungo* (*cv*.T9) and its characterization. Crude protein extracts were further purified by ammonium sulfate fractionation and the precipitate obtained was passed through different columns such as DEAE-cellulose column for ion-exchange, Trypsin-Sepharose 4-B for Affinity and Sephadex G-50 used for Size-exclusion chromatography with the help of Akta prime plus FPLC purification system (**Fig. 4.1**). The purification profile was showed in 15% SDS-PAGE (**Fig. 4.2**). The isolated protein was partially characterized for its purity, mass, presence of isoforms, dimers and trypsin/chymotrypsin inhibitory activity (**Figs 4.3-4.5 and Table 4.1**).

Further, the results from **chapter 5** refer to the evaluation of the insecticidal potential of T9BBI on larval growth and development of non-host insect pest *A. janata* followed by changes in the expression of its midgut tissue proteins. The purified T9BBI showed significant potential against larval midgut trypsin-like proteases of *A. janata* when compared with crude protein extract of black gram T9 variety (**Fig.5.1**). The growth of the larvae fed on leaves coated with different concentrations of T9BBI (0.5-8 μg/cm²) was retarded significantly when compared with larvae fed on control leaves without T9BBI (**Figs 5.2-5.4** and **Table 5.1**). Further, the pupa derived from these larvae also showed a significant loss in their weight when compared with respective control pupa (**Fig 5.5 A & B**). At the end of 23rd day, the mortality rate of larvae/pupae was monitored and found to be significant (**Table 5.1**). A delay in the emergence of pupa was observed in larvae fed on T9BBI. Malformation/abnormality was observed to be at a higher rate during larval to pupal and pupal to adult stage when fed with high concentration (8 μg/cm²) of T9BBI (**Fig 5.5 C and Table 5.1**). 2-D gel electrophoresis of protein samples isolated from midgut tissues of larvae

fed on leaves with and without T9BBI was performed and differential expression of proteins was analysed by using Image Master Platinum 7.0 software (Figs 5.6 & 5.7). Among several protein spots detected with differential expression, eight spots which showed more than 2-fold difference in their expression (up-regulation or down-regulation) were picked and subjected to MALDI-TOF-TOF analysis. The protein spots chosen in this study showed similarity/matching to proteins involved in cell migration during larval growth and development (COP-9 signalosome complex-3 subunit and SOEM-1 protein) and metamorphosis (Cyc-C, PDH) while others are involved in stress response (Heat shock 70 kDa protein cognate and Turandot protein) (Fig 5.8-5.15 and Table 5.2).

In chapter 6, the insecticidal potential of T9BBI was evaluated against larval growth and development of host insect pest S. litura and changes in the expression of their midgut protein was revealed. Here also T9BBI showed significant inhibitory potential against trypsin-like gut proteases of S. litura, when compared with crude protein extract prepared from mature seeds of black gram (cv. T9) (Fig.6.1). The growth of the larvae fed on an artificial diet with T9BBI (0.01-0.1%) was retarded significantly when compared with control larvae fed on the diet without T9BBI (Figs 6.2-6.4). As observed with larvae, the weight of the pupae also decreased significantly when diet was supplemented with T9BBI (Fig 6.5A) &B). At the end of 30th day, the mortality rate of larvae/pupae was remarkable. The delay in the emergence of pupa was more in S. litura as compared to A. janata. Further, malformation/abnormality in pupae/adults was observed at higher concentration (0.1%) of T9BBI (6.5C & Table 6.1). A total of 143 spots were detected during 2-D electrophoresis in protein sample collected from midgut tissue of S. litura (Figs 6.6-6.7). However, five spots which showed a significant difference in their expression were picked and subjected to MALDI-TOF-TOF analysis as described above. During Mascot search, these protein spots showed matching/similarity to those proteins involved in transcription (Zinc finger protein),

cellular energy metabolism (Arginine kinase) as well as structural stability and integrity (Actin-5C) related proteins (Figs 6.8-6.13 and Table 6.2).

In **chapter 7** the insecticidal potential of T9BBI was evaluated on larval growth and development of *H. armigera* and changes in expression pattern of their midgut proteins was monitored. T9BBI also showed inhibitory potential against trypsin-like gut proteases of H. armigera when compared with crude protein (Fig. 7.1). The weight of the larvae and pupae derived from larvae fed on an artificial diet containing T9BBI (0.01-0.1%) was decreased significantly when compared with controls (Figs 7.2-7.4 A &B). However, the larvae/pupae did not show any mortality. Further, the pupal formation was delayed approximately up to 9 days and larval-pupal and pupal-adult malformation was observed upon feeding at high concentration (0.1%) of T9BBI (Fig 7.4C and Table 7.1). A total of 204 spots was detected in 2-D electrophoresis of protein sample obtained from midgut tissue of H. armigera larvae. However, seven spots with significant change in expression were picked for MALDI-TOF-TOF analysis (Figs 7.5 & 7.6). During mascot search, these differentially expressed protein spots showed matching to proteins involved in detoxification (Glutathione S-transferase GSTS4, Cytochrome-P450, Carboxylic ester hydrolase, Tpx) and immune system (Hdd23 like protein) (Figs 7.7-7.11 and Table 7.2). Comparative analysis of the insecticidal effects of T9BBI on three insects chosen in the present study was shown in table 9.1.

In **chapter 8**, an attempt was made to clone T9BBI1 gene from seeds of *V. mungo*. Total RNA was isolated from the *V. mungo* seeds. The *T9BBI1* was synthesized by using the primers of *V. radiata* with the accession No: AY713305 and cloned into pTZ57R/T vector (**Figs 8.1 A-D**). The obtained sequencing results of clone was reported to Genbank with the accession No: KP966296.1. The T9BBI was expressed in *E.coli* shuffle cells using pET-32a vector and confirmed by colony PCR and restriction digestion (**Figs 8.4B & C**). The T9BBI1

was overexpressed using IPTG (**Fig 8.5A**) and purified by using Ni-NTA His binding resin (**Fig. 8.5B**). The purified protein was confirmed by western blot using anti-His IgG antibody (**Fig. 8.5C**).

Major Conclusions:

- 1) The purified PI from seeds of *V. mungo* possessed a molecular mass of 8.2 kDa in MALDI-TOF, existed as isoforms, and possessed inhibitory activity against trypsin and chymotrypsin. Hence named as "**T9BBI**".
- 2) T9BBI possessed inhibitory potential against trypsin-like gut proteases of *A. janata*, *S. litura* and *H. armigera*.
- 3) T9BBI retarded the larval growth and development of chosen pests in the following order: *A. janata >S. litura >H. armigera*.
- 4) T9BBI was shown to be more effective in the management of non-host insect pest *A. janata* as compared to host-pests *S. litura* and *H. armigera*.
- 5) The midgut proteins of the three lepidopteran larvae examined in the present study were modulated differentially upon feeding with T9BBI.
- 6) The larvae of *A. janata* showed modulation in midgut proteins related to cell migration, development and stress response. In contrast, the larvae of *S. litura* showed modulation in proteins related to energy metabolism, transcription and structural stability while the larvae of *H. armigera* showed modulation in detoxification and immune response related proteins.
- 7) *T9BBI1* was successfully cloned, expressed and purified by using Ni-NTA affinity column and further confirmed by Western blotting.
- 8) Taking together the results suggest that T9BBI can be successfully applied in Integrated Pest Management (IPM) of *A. janata*.
- 9) Further, the results obtained with T9BBI with reference to *S. litura* and *H. armigera* paved way to understand the adaptive response of insects when exposed to a biopesticide.

Table. 9.1. Comparative table showing the effects of T9BBI on three lepidopteran insects: *Achaea janata*, *Spodoptera litura* and *Helicoverpa armigera*.

Parameter Examined	A. janata	S. litura	H. armigera
Maximum Reduction in body weight of larvae	80 %	52%	45%
Mortality Rate of larvae	85%	20%	Nil
Delay in Emergence of Pupa	1 week	>1 week	>1 week
Reduction in pupal weight	85%	60%	55%
Larval-Pupal Intermediates	Yes	Yes	Yes
Pupal-Adults Intermediates	Yes	Yes	Yes
Modulation in midgut proteins	Cell Migration, stress response and structural stability and integrity of cell development	Transcription, Energy metabolism and in structural stability and integrity of cell.	Body detoxification and immune system

Chapter 10 Literature cited

- Abdeen, A., Virgos, A., Olivella, E., Villanueva, J., Aviles, X., Gabarra, R., & Prat, S., 2005. Multiple insect resistance in transgenic tomato plants overexpressing two families of plant proteinase inhibitors. *Plant Molecular Biology*, *57*(2), 189-202.
- Agosin, M., 1985. Role of microsomal oxidations in insecticide degradation. *Comprehensive Insect Physiology, Biochemistry and Pharmacology*, 12, 647-712.
- Ahmad, K., 2014. Molecular farming: strategies, expression systems and bio-safety considerations. *Czech Journal of Genetics and Plant Breeding*, 50(1), 1-10.
- Ahmed, I.A.M., Morishima, I., Babiker, E.E. and Mori, N., 2009. Dubiumin, a chymotrypsin-like serine protease from the seeds of *Solanum dubium* Fresen. *Phytochemistry*, 70(4), 483-491.
- Ai, X., Wei, Y., Huang, L., Zhao, J., Wang, Y., & Liu, X., 2018. Developmental control of *Helicoverpa armigera* by ingestion of bacteria expressing dsRNA targeting an arginine kinase gene. *Biocontrol Science and Technology*, 28(3), 253-267.
- Allocati, N., Federici, L., Masulli, M., & Di Ilio, C., 2009. Glutathione transferases in bacteria. *The FEBS journal*, 276(1), 58-75.
- Al-Maiman, S. A., Gassem, M. A., Osman, M. A., Ahmed, I. M., Al-Juhaimi, F. Y., Rahman, I. A., & Weber, C., 2019. Bowman-Birk proteinase inhibitor from tepary bean (*Phaseolus acutifolius*) seeds: purification and biochemical properties. *International Food Research Journal*, 26(4), 1123-1131.
- Altuntas, H., Kilic, A.Y., Uçkan, F. and Ergin, E., 2012. Effects of gibberellic acid on hemocytes of Galleria mellonella L. (Lepidoptera: Pyralidae). *Environmental Entomology*, 41(3), 688-696.
- Amirhusin, B., Shade, R. E., Koiwa, H., Hasegawa, P. M., Bressan, R. A., Murdock, L. L., & Zhu-Salzman, K., 2007. Protease inhibitors from several classes work synergistically against *Callosobruchus maculatus*. *Journal of Insect Physiology*, *53*(7), 734-740.
- Andow, D.A., 2008. The risk of resistance evolution in insects to transgenic insecticidal crops. *Collection of Biosafety Reviews*, *4*, 142-199.
- Aoki, H., Akaike, T., Abe, K., Kuroda, M., Arai, S., Okamura, R. I., & Maeda, H., 1995. Antiviral effect of *oryzacystatin*, a proteinase inhibitor in rice, against herpes simplex virus type 1 *in vitro* and *in vivo*. *Antimicrobial agents and Chemotherapy*, 39(4), 846-849.
- Arnaiz, A., Talavera-Mateo, L., Gonzalez-Melendi, P., Martinez, M., Diaz, I. and Santamaria, M.E., 2018. Arabidopsis Kunitz trypsin inhibitors in defense against spider mites. *Frontiers in Plant Science*, *9*, 986.

- Arunprasanna, V., Kannan, M., Anbalagan, S., & Krishnan, M., 2017. Comparative proteomic analysis of larva and adult heads of silkworm, *Bombyx mori* (Lepidoptera: Bombycidae). *Journal of Entomology*, 1-12.
- Babu, S. R., Subrahmanyam, B., & Santha, I. M., 2012. *In vivo* and *in vitro* effect of *Acacia nilotica* seed proteinase inhibitors on *Helicoverpa armigera* (Hubner) larvae. *Journal of Biosciences*, 37(2), 269-276.
- Banerjee, S., Giri, A. P., Gupta, V. S., & Dutta, S. K., 2017. Structure-function relationship of a bio-pesticidal trypsin/chymotrypsin inhibitor from winged bean. *International Journal of Biological Macromolecules*, 96, 532-537.
- Barbosa, J. A. R., Silva, L. P., Teles, R. C., Esteves, G. F., Azevedo, R. B., Ventura, M. M., & de Freitas, S. M., 2007. Crystal structure of the Bowman-Birk inhibitor from *Vigna unguiculata* seeds in complex with β-Trypsin at 1.55 Å resolution and its structural properties in association with proteinases. *Biophysical Journal*, *92*(5), 1638-1650.
- Bayyareddy, K., Andacht, T. M., Abdullah, M. A., & Adang, M. J., 2009. Proteomic identification of *Bacillus thuringiensis* subsp. israelensis toxin Cry4Ba binding proteins in midgut membranes from *Aedes (Stegomyia) aegypti Linnaeus* (Diptera, Culicidae) larvae. *Insect Biochemistry and Molecular Biology*, 39(4), 279-286.
- Bhattacharyya, A., Mazumdar, S., Leighton, S. M., & Babu, C. R., 2006. A Kunitz proteinase inhibitor from *Archidendron ellipticum* seeds: purification, characterization, and kinetic properties. *Phytochemistry*, 67(3), 232-241.
- Bilal, M., Freed, S., Muhammad, S., Ashraf, M. Z., & Khan, M. B., 2018. Activity of glutathione S-transferase and esterase enzymes in *Helicoverpa armigera* (Hubner) after exposure to entomopathogenic fungi. *Entomological Research*, 48(4), 279-287.
- Blethen, S., 1970. Arginine kinase (arthropod muscle). In *Methods in Enzymology* (Vol. 17, pp. 330-335). Academic Press.
- Bogwitz, M. R., Chung, H., Magoc, L., Rigby, S., Wong, W., O'Keefe, M., & Daborn, P. J., 2005. Cyp12a4 confers lufenuron resistance in a natural population of *Drosophila melanogaster*. *Proceedings of the National Academy of Sciences*, 102(36), 12807-12812.
- Bolter, C. J., & Latoszek-Green, M., 1997. Effect of chronic ingestion of the cysteine proteinase inhibitor, E-64, on Colorado potato beetle gut proteinases. *Entomologia Experimentalis et Applicata*, 83(3), 295-303.
- Bortolozzo, A.S.S., Rodrigues, A.P.D., Arantes-Costa, F.M., Saraiva-Romanholo, B.M., Souza, F.C.R.D., Bruggemann, T.R., Brito, M.V.D., Ferreira, R.D.S., Correia, M.T.D.S., Paiva, P.M.G. and Prado, C.M., 2018. The plant proteinase inhibitor CrataBL plays a role in controlling asthma response in mice. *BioMed Research International*, 2018.
- Bouchard, E., Michaud, D. and Cloutier, C., 2003. Molecular interactions between an insect predator and its herbivore prey on transgenic potato expressing a cysteine proteinase inhibitor from rice. *Molecular Ecology*, 12(9), 2429-2437.

- Bouchard, M.F., Bellinger, D.C., Wright, R.O. and Weisskof, M.G., 2010. Attention-deficit/hyperactivity disorder and urinary metabolites of organophosphate pesticides. *Pediatrics*, 125(6), 1270-1277.
- Briones, N.D., 2005. Environmental sustainability issues in Philippine agriculture. *Asian Journal of Agriculture and Development*, 2(1362-2016-107645), 67-78.
- Browner, M.F., Smith, W. W., & Castelhano, A. L., 1995. Matrilysin-inhibitor complexes: common themes among metalloproteases. *Biochemistry*, *34*(20), 6602-6610.
- Browse, J., Howe, G. A., 2008. New weapons and a rapid response against insect attack. *Plant Physiology*, 146(3), 832-838.
- Campos, J. E., Whitaker, J. R., Yip, T. T., Hutchens, T. W., & Blanco-Labra, A., 2004. Unusual structural characteristics and complete amino acid sequence of a protease inhibitor from *Phaseolus acutifolius* seeds. *Plant Physiology and Biochemistry*, 42(3), 209-214.
- Carriere, Y., Yelich, A.J., Degain, B.A., Harpold, V.S., Unnithan, G.C., Kim, J.H., Mathew, L.G., Head, G.P., Rathore, K.S., Fabrick, J.A. and Tabashnik, B.E., 2019. Gossypol in cottonseed increases the fitness cost of resistance to *Bt* cotton in pink bollworm. *Crop Protection*, 126, p.104914.
- Cater, S. A., Lees, W. E., Hill, J., Brzin, J., Kay, J., & Philip, L. H., 2002. Aspartic proteinase inhibitors from tomato and potato are more potent against yeast proteinase A than cathepsin D. *Biochimica et Biophysica Acta (BBA)-Protein Structure and Molecular Enzymology*, 1596(1), 76-82.
- Charity, J. A., Hughes, P., Anderson, M. A., Bittisnich, D. J., Whitecross, M., & Higgins, T. J. V., 2005. Pest and disease protection conferred by expression of barley β-hordothionin and *Nicotiana alata* proteinase inhibitor genes in transgenic tobacco. *Functional Plant Biology*, 32(1), 35-44.
- Chen, K. S., Kim, S. R., Park, N. S., Kim, I., Kang, P. D., Sohn, B. H., & Sohn, H. D., 2005. Characterization of a silkworm thioredoxin peroxidase that is induced by external temperature stimulus and viral infection. *Insect Biochemistry and Molecular biology*, 35(1), 73-84.
- Chen, W., Geng, S. L., Song, Z., Li, Y. J., Wang, H., & Cao, J. Y., 2019. Alternative splicing and expression analysis of HSF1 in diapause pupal brains in the cotton bollworm, *Helicoverpa armigera*. *Pest Management Science*, 75(5), 1258-1269.
- Chougule, N. P., Hivrale, V. K., Chhabda, P. J., Giri, A. P., & Kachole, M. S., 2003. Differential inhibition of *Helicoverpa armigera* gut proteinases by proteinase inhibitors of pigeon pea (*Cajanus cajan*) and its wild relatives. *Phytochemistry*, 64(3), 681-687.
- Ciftci-Yilmaz, S., Morsy, M. R., Song, L., Coutu, A., Krizek, B. A., Lewis, M. W., & Mittler, R., 2007. The EAR-motif of the Cys2/His2-type zinc finger protein Zat7 plays a key role in the defense response of Arabidopsis to salinity stress. *Journal of Biological Chemistry*, 282(12), 9260-9268.

- Cingel, A., Savic, J., Cosic, T., Zdravkovic-Korac, S., Momcilovic, I., Smigocki, A. and Ninkovic, S., 2014. Pyramiding rice cystatin OCI and OCII genes in transgenic potato (Solanum tuberosum L.) for resistance to Colorado potato beetle (*Leptinotarsa decemlineata Say*). *Euphytica*, 198(3), pp.425-438.
- Clemente, A., Marin-Manzano, M. C., Jimenez, E., Arques, M. C., & Domoney, C., 2012. The anti-proliferative effect of TI1B, a major Bowman-Birk isoinhibitor from pea (*Pisum sativum L.*), on HT29 colon cancer cells is mediated through protease inhibition. *British Journal of Nutrition*, 108(1), 135-144.
- Clemente, M., Corigliano, M.G., Pariani, S.A., Sánchez-Lopez, E.F., Sander, V.A. and Ramos-Duarte, V.A., 2019. Plant serine protease inhibitors: Biotechnology application in agriculture and molecular farming. *International Journal of Molecular Sciences*, 20(6), 1345.
- Clothianidin Registration Status and Related Information; http://www.epa.gov/pesticides/about/intheworks/clothianidinregistration-status.html (updated July 27, 2012) (accessed March 21, 2014).
- Craig, E. A., Ingolia, T. D., & Manseau, L. J., 1983. Expression of *Drosophila* heat-shock cognate genes during heat shock and development. *Developmental Biology*, 99(2), 418-426.
- Dantzger, M., Vasconcelos, I. M., Scorsato, V., Aparicio, R., Marangoni, S., & Macedo, M. L. R., 2015. Bowman-Birk proteinase inhibitor from *Clitoria fairchildiana* seeds: Isolation, biochemical properties and insecticidal potential. *Phytochemistry*, 118, 224-235.
- Datta, R., Kaur, A., Saraf, I., Singh, I.P. and Kaur, S., 2019. Effect of crude extracts and purified compounds of Alpinia galanga on nutritional physiology of a polyphagous lepidopteran pest, *Spodoptera litura* (Fabricius). *Ecotoxicology and Environmental safety*, *168*, 324-329.
- Davis, D. A., Soule, E. E., Davidoff, K. S., Daniels, S. I., Naiman, N. E., & Yarchoan, R., 2012. Activity of human immunodeficiency virus type 1 protease inhibitors against the initial auto cleavage in Gag-Pol polyprotein processing. *Antimicrobial agents and chemotherapy*, 56(7), 3620-3628.
- Dawkar, V.V., Chikate, Y.R., More, T.H., Gupta, V.S. and Giri, A.P., 2016. The expression of proteins involved in digestion and detoxification are regulated in *Helicoverpa armigera* to cope up with chlorpyrifos insecticide. *Insect Science*, 23(1), 68-77.
- Deng, X. W., Dubiel, W., Wei, N., Hofmann, K., & Mundt, K., 2000. Unified nomenclature for the COP9 signalosome and its subunits: an essential regulator of development. *Trends in Genetics*, 16(7), 289.
- Deshimaru, M., Yoshimi, S., Shioi, S., & Terada, S., 2004. Multigene family for Bowman–Birk type proteinase inhibitors of wild soja and soybean: The presence of two BBI-A genes and pseudogenes. *Bioscience, Biotechnology, and Biochemistry*, 68(6), 1279-1286.

Devanand, P., & Rani, P. U., 2011. Insect growth regulatory activity of the crude and purified fractions from *Solanum melongena* L., *Lycopersicum esculentum* Mill. and *Capsicum annuum* L. *Journal of Biopesticides*, 4(2), 118.

Devarshi, A.A. and Yankanchi, S.R., 2017. Ovicidal and toxic effects of certain plant extracts to the castor semi looper, *Achaea janata* L. (Noctuidae: Lepidoptera). *Indian Journal of Agricultural Research*, 51(4), 345-349.

Dhania, N.K., Chauhan, V.K., Chaitanya, R.K. and Dutta-Gupta, A., 2019. Midgut *de novo* transcriptome analysis and gene expression profiling of *Achaea janata* larvae exposed with *Bacillus thuringiensis* (*Bt*)-based biopesticide formulation. *Comparative Biochemistry and Physiology Part D: Genomics and Proteomics*, 30, 81-90.

Domoney, C., Welham, T., Sidebottom, C., & Firmin, J. L., 1995. Multiple isoforms of *Pisum* trypsin inhibitors result from modification of two primary gene products. *FEBS letters*, 360(1), 15-20.

Doronkin, S., Djagaeva, I., & Beckendorf, S. K., 2003. The COP9 signalosome promotes degradation of Cyclin E during early *Drosophila* oogenesis. *Developmental Cell*, 4(5), 699-710.

Douglas, K. T., 1987. Mechanism of action of glutathione-dependent enzymes. *Advances in Enzymology and Related Areas of Molecular Biology*, *59*, 103-167.

Dubiel, D., Rockel, B., Naumann, M., & Dubiel, W., 2015. Diversity of COP9 signalosome structures and functional consequences. *FEBS letters*, 589(19), 2507-2513.

Dufour, A., & Overall, C. M., 2013. Missing the target: matrix metalloproteinase ant targets in inflammation and cancer. *Trends in Pharmacological Sciences*, 34(4), 233-242.

Dunse, K.M., Stevens, J.A., Lay, F.T., Gaspar, Y.M., Heath, R.L. and Anderson, M.A., 2010. Co-expression of potato type I and II proteinase inhibitors gives cotton plants protection against insect damage in the field. *Proceedings of the National Academy of Sciences*, 107(34), 15011-15015.

Dutta, M., Rajak, P., Khatun, S., & Roy, S., 2017. Toxicity assessment of sodium fluoride in *Drosophila melanogaster* after chronic sub-lethal exposure. *Chemosphere*, 166, 255-266.

Edmonds, H.S., Gatehouse, L.N., Hilder, V.A. and Gatehouse, J.A., 1996. The inhibitory effects of the cysteine protease inhibitor, oryzacystatin, on digestive proteases and on larval survival and development of the southern corn rootworm (*Diabrotica undecimpunctata howardi*). *Entomologia Experimentalis et Applicata*, 78(1), 83-94.

Ekengren, S., & Hultmark, D., 2001. A family of Turandot-related genes in the humoral stress response of *Drosophila Biochemical and Biophysical Research Communications*, 284(4), 998-1003.

Elumalai, K., Krishnappa, K., Anandan, A., Govindarajan, M., & Mathivanan, T., 2010. Larvicidal and ovicidal efficacy of ten medicinal plant essential oil against lepidopteran

- pest Spodoptera litura (Lepidoptera: Noctuidae). International Journal of Recent Scientific Research, 1, 1-7.
- Er, A. and Keskin, M., 2016. Influence of abscisic acid on the biology and hemocytes of the model insect *Galleria mellonella* (Lepidoptera: Pyralidae). *Annals of the Entomological Society of America*, 109(2), 244-251.
- Erlanger, B. F., Kokowsky, N., & Cohen, W., 1961. The preparation and properties of two new chromogenic substrates of trypsin. *Archives of biochemistry and biophysics*, 95(2), 271-278.
- EXTOXNET Extension Toxicology Network. A Pesticide Information Project of Cooperative Extension Offices of Cornell University, Michigan State University, Oregon State University, and the University of California at Davis; http://pmep.cce.cornell.edu/profiles/extoxnet/carbaryl-dicrotophos/chlorpyrifos-ext.html (accessed March 21, 2014).
- Falco, M.C. and Silva-Filho, M.C., 2003. Expression of soybean proteinase inhibitors in transgenic sugarcane plants: effects on natural defense against *Diatraea* saccharalis. Plant Physiology and Biochemistry, 41(8), 761-766.
- Fan, J., Han, P., Chen, X., Hu, Q., & Ye, M., 2014. Comparative proteomic analysis of *Bombyx mori* hemocytes treated with destruxin A. *Archives of Insect Biochemistry and Physiology*, 86(1), 33-45.
- Felicioli, R., Garzelli, B., Vaccari, L., Melfi, D., & Balestreri, E., 1997. Activity staining of protein inhibitors of proteases on gelatin-containing polyacrylamide gel electrophoresis. 244 (1), 176-179.
- Ferreira, R. S., Brito, M. V., Napoleao, T. H., Silva, M. C. C., Paiva, P. M. G., & Oliva, M. L. V., 2019. Effects of two protease inhibitors from *Bauhinia bauhinoides* with different specificity towards gut enzymes of *Nasutitermes corniger* and its survival. *Chemosphere*, 222, 364-370.
- Feyereisen, R., 1999. Insect P450 enzymes. *Annual review of entomology*, 44(1), 507-533.
- Foissac, X., Loc, N.T., Christou, P., Gatehouse, A.M. and Gatehouse, J.A., 2000. Resistance to green leafhopper (Nephotettix virescens) and brown planthopper (*Nilaparvata lugens*) in transgenic rice expressing snowdrop lectin (*Galanthus nivalis* agglutinin; GNA). *Journal of Insect Physiology*, 46(4), 573-583.
- Francis, F., Vanhaelen, N. and Haubruge, E., 2005. Glutathione S-transferases in the adaptation to plant secondary metabolites in the Myzus persicae aphid. *Archives of Insect Biochemistry and Physiology: Published in Collaboration with the Entomological Society of America*, 58(3), 166-174.
- Freilich, S., Oron, E., Kapp, Y. A., Nevo-Caspi, Y., Orgad, S., Segal, D., & Chamovitz, D. A., 1999. The COP9 signalosome is essential for development of *Drosophila melanogaster*. *Current Biology*, 9(20), 1187-S4.

- Fritz, M.L., DeYonke, A.M., Papanicolaou, A., Micinski, S., Westbrook, J. and Gould, F., 2018. Contemporary evolution of a Lepidopteran species, *Heliothis virescens*, in response to modern agricultural practices. *Molecular Ecology*, 27(1), pp.167-181.
- Furstenberg-Hagg, J., Zagrobelny, M. and Bak, S., 2013. Plant defense against insect herbivores. *International Journal of Molecular Sciences*, 14(5), 10242-10297.
- Gahloth, D., Shukla, U., Birah, A., Gupta, G. P., Ananda Kumar, P., Dhaliwal, H. S., & Sharma, A. K., 2011. Bio insecticidal activity of *Murraya koenigii* miraculin-like protein against *Helicoverpa armigera* and *Spodoptera litura*. *Archives of Insect Biochemistry and Physiology*, 78(3), 132-144.
- Gahukar, R. T., 2015. Management of pests and diseases of tropical sericultural plants by using plant-derived products: a review. *Journal of Forestry Research*, 26(3), 533-544.
- Gandreddi, V.S., Kappala, V.R., Zaveri, K. and Patnala, K., 2015. Evaluating the role of a trypsin inhibitor from soap nut (*Sapindus trifoliatus L. Var. Emarginatus*) seeds against larval gut proteases, its purification and characterization. *BMC Biochemistry*, 16(1), 23.
- Gatehouse, A.M., Norton, E., Davison, G.M., Babbe, S.M., Newell, C.A. and Gatehouse, J.A., 1999. Digestive proteolytic activity in larvae of tomato moth, *Lacanobia oleracea*; effects of plant protease inhibitors *in vitro* and *in vivo. Journal of Insect Physiology*, 45(6), 545-558.
- Gatehouse, A.M., Shi, Y., Powell, K.S., Brough, C., Hilder, V.A., Hamilton, W.D., Newell, C.A., Merryweather, A., Boulter, D. and Gatehouse, J.A., 1993. Approaches to insect resistance using transgenic plants. *Philosophical Transactions of the Royal Society of London. Series B: Biological Sciences*, 342(1301), 279-286.
- Gatehouse, J. A., 2002. Plant resistance towards insect herbivores: a dynamic interaction. *New Phytologist*, 156(2), 145-169.
- Gatehouse, L. N., Shannon, A. L., Burgess, E. P., & Christeller, J. T., 1997. Characterization of major midgut proteinase cDNAs from *Helicoverpa armigera* larvae and changes in gene expression in response to four proteinase inhibitors in the diet. *Insect Biochemistry and Molecular Biology*, 27(11), 929-944.
- Ghodke, A. B., Chavan, S. G., Sonawane, B. V., & Bharose, A. A., 2013. Isolation and *in vitro* identification of proteinase inhibitors from soybean seeds inhibiting *Helicoverpa* gut proteases. *Journal of Plant Interactions*, 8(2), 170-178.
- Girard, C., Bonade-Bottino, M., Pham-Delegue, M. H., & Jouanin, L., 1998. Two strains of cabbage seed weevil (Coleoptera: Curculionidae) exhibit differential susceptibility to a transgenic oilseed rape expressing *oryzacystatin* I. *Journal of Insect Physiology*, 44(7-8), 569-577.
- Goergen, G., Kumar, P.L., Sankung, S.B., Togola, A. and Tamo, M., 2016. First report of outbreaks of the fall armyworm *Spodoptera frugiperda* (JE Smith) (Lepidoptera, Noctuidae), a new alien invasive pest in West and Central Africa. *Plos One*, 11(10), 165.

- Goettig, P., Magdolen, V., & Brandstetter, H., 2010. Natural and synthetic inhibitors of kallikrein-related peptidases (KLKs). *Biochimie*, 92(11), 1546-1567.
- Gunning, R. V., Moores, G. D., & Devonshire, A. L., 1999. Esterase inhibitors synergise the toxicity of pyrethroids in Australian *Helicoverpa armigera* (Hubner) (Lepidoptera: Noctuidae). *Pesticide Biochemistry and Physiology*, 63(1), 50-62.
- Gupta, S. and Dikshit, A.K., 2010. Biopesticides: An eco-friendly approach for pest control. *Journal of Biopesticides*, 3(Special Issue), 186.
- Habib, H., & Fazili, K. M., 2007. Plant protease inhibitors: a defense strategy in plants. *Biotechnology and Molecular Biology Reviews*, 2(3), 68-85.
- Hamza, R., Perez-Hedo, M., Urbaneja, A., Rambla, J.L., Granell, A., Gaddour, K., Beltran, J.P. and Canas, L.A., 2018. Expression of two barley proteinase inhibitors in tomato promotes endogenous defensive response and enhances resistance to *Tuta absoluta*. *BMC Plant Biology*, *18*(1), 24.
- Hass, G. M., Nau, H., Biemann, K., Grahn, D. T., Ericsson, L. H., & Neurath, H., 1975. Amino acid sequence of a carboxypeptidase inhibitor from potatoes. *Biochemistry*, *14*(6), 1334-1342.
- Haukioja, E. and Neuvonen, S., 1985. Induced long-term resistance of birch foliage against defoliators: defensive or incidental?. *Ecology*, 66(4), 1303-1308.
- Iga, M., Nakaoka, T., Suzuki, Y., & Kataoka, H., 2004. Pigment dispersing factor regulates ecdysone biosynthesis via *Bombyx* neuropeptide G protein-coupled receptor-B2 in the prothoracic glands of *Bombyx mori*. *PloS one*, 9(7), e103239.
- Jacinto, T., Fernandes, K. V., Machado, O. L., & Siqueira-Junior, C. L., 1998. Leaves of transgenic tomato plants overexpressing prosystemin accumulate high levels of cystatin. *Plant Science*, 138(1), 35-42.
- Jadhav, A. R., War, A. R., Nikam, A. N., Adhav, A. S., Gupta, V. S., Sharma, H. C., & Tamhane, V. A., 2016. *Capsicum annuum* proteinase inhibitor ingestion negatively impacts the growth of sorghum pest *Chilo partellus* and promotes differential protease expression. *Biochemistry and Biophysics Reports*, 8, 302-309.
- Jamal, F., Pandey, P.K., Singh, D. and Khan, M.Y., 2013. Serine protease inhibitors in plants: nature's arsenal crafted for insect predators. *Phytochemistry Reviews*, 12(1), 1-34.
- Jamal, F., Singh, D., & Pandey, P. K., 2014. Negative effects of a non-host proteinase inhibitor of ~19.8 kDa from *Madhuca indica* seeds on developmental physiology of *Helicoverpa armigera* (Hubner). *Biomedical Research International*, 2014.
- Janssen, T., Husson, S. J., Meelkop, E., Temmerman, L., Lindemans, M., Verstraelen, K., & Schoofs, L., 2009. Discovery and characterization of a conserved pigment dispersing factor-like neuropeptide pathway in *Caenorhabditis elegans*. *Journal of Neurochemistry*, 111(1), 228-241.

Je, J., Song, C., Hwang, J.E., Chung, W.S. and Lim, C.O., 2014. DREB2C acts as a transcriptional activator of the thermo tolerance-related phytocystatin 4 (AtCYS4) gene. *Transgenic Research*, 23(1), 109-123.

Jedinak, A., & Maliar, T., 2005. Inhibitors of proteases as anticancer drugs-Minireview. *Neoplasma*, 52(3), 185-192.

Johnson, K.S. and Barbehenn, R.V., 2000. Oxygen levels in the gut lumens of herbivorous insects. *Journal of Insect Physiology*, 46(6), 897-903.

Joshi, R.S., Wagh, T.P., Sharma, N., Mulani, F.A., Sonavane, U., Thulasiram, H.V., Joshi, R., Gupta, V.S. and Giri, A.P., 2014. Way toward "dietary pesticides": molecular investigation of insecticidal action of caffeic acid against *Helicoverpa armigera*. *Journal of Agricultural and Food Chemistry*, 62(45), 10847-10854.

Jouanin, L., Bonade-Bottino, M., Girard, C., Morrot, G. and Giband, M., 1998. Transgenic plants for insect resistance. *Plant Science*, *131*(1), 1-11.

Kabsch, W., & Vandekerckhove, J., 1992. Structure and function of actin. *Annual Review of Biophysics and Biomolecular Structure*, 21(1), 49-76.

Kalavagunta, P.K., Pala, R., Pathipati, U.R. and Ravirala, N., 2014. Identification of Naphthol derivatives as novel antifeedants and insecticides. *Journal of Agricultural and Food Chemistry*, 62(28), 6571-6576.

Kashyap, M.P., Singh, A.K., Kumar, V., Tripathi, V.K., Srivastava, R.K., Agrawal, M., Khanna, V.K., Yadav, S., Jain, S.K. and Pant, A.B., 2011. Monocrotophos induced apoptosis in PC12 cells: role of xenobiotic metabolizing cytochrome P450s. *Plos One*, *6*(3), 17757.

Katoch, R., Singh, S.K., Thakur, N., Dutt, S., Yadav, S.K. and Shukle, R., 2014. Cloning, characterization, expression analysis and inhibition studies of a novel gene encoding Bowman-Birk type protease inhibitor from rice bean. *Gene*, 546(2), 342-351.

Kaur, R. and Rup, P.J., 2002. Evaluation of regulatory influence of four plant growth regulators on the reproductive potential and longevity of melon fruit fly (*Bactrocera cucurbitae*). *Phytoparasitica*, 30(3), 224-230.

Kellenberger, C., Boudier, C., Bermudez, I., Bieth, J. G., Luu, B., & Hietter, H., 1995. Serine protease inhibition by insect peptides containing a cysteine knot and a triple-stranded β-sheet. *Journal of Biological Chemistry*, 270(43), 25514-25519.

Kennedy, A. R., 1993. Anti-carcinogenic activity of protease inhibitors overview. In Protease inhibitors as cancer chemopreventive agents (9-64). Springer, Boston, MA.

Kennedy, A.R., 1998. Chemopreventive agents: protease inhibitors. *Pharmacology & Therapeutics*, 78(3), 167-209.

Kennedy, K.D., Anitha Christy, S.A., Buie, L.K. and Borras, T., 2012. Cystatin a, a potential common link for mutant myocilin causative glaucoma. *Plos One*, 7(5), 36301.

- Keppler, D., & Sierra, F., 2005. Role of cystatins in tumor neovascularization. 661-672
- Kervinen, J., Tobin, G. J., Costa, J., Waugh, D. S., Wlodawer, A., & Zdanov, A. (1999). Crystal structure of plant aspartic proteinase prophytepsin: inactivation and vacuolar targeting. *The EMBO journal*, *18*(14), 3947-3955.
- Kim, J. H., & Mullin, C. A., 2003. Anti-feedant effects of proteinase inhibitors on feeding behaviors of adult western corn rootworm (*Diabrotica virgifera*). *Journal of chemical Ecology*, 29(4), 795-810.
- King-Jones, K., & Thummel, C.S., 2005. Nuclear receptor, a perspective from *Drosophila. Nature Reviews Genetics*, 6(4), 311.
- Klomklao, S., Benjakul, S., Kishimura, H., & Chaijan, M., 2011. Extraction, purification and properties of trypsin inhibitor from Thai mung bean (*Vigna radiata*) Food Chemistry, 129(4), 1348-1354.
- Konus, M., Karaagac, S. U., & Iscan, M., 2014. Analysis of Molecular Resistance Mechanisms in *Helicoverpa armigera* (Hubner) (Noctuidae: Lepidoptera) Populations under Pyrethroid Stress in Turkey. *Journal of the Entomological Research Society*, *16*(2), 81.
- Konus, M., Koy, C., Mikkat, S., Kreutzer, M., Zimmermann, R., Iscan, M., & Glocker, M. O., 2013. Molecular adaptations of *Helicoverpa armigera* midgut tissue under pyrethroid insecticide stress characterized by differential proteome analysis and enzyme activity assays. *Comparative Biochemistry and Physiology Part D: Genomics and Proteomics*, 8(2), 152-162.
- Kopper, B.J., Jakobi, V.N., Osier, T.L. and Lindroth, R.L., 2002. Effects of paper birch condensed tannin on whitemarked tussock moth (Lepidoptera: Lymantriidae) performance. *Environmental Entomology*, 31(1), pp.10-14.
- Krishnamoorthy, M., Jurat-Fuentes, J. L., McNall, R. J., Andacht, T., & Adang, M. J., 2007. Identification of novel Cry1Ac binding proteins in midgut membranes from *Heliothis virescens* using proteomic analyses. *Insect Biochemistry and Molecular Biology*, 37(3), 189-201.
- Krowarsch, D., Cierpicki, T., Jelen, F. and Otlewski, J., 2003. Canonical protein inhibitors of serine proteases. *Cellular and Molecular Life Sciences CMLS*, 60 (11), 2427-2444.
- Kuhar, K., Kansal, R., Subrahmanyam, B., Koundal, K. R., Miglani, K., & Gupta, V. K., 2013. A Bowman-Birk protease inhibitor with antifeedant and antifungal activity from *Dolichos biflorus. Acta Physiologiae Plantarum*, *35*(6), 1887-1903.
- Kumar, P., Rao, A. A., Hariharaputran, S., Chandra, N., & Gowda, L. R., 2004. Molecular Mechanism of Dimerization of Bowman-Birk Inhibitors pivotal role of ASP76 in the dimerization. *Journal of Biological Chemistry*, 279(29), 30425-30432.
- Kumar, S. and Singh, A., 2014. Biopesticides for integrated crop management: environmental and regulatory aspects. *J Biofertilizers and Biopesticides*, 5, 121.

- Kumar, S., Singh, G. and Kumar, S.K.A., 2017. Evaluation of some novel insecticides against *Helicoverpa armigera* (Hubner) in black gram (*Vigna mungo*). Journal of Entomology and Zoology Studies 5(3) 183-185
- Kumar, V. and Gowda, L.R., 2013. The contribution of two disulfide bonds in the trypsin binding domain of horse gram (*Dolichos biflorus*) Bowman-Birk inhibitor to thermal stability and functionality. *Archives of Biochemistry and Biophysics*, 537(1), 49-61.
- La Porte, C. J., 2009. Saquinavir, the pioneer antiretroviral protease inhibitor. *Expert Opinion on Drug Metabolism & Toxicology*, 5(10), 1313-1322.
- Laing, W.A., McManus, M.T. and Allan, A.C. eds., 2002. *Protein-protein Interactions in Plant Biology*. Sheffield Academic Press.
- Laity, J. H., Lee, B. M., & Wright, P. E., 2001. Zinc finger proteins: new insights into structural and functional diversity. *Current Opinion in Structural Biology*, 11(1), 39-46.
- Lakshminarayana, M., & Duraimurugan, P., 2014. Assessment of avoidable yield losses due to insect pests in castor (*Ricinus communis L.*). Journal of Oilseed Research, 31(2): 140-144.
- Lakshminarayana, M., & Raoof, M. A., 2005. Insect pests and diseases of castor and their management. *Directorate of Oilseeds Research, Hyderabad*, 78.
- Laparra, J.M. and Haros, C.M., 2019. Plant seed protease inhibitors differentially affect innate immunity in a tumor microenvironment to control hepatocarcinoma. *Food & Function*, 10(7), 4210-4219.
- Laskowski Jr, M., & Kato, I., 1980. Protein inhibitors of proteinases. *Annual Review of Biochemistry*, 49(1), 593-626.
- Law, R. H., Zhang, Q., McGowan, S., Buckle, A. M., Silverman, G. A., Wong, W., & Whisstock, J. C., 2006. An overview of the serpin superfamily. *Genome Biology*, 7(5), 216.
- Lawrence, P. K., & Koundal, K. R., 2002. Plant protease inhibitors in control of phytophagous insects. *Electronic Journal of Biotechnology*, 5(1), 5-6.
- Ledoigt, G., Griffaut, B., Debiton, E., Vian, C., Mustel, A., Evray, G., & Madelmont, J. C., 2006. Analysis of secreted protease inhibitors after water stress in potato tubers. *International Journal of Biological Macromolecules*, 38(3-5), 268-271.
- Li, R., Wang, W., Li, F., Wang, Q., Xu, Y. and Wang, S., 2015. Overexpression of a cysteine proteinase inhibitor gene from Jatropha curcas confers enhanced tolerance to salinity stress. *Electronic Journal of Biotechnology*, 18(5), 368-375.
- Li, X., Schuler, M. A., & Berenbaum, M. R., 2007. Molecular mechanisms of metabolic resistance to synthetic and natural xenobiotics. *Annual Review of Entomology*, *52*, 231-253.

- Llibre, J. M., 2009. First-line boosted protease inhibitor-based regimens in treatment-naive HIV-1-infected patients--making a good thing better. *AIDS Reviews*, 11(4), 215-222.
- Lomate, P. R., & Hivrale, V. K., 2012. Wound and methyl jasmonate induced pigeon pea defensive proteinase inhibitor has potency to inhibit insect digestive proteinases. *Plant Physiology and Biochemistry*, *57*, 193-199.
- Lomate, P. R., & Hivrale, V. K., 2013. Effect of *Bacillus thuringiensis* (*Bt*) Cry1Ac toxin and protease inhibitor on growth and development of *Helicoverpa armigera* (Hubner). *Pesticide Biochemistry and Physiology*, 105(2), 77-83.
- Lopes, A. R., Juliano, M. A., Juliano, L., & Terra, W. R. 2004. Coevolution of insect trypsins and inhibitors. *Archives of Insect Biochemistry and Physiology: Published in Collaboration with the Entomological Society of America*, 55(3), 140-152.
- Lopez-Otin, C. and Bond, J.S., 2008. Proteases: multifunctional enzymes in life and disease. *Journal of Biological Chemistry*, 283(45), 30433-30437.
- Losso, J.N., 2008. The biochemical and functional food properties of the Bowman-Birk inhibitor. *Critical Reviews in Food Science and Nutrition*, 48(1), 94-118.
- LR Macedo, M., FR de Oliveira, C., M Costa, P., C Castelhano, E. and C Silva-Filho, M., 2015. Adaptive mechanisms of insect pests against plant protease inhibitors and future prospects related to crop protection: a review. *Protein and Peptide Letters*, 22(2), 149-163.
- Luo, M., Wang, Z., Li, H., Xia, K. F., Cai, Y., & Xu, Z. F., 2009. Overexpression of a weed (*Solanum americanum*) proteinase inhibitor in transgenic tobacco results in increased glandular trichome density and enhanced resistance to *Helicoverpa armigera* and *Spodoptera litura*. *International Journal of Molecular Sciences*, 10(4), 1896-1910.
- Maass, N., Teffner, M., Rosel, F., Pawaresch, R., Jonat, W., Nagasaki, K., & Rudolph, P., 2001. Decline in the expression of the serine proteinase inhibitor maspin is associated with tumour progression in ductal carcinomas of the breast. *The Journal of Pathology: A Journal of the Pathological Society of Great Britain and Ireland*, 195(3), 321-326.
- Macedo, M. L. R., Durigan, R. A., da Silva, D. S., Marangoni, S., Freire, M. D. G. M., & Parra, J. R. P., 2010. *Adenanthera pavonina* trypsin inhibitor retard growth of Anagasta kuehniella (Lepidoptera: Pyralidae). *Archives of Insect Biochemistry and Physiology: Published in Collaboration with the Entomological Society of America*, 73(4), 213-231.
- Machado, S.W., de Oliveira, C.F.R., Bezerra, C.D.S., Machado Freire, M.D.G., Regina Kill, M., Machado, O.L.T., Marangoni, S. and Macedo, M.L.R., 2013. Purification of a Kunitz-type inhibitor from Acacia polyphylla DC seeds: characterization and insecticidal properties against Anagasta kuehniella Zeller (Lepidoptera: Pyralidae). *Journal of Agricultural and Food Chemistry*, 61(10), 2469-2478.
- Mahapatra, C. T., & Rand, M. D., 2012. Methylmercury tolerance is associated with the humoral stress factor gene Turandot A. *Neurotoxicology and Teratology*, 34(4), 387-394.

- Maheswaran, G., Pridmore, L., Franz, P., & Anderson, M. A., 2007. A proteinase inhibitor from *Nicotiana alata* inhibits the normal development of light-brown apple moth, *Epiphyas postvittana* in transgenic apple plants. *Plant Cell Reports*, 26(6), 773-782.
- Manenti, T., Loeschcke, V., & Sorensen, J. G., 2018. Constitutive up-regulation of Turandot genes rather than changes in acclimation ability is associated with the evolutionary adaptation to temperature fluctuations in *Drosophila simulans*. *Journal of Insect Physiology*, 104, 40-47.
- Mao, Y. B., Tao, X. Y., Xue, X. Y., Wang, L. J., & Chen, X. Y., 2011. Cotton plants expressing CYP6AE14 double-stranded RNA show enhanced resistance to bollworms. *Transgenic Research*, 20(3), 665-673.
- Martinez, M., Santamaria, M.E., Diaz-Mendoza, M., Arnaiz, A., Carrillo, L., Ortego, F. and Diaz, I., 2016. Phytocystatins: defense proteins against phytophagous insects and Acari. *International Journal of Molecular Sciences*, 17(10), 1747.
- Matilla, A., Nicolas, G., Vicente, O. and Sierra, J.M., 1980. Preformed mRNA in Cotyledons of Ungerminated Seeds of *Cicer arietinum* L. *Plant physiology*, 65(6), 1128-1132.
- Matten, S.R., Frederick, R.J. and Reynolds, A.H., 2012. United States Environmental Protection Agency insect resistance management programs for plant-incorporated protectants and use of simulation modeling. In *Regulation of agricultural biotechnology: the United States and Canada*, 175-267. Springer, Dordrecht.
- McNall, R. J., & Adang, M. J., 2003. Identification of novel Bacillus thuringiensis Cry1Ac binding proteins in *Manduca sexta* midgut through proteomic analysis. *Insect Biochemistry and Molecular Biology*, 33(10), 999-1010.
- McPhalen, C. A., Svendsen, I., Jonassen, I., & James, M. N. G., 1985. Crystal and molecular structure of chymotrypsin inhibitor 2 from barley seeds in complex with subtilisin Novo. *Proceedings of the National Academy of Sciences*, 82(21), 7242-7246.
- Meiners, J.P., Elden, T.C., Summerfield, R.S. and Bunting, A.H., 1978. Advances in legume science. Kew: International Legume Conference.
- Mello, M. O., Tanaka, A. S., & Silva-Filho, M. C., 2003. Molecular evolution of Bowman-Birk type proteinase inhibitors in flowering plants. *Molecular phylogenetics and evolution*, 27(1), 103-112.
- Mendoza-Blanco, W. and Casaretto, J.A., 2012. The serine protease inhibitors and plant-insect interaction. *IDESIA* (*Chile*) *Enero-Abril*, 2012, 30(1).
- Merzendorfer, H., Kim, H. S., Chaudhari, S. S., Kumari, M., Specht, C. A., Butcher, S., & Muthukrishnan, S., 2012. Genomic and proteomic studies on the effects of the insect growth regulator diflubenzuron in the model beetle species *Tribolium castaneum*. *Insect Biochemistry and Molecular Biology*, 42(4), 264-276.

- Meyskens, F. L., & Szabo, E., 2005. Diet and cancer: the disconnect between epidemiology and randomized clinical trials. *Cancer Epidemiology and Prevention Biomarkers*, 14(6), 1366-1369.
- Mohanraj, S.S., Gujjarlapudi, M., Lokya, V., Mallikarjuna, N., Dutta-Gupta, A. and Padmasree, K., 2019. Purification and characterization of Bowman-Birk and Kunitz isoinhibitors from the seeds of *Rhynchosia sublobata* (Schumach.) Meikle, a wild relative of pigeon pea. *Phytochemistry*, *159*,159-171.
- Mohanraj, S.S., Tetali, S.D., Mallikarjuna, N., Dutta-Gupta, A. and Padmasree, K., 2018. Biochemical properties of a bacterially-expressed Bowman-Birk inhibitor from *Rhynchosia sublobata* (Schumach.) Meikle seeds and its activity against gut proteases of *Achaea janata. Phytochemistry*, 151, 78-90.
- Moon, J., Salzman, R. A., Ahn, J. E., Koiwa, H., & Zhu-Salzman, K., 2004. Transcriptional regulation in cowpea bruchid guts during adaptation to a plant defence protease inhibitor. *Insect Molecular Biology*, *13*(3), 283-291.
- Muddanuru, T., Polumetla, A.K., Maddukuri, L. and Mulpuri, S., 2019. Development and evaluation of transgenic castor (Ricinus communis L.) expressing the insecticidal protein Cry1Aa of *Bacillus thuringiensis* against lepidopteran insect pests. *Crop Protection*, 119, 113-125.
- Mueller, R., & Weder, J. K., 1989. Isolation and characterization of two trypsin-chymotrypsin inhibitors from lentil seeds (*Lens Culinaris medic.*) 1. *Journal of Food Biochemistry*, 13(1), 39-63.
- Mundt, K. E., Porte, J., Murray, J. M., Brikos, C., Christensen, P. U., Caspari, T., & Carr, A. M., 1999. The COP9/signalosome complex is conserved in fission yeast and has a role in S phase. *Current Biology*, *9*(23), 1427-1433.
- Muricken, D.G. and Gowda, L.R., 2010. Functional expression of horse gram (Dolichos biflorus) Bowman-Birk inhibitor and its self-association. *Biochimica et Biophysica Acta* (*BBA*)-*Proteins and Proteomics*, 1804(7), 1413-1423.
- Naggie, S., & Hicks, C., 2010. Protease inhibitor-based antiretroviral therapy in treatment-naive HIV-1-infected patients: the evidence behind the options. *Journal of Antimicrobial Chemotherapy*, 65(6), 1094-1099.
- Nakahata, A.M., Bueno, N.R., Rocha, H.A., Franco, C.R., Chammas, R., Nakaie, C.R., Jasiulionis, M.G., Nader, H.B., Santana, L.A., Sampaio, M.U. and Oliva, M.L.V., 2006. Structural and inhibitory properties of a plant proteinase inhibitor containing the RGD motif. *International Journal of Biological Macromolecules*, 40(1), 22-29.
- Ningshen, T.J., Chauhan, V.K., Dhania, N.K. and Dutta-Gupta, A., 2017. Insecticidal effects of hemocoelic delivery of Bacillus thuringiensis Cry toxins in Achaea janata larvae. *Frontiers in Physiology*, 8, 289.
- Ninkovic, S., Miljus-Dukic, J., Radovic, S., Maksimovic, V., Lazarevic, J., Vinterhalter, B., & Smigocki, A., 2007. *Phytodecta fornicata Brüggemann* resistance mediated by

- oryzacystatin II proteinase inhibitor transgene. Plant Cell, Tissue and Organ Culture, 91(3), 289-294.
- Nobar, S. M., Guy-Crotte, O., Rabaud, M., & Bieth, J. G., 2004. Inhibition of human pancreatic proteinases by human plasma α 2-antiplasmin and antithrombin. *Biological Chemistry*, 385(5), 423-427.
- Noma, T., Colunga-Garcia, M., Brewer, M., Landis, J. and Gooch, A., 2010. Oriental leafworm, Spodoptera litura. *Michigan State University's invasive species fact sheets. Feburary*.
- Odani, S. and Ikenaka, T., 1972. Studies on soybean trypsin inhibitors: IV. Complete amino acid sequence and the anti-proteinase sites of Bowman-Birk soybean proteinase inhibitor. *The Journal of Biochemistry*, 71(5), 839-848.
- Oliva, M. L. V., & Sampaio, M. U., 2008. *Bauhinia* Kunitz-type proteinase inhibitors: structural characteristics and biological properties. *Biological Chemistry*, 389(8), 1007-1013.
- Oliva, M. L. V., Silva, M. C., Sallai, R. C., Brito, M. V., & Sampaio, M. U., 2009. A novel sub-classification for Kunitz proteinase inhibitors from leguminous seeds. *Biochimie*, 92(11), 1667-1673.
- Oliva, M.L.V., Souza-Pinto, J.C., Batista, I.F., Araujo, M.S., Silveira, V.F., Auerswald, E.A., Mentele, R., Eckerskorn, C., Sampaio, M.U. and Sampaio, C.A., 2000. Leucaena leucocephala serine proteinase inhibitor: primary structure and action on blood coagulation, kinin release and rat paw edema. *Biochimica et Biophysica Acta (BBA)-Protein Structure and Molecular Enzymology*, 1477(1-2), 64-74.
- Oliveira, A. S., Migliolo, L., Aquino, R. O., Ribeiro, J. K., Macedo, L. L., Andrade, L. B., & Mauricio, P., 2007. Purification and characterization of a trypsin—papain inhibitor from *Pithecelobium dumosum* seeds and its *in vitro* effects towards digestive enzymes from insect pests. *Plant Physiology and Biochemistry*, 45(10-11), 858-865.
- Otlewski, J., Krowarsch, D., & Apostoluk, W., 1999. Protein inhibitors of serine proteinases. *Acta Biochimica Polonica*, 46(3), 531-565.
- Ottea, J. A., & Plapp Jr, F. W., 1984. Glutathione S-transferase in the house fly: biochemical and genetic changes associated with induction and insecticide resistance. *Pesticide Biochemistry and Physiology*, 22(2), 203-208.
- Page, M.J. and Di Cera, E., 2008. Evolution of peptidase diversity. *Journal of Biological Chemistry*, 283(44), 30010-30014.
- Paiva, P. M. G., Oliva, M. L. V., Fritz, H., Coelho, L. C. B. B., & Sampaio, C. A. M., 2006. Purification and primary structure determination of two Bowman-Birk type trypsin isoinhibitors from *Cratylia mollis* seeds. *Phytochemistry*, 67(6), 545-552.
- Parde, V. D., Sharma, H. C., & Kachole, M. S., 2010. *In vivo* inhibition of *Helicoverpa armigera* gut pro-proteinase activation by non-host plant protease inhibitors. *Journal of Insect Physiology*, 56(9), 1315-1324.

- Pariani, S., Contreras, M., Rossi, F.R., Sander, V., Corigliano, M.G., Simón, F., Busi, M.V., Gomez-Casati, D.F., Pieckenstain, F.L., Duschak, V.G. and Clemente, M., 2016. Characterization of a novel Kazal-type serine proteinase inhibitor of *Arabidopsis thaliana*. *Biochimie*, 123, 85-94.
- Pekkarinen, A.I., Longstaff, C. and Jones, B.L., 2007. Kinetics of the inhibition of Fusarium serine proteinases by barley (*Hordeum vulgare L.*) inhibitors. *Journal of Agricultural and Food Chemistry*, 55(7), 2736-2742.
- Perea, D., Molohon, K., Edwards, K., & Diaz-Benjumea, F. J., 2013. Multiple roles of the gene zinc finger homeodomain-2 in the development of the *Drosophila* wing. *Mechanisms of Development*, 130(9-10), 467-481.
- Pereira, R. D. A., Valencia-Jiménez, A., Magalhaes, C. P., Prates, M. V., Melo, J. A. T., de Lima, L. M., ... & Grossi-de-Sa, M. F., 2007. Effect of a Bowman-Birk proteinase inhibitor from *Phaseolus coccineus* on *Hypothenemus hampei* gut proteinases *in vitro*. *Journal of Agricultural and Food Chemistry*, 55(26), 10714-10719.
- Pettit, S. C., Everitt, L. E., Choudhury, S., Dunn, B. M., & Kaplan, A. H., 2004. Initial cleavage of the human immunodeficiency virus type 1 GagPol precursor by its activated protease occurs by an intramolecular mechanism. *Journal of Virology*, 78(16), 8477-8485.
- Pollard, T. D., & Cooper, J. A., 2009. Actin, a central player in cell shape and movement. *Science*, 326(5957), 1208-1212.
- Prakash, B., Selvaraj, S., Murthy, M. R. N., Sreerama, Y. N., Rao, D. R., & Gowda, L. R., 1996. Analysis of the amino acid sequences of plant Bowman-Birk inhibitors. *Journal of Molecular Evolution*, 42(5), 560-569.
- Prasad, E. R., Dutta-Gupta, A., & Padmasree, K., 2009. Inhibitors from pigeon pea active against lepidopteran gut proteinases. *Journal of Economic Entomology*, 102(6), 2343-2349.
- Prasad, E. R., Dutta-Gupta, A., & Padmasree, K., 2010a. Insecticidal potential of Bowman-Birk proteinase inhibitors from red gram (*Cajanus cajan*) and black gram (*Vigna mungo*) against lepidopteran insect pests. *Pesticide Biochemistry and Physiology*, 98(1), 80-88.
- Prasad, E.R., Dutta-Gupta, A. and Padmasree, K., 2010b. Purification and characterization of a Bowman-Birk proteinase inhibitor from the seeds of black gram (*Vigna mungo*). *Phytochemistry*, 71(4), 363-372.
- Prasad, E.R., Komera, V.R., Padmasree, K. and Dutta-Gupta, A., 2011. Plant proteinase inhibitors and their potential in insect pest management. *Entomology: Ecology and Biodiversity, Scientific Publishers, Jodhpur, India*, 268-291.
- Qi, X. L., Su, X. F., Lu, G. Q., Liu, C. X., Liang, G. M., & Cheng, H. M., 2015. The effect of silencing arginine kinase by RNAi on the larval development of *Helicoverpa armigera*. *Bulletin of entomological research*, 105(5), 555-565.

- Qiu, L., Wu, T., Dong, H., Wu, L., Cao, J. and Huang, L., 2013. High-level expression of sporamin in transgenic Chinese cabbage enhances resistance against diamondback moth. *Plant Molecular Biology Reporter*, *31*(3), 657-664.
- Quilis, J., López-García, B., Meynard, D., Guiderdoni, E. and San Segundo, B., 2014. Inducible expression of a fusion gene encoding two proteinase inhibitors leads to insect and pathogen resistance in transgenic rice. *Plant biotechnology journal*, 12(3), 367-377.
- Quillien, L., Ferrasson, E., Molle, D., & Gueguen, J., 1997. Trypsin inhibitor polymorphism: multigene family expression and posttranslational modification. *Journal of Protein Chemistry*, 16(3), 195-203.
- Radyuk, S. N., Klichko, V. I., Spinola, B., Sohal, R. S., & Orr, W. C., 2001. The peroxiredoxin gene family in *Drosophila melanogaster*. Free Radical Biology and Medicine, 31(9), 1090-1100.
- Rai, K.K. and Rai, A.C., 2020. Recent Transgenic Approaches for Stress Tolerance in Crop Plants. In *Sustainable Agriculture in the Era of Climate Change* (pp. 533-556). Springer, Cham.
- Rajapakse, C. N. K., & Walter, G. H., 2007. Polyphagy and primary host plants: oviposition preference versus larval performance in the lepidopteran pest Helicoverpa armigera. Arthropod-Plant Interactions, I(1), 17-26.
- Rani, P.U. and Devanand, P., 2013. Bioactivities of caffeic acid methyl ester (methyl-(E)-3-(3, 4-dihydroxyphenyl) prop-2-enoate): a hydroxyl cinnamic acid derivative from Solanum melongena L. fruits. *Journal of Pest Science*, 86(3), 579-589.
- Rani, P.U., Madhusudhanamurthy, J. and Sreedhar, B., 2014. Dynamic adsorption of α-pinene and linalool on silica nanoparticles for enhanced antifeedant activity against agricultural pests. *Journal of Pest Science*, 87(1), 191-200.
- Rao, M.S.A., Suresh, G., Yadav, P.A., Prasad, K.R., Rani, P.U., Rao, C.V. and Babu, K.S., 2015. Piscidinols H–L, apotirucallane triterpenes from the leaves of Walsura trifoliata and their insecticidal activity. *Tetrahedron*, 71(9), 1431-1437.
- Rashid, M., Khan, R. A., & Zhang, Y. L., 2013. Over-expression of Cytochrome P450s in *Helicoverpa armigera* in Response to Bio-insecticide, Cantharidin. *International Journal of Agriculture & Biology*, 15(5).
- Rauf, I., Javaid, S., Naqvi, R. Z., Mustafa, T., Amin, I., Mukhtar, Z., & Mansoor, S., 2019. In-planta expression of insecticidal proteins provides protection against lepidopteran insects. *Scientific Reports*, *9*(1), 6745.
- Richardson, M., 1991. Seed storage proteins: the enzyme inhibitors. *Amino acids*, *Proteins and Nucleic Acids*.
- Richardson, M., Campos, F. A. P., Xavier-Filho, J., Macedo, M. L. R., Maia, G. M. C., & Yarwood, A., 1986. The amino acid sequence and reactive (inhibitory) site of the major trypsin isoinhibitor (DE5) isolated from seeds of the *Brazilian Carolina* tree

- (Adenanthera pavonina L.). Biochimica et Biophysica Acta (BBA)-Protein Structure and Molecular Enzymology, 872(1-2), 134-140.
- Ridky, T., & Leis, J., 1995. Development of drug resistance to HIV-1 protease inhibitors. *Journal of Biological Chemistry*, 270(50), 29621-29623.
- Rocha, I. F., Maller, A., Simão, R. D. C. G., Kadowaki, M. K., Alves, L. F. A., Huergo, L. F., & da Conceicao Silva, J. L., 2016. Proteomic profile of hemolymph and detection of induced antimicrobial peptides in response to microbial challenge in *Diatraea saccharalis* (Lepidoptera: Crambidae). *Biochemical and Biophysical Research Communications*, 473(2), 511-516.
- Rudek, M. A., Venitz, J., & Figg, W. D., 2002. Matrix metalloproteinase inhibitors: do they have a place in anticancer therapy? *Pharmacotherapy: The Journal of Human Pharmacology and Drug Therapy*, 22(6), 705-720.
- Rustgi, S., Boex-Fontvieille, E., Reinbothe, C., von Wettstein, D. and Reinbothe, S., 2018. The complex world of plant protease inhibitors: Insights into a Kunitz-type cysteine protease inhibitor of Arabidopsis thaliana. *Communicative & Integrative Biology*, 11(1), 136.
- Ryan, C. A., 1990. Protease inhibitors in plants: genes for improving defenses against insects and pathogens. *Annual Review of Phytopathology*, 28(1), 425-449.
- Saikhedkar, N. S., Joshi, R. S., Yadav, A. K., Seal, S., Fernandes, M., & Giri, A. P., 2019. Phyto-inspired cyclic peptides derived from plant Pin-II type protease inhibitor reactive center loops for crop protection from insect pests. *Biochimica et Biophysica Acta (BBA)-General Subjects*, 1863(8), 1254-1262.
- Sakamoto, H., Maruyama, K., Sakuma, Y., Meshi, T., Iwabuchi, M., Shinozaki, K., & Yamaguchi-Shinozaki, K., 2004. *Arabidopsis* Cys2/His2-type zinc-finger proteins function as transcription repressors under drought, cold, and high-salinity stress conditions. *Plant Physiology*, *136*(1), 2734-2746.
- Salehipour-Shirazi, G., Ferguson, L. V., & Sinclair, B. J., 2017. Does cold activate the Drosophila melanogaster immune system?. *Journal of insect physiology*, *96*, 29-34.
- Salu, B.R., Pando, S.C., Brito, M.V.D., Medina, A.F., Odei-Addo, F., Frost, C., Naude, R., Sampaio, M.U., Emsley, J., Maffei, F.H.A. and Oliva, M.L.V., 2019. Improving the understanding of plasma kallikrein contribution to arterial thrombus formation using two plant protease inhibitors. *Platelets*, *30*(3), 305-313.
- Sasaki, D. Y., Jacobowski, A. C., de Souza, A. P., Cardoso, M. H., Franco, O. L., & Macedo, M. L. R., 2015. Effects of proteinase inhibitor from *Adenanthera pavonina* seeds on short-and long term larval development of *Aedes aegypti*. *Biochimie*, *112*, 172-186.
- Schagger, H., & Von Jagow, G., 1987. Tricine-sodium dodecyl sulfate-polyacrylamide gel electrophoresis for the separation of proteins in the range from 1 to 100 kDa. *Analytical Biochemistry*, 166(2), 368-379.

- Schon, A., Ingaramo, M., & Freire, E., 2003. The binding of HIV-1 protease inhibitors to human serum proteins. *Biophysical Chemistry*, 105(2-3), 221-230.
- Schuler, M. A., 2012. Insect P450s: mounted for battle in their war against toxins. *Molecular Ecology*, 21(17), 4157-4159.
- Schwechheimer, C., & Deng, X. W., 2000. COP9 signalosome revisited: a novel mediator of protein degradation. *Trends in Cell Biology*, 11(10), 420-426.
- Scott, I.M., Thaler, J.S. and Scott, J.G., 2010. Response of a generalist herbivore Trichoplusia ni to jasmonate-mediated induced defense in tomato. *Journal of Chemical Ecology*, *36*(5), 490-499.
- Seeram, S. S., Hiraga, K., & Oda, K., 1997. Resynthesis of reactive site peptide bond and temporary inhibition of *Streptomyces* metalloproteinase inhibitor. *The Journal of Biochemistry*, 122(4), 788-794.
- Shafeeq, T., UlAbdin, Z., & Lee, K. Y., 2017. Induction of stress-and immune-associated genes in the Indian meal moth *Plodia interpunctella* against envenomation by the ectoparasitoid Bracon hebetor. *Archives of Insect Biochemistry and Physiology*, 96(2), 214.
- Shamsi, T.N., Parveen, R. and Fatima, S., 2016. Characterization, biomedical and agricultural applications of protease inhibitors: A review. *International Journal of Biological Macromolecules*, 91, 1120-1133.
- Sharma, H.C., Pampapathy, G., Dhillon, M.K. and Ridsdill-Smith, J.T., 2005. Detached leaf assay to screen for host plant resistance to *Helicoverpa armigera*. *Journal of Economic Entomology*, 98(2), 568-576.
- Shayegan, D., Jalali Sendi, J., Sahragard, A. and Zibaee, A., 2019. Antifeedant and cytotoxic activity of gibberellic acid against *Helicoverpa armigera* (Hübner) (Lepidoptera: Noctuidae). *Physiological Entomology*, 44(2), 169-176.
- Shevchenko, A., 1996. Wilm M, Vorm O, and Mann M. Mass spectrometric sequencing of proteins silver-stained polyacrylamide gels. *Anal Chem*, 68, 850-858.
- Shin, S. W., Park, S. S., Park, D. S., Kim, M. G., Kim, S. C., Brey, P. T., & Park, H. Y., 1998. Isolation and characterization of immune-related genes from the fall webworm, *Hyphantria cunea*, using PCR-based differential display and subtractive cloning. *Insect Biochemistry and Molecular Biology*, 28(11), 827-837.
- Siddiqui, H.A., Asif, M., Asad, S., Naqvi, R.Z., Ajaz, S., Umer, N., Anjum, N., Rauf, I., Sarwar, M., Arshad, M. and Amin, I., 2019. Development and evaluation of double gene transgenic cotton lines expressing Cry toxins for protection against chewing insect pests. *Scientific Reports*, 9(1), pp.1-7.
- Silverman, G. A., 2001. The serpins are an expanding superfamily of structurally similar but functionally diverse proteins. Evolution, novel functions, mechanism of inhibition and a revised nomenclature. *J. Biol. Chem*, 276, 33293-33296.

- Singh, D., Jamal, F., & Pandey, P. K., 2014. Kinetic assessment and effect on developmental physiology of a trypsin inhibitor from *Eugenia jambolana* (Jambul) seeds on *Helicoverpa armigera* (Hubner). *Archives of Insect Biochemistry and Physiology*, 85(2), 94-113.
- Singh, R.R. and Rao, A.A., 2002. Reductive unfolding and oxidative refolding of a Bowman-Birk inhibitor from horse gram seeds (*Dolichos biflorus*): evidence for 'hyperreactive'disulfide bonds and rate-limiting nature of disulfide isomerization in folding. *Biochimica et Biophysica Acta (BBA)-Protein Structure and Molecular Enzymology*, 1597(2), 280-291.
- Singh, S., Kumar, S. and Basappa, H., 2005. Validation of IPM technologies for the castor crop in rainfed agro-ecosystem. *Annals of Plant Protection Sciences*, 13(1), 105-110.
- Smigocki, A.C., Ivic-Haymes, S., Li, H. and Savic, J., 2013. Pest protection conferred by a *Beta vulgaris* serine proteinase inhibitor gene. *Plos One*, 8(2), 573.
- Smith-Pardo, A., 2014. The old world bollworm *Helicoverpa armigera* (Hubner) (Lepidoptera: noctuidae: Heliothinae) its biology, economic importance and its recent introduction into the Western Hemisphere. *Bol. Mus. Entomol. Univ. Valle*, 6(1), 18-28.
- Solomon, M., Belenghi, B., Delledonne, M., Menachem, E. and Levine, A., 1999. The involvement of cysteine proteases and protease inhibitor genes in the regulation of programmed cell death in plants. *The Plant Cell*, 11(3), 431-443.
- Srikanth, S. and Chen, Z., 2016. Plant protease inhibitors in therapeutics-focus on cancer therapy. *Frontiers in pharmacology*, 7, p.470.
- Srinivasa Rao, M., Rama Rao, C.A., Srinivas, K., Pratibha, G., Vidya Sekhar, S.M., Sree Vani, G. and Venkateswarlu, B., 2012. Intercropping for management of insect pests of castor, *ricinus communis*, in the semi-arid tropics of India. *Journal of Insect Science*, 12(1), 14.
- Srinivasan, A., Giri, A.P. and Gupta, V.S., 2006. Structural and functional diversities in lepidopteran serine proteases. *Cellular & Molecular Biology Letters*, 11(1), 132-154.
- Srinivasan, T., Kumar, K.R.R. and Kirti, P.B., 2009. Constitutive expression of a trypsin protease inhibitor confers multiple stress tolerance in transgenic tobacco. *Plant and Cell Physiology*, 50(3), 541-553.
- Srivastava, K., Sharma, D., Anal, A.K.D. and Sharma, S., 2015. Integrated Management of *Spodoptera litura*: a review. *International Journal of Life Sciences Scientific Reports*, 4(1), 1536-1538.
- Sujatha, M., Devi, P. V., & Reddy, T. P., 2011. Insect Pests of Castor (*Ricinus communis L*) and their Management Strategies. BS Publications, CRC Press.
- Sun, X., Yang, S., Sun, M., Wang, S., Ding, X., Zhu, D., Ji, W., Cai, H., Zhao, C., Wang, X. and Zhu, Y., 2014. A novel *Glycine soja* cysteine proteinase inhibitor GsCPI14,

- interacting with the calcium/calmodulin-binding receptor-like kinase GsCBRLK, regulated plant tolerance to alkali stress. *Plant Molecular Biology*, 85(1-2), 33-48.
- Swaney, K. F., & Li, R., 2016. Function and regulation of the Arp2/3 complex during cell migration in diverse environments. *Current Opinion in Cell Biology*, 42, 63-72.
- Swaroopa Rani, T., & Podile, A. R., 2014. Extracellular matrix-associated proteome changes during non-host resistance in citrus—Xanthomonas interactions. *Physiologia plantarum*, 150(4), 565-579.
- Swathi, M., Lokya, V., Swaroop, V., Mallikarjuna, N., Kannan, M., Dutta-Gupta, A. and Padmasree, K., 2014. Structural and functional characterization of proteinase inhibitors from seeds of *Cajanus cajan* (cv. ICP 7118). *Plant Physiology and Biochemistry*, 83, 77-87.
- Swathi, M., Mishra, P.K., Lokya, V., Swaroop, V., Mallikarjuna, N., Dutta-Gupta, A. and Padmasree, K., 2016. Purification and partial characterization of trypsin-specific proteinase inhibitors from pigeon pea wild relative *Cajanus platycarpus* L. (Fabaceae) active against gut proteases of lepidopteran pest *Helicoverpa armigera*. *Frontiers in physiology*, 7, 388.
- Swathi, M., Mohanraj, S.S., Swaroop, V., Gujjarlapudi, M., Mallikarjuna, N., Dutta-Gupta, A. and Padmasree, K., 2015. Proteinase inhibitors from *Cajanus platycarpus* accessions active against pod borer *Helicoverpa armigera*. *Acta Physiologiae Plantarum*, *37*(11), 242.
- Swiatkiewicz, S., Swiatkiewicz, M., Arczewska-Wlosek, A. and Jozefiak, D., 2014. Genetically modified feeds and their effect on the metabolic parameters of food-producing animals: A review of recent studies. *Animal Feed Science and Technology*, 198, 1-19.
- Tabashnik, B.E., Mota-Sanchez, D., Whalon, M.E., Hollingworth, R.M. and Carriere, Y., 2014. Defining terms for proactive management of resistance to *Bt* crops and pesticides. *Journal of Economic Entomology*, *107*(2), 496-507.
- Talekar, N. S., Opena, R. T., & Hanson, P., 2006. *Helicoverpa armigera* management: a review of AVRDC's research on host plant resistance in tomato. *Crop Protection*, 25(5), 461-467.
- Tan, Y., Li, M. and Ma, F., 2015. Overexpression of MpCYS2, a phytocystatin gene from *Malus prunifolia* (Willd.) Borkh, confers drought tolerance and protects against oxidative stress in *Arabidopsis*. *Plant Cell, Tissue and Organ Culture* (*PCTOC*), *123*(1), 15-27.
- Tanpure, R.S., Barbole, R.S., Dawkar, V.V., Waichal, Y.A., Joshi, R.S., Giri, A.P. and Gupta, V.S., 2017. Improved tolerance against Helicoverpa armigera in transgenic tomato over-expressing multi-domain proteinase inhibitor gene from *Capsicum annuum*. *Physiology and Molecular Biology of Plants*, 23(3), 597-604.
- Tay, W.T., Walsh, T.K., Downes, S., Anderson, C., Jermiin, L.S., Wong, T.K., Piper, M.C., Chang, E.S., Macedo, I.B., Czepak, C. and Behere, G.T., 2017. Mitochondrial

- DNA and trade data support multiple origins of *Helicoverpa armigera* (Lepidoptera, Noctuidae) in Brazil. *Scientific Reports*, 7, 45302.
- Telang, M. A., Giri, A. P., Pyati, P. S., Gupta, V. S., Tegeder, M., & Franceschi, V. R., 2009. Winged bean chymotrypsin inhibitors retard growth of *Helicoverpa armigera*. *Gene*, 431(1-2), 80-85.
- Telang, M., Srinivasan, A., Patankar, A., Harsulkar, A., Joshi, V., Damle, A., & Birah, A., 2003. Bitter gourd proteinase inhibitors: potential growth inhibitors of *Helicoverpa armigera* and *Spodoptera litura*. *Phytochemistry*, 63(6), 643-652.
- Vasudev, A., & Sohal, S., 2016. Partially purified *Glycine max* proteinase inhibitors: potential bioactive compounds against tobacco cutworm, *Spodoptera litura* (Fabricius, 1775) (Lepidoptera: Noctuidae). *Turkish Journal of Zoology*, 40(3), 379-387.
- Velmurugan, G.; Venkatesh, B. D. D.; Ramasamy, S. Prolonged monocrotophos intake induces cardiac oxidative stress and myocardial damage in rats. Toxicology, 2013, 307, 103–108.
- Wang, H. X., & Ng, T. B., 2001. Examination of lectins, polysaccharopeptide, polysaccharide, alkaloid, coumarin and trypsin inhibitors for inhibitory activity against human immunodeficiency virus reverse transcriptase and glycohydrolases. *Planta Medica*, 67(07), 669-672.
- Wang, J., Shi, Z. Y., Wan, X. S., Shen, G. Z., & Zhang, J. L., 2008. The expression pattern of a rice proteinase inhibitor gene OsPI8-1 implies its role in plant development. *Journal of Plant Physiology*, 165(14), 1519-1529.
- Wang, W. and Wang, X., 2017. Single-cell CRISPR screening in drug resistance, 207-210.
- Wang, W., Zhao, P., Zhou, X.M., Xiong, H.X. and Sun, M.X., 2015. Genome-wide identification and characterization of cystatin family genes in rice (Oryza sativa L.). *Plant Cell Reports*, *34*(9), 1579-1592.
- War, A.R. and Sharma, H.C., 2014. Effect of jasmonic acid and salicylic acid-induced resistance in groundnut on *Helicoverpa armigera*. *Physiological Entomology*, 39(2), 136-142.
- Wei, J., Guo, Y., Liang, G., Wu, K., Zhang, J., Tabashnik, B.E. and Li, X., 2015. Cross-resistance and interactions between *Bt* toxins Cry1Ac and Cry2Ab against the cotton bollworm. *Scientific Reports*, 5(1), 1-7.
- Wei, N., & Deng, X. W., 1999. Making sense of the COP9 signalosome: a regulatory protein complex conserved from *Arabidopsis* to human. *Trends in Genetics*, 15(3), 98-103.
- Wei, N., Chamovitz, D. A., & Deng, X. W., 1994. Arabidopsis COP9 is a component of a novel signaling complex mediating light control of development. *Cell*, 78(1), 117-124.

- Wilson, K. A., & Chen, J. C., 1983. Amino acid sequence of mung bean trypsin inhibitor and its modified forms appearing during germination. *Plant Physiology*, 71(2), 341-349.
- Winer, A., Adams, S. and Mignatti, P., 2018. Matrix metalloproteinase inhibitors in cancer therapy: turning past failures into future successes. *Molecular Cancer Therapeutics*, 17(6), 1147-1155.
- Wolfson, J. L., & Murdock, L. L., 1987. Suppression of larval Colorado potato beetle growth and development by digestive proteinase inhibitors. *Entomologia Experimentalis et Applicata*, 44(3), 235-240.
- Wu, S. Y., Tong, X. L., Li, C. L., Ding, X., Zhang, Z. L., Fang, C. Y., ... & Dai, F. Y., 2019. BmBlimp-1 gene encoding a C2H2 zinc finger protein is required for wing development in the silkworm *Bombyx mori. International journal of biological sciences*, 15(12), 2664.
- Wu, Y., Long, Q., Xu, Y., Guo, S., Chen, T., Wang, L., & Walker, B., 2017. A structural and functional analogue of a Bowman–Birk-type protease inhibitor from *Odorrana schmackeri*. *Bioscience Reports*, *37*(2), BSR20160593.
- Xie, X. J., Hsu, F. N., Gao, X., Xu, W., Ni, J. Q., Xing, Y., ... & Zheng, Y., 2015. CDK8-cyclin C mediates nutritional regulation of developmental transitions through the ecdysone receptor in *Drosophila*. *PLos Biology*, *13*(7), 207.
- Yadav, P.A., Suresh, G., Rao, M.S.A., Shankaraiah, G., Rani, P.U. and Babu, K.S., 2014. Limonoids from the leaves of Soymida febrifuga and their insect antifeedant activities. *Bioorganic & Medicinal Chemistry Letters*, 24(3), 888-892.
- Yan, Y., Zhang, Y., Huaxia, Y., Wang, X., Yao, P., Guo, X., & Xu, B., 2014. Identification and characterisation of a novel 1-Cys thioredoxin peroxidase gene (AccTpx5) from *Apis cerana cerana*. *Comparative Biochemistry and Physiology Part B: Biochemistry and Molecular Biology*, 172, 39-48.
- Yang, P. J., Zhan, M. Y., Ye, C., Yu, X. Q., & Rao, X. J., 2017. Molecular cloning and characterization of a short peptidoglycan recognition protein from silkworm *Bombyx mori. Insect molecular biology*, 26(6), 665-676.
- Yasur, J. and Rani, P.U., 2015. Lepidopteran insect susceptibility to silver nanoparticles and measurement of changes in their growth, development and physiology. *Chemosphere*, 124, 92-102.
- Yi, J., Wu, H., Liu, J., Lai, X., Guo, J., Li, D., & Zhang, G., 2018. Molecular characterization and expression of six heat shock protein genes in relation to development and temperature in *Trichogramma chilonis*. *PloS one*, *13*(9), 203.
- Yuan, C., Ding, X., Xia, L., Yin, J., Huang, S., & Huang, F., 2011. Proteomic analysis of BBMV in *Helicoverpa armigera* midgut with and without Cry1Ac toxin treatment. *Biocontrol Science and Technology*, 21(2), 139-151.

- Zhang, K., Pan, G., Zhao, Y., Hao, X., Li, C., Shen, L., Zhang, R., Su, J. and Cui, H., 2017. A novel immune-related gene HDD1 of silkworm *Bombyx mori* is involved in bacterial response. *Molecular Immunology*, 88, 106-115.
- Zhang, Y., & Lu, Z., 2015. Peroxiredoxin 1 protects the pea aphid *Acyrthosiphon pisum* from oxidative stress induced by *Micrococcus luteus* infection. *Journal of Invertebrate Pathology*, 127, 115-121.
- Zhao, Q., Ma, D., Huang, Y., He, W., Li, Y., Vasseur, L., & You, M., 2018. Genome-wide investigation of transcription factors provides insights into transcriptional regulation in *Plutella xylostella*. *Molecular Genetics and Genomics*, 293(2), 435-449.
- Zhong, Y., Ahmed, S., Deng, G., Fan, W., Zhang, P. and Wang, H., 2019. Improved insect resistance against *Spodoptera litura* in transgenic sweet potato by overexpressing Cry1Aa toxin. *Plant Cell Reports*, 38(11), 1439-1448.
- Zhou, J., Shang, Y., Wang, K., Sun, S., & Yu, J., 2019. COP9 signalosome CSN4 and 5 subunits are involved in jasmonate-dependent defense against root-knot nematode in tomato. *Frontiers in Plant Science*, 10, 1223.
- Zhu, W., Bai, X., Li, G., Chen, M., Wang, Z., & Yang, Q., 2019. SpCYS, a cystatin gene from wild potato (*Solanum pinnatisectum*), is involved in the resistance against *Spodoptera litura*. Theoretical and Experimental Plant Physiology, 1-12.
- Zhu, Z., Chai, Y., Jiang, Y., Li, W., Hu, H., Li, W., & Ou, G., 2016. Functional coordination of WAVE and WASP in *C. elegans* neuroblast migration. *Developmental Cell*, 39(2), 224-238.
- Zhu-Salzman, K. and Zeng, R., 2015. Insect response to plant defensive protease inhibitors. *Annual Review of Entomology*, 60, 233-252.

Publications & conference attended

Publications:

- 1) Swathi, M., Lokya, V., Swaroop, V., Mallikarjuna, N., Kannan, M., Dutta-Gupta, A., & Padmasree, K. (2014). Structural and functional characterization of proteinase inhibitors from seeds of *Cajanus cajan* (cv. ICP 7118). *Plant physiology and biochemistry*, 83, 77-87.
- 2) Swathi, M., Mohanraj, S. S., Swaroop, V., Gujjarlapudi, M., Mallikarjuna, N., Dutta-Gupta, A., & Padmasree, K. (2015). Proteinase inhibitors from Cajanus platycarpus accessions active against pod borer Helicoverpa armigera. *Acta physiologiae plantarum*, *37*(11), 242.
- 3) Swathi, M., Mishra, P. K., Lokya, V., Swaroop, V., Mallikarjuna, N., Dutta-Gupta, A., & Padmasree, K. (2016). Purification and partial characterization of trypsin-specific proteinase inhibitors from pigeon pea wild relative Cajanus platycarpus L.(Fabaceae) active against gut proteases of lepidopteran pest Helicoverpa armigera. *Frontiers in physiology*, 7, 388.

Presentation of work related to Thesis:

- 1. V. Swaroop, M. Swathi, V. Lokya, P.K. Mishra, N. Mallikarjuna, A. Dutta-Gupta, K. Padmasree (2015). Identification, Purification and biochemical characterization of proteinase inhibitors from *Cajanus platycarpus*, a wild relative of pigeonpea. ISPP South Zonal Seminar on Crop Physiology–Emerging Challenges and Opportunities for Sustainable Agriculture. Department of crop physiology, S.V. Agricultural College and RARS, Tirupathi plant physiology club (APAU) and Indian society for plant physiology, New Delhi, 3rd March, pp. 133 (Poster). Received Best poster Award.
- 2. V.Swaroop and K. Padmasree (2017) Biochemical characterization and pharmacological activities of purified proteinase inhibitors (PIs) from the seeds of *Vigna mungo* (*cv*.T9). **International Conference on Innovations in Pharma and Biopharma Industry** (**ICIPBI-2017**); **Challenges and Opportunities for Academy and Industry**, 20-22 Dec, University of Hyderabad, Hyderabad, p28, pp. 82 (Poster).
- 3. V. Swaroop Kumar, Vadthya Lokya, Kollipara Padmasree (2019). Role of Arginine Kinase in retardation of *Spodoptera litura* larval growth and development upon feeding with purified T9BBI from *Vigna mungo* (cv.T9). **Eighth International Symposium on Molecular Insect Science**", held at Melia Sitges, Sitges, Spain on 7-10th July 2019 (Poster).

FISEVIER

Contents lists available at ScienceDirect

Plant Physiology and Biochemistry

journal homepage: www.elsevier.com/locate/plaphy



Research article

Structural and functional characterization of proteinase inhibitors from seeds of *Cajanus cajan* (cv. ICP 7118)



Marri Swathi ^a, Vadthya Lokya ^b, Vanka Swaroop ^b, Nalini Mallikarjuna ^c, Monica Kannan ^d, Aparna Dutta-Gupta ^e, Kollipara Padmasree ^{b, *}

- ^a Department of Plant Sciences, School of Life Sciences, University of Hyderabad, Hyderabad 500046, India
- ^b Department of Biotechnology & Bioinformatics, School of Life Sciences, University of Hyderabad, Hyderabad 500046, India
- ^c Legumes Cell Biology, Grain Legumes Program, ICRISAT, Patancheru, Hyderabad 502324, India
- ^d Proteomics Facility, School of Life Sciences, University of Hyderabad, Hyderabad 500046, India
- ^e Department of Animal Sciences, School of Life Sciences, University of Hyderabad, Hyderabad 500046, India

ARTICLE INFO

Article history: Received 28 February 2014 Accepted 11 July 2014 Available online 21 July 2014

Keywords:
Achaea janata
Activity staining
BBI
Castor
Isoinhibitors
MALDI-TOF/TOF
Two-dimensional (2-D) gel electrophoresis

ABSTRACT

Proteinase inhibitors (C11PI) from mature dry seeds of Cajanus cajan (cv. ICP 7118) were purified by chromatography which resulted in 87-fold purification and 7.9% yield. SDS-PAGE, matrix assisted laser desorption ionization time-of-flight (MALDI-TOF/TOF) mass spectrum and two-dimensional (2-D) gel electrophoresis together resolved that C11PI possessed molecular mass of 8385.682 Da and existed as isoinhibitors. However, several of these isoinhibitors exhibited self association tendency to form small oligomers. All the isoinhibitors resolved in Native-PAGE and 2-D gel electrophoresis showed inhibitory activity against bovine pancreatic trypsin and chymotrypsin as well as Achaea janata midgut trypsin-like proteases (AjPs), a devastating pest of castor plant. Partial sequences of isoinhibitor (pl 6.0) obtained from MALDI-TOF/TOF analysis and N-terminal sequencing showed 100% homology to Bowman-Birk Inhibitors (BBIs) of leguminous plants. C11PI showed non-competitive inhibition against trypsin and chymotrypsin. A marginal loss (<15%) in C11PI activity against trypsin at 80 °C and basic pH (12.0) was associated with concurrent changes in its far-UV CD spectra. Further, in vitro assays demonstrated that C11PI possessed significant inhibitory potential (IC₅₀ of 78 ng) against AjPs. On the other hand, in vivo leaf coating assays demonstrated that C11PI caused significant mortality rate with concomitant reduction in body weight of both larvae and pupae, prolonged the duration of transition from larva to pupa along with formation of abnormal larval-pupal and pupal-adult intermediates. Being smaller peptides, it is possible to express C11PI in castor to protect them against its devastating pest A. janata.

© 2014 Elsevier Masson SAS. All rights reserved.

1. Introduction

The castor oil plant, *Ricinus communis*, is a plant species of the Euphorbiaceae family. Castor seed is the source of castor oil which has a wide variety of uses. The seeds contain between 40-60% of oil that is rich in triglycerides, mainly ricinolein. Castor seed oil has special chemical and physical properties. Its bio-degradable and eco-friendly nature makes it a vital industrial raw material for more

Abbreviations: AjPs, Achaea janata midgut trypsin-like proteases; AjPls, Achaea janata midgut trypsin-like proteinase inhibitors; BBls, Bowman-Birk inhibitors; IEF, isoelectric focusing; MALDI-TOF/TOF MS, matrix assisted laser desorption ionization time-of-flight mass spectrometry; Pls, proteinase inhibitors.

E-mail addresses: kpssl@uohyd.ac.in, kpssl@uohyd.ernet.in, padmasree_kollipara@yahoo.com (K. Padmasree).

than 700 industrial products, including high quality lubricants, paints, coatings, plastics, soaps, medications for skin infections and cosmetics (Ogunniyi, 2006). The recent application of castor oil is its use as biofuel for the production of biodiesel with reduced sulfur emission. Further, traditional ayurvedic medicine considered castor oil as the king of medicinals for curing arthritic diseases (Kalaiselvi et al., 2003). It has many therapeutical uses including anti-inflammatory and free radical scavenging activity (Ilavarasan et al., 2006; Saini et al., 2010), anti-diabetic effect (Rao et al., 2010) and hepato-protective activity (Visen et al., 1992).

Among the pests that damage the castor field, *Achaea janata* (castor semilooper) is a major feeder which causes about 30–70% loss in its production. Several recent studies indicated that among pest management methods used for crop protection, development of insect resistance by incorporating genes that express proteins with insecticidal activity is a novel approach (Dunse et al., 2010;

^{*} Corresponding author. Tel.: +91 40 23134507.

ORIGINAL ARTICLE



Proteinase inhibitors from *Cajanus platycarpus* accessions active against pod borer *Helicoverpa armigera*

Marri Swathi¹ · Soundappan S. Mohanraj¹ · Vanka Swaroop⁴ · Mariyamma Gujjarlapudi⁴ · Nalini Mallikarjuna² · Aparna Dutta-Gupta³ · Kollipara Padmasree⁴

Received: 22 February 2015/Revised: 26 July 2015/Accepted: 8 October 2015/Published online: 24 October 2015 © Franciszek Górski Institute of Plant Physiology, Polish Academy of Sciences, Kraków 2015

Abstract Cajanus platycarpus, a wild relative of Cajanus cajan, is an important source for various agronomically desirable traits, including resistance towards pod borer, Helicoverpa armigera. In the present study, the inhibitory activity of proteinase inhibitors (PIs) present in crude protein extracted from different accessions of C. platycarpus and cultivars of C. cajan was evaluated against H. armigera under in vitro and in vivo conditions. The PIs active against H. armigera gut trypsin-like proteinases (HGPs), referred to as 'HGPIs', were more pronounced in mature dry seeds of C. platycarpus accessions when compared with cultivars, which is also evident through gelatin activity staining studies. Therefore, the inhibitory activity of HGPIs was further evaluated in various plant organs of C. platycarpus accessions, such as leaves, flowers, pods, developing seeds at 8-10 days (DAP-I), 18-20 days (DAP-II), and 28-32 days after pollination (DAP-III). However, the HGPI activity was more pronounced in mature dry seeds > DAP-III > DAP-II > DAP-I > flowers > pods > leaves. The observed quantitative allocation of HGPIs closely resembled "Optimal Defense

Communicated by M. J. Reigosa.

- Department of Plant Sciences, School of Life Sciences, University of Hyderabad, Hyderabad, India
- Legumes Cell Biology, Grain Legumes Program, ICRISAT, Patancheru, Hyderabad, India
- Department of Animal Biology, School of Life Sciences, University of Hyderabad, Hyderabad, India
- Department of Biotechnology and Bioinformatics, School of Life Sciences, University of Hyderabad, Hyderabad 500 046, India

Theory". Further, bioassays demonstrated that there was a significant reduction in the body weight of the larvae fed upon crude PI extracts of *C. platycarpus* accessions with concomitant increase in mortality rate and the formation of larval—pupal intermediates. Nevertheless, such changes were not observed when the larvae were fed on crude PI extracts of *C. cajan* cultivars. These results suggest that the PI gene(s) from *C. platycarpus* accessions could be exploited in the management of *H. armigera* by introgression into *C. cajan* cultivars.

Keywords Gelatin activity staining · Optimal defense · Pigeonpea · Proteinase inhibitor · Proteinases

Abbreviations

CI Chymotrypsin inhibitor DAP Days after pollination

HGPs Helicoverpa armigera gut (trypsin-like)

proteinases

HGPIs Helicoverpa armigera gut (trypsin-like)

proteinase inhibitors Proteinase inhibitors Trypsin inhibitor

Introduction

PIs

ΤI

Pigeonpea (*Cajanus cajan* L. Millsp) is one of the most important crops cultivated in southern Asia and eastern Africa (Sujana et al. 2008). Although more than 200 species of insects are known to infest this crop, its production is most affected by pod borer *Helicoverpa armigera* (Reed and Lateef 1990). *H. armigera* is polyphagous and well







Purification and Partial Characterization of Trypsin-Specific Proteinase Inhibitors from Pigeonpea Wild Relative Cajanus platycarpus L. (Fabaceae) Active against Gut Proteases of Lepidopteran Pest Helicoverpa armigera

OPEN ACCESS

Edited by:

Arash Zibaee, University of Gilan, Iran

Reviewed by:

Jan Adrianus Veenstra, University of Bordeaux 1, France Samar Ramzi, University of Gilan, Iran Jalal Jalali Sendi, University of Gilan, Iran

*Correspondence:

Kollipara Padmasree kpssl@uohyd.ac.in; kpssl@uohyd.ernet.in

[†]These authors have contributed equally to this work.

Specialty section:

This article was submitted to Invertebrate Physiology, a section of the journal Frontiers in Physiology

Received: 07 April 2016 Accepted: 22 August 2016 Published: 07 September 2016

Citation:

Swathi M, Mishra PK, Lokya V,
Swaroop V, Mallikarjuna N,
Dutta-Gupta A and Padmasree K
(2016) Purification and Partial
Characterization of Trypsin-Specific
Proteinase Inhibitors from Pigeonpea
Wild Relative Cajanus platycarpus L.
(Fabaceae) Active against Gut
Proteases of Lepidopteran Pest
Helicoverpa armigera.
Front. Physiol. 7:388.
doi: 10.3389/fphys.2016.00388

Marri Swathi¹, Prashant K. Mishra², Vadthya Lokya^{2†}, Vanka Swaroop^{2†}, Nalini Mallikarjuna³, Aparna Dutta-Gupta⁴ and Kollipara Padmasree^{2*}

¹ Department of Plant Sciences, School of Life Sciences, University of Hyderabad, Hyderabad, India, ² Department of Biotechnology and Bioinformatics, School of Life Sciences, University of Hyderabad, Hyderabad, India, ³ Legumes Cell biology, Grain Legumes Program, ICRISAT, Hyderabad, India, ⁴ Department of Animal Biology, School of Life Sciences, University of Hyderabad, Hyderabad, India

Proteinase inhibitors (PIs) are natural defense proteins of plants found to be active against gut proteases of various insects. A pigeonpea wild relative Cajanus platycarpus was identified as a source of resistance against Helicoverpa armigera, a most devastating pest of several crops including pigeonpea. In the light of earlier studies, trypsin-specific Pls (CpPI 63) were purified from mature dry seeds of C. platycarpus (ICPW-63) and characterized their biochemical properties in contributing to *H. armigera* resistance. CpPI 63 possessed significant H. armigera gut trypsin-like proteinase inhibitor (HGPI) activity than trypsin inhibitor (TI) activity. Analysis of CpPI 63 using two-dimensional (2-D) electrophoresis and matrix assisted laser desorption ionization time-of-flight (MALDI-TOF) mass spectrometry revealed that it contained several isoinhibitors and small oligomers with masses ranging between 6 and 58 kDa. The gelatin activity staining studies suggest that these isoinhibitors and oligomers possessed strong inhibitory activity against H. armigera gut trypsin-like proteases (HGPs). The N-terminal sequence of the isoinhibitors (pl 6.6 and pl 5.6) of CpPl 63 exhibited 80% homology with several Kunitz trypsin inhibitors (KTIs) as well as miraculin-like proteins (MLPs). Further, modification of lysine residue(s) lead to 80% loss in both TI and HGPI activities of CpPI 63. In contrast, the TI and HGPI activities of CpPI 63 were stable over a wide range of temperature and pH conditions. The reported results provide a biochemical basis for pod borer resistance in C. platycarpus.

Keywords: gelatin activity staining, Kunitz trypsin inhibitor, mass spectrometry, miraculin-like proteins, two-dimensional electrophoresis

1

Effects of Vigna mungo (cv.T9) Seed Proteinase Inhibitor on Larval Growth and Expression of Midgut Proteins in Noctuid Lepidopteran Pests - A Comparative Study

by V Swaroop Kumar

Submission date: 13-Aug-2020 02:33PM (UTC+0530)

Submission ID: 1369103319

File name: V Swaroop Kumar Thesis for plagiarism check.docx (106.15K)

Word count: 24292

Character count: 133040

Effects of Vigna mungo (cv.T9) Seed Proteinase Inhibitor on Larval Growth and Expression of Midgut Proteins in Noctuid Lepidopteran Pests - A Comparative Study

ORIGINALITY REPORT

9%

2%

8%

7%

SIMILARITY INDEX

INTERNET SOURCES

PUBLICATIONS

STUDENT PAPERS

PRIMARY SOURCES



Submitted to University of Hyderabad, Hyderabad

2%

Student Paper

2

Vadthya Lokya, Marri Swathi, Nalini Mallikarjuna, Kollipara Padmasree. "Response of Midgut Trypsin- and Chymotrypsin-Like Proteases of Helicoverpa armigera Larvae Upon Feeding With Peanut BBI: Biochemical and Biophysical Characterization of PnBBI", Frontiers in Plant Science, 2020

1%

1%

Publication

3

E.R. Prasad, A. Dutta-Gupta, K. Padmasree. "Insecticidal potential of Bowman–Birk proteinase inhibitors from red gram (Cajanus cajan) and black gram (Vigna mungo) against lepidopteran insect pests", Pesticide Biochemistry and Physiology, 2010

Publication

Swathi, Marri, Vadthya Lokya, Vanka Swaroop,